Fundamental Study on Removal of Iron Directly from Titanium Ore by Selective Chlorination

(選択塩化法によるチタン鉱石からの鉄の直接除去に関する基礎的研究)

Jungshin Kang

(姜 正信)

博士論文

Fundamental Study on Removal of Iron Directly from Titanium Ore by Selective Chlorination

(選択塩化法によるチタン鉱石からの鉄の直接除去に関する基礎的研究)

Jungshin Kang

(姜 正信)

Table of contents

List of Tables

x

List of Figures

XIII

XVI

XVII

Chapter 1 Introduction

1.1 Titanium metal and its alloys

1.1.1 Properties and market consumption of titanium metal

Titanium (atomic number: 22; Ti) is well known for its excellent physical and chemical properties such as its high specific strength (strength to weight ratio), high corrosion resistance, nontoxicity, and low thermal expansion. Some of these properties can be enhanced or adjusted for obtaining desired properties by alloying titanium with other metal elements such as aluminum (Al), vanadium (V), or molybdenum (Mo). For comparison of titanium with common metals, Table 1-1 lists the physical and chemical properties of titanium, one of its alloys (Ti-6Al-4V), iron (Fe), and aluminum.[1-6] Owing to their superior properties, titanium and its alloys are used in very diverse fields such as the aerospace industry, chemical plants, power generation plants, seawater desalination plants, and the automotive industry.

The demand for titanium and its alloys has gradually increased, and this increased market demand has resulted in an increase in the production of titanium metal. Fig. 1-1 shows that the total global titanium metal production has steadily increased from 2002 to 2010.[7-16] In addition, the portion of the titanium metal production in China has remarkably increased to 38.0 % of global titanium metal production in 2010. Even though the portion of the titanium metal production in Japan has slightly decreased, Japan is still the second largest titanium metal producer in the world.

Conventionally, the defense and aerospace industry has a huge influence on the market consumption of titanium metal, because the use of titanium metal or its alloys for aircraft has several advantages such as weight reduction with good mechanical properties, service at high operating temperature, and high corrosion resistance.[17]

Fig. 1-2 shows the relationship between the production of titanium metal and the estimated percentages of titanium metal consumption in the aerospace industry in the United States of America (USA) from 2002 to 2010.[7-16] As shown in Fig. 1-2, the trend for the production of titanium metal in the USA is similar to the trend for the percentage of titanium metal consumed in the aerospace industry in the USA. Therefore, the

aerospace industry is considered to play an important role in the growth of the titanium industry. This relationship was also analyzed by Gambogi[15] and Bedinger,[18,19] who forecasted that the consumption of titanium metal in the aerospace industry will continue to increase in the near future. As a result, it is expected that production of titanium metal will also increase.

1.1.2 Constraints for increasing the use of titanium metal

Titanium is the ninth most abundant element in the Earth's crust. From the viewpoint of reserves of the mineral resources of titanium, the amount of ilmenite, which is the principal mineral resource for titanium, is unlimited (*see* section 1.3.2). However, global production of titanium is much lower than that of iron or aluminum. Fig. 1-3 shows the global production of iron, aluminum, nickel (Ni), and titanium in 2012.[19-22] As shown in Fig. 1-3, global production of titanium was 13000 times and 230 times lower than those of iron and aluminum, respectively. It is worth noting that global production of nickel was 9 times higher than that of titanium even though titanium is more abundant in the Earth's crust than nickel: nickel is the 21st most abundant element.[6] The principal reason for this result is that the removal of impurities such as iron and oxygen is technically difficult for producing high-purity titanium metal (*see* section 1.1 and 1.3).[23]

The difficulty of the production of titanium metal results in high processing costs for titanium. Fig. 1-4 shows processing costs for steel, aluminum, and titanium from ore to ingot.[24, 25] As shown in Fig. 1-4, the processing cost for titanium ore is 15 times higher than that for iron ore. In addition, processing costs for titanium increase whenever the processing stage proceeds. The results in Fig. 1-4 show that all processing steps for titanium production must be improved and become more effective to reduce the cost of titanium. Furthermore, it shows the importance of development of an effective titanium ore upgrading process, because the cost burden in an early processing stage is carried over the entire process. Therefore, to extend the use of titanium in our society, development of effective titanium smelting processing is required.

1.1.3 Brief overview of developments for early stages of titanium metal production

Since Gregor first reported the existence of titanium oxide in iron-containing sand in 1791, many attempts have been made to extract pure titanium metal, for example, by using potassium hexafluorotitanate (K_2TiF_6), titanium dioxide (TiO_2), or $TiCl_4 \cdot 4NH_3$ as starting materials.[26-28] However, all attempts ended in failure because of the strong chemical affinity between titanium and oxygen. In 1887, Nilson and Petersson produced 94.7 % titanium by reducing titanium tetrachloride ($TiCl_4$) with sodium (Na) in an air-tight steel reactor.[28]

In 1910, Hunter, inspired by Nilson and Petersson, produced 96.3 – 99.9 % titanium through reduction of $TiCl_4$ by sodium at 1173 K by taking extra care to prevent intrusion of air during and after the experiment.[28,29] Thereafter, a process for producing titanium metal by sodiothermic reduction has been called the Hunter process. The Hunter process was scaled up in 1950s after several improvements and was used as a batch-type commercial titanium production process in industry until 1993. However, currently, only a small amount of titanium for limited purposes such as electronic materials is produced using the Hunter process.[26] The main reason is its ineffective treatment of the sodium chloride (NaCl) produced by the sodiothermic reduction reaction.

$$TiCl_4\ (g) + 4\ Na\ (l) = Ti\ (s) + 4\ NaCl\ (l) \qquad\qquad (1\text{-}1)$$
$$\Delta H^{\circ}_r = -1122\ kJ,\ \Delta G^{\circ}_r = -590\ kJ\ at\ 1200\ K^{[30]}$$
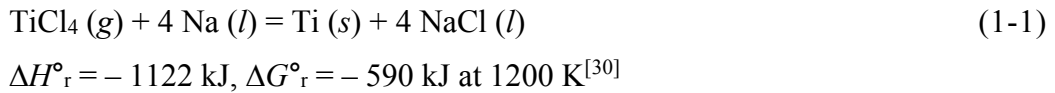
Eq. 1-1 shows the total reaction for the sodiothermic reduction in the Hunter process. In order to obtain titanium metal, a large amount of NaCl and a small amount of Na must be separated from titanium metal after reduction. The vapor pressures of NaCl at high temperatures are very low. For example, the vapor pressure of NaCl at 1200 K is 0.003 atm.[30] As a result, it is impossible to utilize vacuum distillation to remove NaCl. Therefore, leaching treatment using water or dilute hydrochloric (HCl) acid is essential to remove NaCl from the mixture of NaCl and titanium.[3,28,31,32] Even though NaCl is recovered from the aqueous NaCl solution, the effective recovery of sodium and chlorine gas (Cl_2) by electrolysis requires a high amount of energy and has a high cost at present.[26]

To overcome the disadvantages of the Hunter process, in recent years, a continuous type of the Hunter process called the Armstrong process (or Armstrong/ITP process) has been developed.[31,33-36] However, currently, this process is not used as a large-scale industrial titanium production process.

In 1925, van Arkel and de Boer developed the iodide process, also known as the van Arkel-de Boer process, for production of high-purity titanium, zirconium, and hafnium metal.[26,37-39] In the iodide process, iodine gas (I_2) or titanium tetraiodide (TiI_4) can be used as a precursor material. For example, when TiI_4 is used, TiI_4 reacts with crude titanium metal placed in a reactor and TiI_2 is produced by Eq. 1-2. The produced subhalide titanium iodide is decomposed on a high-temperature filament wire such as a tungsten (W) wire, and deposition of high-purity titanium metal and release of TiI_4 gas occur through the disproportionation reaction shown in Eq. 1-3. However, currently, this process is not used as a large-scale industrial titanium production process owing to its low productivity, although high-purity titanium metal can be obtained.

$$TiI_4\ (g) + Ti\ (s) = 2\ TiI_2\ (g) \tag{1-2}$$
$$2\ TiI_2\ (g) = TiI_4\ (g) + Ti\ (s) \tag{1-3}$$

1.1.4 Titanium metal production process: Kroll process

In 1940, Kroll reported a novel titanium metal production process called the Kroll process.[40,41] Since the Kroll's invention, the Kroll process has been using as the large-scale titanium metal production process in industrial manufacturing. As shown in Fig. 1-5, the principal procedures of the Kroll process include (i) the chlorination of a high-grade TiO_2 feed by Cl_2 gas in the presence of carbon to produce $TiCl_4$ (the carbo-chlorination process), (ii) the reduction of $TiCl_4$ by magnesium (Mg) to produce titanium metal, and (iii) the electrolysis of magnesium chloride ($MgCl_2$) to recover Mg and Cl_2 gas from the by-product.[23,26,42,43]

The first stage of the Kroll process is the carbo-chlorination process. In this process, a high-grade TiO_2 feed with a purity of above 90 % TiO_2 is chlorinated by Cl_2 gas in the presence of carbon. Fig. 1-6 shows a schematic of the carbo-chlorination process, in which the fluidized bed and distillation equipment are integrated.[43,44]

Generally, rutile, synthetic rutile, or upgraded ilmenite (UGI) is used as the high-grade TiO_2 feed. The carbo-chlorination process is carried out in the fluidized bed chlorinator at 1073 – 1273 K. When the carbo-chlorination process is conducted, titanium oxides and almost all other impurities in the high-grade TiO_2 feed, including iron oxides but not silica (SiO_2), are chlorinated by Cl_2 gas as follows:

$$TiO_2\ (s) + 2\ C\ (s) + 2\ Cl_2\ (g) \quad = TiCl_4\ (g) + 2\ CO\ (g) \tag{1-4}$$
$\Delta H^{\circ}_r = -53\ kJ,\ \Delta G^{\circ}_r = -350\ kJ$ at 1300 K[30]

$$FeO\ (s) + C\ (s) + Cl_2\ (g) \quad = FeCl_2\ (g) + CO\ (g) \tag{1-5}$$
$\Delta H^{\circ}_r = -41\ kJ,\ \Delta G^{\circ}_r = -193\ kJ$ at 1300 K[30]
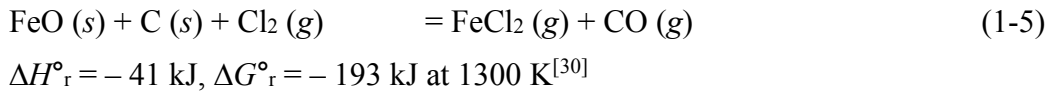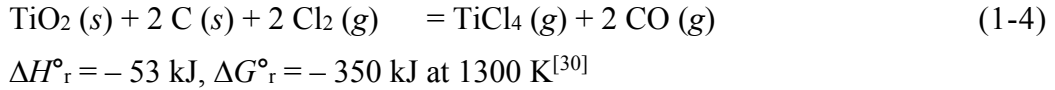
Among the chlorinated impurities produced in the carbo-chlorination process, the $FeCl_x$ (x = 2,3) and aluminum chloride ($AlCl_3$) have boiling temperatures (T_b) that are greatly different from boiling temperature of $TiCl_4$ (T_b = 408 K). As a result, these chlorides are condensed and removed by simple distillation. However, the boiling temperatures of vanadium oxytrichloride ($VOCl_3$), tin tetrachloride ($SnCl_4$), and silicon tetrachloride ($SiCl_4$) are close to that of $TiCl_4$. Therefore, these chlorides are removed by multiple distillation. In general, $VOCl_3$ and VCl_4 are reacted with hydrogen sulfide (H_2S) before distillation and removed from crude $TiCl_4$.[45,46] After the distillation, $TiCl_4$ with a purity of above 99.98 % is obtained and used as a reactant for the magnesiothermic reduction stage.

In the chlorinator, if the purity of the TiO_2 feed is low, a large amount of chloride waste is generated and chlorine loss increases. Generation of chloride waste leads to clogging of the pipes in the chlorinator. In addition, treatment or disposal of the chloride waste is costly in some countries such as Japan, which has strict environmental regulations for the disposal and treatment of industrial waste.[47] Furthermore, the naturally occurring radioactive materials (NORMs) such as thorium (Th) and uranium (U) in the TiO_2 feed are also enriched in the chloride waste. When a feed material containing NORMs is used, waste management becomes costly because the treatment of radioactive materials needs very special care. Therefore, Japan imports TiO_2 feed with a very low NROMs content.

The amounts of alkaline metals or alkaline earth metals in the feed must also be considered. The vapor pressures of alkaline metal chlorides or alkaline earth metal chlorides are low compared to those of other chlorides. For example, the vapor pressure of $CaCl_2$ at 1300 K is 5.6×10^{-5} atm. Therefore, the environment inside the chlorinator becomes very corrosive at high temperatures when the chlorinated alkaline metals or alkaline earth metals remain in the bottom of the chlorinator. These alkaline metal chlorides or alkaline earth metal chlorides damage the refractory materials inside the chlorinator. Therefore, controlling the purity (or grade) of TiO_2 feed is one of the most important issues in the carbo-chlorination process.

Currently, a purity of above 90 % TiO_2 is used as the feedstock for the chlorinator in the world. In addition, feedstock with a purity of above 95 % TiO_2 is used in Japan. However, the use of high-grade TiO_2 feed has become more difficult nowadays, mainly because the price of high-grade TiO_2 feed has increased owing to the increase in consumption of TiO_2 feed in China and other developing countries (*see* section 1.2.1). In this situation, titanium metal production companies in Japan have started to investigate the usage of lower grade feed, of about 90 % TiO_2, instead of the 95 % TiO_2 feed. In 2012, 40 % of the total feedstock used in the chlorinator by Osaka Titanium Technologies Co., Ltd. was TiO_2 feed with a purity of about 90 – 92 %. However, this approach is still in limited use owing to certain unresolved technical problems in the current production process, such as pipe clogging, increase of chlorine loss, and damage to the refractory materials of the chlorinator.

The second stage of the Kroll process is the magnesiothermic reduction process. Fig. 1-7 (a) shows the schematic of the reduction process. In this process, high-purity $TiCl_4$ injected reacts with molten Mg contained in a steel retort in advance at 1173 K under an Ar gas atmosphere.[43] Titanium metal is produced by the reaction shown in Eq. 1-6, and $MgCl_2$ is produced as by-product. The produced $MgCl_2$ is periodically tapped out from the retort and moved to electrolysis plant for recovering Mg and Cl_2 from it.

$$TiCl_4\ (g) + 2\ Mg\ (l) = Ti\ (s) + 2\ MgCl_2\ (l) \tag{1-6}$$
$$\Delta H^{\circ}_r = -420\ kJ,\ \Delta G^{\circ}_r = -612\ kJ\ at\ 1200\ K^{[30]}$$
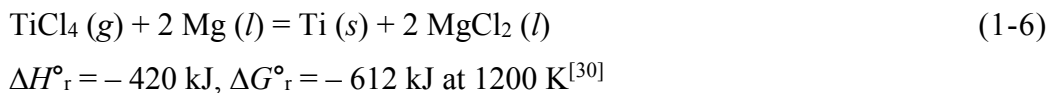
As shown in Eq. 1-6, magnesiothermic reduction is a highly exothermic reaction. Fig. 1-8 shows the binary phase diagram of the Ti-Fe system.[48] As shown in Fig. 1-8, the eutectic temperature of Ti rich-Fe alloy is 1358 K (1085 °C). Therefore, control of the reaction temperature is very important, because the steel retort might be broken by the production of liquid Ti–Fe alloy if the temperature control fails, depending on conditions. Consequently, in the Kroll process, control of the reaction temperature is delicately carried out by controlling the injection rate of $TiCl_4$ and by cooling the steel retort. This leads to a slow reaction rate for titanium production, and generally, about 90 hours are required for the production of 10 tons of sponge titanium.[49,50]

After the reduction reaction is completed, sponge-like titanium metal with a porous structure is produced, in which unreacted Mg and $MgCl_2$ remain. The vapor pressures of Mg and $MgCl_2$ at 1300 K are 0.59 atm and 0.05 atm, respectively,[30] which are high enough for the Mg and $MgCl_2$ to evaporate. Therefore, the Mg and $MgCl_2$ in the sponge titanium are removed by vacuum distillation at around 1273 K, as schematically shown in Fig. 1-7 (b).[26,49,50] This vacuum distillation also requires about 90 hours per 10 ton of titanium.[49,50] Furthermore, before the sponge titanium is removed from the retort, a certain time is needed for cooling the retort after the vacuum distillation is conducted. Therefore, normally, production speed of titanium metal is about 1 ton/day·reactor, which is very small compared to other large-scale metal production processes.[26] From these facts, it can be inferred that a change from batch-type production to continuous production and improvement of the low reaction rate are required to reduce the high processing cost of titanium metal.

The last important process in the Kroll process is the electrolysis of $MgCl_2$. As mentioned before, in this process, Mg and Cl_2 gas are recovered from the $MgCl_2$ produced in the reduction process and are reused for the reduction process and the carbo-chlorination process, respectively. The most important issue in the electrolysis process is its energy efficiency. For the electrolysis process in the Kroll process, a highly energy efficient technology for the molten salt electrolysis of $MgCl_2$ has been developed. The establishment of this industrial method for electrolysis of $MgCl_2$ is one significant reason why the Kroll process is used as the industrial titanium metal production process.[23]

Fig. 1-9 shows a schematic of the fundamental concept of the electrochemical cell for $MgCl_2$ electrolysis.[51] Electrolysis of the $MgCl_2$ is performed by using molten salt

consisting of about 18 – 23 % $MgCl_2$, 48 – 58 % NaCl, and 20 – 28 % $CaCl_2$ at about 943 K.[51] When the electrolysis is carried out, liquid Mg is produced at the cathode and Cl_2 gas is produced at the anode, as shown in Eq. 1-7. Because the density of the liquid Mg produced is lower than that of the electrolyte, the regenerated Mg floats. The design of electrode and the electrolyte flow in the electrolysis cell are technologically important issues in order to separate Mg and Cl_2 efficiently. Therefore, the structure of an actual industrial electrochemical cell for $MgCl_2$ electrolysis is complicated. In recent years, an electrochemical cell using bipolar (or multi-polar) electrodes, as schematically shown in Fig. 1-9 (b), has been used to enhance the efficiency of the electrolysis. By reducing the IR drop and preventing the reaction between the Mg and Cl_2 gas produced, the current and energy efficiencies of $MgCl_2$ electrolysis have reached 70 – 80 % and 55 – 60 %, respectively, in the modern industrial electrolysis employed in titanium industry.[23] These results show that high-efficiency electrolysis of $MgCl_2$ can be carried out. In addition, the heat loss during electrolysis can be reduced. This highly energy efficient electrolysis technology has allowed Japan to lead the global titanium metal production, even though the energy cost is high.

$$\text{Cathode: } Mg^{2+} \text{ (in molten salt)} + 2\ e^- = Mg\ (l) \tag{1-7}$$
$$\text{Anode: }\quad 2\ Cl^- \text{ (in molten salt)} \qquad = Cl_2\ (g) + 2\ e^-$$
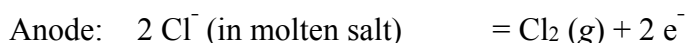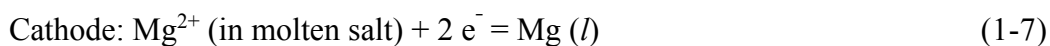
1.1.5 New titanium metal production processes

To overcome the disadvantages of the Kroll process, many studies have been conducted. However, unfortunately, none of the studied processes have been commercialized. These past studies can be roughly classified into two groups: electrolysis using molten salt and metallothermic reduction. Molten salt must be used for electrolysis method for titanium production, because the standard electrode potential for titanium deposition is greatly negative. In addition, only a limited number of reducing agents such as calcium (Ca), magnesium, sodium or hydrogen gas (H_2) can be used for the metallothermic reduction method for titanium, depending on the starting materials.[23] Fig. 1-10 shows the relationship between the starting materials and reducing agents for several reduction processes. As shown in Fig. 1-10, selection of the reducing agent depends on

the starting material. For example, magnesium can be the reducing material for $TiCl_4$, however, it cannot be the reducing material for TiO_2. This is because when magnesium is used as a reducing agent for TiO_2, the concentration of oxygen cannot be sufficiently lowered to produce commercial titanium metal. The important studies conducted on this topic so far are well summarized by Zheng and Takeda in their theses.[32,52]

In recent years, new titanium metal production processes such as the FFC process,[53-56] OS process,[57-62] EMR/MSE process,[63-65] PRP process,[66,67] and the subhalide process[68-70] have been proposed. Table 1-2 lists the advantages and disadvantages of these processes. Many studies have focused on increasing the productivity by establishing a continuous process (or a semi-continuous process) or developing a high-speed process. In this thesis, among these processes, the FFC process, OS process, and EMR/MSE process are briefly reviewed.

Fig. 1-11 (a) shows the schematic of the FFC process.[53-56] Fray and his coworkers showed that ionization of oxygen in TiO_2 and discharge of the ionized oxygen at the cathode can proceed without Ca deposition at the cathode. In other words, titanium metal can be directly obtained from TiO_2 using the electrochemical method by electrons as the reducing agent. The main reactions at the anode and cathode are as follows:

$$\text{Cathode: } TiO_2 + 4\ e^- = Ti + 2\ O^{2-} \qquad\qquad (1\text{-}8)$$
$$\text{Anode: }\quad C + x\ O^{2-} = CO_x + 2x\ e^-$$

As shown in Eq. 1-8, the oxide ion dissolved in molten salt or generated after reduction of TiO_2 at the cathode oxidized at the anode to form CO_x gas. The advantage of the FFC process is that it is semi-continuous, because titanium can be easily collected by exchanging the cathode. However, post treatment such as water leaching is required to remove the $CaCl_2$ adhered to the titanium. In addition, suppression of impurity contamination is required such as carbon contamination when a carbon anode is used.

An interesting result obtained by utilizing the FFC process is that $CaTiO_3$ can also be used as a starting material to produce titanium metal, as shown by Chen and his coworkers.[71] Chen and his coworkers also reported that perovskitization of TiO_2 in $CaCl_2$ can increase the reduction speed and efficiency. On the basis of their results, it can

be expected that the development of the effective method for production of calcium titanate ($CaTiO_3$) from titanium ore has the potential to be useful in the future.

Fig. 1-11 (b) shows the schematic of the OS process.[57-62] The OS process is based on the direct reduction of TiO_2 by Ca produced by electrolysis of calcim oxide (CaO) dissolved in $CaCl_2$ molten salt. This process is the calciothermic reduction of TiO_2 by the electrochemically generated metal reductant, and not a direct electrochemical reduction. These reactions can proceed in a single electrochemical cell. Production of Ca from CaO is possible because the solubility of CaO in $CaCl_2$ at high temperatures is high. For example, 19.4 mol% CaO can be dissolved in $CaCl_2$ at 1173 K.[58] The reactions at anode and cathode and the calciothermic reduction of TiO_2 by the electrochemically generated Ca are as follows:

$$\text{Cathode: } Ca^{2+} + 2\ e^- = Ca \qquad\qquad (1\text{-}9)$$
$$\text{Anode: } \quad C + x\ O^{2-} = CO_x + 2x\ e^-$$

$$TiO_2 + 2\ Ca = Ti + 2\ O^{2-} + 2\ Ca^{2+} \qquad\qquad (1\text{-}10)$$
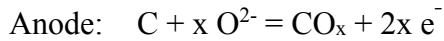
The advantage of the OS process is that it is semi-continuous, because TiO_2 powder, the staring material, can be successively supplied into the electrochemical cell and can be reduced by the regenerated Ca. However, post-treatment such as water leaching of the obtained titanium powder and suppression of carbon contamination are required. One interesting result of the OS process is that the use of $CaTiO_3$ as starting material is also possible, as was reported by Suzuki and coworkers.[58] This result also shows that a method for upgrading low-grade titanium ore to produce $CaTiO_3$ has the potential to be useful in the future.

Fig. 1-11 (c) shows the schematic of the EMR/MSE process developed by Okabe and coworkers.[63-65] Okabe and coworkers showed that reduction of metal oxides by a metal reducing agent proceeds when an electrically conducting medium exists for transference of electrons and when electroneutrality conditions are satisfied. As shown in Fig. 1-11 (c), when a Ca alloy is used as the reducing agent, the reactions shown in Eq. 1-11 proceed at the anode and cathode. Therefore, titanium metal can be obtained at the cathode through the EMR (electronically mediated reaction). In addition, when MSE

(molten salt electrolysis) is conducted after the EMR is completed, regeneration of the reducing agent, such as the Ca alloy in this case, is possible, as shown in Eq. 1-12.

Cathode: $TiO_2 + 4 e^- = Ti + 2 O^{2-}$ (1-11)

Anode: $2 Ca (alloy) = 2 Ca^{2+} + 4 e^-$

Cathode: $Ca^{2+} (salt) + 2 e^- = Ca$ (1-12)

Anode: $C + x O^{2-} = CO_x + 2x e^-$
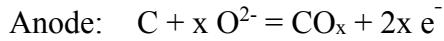
The advantage of the EMR/MSE process is that contamination by impurities can be suppressed, because the TiO_2 reduction cell can be separated from the reducing agent (Ca metal) production cell owing to the characteristics of the EMR. In addition, the reduction and electrolysis operation can be independently conducted. Furthermore, this process is semi-continuous, because titanium can be easily collected by exchanging the cathode. However, the separation of titanium and molten salt is difficult, and structure of the electrochemical cell is complicated.

1.2   Titania pigment

1.2.1   Properties and market consumption of titania pigment

Pigment can change the color of a material, for example, by coating, and the pigment industry is one of the most important industries for mankind. The pigment can be roughly classified into white pigments such as titania (TiO_2) or zinc sulfide (ZnS) and colored pigments such as iron oxides or chromates.[72] Titania is widely used as a white pigment because titania pigment has superior properties such as a high opaqueness due to its high refractive index, high brightness, chemical stability, and nontoxicity.[27,72] Table 1-3 compares the properties of various kinds of white pigments.[73,74] As shown in Table 1-3, owing to its excellent properties as a white pigment, titania is mainly used for coatings, polymers, and paper. Among these several uses, for example, 60 % and 25 % of the titania pigment used in the USA were estimated to be consumed in application for paint and plastic, respectively, in 2013.[19]

As implied by these statistics, titania pigment is indispensable for the production of several essential commodities in our daily lives. Thus, it is generally accepted that the consumption of titania pigment is related to the gross domestic product (GDP).[72] Fig. 1-12 (a) shows the trend of the global capacity for titania pigment production and the trend of the annual percent changes of world output.[7-15,18,19,75-81] As shown in Fig. 1-12 (a), the global capacity for titania pigment production has increased gradually in order to satisfy the increase in demand from the market. The increase in the total volume of the world economy implies the increase in demand for titania pigment. In addition, Fig. 1-12 (b) shows that, in the recent years, the Chinese market has led the global production of titania pigment, because the demand for titania pigment in China has rapidly increased owing to the rapid growth of the Chinese economy.

The International Monetary Fund (IMF) forecasted that the annual percent change of world output will be 3.9 % in 2015 and 3.9 % in 2019.[79] Specifically, the average growth rate of emerging and developing Asia such as China and India is expected to become 6.8 % in 2015 and 6.5 % in 2019. On the basis of these forecasts, it can be expected that the demand for titania pigment will continue to increase in the near future, especially in the developing countries in Asia. One interesting fact is that the volume of the titania pigment market is larger than that of titanium metal market. For example, 5.6 Mt of TiO_2 was produced while 0.16 Mt of titanium metal was produced in 2011.[18,82] Therefore, the production of TiO_2 pigment plays an important role in the overall titanium industry.

1.2.2 Factors determining the price of titania pigment

Podolsky and Reid reported that the price of the feedstock for producing titania pigment such as synthetic rutile or upgraded ilmenite is the most important factor determining the price of titania pigment.[72] Fig. 1-13 shows the trend of the producer price index (PPI) of titania pigment in the USA and the trends of the prices of rutile and ilmenite in the USA.[83-87] As shown in Fig 1-13, the shape of the trend of the PPI of titania pigment is very similar to that of the price of rutile in the USA. The analysis results of Bedinger[84] show that the increased global demand for titania pigment led to the increase

in the price of rutile. In addition, it is expected that the increased price of the rutile also caused the increased price of the titania pigment.

The strong relationship between the PPI of titania pigment and the price of rutile also shows the need for development of an effective titanium ore upgrading process to reduce the price of the titania pigment. Reductions in the price of the rutile lead to reductions in the price of titania pigment as well as in the price of titanium metal.

1.2.3 Titania pigment production process 1: Chloride process

The chloride process for the production of titania pigment was first developed by DuPont.[88] In 2011, DuPont produced 19 % of the global titania pigment, and it is currently the largest titania pigment producer in the world.[82] Fig. 1-14 shows the flowchart of the chloride process.[27,88-95]

As shown in Fig. 1-14, the chloride process mainly consists of the carbo-chlorination process and oxidation process. The carbo-chlorination process, which includes distillation, is identical to the carbo-chlorination process in the Kroll process explained in section 1.1.4. The feedstock for the carbo-chlorination process in almost all chloride processes in the world is high-grade TiO_2 feed in order to decrease the amount of chloride waste produced, chlorine loss, and damage to the refractory materials inside the chlorinator. Unlike the other chloride processes, the chloride process adopted in DuPont uses low-grade titanium ore feed directly. However, considering environmental burden caused by the chloride process, the use of high-grade TiO_2 feed is still indispensable for the carbo-chlorination process. Therefore, an effective method for producing high-grade TiO_2 feed from low-grade titanium ore is important.

The high-purity $TiCl_4$ produced in the carbo-chlorination process is oxidized to produce high-purity TiO_2 under an oxidative atmosphere. Before $TiCl_4$ reacts with O_2 gas in the reactor, $TiCl_4$ is preheated to 573 K – 923 K and O_2 gas is preheated to at least 1473 K to obtain a high reaction rate.[27,92] The preheated $TiCl_4$ and O_2 gas are fed separately into the reactor and react at 1173 – 1873 K, as shown in Eq. 1-13.[92] The Cl_2 gas produced by the reaction is recycled and used as a chlorinating agent for the carbo-chlorination process.

$$TiCl_4 \ (g) + O_2 \ (g) = TiO_2 \ (s, \text{rutile}) + 2 \ Cl_2 \ (g) \tag{1-13}$$

$$\Delta H^\circ_r = -174 \text{ kJ}, \ \Delta G^\circ_r = -98 \text{ kJ at } 1400 \text{ K}^{[30]}$$
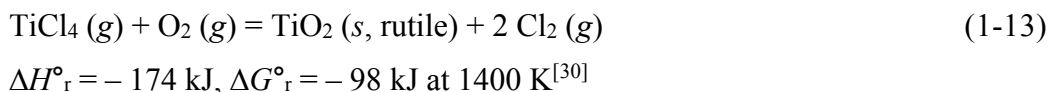
Rutile-type TiO_2 is preferred to anatase-type TiO_2 because of its high refractive index. Therefore, several studies on the conditions for the production of rutile-type TiO_2 were conducted. The results showed that the addition of a small amount of $AlCl_3$ and $SiCl_4$ in $TiCl_4$ enhanced the production of rutile-type TiO_2 and decreased the particle size by restraining agglomeration.[92,94] Furthermore, a high reaction temperature and high pressure also enhanced the production of rutile-type TiO_2.[90, 92] On the contrary, addition of a small amount of $SiCl_4$ and PCl_3 to the $TiCl_4$ enhanced the production of anatase-type TiO_2.[95] Under certain conditions, TiO_2 with the anatase crystallographic type is produced instead of TiO_2 with the rutile crystallographic type.

The investigation of the use of $AlCl_3$ and $SiCl_4$ in the oxidation process also has other purposes and aspects. Normally, TiO_2 produced is coated by Al_2O_3 or a mixture of Al_2O_3 and SiO_2 after the oxidation process in order to improve the durability and other properties through surface treatment using a wet-processing method.[93] However, if $AlCl_3$ and $SiCl_4$ are added in the oxidation process, this wet-processing method might be skipped or simplified under certain conditions. After oxidation, the TiO_2 produced is rapidly cooled to below 873 K to restrain agglomeration. Afterward, finishing treatments such as surface treatment, filtration, washing, drying, and grinding are performed.[27,88]

The disadvantage of the chloride process is that there are few effective methods for recycling the chloride waste produced, even though the amount of chloride waste produced is not large when high-grade TiO_2 feed is used. In addition, the use of Cl_2 gas has safety and environmental issues. Moreover, the capital investment required for the chloride process is higher than that for the sulfate process.[96] However, the chloride process is semi-continuous and uses high-temperature reactions that is suitable for high-speed processing.[74] In addition, it is easy to control the impurities affecting the whiteness of the titania pigment because the chlorination and distillation are used.[74] Therefore, the quality of the titania pigment is generally better than that of the titania pigment produced by the sulfate process. Furthermore, production of uniform titania pigment particles is possible.[74]

1.2.4 Titania pigment production process 2: Sulfate process

The sulfate process is the conventional method for producing titania pigment and was developed earlier than the chloride process. Fig 1-15 shows a representative flowchart of the sulfate process.[27,44,74,97,98] Unlike the chloride process, the sulfate process can use ilmenite or titania slag as a feedstock.

The first stage of the sulfate process is the digestion process, in which the ilmenite or titania slag reacts with concentrated sulfuric acid (H_2SO_4). During the leaching reaction, a reductant and/or additives are supplied into the reactor for ferric reduction and acceleration of the leaching reaction, respectively. Normally, iron scrap is used as the reductant. In addition, iron, titanium (III) salt, thiosulfate salt (e.g., sodium thiosulfate), or sulfur dioxide is used as the accelerant. In general, the leaching reaction is conducted using $80 - 98$ % H_2SO_4 at $443 - 493$ K for $1 - 12$ hours.[27] The reaction between iron in the ilmenite or titania slag and H_2SO_4 transforms iron into the iron sulfate ($FeSO_4$), and titanium is transformed to titanyl sulfate ($TiOSO_4$), as shown in Eq. 1-14. In addition, the ferric ion is reduced to a ferrous ion by reacting with the reductant, as shown in Eq. 1-15.

$$FeO \cdot TiO_2 \ (s) + 2 \ H_2SO_4 \ (l)$$
$$= FeSO_4 \ (l) + TiOSO_4 \ (l) + 2 \ H_2O \ (l) \qquad (1\text{-}14)$$

$$Fe_2(SO_4)_3 \ (l) + Fe \ (s) = 3 \ FeSO_4 \ (l) \qquad (1\text{-}15)$$
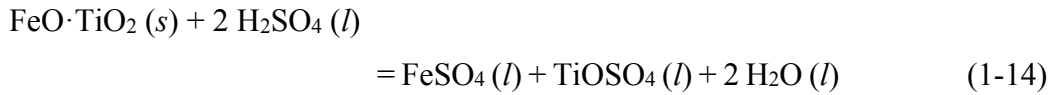
Before crystallization, the unreacted solids such as unreacted ilmenite are separated from the leach liquor produced in the digestion process. In the crystallization process, the temperature of the filtered leach liquor is decreased to about $283 - 303$ K by cooling, and the $FeSO_4$ in leach liquor is precipitated as $FeSO_4 \cdot 7 \ H_2O$, as shown in Eq. 1-16.[97,98] Then, the crystallized $FeSO_4 \cdot 7H_2O$ is separated from the leach liquor.

$$Fe(SO_4) \ (l) + 7 \ H_2O \ (l) = FeSO_4 \cdot 7 \ H_2O \ (s) \qquad (1\text{-}16)$$
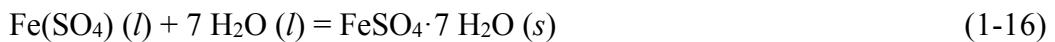
After the crystallization process, hydrolysis process is conducted at $367 - 383$ K for $3 - 12$ hours.[27,97,98] During the hydrolysis process, hydrated titanium oxides are

precipitated, because the sulfate ions in the $TiOSO_4$ solution are replaced by hydroxyl ions, as shown in Eq. 1-17. In some cases, hydrated titanium oxide or TiO_2 particles are placed in the rector in advance to act as seeds for precipitation.

$$TiOSO_4 \ (l) + 2 \ H_2O \ (l) = TiO(OH)_2 \ (s) + H_2SO_4 \ (l) \qquad\qquad (1\text{-}17)$$
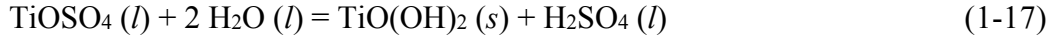
The purification of $TiO(OH)_2$ is conducted after the hydrolysis. Normally, filtration and washing with water or diluted acid are followed by bleaching to purify the $TiO(OH)_2$. The bleaching is performed by using $3 - 10 \ \%$ diluted acid with Zn or Al powder at $323 - 363$ K to reduce the impurities for removal from $TiO(OH)_2$.

For the purification, another method related to solvent extraction of $TiOSO_4$ from the leach liquor generated in the crystallization process was also studied by BHP Billiton. The solvent extraction is carried out using a solvent such as trioctylphosphine oxide or butyl dibutylphosphonate and a modifier such as methyl isobutyl ketone, di-isobutyl ketone, or isotridecanol at 323 K. In addition, $TiOSO_4$ is extracted by reacting the mixture of $TiOSO_4$ and the solvent with H_2O.[97,98]

Finally, the calcination process using $TiO(OH)_2$ as a feed is conducted to produce titania pigment at $1073 - 1373$ K, depending on the production conditions such as the pigment type, as shown in Eq. 1-18.[27]

$$TiO(OH)_2 \ (s) = TiO_2 \ (s) + H_2O \ (g) \qquad\qquad (1\text{-}18)$$

In the sulfate process, the iron in the titanium ore is removed by digestion and crystallization, as mentioned above. It can be inferred that when low-grade titanium ore is used as the feedstock, a large amount of iron waste is produced, and a large amount of H_2SO_4 acid is required to remove the iron from the titanium ore. In addition, the generation of a large amount of iron waste increases the treatment or disposal cost for iron waste. As a result, the use of high-grade TiO_2 feed is preferred. Therefore, it is expected that an effective and inexpensive process for production of high-grade TiO_2 feed from low-grade titanium ore is also important for the sulfate process.

The level of technological difficulty of the sulfate process is not high, even though multiple steps are required for removing iron from titanium ore.[99] In addition, low-grade

titanium ore can be used as feedstock. Furthermore, the capital cost and energy consumption are low.[96,99] However, large amounts of $FeSO_4$ waste and acid waste solution are generated because a large amount of highly concentrated H_2SO_4 is used for removing iron from titanium ore.[96,99] In addition, productivity is low because the sulfate process is a batch-type process and does not use high-temperature reaction. Moreover, production of uniform titania pigment particles and control of the impurities related to the whiteness of the pigment are relatively more difficult than the chloride process.[74] Comparisons of the sulfate process and the chloride process are shown in Table 1-4.

1.3   Titanium mineral concentrates and their upgrading

1.3.1   Classification of titanium mineral concentrates

There are various types of titanium mineral concentrates, as shown in Table 1-5.[27,72,99-102] Table 1-5 lists the major titanium minerals, their chemical formulas, and the TiO_2 content in each mineral. Among these titanium minerals, only ilmenite (including leucoxene) and rutile are important titanium minerals from the viewpoint of mine production and mineral reserves (*see* Fig. 1-17). Therefore, only these two titanium minerals are used as feedstock for the titanium smelting process.

Ilmenite and rutile are geologically occurred in igneous and metamorphic rocks. [72,100] Over a long time, these titanium minerals are weathered and eroded and moved by fluvial transportation. Consequently, ilmenite and rutile are also found in the form of sedimentary deposits on costal shorelines. Therefore, titanium minerals can also be simply classified into rock-type deposits and sedimentary-type deposits by deposits types. Fig. 1-16 shows an example of the important titanium mineral mining sites in the world.[100,103] As shown in Fig. 1-16, many industrial titanium mineral mining sites are located near costal shorelines. Most representative titanium mineral mining sites for the sedimentary deposits are located in Australia, the USA, India, South Africa, and Sierra Leone. In addition, representative titanium mineral mining sites for rock-type deposits are located in the Canada and Norway.

1.3.2 Current status of the global production of titanium mineral concentrates

Fig. 1-17 (a) shows the global production of ilmenite and rutile, and Fig. 1-17 (b) shows the global reserves of ilmenite and rutile from 2002 to 2012.[104-114] As shown in Fig. 1-17 (a), the production of ilmenite was about nine times larger than that of rutile in 2012, and ilmenite production was about 90 % of the total titanium mineral production in 2012. In addition, the reserves of ilmenite were about fifteen times larger than those of rutile in 2012, and reserves of ilmenite were above 90 % of the total reserves of titanium minerals over these ten years. These results show that the ilmenite is a more important titanium mineral than rutile. In addition, it is expected that the ilmenite will still play an important role in the titanium smelting process in the near future, because the percentage of the reserves of ilmenite has slightly and gradually increased.

Fig. 1-18 shows the global production of titanium feedstock in 2011 by various companies reported by Iluka.[82] As shown in Fig. 1-18, 48 % of titanium feedstock in the world was produced by the top three companies: Iluka, Rio Tinto, and Tronox. Therefore, in this section, the mining processes and the upgrading processes for low-grade titanium ore are explained by mainly referring to the processes adopted by Iluka or Rio Tinto.

1.3.3 Processing of mineral sands for separation of valuable heavy minerals

The mined mineral sands are processed through multiple steps, as shown in Fig. 1-19, for obtaining valuable heavy minerals such as ilmenite, rutile, or zircon.[115,116] The mined mineral sands roughly consist of slimes/clay, valuable heavy minerals, non-valuable heavy minerals, and quartz. Among these components, valuable heavy minerals make up around 10 % of the sands.[115] The first step in the mineral sand processing is screening. After the oversized mineral sand particles are screened, slimes/clays are also removed from the mineral sands by hydrocyclones.

After the hydrocyclones process for removing slimes/clays, quartz is separated from the mineral sands by spiral separation. As a result, heavy minerals are obtained. Afterward, in some operations, ilmenite-rich concentrates are separated from the heavy minerals by wet high intensity magnets separation (WHIMS) before the heavy minerals

are sent to the mineral separation plant (MSP). The ilmenite-rich concentrates can be separated by WHIMS because the ilmenite is magnetic.

The first step in the MSP is magnetic separation using rare earth drum magnets to separate ilmenite from non-magnetic heavy minerals. After magnetic separation, rutile is separated from the remaining non-magnetic heavy minerals by electrostatic separation, because the rutile is conductive and non-magnetic. When the ilmenite is weathered severely, its magnetic property becomes weak in some cases. As a result, there is a possibility that small amount of ilmenite is mixed with the rutile. Therefore, magnetic separation is also conducted to separate the ilmenite from the rutile obtained. Afterward, zircon is separated from the non-magnetic and non-conductive heavy minerals by gravity, electrostatic, and magnetic separations.

As shown in Table 1-5, the ilmenite, which is the most important titanium ore, consists of approximately 50 % titanium oxides and 50 % iron oxides. In addition, this low-grade titanium ore cannot be used as a feedstock for the chloride process or the Kroll process, as mentioned in section 1.1.4 and 1.2.3. As a result, upgrading low-grade titanium ore is required before it can be used as a feedstock for the chloride or Kroll process. In other words, removal of iron from the ilmenite is necessary after the mineral sands processing. Currently, the Becher process, the Benilite process, or the slag and UGS processes are used for upgrading low-grade titanium ore in industry.

1.3.4   Titanium ore upgrading process 1: Becher process

The Becher process was developed by the Western Australian Government Chemical Laboratories in 1960s. Fig. 1-20 shows the flowchart of the Becher process for upgrading low-grade titanium ore.[72,117-121] The important stages of the Becher process are carbothermic reduction of the feed and aeration leaching before the acid leaching process.

The first step of the Becher process is the carbothermic reduction of low-grade ilmenite. The carbothermic reduction of low-grade ilmenite is conducted in the presence of a mixture of coal and char at 1373 – 1423 K for approximately 12 hours.[122] As a result, almost all iron oxides in the low-grade ilmenite are transformed to iron metal, as shown in Eq. 1-19. Afterward, the reduced ilmenite is separated from the non-magnetic materials

and char by the screen and magnetic separator, because the reduced ilmenite has strong magnetic property owing to the presence of iron metal.

$$FeO \cdot TiO_2 \ (s) + C \ (s) = Fe \cdot TiO_2 \ (s) + CO \ (g) \tag{1-19}$$
$$\Delta H°_r = 155 \text{ kJ}, \ \Delta G°_r = -53 \text{ kJ at } 1400 \text{ K}^{[30]}$$
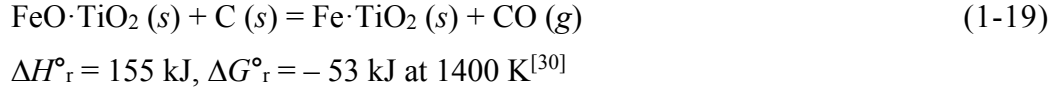
For the removal of iron from the reduced ilmenite, an aeration leaching step is conducted after the carbothermic reduction. The basic concept of the aeration leaching step is the removal of iron from the reduced ilmenite by oxidation of iron using air in water, as shown in Eqs. 1-20 and 1-21.

$$Fe \ (ore) = Fe^{2+} \ (in \ solution) + 2 \ e^- \tag{1-20}$$
$$O_2 \ (g) + 2 \ H_2O \ (l) + 4 \ e^- = 4 \ OH^- \tag{1-21}$$
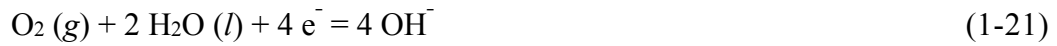
When the ferrous ion exists at high pH, iron hydroxide ($Fe(OH)_2$) is produced. This production of $Fe(OH)_2$ decreases the removal rate of iron from the reduced ilmenite, because $Fe(OH)_2$ precipitates in the pores of the reduced ilmenite particles. This phenomenon is called in-situ rusting. To prevent this phenomenon, ammonium chloride (NH_4Cl) is also used in the aeration leaching step. When the NH_4Cl is used, a high local pH near the reduced ilmenite particles can be prevented because NH_4Cl acts as a buffer for the hydroxyl ions by the reaction shown in Eq. 1-22. In addition, as shown in Eq. 1-23, the reaction between the NH_3 produced by Eq. 1-22 and iron ions moves the iron away from the reduced ilmenite particles without precipitation. Furthermore, passive films that might be formed in the aeration leaching step are removed by the chloride ions of NH_4Cl. In summary, NH_4Cl accelerates rusting in the aeration leaching step. The complex ions produced by Eq. 1-23 are precipitated as iron oxides by dissociation, oxidation, and hydrolysis in the solution. This aeration leaching is conducted by using 0.1 M NH_4Cl at 338 – 348 K for 12 – 18 hours.

$$NH^{4+} + OH^- = NH_3 \ (aq.,g) + H_2O \ (l) \tag{1-22}$$
$$[Fe(H_2O)_6]^{2+} + x \ NH_3 \ (aq.,g) = [Fe(NH_3)_x \ (H_2O)_{6-x}]^{2+} + x \ H_2O \ (l) \tag{1-23}$$
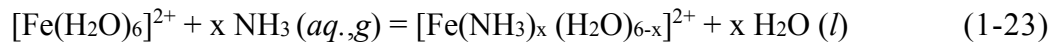
After the aeration leaching step, acid leaching using H_2SO_4 or HCl is conducted to remove residual iron in the upgraded TiO_2 produced. Afterward, high-grade TiO_2 feed with a purity of 90 – 93 % TiO_2 is produced.[44,72,117-121]

The Becher process can use various types of ilmenite as feedstock.[72,99,117-121] In addition, aeration leaching is the most cost-effective method for removal of iron from low-grade ilmenite, because it is not based on acid leaching which consumes chemicals. However, for the production of high-grade TiO_2 feed, multiple steps are required. Furthermore, the energy consumption is relatively high, because iron oxides must be reduced to metallic iron in the carbothermic reduction. Moreover, removal of residual iron and other impurities by acid leaching is still necessary, because the upgraded TiO_2 produced by aeration leaching is insufficient in terms of its impurity content. Finally, the iron removed from the low-grade ilmenite is dumped as waste.

1.3.5 Titanium ore upgrading process 2: Benilite process

Fig. 1-21 shows the flowchart of the Benilite process for upgrading low-grade titanium ore.[123-125] As shown in Fig. 1-21, the first step is the carbothermic reduction of ilmenite in the presence of coal, coke, or fuel oil to convert almost all iron oxides to FeO, as shown in Eq. 1-24. This carbothermic reduction is conducted at 973 – 1473 K.

$$Fe_2O_3 \text{ } (s) + TiO_2 \text{ } (s) + C \text{ } (s) = 2 \text{ } FeO \text{ } (s) + TiO_2 \text{ } (s) + CO \text{ } (g) \qquad (1\text{-}24)$$
$$\Delta H°_r = 155 \text{ kJ}, \Delta G°_r = -74 \text{ kJ at } 1100 \text{ K}^{[30]}$$
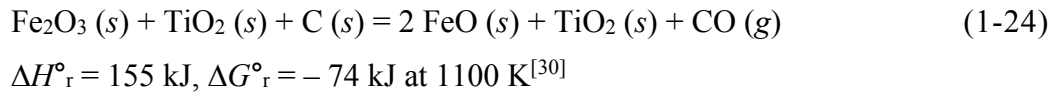
After the carbothermic reduction, the partially reduced ilmenite containing FeO reacts with 18 – 20 % HCl at 373 – 423 K for 6 – 14 hours, as shown in Eq. 1-25. The concentrated HCl leaching reaction removes iron from the low-grade titanium ore as iron chlorides, and upgraded TiO_2 is produced. Afterward, the upgraded TiO_2 is washed with water. Then, the upgraded TiO_2 is calcined at 973 – 1473 K to remove the water. Consequently, high-grade TiO_2 with a purity of above 95 % TiO_2 is produced.

$$FeO \cdot TiO_2 \text{ } (s) + 2 \text{ } HCl \text{ } (l) = FeCl_2 \text{ } (aq.) + TiO_2 \text{ } (s) + H_2O \text{ } (l) \qquad (1\text{-}25)$$
$$\Delta H°_r = -127 \text{ kJ}, \Delta G°_r = -76 \text{ kJ at } 400 \text{ K}^{[30]}$$
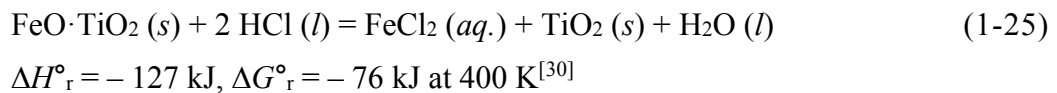
In order to recover HCl from the acid waste solution generated in the acid leaching process, a regeneration process is conducted. This regeneration of the spent acid solution is carried out by spraying the spent acid solution to react with air. As a result, iron chlorides in the acid waste solution are transformed to iron oxides, and HCl is regenerated by the pyrohydrolysis reaction. Afterward, the regenerated HCl is diluted with the spent solution generated by washing step or with fresh water to produce 18 – 20 % HCl, which is recycled as a chlorinating agent for the acid leaching process.

The Benilite process is relatively simpler than other hydrometallurgical titanium ore upgrading processes.[72,99,123-125] In addition, it is suitable for the removal of impurities in the low-grade ilmenite owing to the use of the concentrated HCl as a chlorinating agent. However, highly concentrated HCl is required, and a large amount of acid waste solution is dumped out even though regeneration process is implemented to recover the HCl. Furthermore, iron is dumped out as waste.

1.3.6   Titanium ore upgrading process 3: Slag and UGS processes

The one of the major titanium ore upgrading processes used in the current industry are the slag and UGS processes. Fig. 1-22 shows the flowchart of the slag and UGS processes for upgrading low-grade titanium ore.[72,126-128] The main steps of the slag and UGS processes to produce high-grade TiO_2 are a reduction process and an acid leaching process. The reduction step of the slag process in Fig. 1-22 uses high-temperature reactions for the removal of the iron from low-grade titanium ore as pig iron (Fe-C alloy). When the titanium ore reacts with the carbon powder reductant at 1923 – 1973 K in an electric furnace, the iron in the titanium ore is reduced and removed separately as liquid Fe-C alloy (pig iron) by the reaction shown in Eq. 1-26. However, the purity of the titanium oxide obtained is not high enough, because the titania slag still contains FeO as an impurity. As a result, the purity of TiO_2 in titania slag is generally 75 – 86 %. Therefore, the UGS process using concentrated HCl is conducted to upgrade titania slag into high-grade TiO_2 feed.
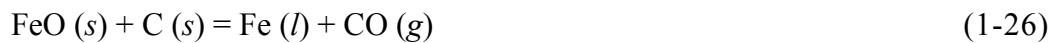
$$FeO\ (s) + C\ (s) = Fe\ (l) + CO\ (g) \qquad\qquad (1\text{-}26)$$
$$\Delta H^{\circ}_r = 162\ kJ,\ \Delta G^{\circ}_r = -145\ kJ\ at\ 1973\ K^{[129]}$$

Before the acid leaching is conducted, oxidation and reduction of the produced titania slag are carried out. The oxidation of the titania slag is conducted at 1273 – 1298 K to oxidize all low-valence titanium oxides as TiO_2 in order to prevent the loss of titanium during the acid leaching process. In addition, the reduction of titania slag is conducted at 1073 – 1123 K under a mixture of CO and H_2 gases in order to reduce the Fe_2O_3 produced during the oxidization process to synthesize FeO, which increases the reaction rate during the acid leaching process.

After the oxidation and reduction of the titania slag, an acid leaching process using 18 – 20 % HCl is conducted at 418 – 428 K to remove iron in the titania slag as iron chlorides. Afterward, the upgraded TiO_2 produced by the acid leaching process is washed, dried, and calcined at 873 – 1073 K to produce high-grade TiO_2 feed with a purity of about 95 % TiO_2. In addition, regeneration of the acid waste solution produced by the acid leaching process is conducted. The principle of the regeneration of HCl in the UGS process is identical to that in the Benilite process. The regenerated HCl is recycled and is reused as a chlorinating agent for the acid leaching process, along with fresh HCl.

The main advantage of the slag process is that the iron in the low-grade titanium ore is removed as pig iron and not wasted.[72,99,126,128] In addition, the slag process is a large-scale and high-speed process, because the operation temperature of the carbothermic reduction is high, at 1923 – 1973 K. However, low-purity TiO_2 feed is produced by the slag process. In addition, the slag process consumes a high amount of energy owing to the high reaction temperature. Furthermore, to obtain high-grade TiO_2 feed, an additional process, the UGS process, is required. In the UGS process, highly concentrated HCl is used for removing iron from titania slag. As a result, a large amount of acid waste solution is generated even though a regeneration process of the spent acid is implemented for the spent acid. Finally, multiple steps are required for the production of high-grade TiO_2 feed in the slag and UGS processes.

The advantages and disadvantages of the current titanium ore upgrading processes used in industry are summarized in Table 1-6. As shown in Table 1-6, various problems exist in the current titanium ore upgrading processes. To overcome these disadvantages, several studies were conducted in the past.

1.4   Flowchart of titanium processing: from ore to metal and pigment

Before the studies conducted in the past are introduced in the next section, the current titanium ore upgrading processes explained so far are summarized in Fig. 1-23. Fig. 1-23 shows the current flowchart of titanium processing from titanium ore to titanium metal and titania pigment.

As shown in Fig. 1-23, even though ilmenite and rutile are used as feedstocks in the titanium smelting industry, ilmenite is far more important than rutile, because production of ilmenite is much higher than that of rutile. In addition, among the two types of ilmenite, i.e., rock-type and sand-type ores, sand-type ilmenite dominates the production. These results show that any titanium ore upgrading process that will be developed in the future must be able to use sand-type ilmenite as a feedstock.

Low-grade titanium ore is necessary to be upgraded before use as a feedstock for the sulfate, chloride, and Kroll processes. There are four major processes for upgrading ilmenite: the slag, UGS, Becher, and Benilite processes. Among these processes, the slag process is the only process that uses a pyrometallurgical method and is suitable for removing iron directly from ilmenite. All the other processes use hydrometallurgical method. In addition, these processes use concentrated acid for removal of the iron in ilmenite to produce high-grade TiO_2 feed. Therefore, when these processes are used, the generation of a large amount of acid waste solution containing heavy metals is inevitable. Moreover, unfortunately, there is no effective method to recover the chlorine.

In this thesis, a novel titanium ore upgrading process using a pyrometallurgical method is investigated. This is because when a pyrometallurgical method is used, the reaction rate is high and the generation of a large amount of acid waste solution is avoidable. This leads to an environmentally friendly process. In addition, an effective method for recovering the chlorine can be developed, because it is a dry process.

1.5   New titanium ore upgrading process: selective chlorination

The chlorination method used in the chloride process or the Kroll process simultaneously chlorinates both the titanium oxides and iron oxides in a low-grade titanium ore. However, the selective chlorination method chlorinates only iron oxides in

a low-grade titanium ore as volatile iron chlorides by using chlorinating agent such as HCl or metal chloride at high temperatures for the production of high-grade TiO_2 feed. Fig. 1-24 shows a schematic of the concept of selective chlorination.

As shown in Fig. 1-24, iron in the low-grade titanium ore is removed as iron chlorides in the selective chlorination method, whereas iron is removed as pig iron in the slag process. As a result, an effective method to recover the iron and chlorine from the iron chloride waste is required when the selective chlorination method is used. Meanwhile, the reaction temperature of the selective chlorination is not higher than that of the slag process, because the iron in the low-grade titanium ore is chlorinated as iron chlorides and not as pig iron. Thus, the use of a selective chlorination method is favorable for reducing energy consumption.

Table 1-7 lists the selective chlorination processes using pyrometallurgical method developed in the past.[32,130-143] As shown Table 1-7, many studies conducted in the past used Cl_2 gas as a chlorinating agent for the selective removal of iron form low-grade titanium ore. In addition, recently, the use of metal chlorides such as $CaCl_2$ or $MgCl_2$ has been suggested for selective chlorination of low-grade titanium ore. Accordingly, selective chlorination methods studied in the past can be roughly classified into two groups: selective chlorination using Cl_2 gas or selective chlorination using metal chlorides.

1.5.1   Selective chlorination using chlorine gas

The majority of the studies related to the selective chlorination of low-grade titanium ore used Cl_2 gas as a chlorinating agent, as shown in Table 1-7. Most of the studies carried out in the past were conducted under a CO atmosphere or in the presence of carbon to control the oxygen chemical potential in the reaction system.

When the selective chlorination was conducted under a mixture of Cl_2 and CO gases, the reactions shown in Eqs. 1-27 and 1-28 were suggested as total reactions by Doraiswamy[130] and Rhee.[140] In addition, Lakshmanan[132] mentioned the generation of $FeCl_3$ after the selective chlorination of low-grade titanium ore. After selective chlorination, high-grade TiO_2 feeds were produced from low-grade titanium ore, as shown in Table 1-7.

$$FeO \cdot TiO_2 \ (s) + CO \ (g) + 3/2 \ Cl_2 \ (g) = FeCl_3 \ (g) + TiO_2 \ (s) + CO_2 \ (g) \qquad (1\text{-}27)$$

$$Fe_2O_3 \ (s) + 3 \ CO \ (g) + 3 \ Cl_2 \ (g) = 2 \ FeCl_3 \ (g) + 3 \ CO_2 \ (g) \qquad (1\text{-}28)$$
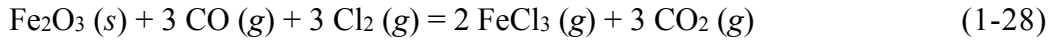
Fukushima[135] and Fuwa[137] developed the selective chlorination of low-grade titanium ore using Cl_2 gas in the presence of carbon as a part of the Mitsubishi process. One feature of the Mitsubishi process is that a roasted titanium ore is used as a feedstock for the selective chlorination. Fukushima mentioned that the use of the roasted ilmenite as a feedstock can prevent the clogging of pipes in a chlorinator, because the iron in the titanium ore is removed as $FeCl_3$ and not $FeCl_2$. They suggested the following chlorination reaction in a chlorinator:

$$Fe_2O_3 \cdot TiO_2 \ (s) + 3/2 \ C \ (s) + 3 \ Cl_2 \ (g)$$
$$= 2 \ FeCl_3 \ (g) + TiO_2 \ (s) + 3/2 \ CO_2 \ (g) \qquad (1\text{-}29)$$
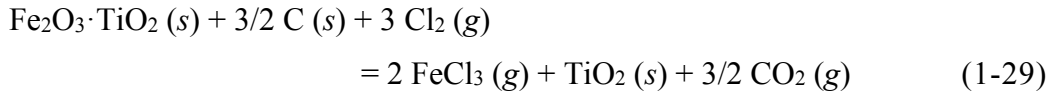
Neurgaonkar[138] reported that 94 % TiO_2 feed was obtained when the selective chlorination of low-grade titanium ore was conducted under a mixture of Cl_2 and O_2 gases in the presence of carbon. Neurgaonkar explained that oxygen suppressed the chlorination of TiO_2 more than that of Fe_2O_3 at 1273 K. In addition, Deventer[139] and Rhee[141] also reported that high-grade TiO_2 feed was obtained from low-grade titanium ore when the selective chlorination was conducted using Cl_2 gas in the presence of carbon.

In 1994, selective chlorination process using Cl_2 under reducing atmosphere was reported by Ichimura, Ishihara Sangyo Kaisha, LTD.[142] Most studies in the past used C or CO gas as a reducing agent. However, Ichimura developed the selective chlorination using Cl_2 in the presence of TiO_x $(0 < x < 2)$. In this process, the oxygen chemical potential (p_{O_2}) in the reaction system is controlled by TiO_x $(0 < x < 2)$. When this selective chlorination was conducted using titania slag as a feedstock, 93 % TiO_2 was produced.

In addition, Athavale[133] developed a selective chlorination of low-grade titanium ore using highly concentrated HCl as a chlorinating agent. In Athavale's experiment, 98 % HCl produced by the reaction between Cl_2 gas and H_2 gas was used to remove iron from the ore, as shown in Eq. 1-30. As a result, 90 % of the iron oxide in the titanium ore was removed, and high-grade TiO_2 feed was produced.

$$Fe_2O_3 \cdot TiO_2 \ (s) + 6 \ HCl \ (g) = 2 \ FeCl_3 \ (g) + TiO_2 \ (s) + 3 \ H_2O \ (g) \qquad (1\text{-}30)$$
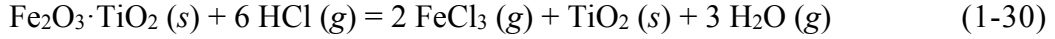
As shown in the above discussion, many studies in the past used Cl_2 gas as a chlorinating agent. However, when Cl_2 gas is used, installation of the reactor becomes costly, and environmental issues arise for operation.

1.5.2 Selective chlorination using metal chloride

To mitigate the disadvantages of the selective chlorination using Cl_2 gas, selective chlorination using a metal chloride was proposed. In 1972, Othmer[134,136] suggested the use of $TiCl_4$ as a chlorinating agent for the selective chlorination of low-grade titanium ore, as shown in Eqs. 1-31 and 1-32. When the selective chlorination is conducted under reducing and oxidative atmospheres, the reactions in Eq. 1-31 and Eq. 1-32 proceed, respectively. However, the actual experimental results were not provided. In addition, thermodynamic analysis of the selective chlorination considering chemical potentials of chlorine and oxygen was not carried out.

$$2 \ FeO \ (s) + TiCl_4 \ (g) = 2 \ FeCl_2 \ (l, g) + TiO_2 \ (s) \qquad (1\text{-}31)$$
$$2 \ Fe_2O_3 \ (s) + 3 \ TiCl_4 \ (g) = 4 \ FeCl_3 \ (g) + 3 \ TiO_2 \ (s) \qquad (1\text{-}32)$$
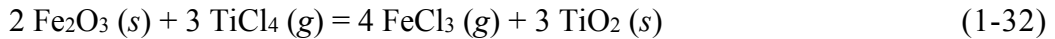
Selective chlorination processes using $MgCl_2$ and $CaCl_2$ were proposed by Matsuoka[143] and Zheng,[32] respectively. Matsuoka suggested that when the selective chlorination of low-grade titanium ore was conducted using $MgCl_2$, iron in the ore was removed by the reaction shown in Eq. 1-33. In addition, Zheng suggested that when the selective chlorination of low-grade titanium ore was conducted using $CaCl_2$ in the presence of H_2O, iron was removed from the ore by the reactions shown in Eqs. 1-34 or 1-35 and 1-36. However, in both studies, an insufficient amount of iron was removed from the ore. For example, Zheng reported that the concentration of iron in the ore decreased from 51.3 % to 16.7 % when the selective chlorination was carried out at 1293 K for 12 hours (*see* Table 1-7). In addition, the other disadvantage is that $CaTiO_3$ was obtained as a product of the selective chlorination. The iron free $CaTiO_3$ can be used as a feedstock for the production of titanium metal when the FFC or OS process is used, as

mentioned in section 1.1.5. However, the development of these processes is still in the stage of fundamental study, and they are not used in industrial operation. Furthermore, TiO_2 feed containing alkali earth metals cannot be used as a feedstock for the Kroll process, which is the current titanium metal production process.

$$FeO\ (s) + MgCl_2\ (g) = FeCl_2\ (l, g) + MgO\ (s) \tag{1-33}$$

$$FeO{\cdot}TiO_2\ (s) + CaCl_2\ (l) = FeCl_2\ (l, g) + CaTiO_3\ (s) \tag{1-34}$$
or
$$CaCl_2\ (l) + H_2O\ (g) + TiO_2\ (s) = 2\ HCl\ (g) + CaTiO_3\ (s) \tag{1-35}$$
$$FeO\ (s) + 2\ HCl\ (g) = FeCl_2\ (l, g) + H_2O\ (g) \tag{1-36}$$
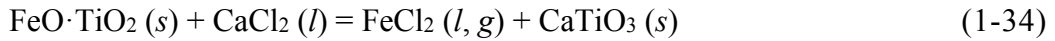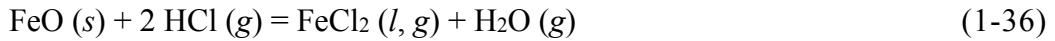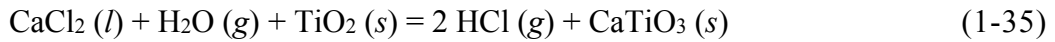
1.6   Objective of thesis

In the current titanium smelting industry, the use of high-grade TiO_2 feed for the production of titanium metal or titania pigment is indispensable, as explained in sections 1.1 to 1.4. This is because when low-grade titanium ore is used as a feedstock for the chloride process or the Kroll process, operating problems such as clogging of pipes in the chlorinator and increase of chlorine loss occur owing to the generation of a large amount of chloride waste. In addition, damage to the refractory materials inside the chlorinator occurs because of condensation of alkaline metals or alkaline earth metals such as $CaCl_2$.

However, as explained in section 1.3, the current titanium ore upgrading processes used in industry have several problems. For example, a large amount of acid waste solution containing heavy metals is generated when concentrated acid is used for the removal of iron from low-grade titanium ore. The treatment or disposal of this large amount of acid waste solution is costly and is a major issue in some countries with strict environmental regulations. In addition, it is difficult to recover chlorine from the iron chloride waste when acid leaching is used because the iron is not removed in a dry form.

Even though new titanium ore upgrading processes such as selective chlorination have been suggested, many of these processes have disadvantages such as the use of Cl_2 gas as a chlorinating agent. In addition, when selective chlorination using metal chlorides

such as CaCl$_2$ is considered, iron was not completely removed from low-grade titanium ore.

In order to overcome the disadvantages of the current and developed titanium ore upgrading processes, in this thesis, selective chlorination using CaCl$_2$, MgCl$_2$, or TiCl$_4$ as a chlorine source was investigated for the production of high-grade TiO$_2$ feed. Fig. 1-25 shows the flowchart of the novel selective chlorination process using CaCl$_2$ or MgCl$_2$ for upgrading low-grade titanium ore and the Kroll process from the viewpoint of circulation of chlorine gas and chloride waste. The detailed flowcharts for the selective chlorination are introduced in chapters 3 − 8. In addition, Fig. 1-26 shows the flowchart of the novel environmentally friendly selective chlorination process using TiCl$_4$ for upgrading low-grade titanium ore and titania slag from the viewpoint of circulation of chloride waste, in addition to the flowchart of the Kroll process.

The selective chlorination processes developed in this thesis have the following advantages in common. (i) A high-grade TiO$_2$ feed can be obtained directly from low-grade titanium ore in a single step. (ii) A highly concentrated acid or Cl$_2$ gas is not used. (iii) Various types of low-grade titanium ore can be used as starting materials. In addition, the selective chlorination using TiCl$_4$ has the following advantages. (iv) Recovery of chlorine is possible, because the chloride wastes such as FeCl$_x$ (x = 2,3) produced by the reaction are generated in a dry form. (v) Finally, the TiCl$_4$ used as a chlorinating agent is easy to obtain, because a large amount of TiCl$_4$ is circulated in the current titanium metal production process, the Kroll process.

1.7 Thesis outline

In chapter 1, the current status of titanium metal, titania pigment, titanium mineral concentrates and upgraded TiO$_2$ feed is briefly introduced. In addition, the industrial processes used for the production of these materials are explained, along with titanium ore upgrading processes developed in the past, in order to illustrate the importance of developing an environmentally friendly and effective titanium ore upgrading process.

In chapter 2, thermodynamic consideration is carried out for the removal of iron from low-grade titanium ore through selective chlorination. In this chapter, thermodynamic study of the chlorination reactions of metal or metal oxides at elevated

temperatures is conducted. Subsequently, various chlorination reactions are analyzed by utilizing chemical potential diagrams, and the usefulness of this thermodynamic study for analyzing the selective chlorination of titanium ore are addressed. In addition, chlorination reactions using various types of chlorinating agents are discussed from different viewpoints.

In chapter 3, the selective chlorination of low-grade titanium ore at 1100 K using $CaCl_2$ as the chlorine source at 1100 K is investigated to determine its feasibility for the direct production of high-grade TiO_2 feed. Thermodynamic analysis of the potential region for selective chlorination using $CaCl_2$ is conducted utilizing the chemical potential diagrams for the Fe-O-Cl and Ti-O-Cl systems. Verification of the selective chlorination is conducted and the influence of particle size, type of titanium ore, reaction atmosphere, and CaO activity on the selective chlorination is investigated.

In chapter 4, a fundamental study is conducted into the selective chlorination of low-grade titanium ore at 1240 K using $CaCl_2$ as the chlorine source to produce a high-grade $CaTiO_3$ feed directly, with a view to its potential for scale-up. The potential region for selective removal of iron from titanium ore by $CaCl_2$ is determined by considering the chemical potentials of chlorine and oxygen. The feasibility of selective chlorination process is verified, and the influence of reaction temperature, reaction time, particle size, and type of titanium ore, and weight of titanium ore on the amount of iron removed from the titanium ore is investigated.

In chapter 5, a process for the selective chlorination of low-grade titanium at 1000 K using $MgCl_2$ as a chlorine source at 1000 K is developed in order to produce high-grade TiO_2 feed directly. Thermodynamic analysis of the appropriate potential region for selective chlorination is conducted by utilizing the combined chemical potential diagram for the Fe-O-Cl and Ti-O-Cl systems. From experimental data, the mechanism for selective chlorination is verified, and the influence of the reaction system atmosphere, particle size, and titanium ore type on selective chlorination is studied.

In chapter 6, in order to produce high-grade TiO_2 feed directly, a fundamental study on the selective chlorination of low-grade titanium ore at 1100 K using $TiCl_4$ as a chlorinating agent under low p_{O_2} is carried out. The potential region for the selective removal of iron from titanium ore by $TiCl_4$ under low p_{O_2} is thermodynamically analyzed by considering the chemical potentials of chlorine and oxygen. This analyzed potential

region is examined by experimental results. Furthermore, in the experiments, the influence of the type and particle size of the titanium ore and the atmosphere of the reaction system on the amount of iron removed from the titanium ore is investigated. This confirms the feasibility of developing an environmentally friendly method for upgrading titanium ore.

In chapter 7, the selective removal of iron from low-grade titanium ore at 1200 K by $TiCl_4$ under high p_{O_2} is studied for the direct production of high-grade TiO_2 feed. Through thermodynamic study, the potential region for selective chlorination using $TiCl_4$ under high p_{O_2} is determined and the differences of the potential regions depending on the oxygen chemical potential are analyzed. This potential region for selective chlorination using $TiCl_4$ under high p_{O_2} is experimentally verified. In the experiments, the influence of the reaction temperature, particle size and type of titanium ore, and reaction system atmosphere on the selective chlorination of titanium ore is investigated.

In chapter 8, a fundamental investigation on the selective chlorination of titania slag using $TiCl_4$ at 1100 K is carried out in order to produce a high-grade TiO_2 feed directly. In the experiments, four types of titania slags prepared in advance under identical conditions at each stage of the UGS process are used as the feedstocks. The experimental results identify the possibility of using the developed selective chlorination with $TiCl_4$ in place of the current UGS process, especially when environmental issues are taken into consideration.

In chapter 9, a novel and environmentally friendly process that does not discharge waste solution or chloride waste for the upgrading of titanium ore is proposed. At first, the current flowchart for titanium and the major upgrading processes are reviewed, and the relative advantages and disadvantages of each are discussed. Thereafter, a selective chlorination process using metal chloride and the recovery of chlorine from chloride waste are discussed in addition to the Kroll process for establishing the environmentally sound titanium smelting process from titanium ore to titanium metal.

In chapter 10, the objectives and importance of this thesis, the findings in each chapter, and the contribution that this thesis makes to the future development of titanium smelting processes are described.

References

[1]   E. Bardal: "*Corrosion and protection*", Springer-Verlag, London, United Kingdom, 2004.

[2]   J.R. Davis: "*Metals handbook - desk edition*", 2nd ed., ASM international, Materials Park, OH, United States of America, 1998.

[3]   M.J. Donachie, Jr.: "*Titanium: A Technical Guide*", ASM international, Materials Park, OH, United States of America, 1988.

[4]   National Association of Corrosion Engineers: "*NACE Basic Corrosion Course*", 11th ed., National Association of Corrosion Engineers, Houston, Texas, United States of America, 1980.

[5]   J.R. Davis: "*Metals Handbook - Properties and Selection: Nonferrous Alloys and Special-Purpose Materials*", 10th ed., vol. 2, ASM international, Materials Park, OH, United States of America, 1990.

[6]   F.W Clarke and H.S. Washington: "*The average chemical composition of igneous rocks*", Proceedings of the National Academy of Sciences of the United States of America, 1922, vol. 8, pp. 108-115.

[7]   J. Gambogi: "*Mineral Commodity Summaries: Titanium and Titanium Dioxide*", U.S. Geological Survey, Washington DC, January, 2004, pp. 178-179.

[8]   J. Gambogi: "*Mineral Commodity Summaries: Titanium and Titanium Dioxide*", U.S. Geological Survey, Washington DC, January, 2005, pp. 178-179.

[9]   J. Gambogi: "*Mineral Commodity Summaries: Titanium and Titanium Dioxide*", U.S. Geological Survey, Washington DC, January, 2006, pp. 180-181.

[10]   J. Gambogi: "*Mineral Commodity Summaries: Titanium and Titanium Dioxide*", U.S. Geological Survey, Washington DC, January, 2007, pp. 176-177.

[11]   J. Gambogi: "*Mineral Commodity Summaries: Titanium and Titanium Dioxide*", U.S. Geological Survey, Washington DC, January, 2008, pp. 180-181.

[12]   J. Gambogi: "*Mineral Commodity Summaries: Titanium and Titanium Dioxide*", U.S. Geological Survey, Washington DC, January, 2009, pp. 176-177.

[13]   J. Gambogi: "*Mineral Commodity Summaries: Titanium and Titanium Dioxide*", U.S. Geological Survey, Washington DC, January, 2010, pp. 174-175.

[14]   J. Gambogi: "*Mineral Commodity Summaries: Titanium and Titanium Dioxide*", U.S. Geological Survey, Washington DC, January, 2011, pp. 172-173.

[15]   J. Gambogi: "*Mineral Commodity Summaries: Titanium and Titanium Dioxide*", U.S. Geological Survey, Washington DC, January, 2012, pp. 172-173.

[16] K. Nikami: "*Wishing for the Development of the Titanium Industry (Part 2) A View of the Standing Position of Titanium Metal in the Near Future based on the Ten-Years Activity of Rare Metal Workshop*", Titanium Japan, 2013, vol. 61 (1), pp. 35-40. (in Japanese)

[17] R.R. Boyer: "*An overview on the use of titanium in the aerospace industry*", Materials Science and Engineering: A, 1996, vol. 213 (1), pp. 103-114.

[18] G.M. Bedinger: "*Mineral Commodity Summaries: Titanium and Titanium Dioxide*", U.S. Geological Survey, Washington DC, January, 2013, pp. 172-173.

[19] G.M. Bedinger: "*Mineral Commodity Summaries: Titanium and Titanium Dioxide*", U.S. Geological Survey, Washington DC, February, 2014, pp. 170-171.

[20] N. Kemori: "*Nickel Industry: Past, Present, and Future*", The 60th Rare Metal Workshop, The University of Tokyo, Tokyo, Japan, 2014, pp. 1-30. (in Japanese)

[21] M.D. Fenton: "*Mineral Commodity Summaries: Iron and Steel*", U.S. Geological Survey, Washington DC, February, 2014, pp. 78-79.

[22] E.L. Bray: "*Mineral Commodity Summaries: Aluminum*", U.S. Geological Survey, Washington DC, February, 2014. pp. 16-17.

[23] T.H. Okabe and J. Kang: "*The Latest Technological Trend of Rare Metals*", CMC Publishing Co. LTD., Tokyo, 2012, Chap. 6-1, pp. 83-94. (in Japanese)

[24] K. Faller and F.H.S. Froes: "*The use of titanium in family automobiles: current trends*", JOM, 2001, vol. 53 (4), pp. 27-28.

[25] F.H. Froes, H. Friedrich, J. Kiese, and D. Bergoint: "*Titanium in the family automobile: the cost challenge*", JOM, 2004, vol. 56 (2), pp. 40-44.

[26] G. Adachi: "*Handbook of Rare Metal*", Maruzen Publishing Co., LTD, Tokyo, 2011. (in Japanese)

[27] F. Habashi: "*Handbook of Extractive Metallurgy*", vol. 2, VCH Verlagsgesellschaft mbH, Weinheim, Germany, 1997.

[28] M.A. Hunter: "*Metallic Titanium*", Journal of the American Chemical Society, 1910, vol. 32 (3), pp. 330-336.

[29] P.C. Turner, A.D. Hartman, J.S. Hansen, and S.J. Gerdemann: "*Low cost titanium-myth or reality*", EPD Congress 2001, 2001 TMS Annual Meeting, New Orleans, Louisiana, USA, 2001.

[30] I. Barin: "*Thermochemical Data of Pure Substances*", 3rd ed., VCH Verlagsgesellschaft mbH, Weinheim, Germany, 1995.

[31]   R.P. Anderson, D.R. Armstrong, and S.S. Borys: "*Method of making metals and other elements from the halide vapor of the metal*", United States Patent 5958106, 1999.

[32]   H. Zheng: "*Development of a Novel Titanium Production Process Using Selective Chlorination*", Doctoral Thesis, The University of Tokyo, 2007.

[33]   R.P. Anderson, D.R. Armstrong, and S.S. Borys: "*Method of making metals and other elements*", United States Patent 5779761, 1998.

[34]   R.P. Anderson, D.R. Armstrong, and L.E. Jacobsen: "*Method and apparatus for controlling the size of powder produced by the Armstrong process*", United States Patent 7351272 B2, 2008.

[35]   M. Jackson and K. Dring: "*A review of advances in processing and metallurgy of titanium alloys*", Materials Science and Technology, 2006, vol. 22 (8), pp. 881-887.

[36]   EHKTechnologies: "*Summary of emerging titanium cost reduction technologies*", U.S. Department of Energy and Oak Ridge National Laboratory, January, 2004.

[37]   A.E. van. Arkel, and J.H. de Boer: "*Process of precipitating metals on an incandescent body*", United States Patent 1671213, 1928.

[38]   B. Lustman and F. Kerze: "*Chapter 5: Iodie-decomposition process for production of zirconium*", The metallurgy of zirconium, McGraw-Hill New York, United States of America, 1955.

[39]   A.C. Loonam: "*Principles and Applications of the Iodide Process*", Journal of The Electrochemical Society, 1959, vol. 106 (3), pp. 238-244.

[40]   W. Kroll: "*The production of ductile titanium*", Transactions of the Electrochemical Society, 1940, vol. 78 (1), pp. 35-47.

[41]   W. Kroll: "*Method for manufacturing titanium and alloys thereof*", United States Patent 2205854, 1940.

[42]   S. Kogi: "*Process for Production of Titanium Sponge*", Journal of the Mining and Metallurgical Institute of Japan, 1981, vol. 97 (1122), pp. 854-860. (in Japanese)

[43]   N. Nakamura: "*Current state of titanium sponge production technology*", Molten Salts, 2013, vol. 56 (3), pp. 121-124. (in Japanese)

[44]   T. Tomonari: "*Titanium Industry-Its Growing Steps and Future Possibilities*", The Japan Titanium Society, Tokyo, Japan, 2001. (in Japanese)

[45]   A. Yajima, R. Matsuzaki, and Y. Saeki: "*Reaction between vanadium trichloride oxide and hydrogen sulfide*", Bulletin of the Chemical Society of Japan, 1978, vol. 51 (4), pp. 1098-1100.

[46]   F. Cardarelli: "*Materials handbook: a concise desktop reference*", 2nd ed., Springer-Verlag, London, United Kingdom, 2008.

[47]   T. Wako: "*Industrial Wastewater Management in Japan*", Conference of WEPA Dialogue in Sri Lanka, 2012.
         http://www.env.go.jp/en/focus/docs/files/20120801-51.pdf.

[48]   T.B. Massalski: "*Binary alloy phase diagrams*", 2nd ed., ASM international, Materials Park, OH, United States of America, 1990.

[49]   T. Fukuyama, M. Koizumi, M. Hanaki, and S. Kosemura: "*Production of Titanium Sponge and Ingot at Toho Titanium Co., Ltd*", Shigen-to-Sozai, 1993, vol. 109, pp. 1157-1163. (in Japanese)

[50]   A. Moriya and A. Kanai: "*Titanium Sponge Production at Sumitomo Sitix Corporation*", Shigen-to-Sozai, 1993, vol. 109, pp. 1164-1169. (in Japanese)

[51]   T.H. Okabe: "*Integration of Electricity and Technology: Titanium Metal Production Method*", The Journal of the Institute of Electrical Engineers of Japan, 2006, vol. 126 (12), pp. 801-805. (in Japanese)

[52]   O. Takeda: "*A Novel Titanium Production Process Using Subhalide*", Doctoral Thesis, The University of Tokyo, 2006. (in Japanese)

[53]   G.Z. Chen, D.J. Fray, and T.W. Farthing: "*Direct electrochemical reduction of titanium dioxide to titanium in molten calcium chloride*", Nature, 2000, vol. 407 (6802), pp. 361-364.

[54]   D.J. Fray: "*Emerging molten salt technologies for metals production*", JOM, 2001, vol. 53 (10), pp. 26-31.

[55]   G.Z. Chen, T.W. Farthing, and D.J. Fray: "*Removal of oxygen from metal oxides and solid solutions by electrolysis in a fused salt*", United States Patent 2004/0159559 A1, 2004.

[56]   K.S. Mohandas and D.J. Fray: "*FFC Cambridge process and removal of oxygen from metal-oxygen systems by molten salt electrolysis: an overview*", Trans. Indian Inst. Met., 2004, vol. 57 (6), pp. 579-592.

[57]   K. Ono and R.O. Suzuki: "*A new concept for producing Ti sponge: calciothermic reduction*", JOM, 2002, vol. 54 (2), pp. 59-61.

[58]   R.O. Suzuki and S. Inoue: "*Calciothermic reduction of titanium oxide in molten $CaCl_2$*", Metallurgical and Materials Transactions B, 2003, vol. 34B (3), pp.277-285.

[59] R.O. Suzuki, K. Ono, and K. Teranuma: "*Calciothermic reduction of titanium oxide and in-situ electrolysis in molten $CaCl_2$*", Metallurgical and Materials Transactions B, 2003, vol. 34B (3), pp. 287-295.

[60] R.O. Suzuki and S. Fukui: "*Reduction of TiO_2 in Molten $CaCl_2$ by Ca Deposited during CaO Electrolysis*", Materials Transactions, 2004, vol. 45 (5), pp. 1665-1671.

[61] R.O. Suzuki: "*Calciothermic reduction of TiO_2 and in situ electrolysis of CaO in the molten $CaCl_2$*", Journal of Physics and Chemistry of Solids, 2005, vol. 66 (2), pp. 461-465.

[62] R.O. Suzuki: "*Direct reduction processes for titanium oxide in molten salt*", JOM, 2007, vol. 59 (1), pp. 68-71.

[63] T.H. Okabe and Y. Waseda: "*Producing titanium through an electronically mediated reaction*", JOM, 1997. vol. 49 (6), pp. 28-32.

[64] T. Abiko, I. Park, and T.H. Okabe: "*Reduction of titanium oxide in molten salt medium*", 10th World Conference on Titanium, Hamburg, Germany, 2003.

[65] I. Park, T. Abiko, and T.H. Okabe: "*Production of titanium powder directly from TiO_2 in $CaCl_2$ through an electronically mediated reaction (EMR)*", Journal of Physics and Chemistry of Solids, 2005, vol. 66 (2) pp. 410-413.

[66] T.H. Okabe, T. Oda, and Y. Mitsuda: "*Titanium powder production by preform reduction process (PRP)*", Journal of Alloys and Compounds, 2004, vol. 364 (1), pp. 156-163.

[67] H. Zheng, H. Ito, and T.H. Okabe: "*Production of titanium powder by the calciothermic reduction of titanium concentrates or ore using the preform reduction process*", Materials Transactions, 2007, vol. 48 (8), pp. 2244-2251.

[68] O. Takeda and T.H. Okabe: "*High-speed titanium production by magnesiothermic reduction of titanium trichloride*", Materials Transactions, 2006, vol. 47 (4), pp. 1145-1154.

[69] O. Takeda and T.H. Okabe: "*Fundamental study on magnesiothermic reduction of titanium dichloride*", Metallurgical and Materials Transactions B, 2006, vol. 37 (5), pp. 823-830.

[70] O. Takeda and T.H. Okabe: "*Fundamental study on synthesis and enrichment of titanium subchloride*", Journal of Alloys and Compounds, 2008, vol. 457 (1), pp. 376-383.

[71] K. Jiang, X. Hu, M. Ma, D. Wang, G. Qiu, X. Jin, and G.Z. Chen: "*Perovskitization‐Assisted Electrochemical Reduction of Solid TiO_2 in Molten*

$CaCl_2$", Angewandte Chemie International Edition, 2006, vol. 45 (3), pp. 428-432.

[72]   J.E. Kogel, N.C. Trivedi, J.M. Barker, and S.T. Krukowski: "*Industrial minerals & rocks: commodities, markets, and uses*", 7th ed., Society for Mining, Metallurgy, and Exploration, Inc. (SME), Littleton, Colorado, United States of America, 2006.

[73]   G. Buxbaum: "*Industrial inorganic pigments*", 2nd ed., Wiley-VCH Verlag GmbH, Weinheim, Germany, 1998.

[74]   M. Matsunaga: "*Titanium Dioxide Pigment*", Journal of the Japan Society of Colour Material, 1981, vol. 54 (11), pp. 680-689. (in Japanese)

[75]   J. Gambogi: "*Mineral Commodity Summaries: Titanium and Titanium Dioxide*", U.S. Geological Survey, Washington DC, January, 2003, pp. 180-181.

[76]   J. Gambogi: "*Mineral Commodity Summaries: Titanium and Titanium Dioxide*", U.S. Geological Survey, Washington DC, January, 2002, pp. 178-179.

[77]   J. Gambogi: "*Mineral Commodity Summaries: Titanium and Titanium Dioxide*", U.S. Geological Survey, Washington DC, January, 2001, pp. 176-177.

[78]   J. Gambogi: "*Mineral Commodity Summaries: Titanium and Titanium Dioxide*", U.S. Geological Survey, Washington DC, January, 2000, pp. 180-181.

[79]   International Monetary Fund: "*World Economic Outlook-Recovery Strengthens*", Remains Uneven, International Monetary Fund, Washington, United States of America, 2014.

[80]   International Monetary Fund: "*World Economic Outlook-Transitions and Tensions*", International Monetary Fund, Washington, United States of America, 2013.

[81]   International Monetary Fund: "*World Economic Outlook-Globalization and Inflation*", International Monetary Fund, Washington, United States of America, 2006.

[82]   R. Porter: "*Mineral Sands Industry Fact Book*", Iluka, 2013.
http://www.iluka.com/docs/industry-company-information/mineralsands-industry-fact-book

[83]   G.M. Bedinger: "*Mineral Commodity Summaries: Titanium Mineral Concentrates*", U.S. Geological Survey, Washington DC, February, 2014, pp. 172-173.

[84]   G.M. Bedinger: "*2011 Minerals Yearbook-Titanium*", U.S. Geological Survey, Washington DC, 2013.

[85]   J. Gambogi: "*Mineral Commodity Summaries: Titanium Mineral Concentrates*", U.S. Geological Survey, Washington DC, January, 2010, pp. 172-173.

[86]   J. Gambogi: "*Mineral Commodity Summaries: Titanium Mineral Concentrates*", U.S. Geological Survey, Washington DC, January, 2007, pp. 174-175.

[87]   J. Gambogi: "*2007 Minerals Yearbook-Titanium*", U.S. Geological Survey, Washington DC, 2007.

[88]   D.S. Ensor: "*History of Manufacture of Fine Particles in High-Temperature Aerosol Reactors*", Aerosol Science and Technology: History and Reviews, RTI Press, Research Triangle Park, NC, United States of America, 2011.

[89]   I.J. Krchma and H.H. Schaumann: "*Production of titanium dioxide*", United States Patent 2559638, 1951.

[90]   M.K. Akhtar, Y. Xiong, and S.E. Pratsinis: "*Vapor Synthesis of Titania Powder by Titanium Tetrachloride Oxidation*", AIChE Journal, 1991, vol. 37 (10), pp. 1561-1570.

[91]   M.K. Akhtar, S. Vemury, and S.E. Pratsinis: "*Competition between TiCl$_4$ Hydrolysis and Oxidation and its Effect on Product TiO$_2$ Powder*", AIChE Journal, 1994, vol. 40 (7), pp. 1183-1192.

[92]   R.A. Gonzalez: "*Process for preparing improved TiO$_2$ by silicon halide addition*", United States Patent 5562764, 1996.

[93]   Q.H. Powell, G.P. Fotou, and T.T. Kodas: "*Gas-phase coating of TiO$_2$ with SiO$_2$ in a continuous flow hot-wall aerosol reactor*", Journal of Materials Research, 1997, vol. 12 (2), pp. 552-559.

[94]   N.S. Subramanian, R.B. Diemer, Jr., and P.L. Gai: "*Process for making durable rutile titanium dioxide pigment by vapor phase deposition of surface treatments*", United States Patent 6852306 B2, 2005.

[95]   A.H. Angerman and C.G. Moore: "*Production of Anatase TiO$_2$ by the Chloride Process*", United States Patent 3856929, 1974.

[96]   K.K. Sahu, T.C. Alex, D. Mishra, and A. Agrawal: "*An overview on the production of pigment grade titania from titania-rich slag*", Waste Management & Research, 2006, vol. 24 (1), pp. 74-79.

[97]   E.G. Roche, A.D. Stuart, and P.E. Grazier: "*Production of Titania*", United States Patent 7485269 B2, 2009.

[98]   E.G. Roche, A.D. Stuart, P.E. Grazier, and H. Liu: "*Production of Titania*", United States Patent 7485268 B2, 2009.

[99]   W. Zhang, Z. Zhu, and C.Y. Cheng: "*A literature review of titanium metallurgical processes*", Hydrometallurgy, 2011, vol. 108 (3), pp. 177-188.

[100] E.R. Force: "*Geology of titanium-mineral deposits*", The Geological Society of America, Inc., Boulder, Colorado, United States of America, 1991.

[101] T.S. Mackey: "*Upgrading ilmenite into a high-grade synthetic rutile*", JOM, 1994, vol. 46 (4), pp. 59-64.

[102] D. Filippou and G. Hudon: "*Iron removal and recovery in the titanium dioxide feedstock and pigment industries*", JOM, 2009, vol. 61 (10), pp. 36-42.

[103] P. Benjamin: "*Mineral Sands Geology and Exploration*", Iluka, 2011. http://www.iluka.com/docs/company-presentations/mineral-sands-technical-presentation-sydney-3-may-2011.pdf

[104] G.M. Bedinger: "*Mineral Commodity Summaries: Titanium Mineral Concentrates*", U.S. Geological Survey, Washington DC, January, 2013, pp. 174-175.

[105] G.M. Bedinger: "*Mineral Commodity Summaries: Titanium Mineral Concentrates*", U.S. Geological Survey, Washington DC, February, 2014, U.S. Geological Survey. pp. 172-173.

[106] J. Gambogi: "*Mineral Commodity Summaries: Titanium Mineral Concentrates*", U.S. Geological Survey, Washington DC, January, 2004, pp. 176-177.

[107] J. Gambogi: "*Mineral Commodity Summaries: Titanium Mineral Concentrates*", U.S. Geological Survey, Washington DC, January, 2005, pp. 176-177.

[108] J. Gambogi: "*Mineral Commodity Summaries: Titanium Mineral Concentrates*", U.S. Geological Survey, Washington DC, January, 2006, pp. 178-179.

[109] J. Gambogi: "*Mineral Commodity Summaries: Titanium Mineral Concentrates*", U.S. Geological Survey, Washington DC, January, 2007, pp. 174-175.

[110] J. Gambogi: "*Mineral Commodity Summaries: Titanium Mineral Concentrates*", U.S. Geological Survey, Washington DC, January, 2008, pp. 178-179.

[111] J. Gambogi: "*Mineral Commodity Summaries: Titanium Mineral Concentrates*", U.S. Geological Survey, Washington DC, January, 2009, pp. 174-175.

[112] J. Gambogi: "*Mineral Commodity Summaries: Titanium Mineral Concentrates*", U.S. Geological Survey, Washington DC, January, 2010, pp. 172-173.

[113] J. Gambogi: "*Mineral Commodity Summaries: Titanium Mineral Concentrates*", U.S. Geological Survey, Washington DC, January, 2011, pp. 174-175.

[114] J. Gambogi: "*Mineral Commodity Summaries: Titanium Mineral Concentrates*", U.S. Geological Survey, Washington DC, January, 2012, pp. 174-175.

[115] R. Porter: "*Mineral Sands Briefing Paper*", Iluka, 2010. http://www.iluka.com/docs/mineral-sands-briefing-papers/mineral-sands-physical-flow-information-october-2010

[116]   G. Jones: "*Mineral Sands: An Overview of the Industry*", Iluka, 2009.
http://www.iluka.com/docs/company-presentations/mineral-sands---an-
overview-of-the-industry-by-greg-jones-manager-development-geology

[117]   K.S. Geetha and G.D. Surender: "*Experimental and modelling studies on the
aeration leaching process for metallic iron removal in the manufacture of
synthetic rutile*", Hydrometallurgy, 2000, vol. 56 (1), pp. 41-62.

[118]   R.G. Becher, R.G. Canning, B.A. Goodheart, and S. Uusna: "*A new process for
upgrading ilmenitic mineral sands*", Proceeding of the Australasian Institute of
Mining and Metallurgy, 1965, vol. 21, pp. 21-44.

[119]   S. Jayasekera, Y. Marinovich, J. Avraamides, and S.I. Bailey: "*Pressure
leaching of reduced ilmenite: electrochemical aspects*", Hydrometallurgy,
1995, vol. 39 (1), pp. 183-199.

[120]   W. Hoecker: "*Process for the production of synthetic rutile*", United States
Patent 5601630, 1997.

[121]   J.B. Farrow, I.M. Ritchie, P. Mangano: "*The reaction between reduced ilmenite
and oxygen in ammonium chloride solutions*", Hydrometallurgy, 1987, vol. 18
(1), pp. 21-38.

[122]   Iluka: "*Synthetic Rutile*", Iluka.
http://www.iluka.com/docs/3.3-operations/synthetic-rutile.pdf

[123]   J.H. Chen: "*Beneficiation of Titaniferous Ores*", United States Patent 3825419,
1974.

[124]   J.H. Chen: "*Pre-leaching or reduction treatment in the beneficiation of
titaniferous iron ores*", United States Patent 3967954, 1976.

[125]   J.H. Chen and L.W. Huntoon: "*Beneficiation of ilmenite ore*", United States
Patent 4019898, 1977.

[126]   K. Borowiec, A.E. Grau, M. Gueguin, and J-F. Turgeon: "*Method to upgrade
titania slag and resulting product*", United States Patent 5830420, 1998.

[127]   G.E. Williams and J.D. Steenkamp: "*Heavy Mineral Processing at Richards Bay
Minerals*", Southern African Pyrometallurgy 2006, 2006, pp. 181-188.

[128]   M. Gueguin and F. Cardarelli: "*Chemistry and mineralogy of titania-rich slags.
Part 1-hemo-ilmenite, sulphate, and upgraded titania slags*", Miner. Process.
Extr. Metall. Rev., 2007, vol. 28, pp. 1–58.

[129]   A. Roine et al.: "*HSC Chemistry$^{®}$ version 7.11*", Outotec Oy Information
Center, Finland, 2011.

[130]   L.K. Doraiswamy, H.C. Bijawat, and M.V. Kunte: "*Chlorination of ilmenite in
a fluidized bed*", Chemical Engineering Progress, 1959, vol. 55 (10), pp. 80-88.

[131] W.E. Dunn: "*High-temperature chlorination of TiO₂ bearing minerals*", Transactions of the Metallurgical Society of AIME, 1960, vol. 218 (1), pp. 6-12.

[132] C.M. Lakshmanan, H.E. Hoelscher, and B. Chennakesavan: "*The kinetics of ilmenite beneficiation in a fluidised chlorinator*", Chemical Engineering Science, 1965, vol. 20 (12), pp. 1107-1113.

[133] A.S. Athavale and V.A. Altekar: "*Kinetics of Selective Chlorination of Ilmenite Using Hydrogen Chloride in a Fluidized Bed*", Industrial & Engineering Chemistry Process Design and Development, 1971, 10 (4), pp. 523-530.

[134] D.F. Othmer and R. Nowak: "*Halogen affinities–A new ordering of metals to accomplish difficult separations*", AIChE J., 1972, 18 (1), pp. 217-220.

[135] S. Fukushima and E. Kimura: "*Ilmenite Upgrading: Particularly Concerning Mitsubishi Process*", Titanium·Zirconium, 1975, vol. 23 (2), pp. 67-74. (in Japanese)

[136] D.F. Othmer: "*Manufacture of titanium chloride, synthetic rutile and metallic iron from titaniferous materials containing iron*", United States Patent 3859077, 1975.

[137] A. Fuwa, E. Kimura, and S. Fukushima: "*Kinetics of Iron Chlorination of Roasted Ilmenite Ore, Fe₂TiO₅ in a Fluidized-Bed Reactor*", Metallurgical Transactions B, 1978, vol. 9B (4), pp. 643-652.

[138] V.G. Neurgaonkar, A.N. Gokarn, and K. Joseph: "*Beneficiation of ilmenite to rutile by selective chlorination in a fluidised bed*", Journal of Chemical Technology and Biotechnology, 1986, vol. 36 (1), pp. 27-30.

[139] J.S.J. Van Deventer: "*Kinetics of the selective chlorination of ilmenite*", Thermochimica Acta, 1988, vol. 124, pp. 205-215.

[140] K.I. Rhee and H.Y. Sohn: "*The selective chlorination of iron from llmenite ore by CO-Cl₂ mixtures: Part I. intrinsic kinetics*", Metallurgical Transactions B, 1990, vol. 21B (2), pp. 321-330.

[141] K.I. Rhee and H.Y. Sohn: "*The selective carbochlorination of iron from titaniferous magnetite ore in a fluidized bed*", Metallurgical Transactions B, 1990, vol. 21B (2), pp. 341-347.

[142] K. Ichimura, S. Oka, and Y. Takahashi: "*Method to produce high-grade TiO₂ feed*", Japan Patent 1994-191847, 1994. (in Japanese)

[143] R. Matsuoka: "*Iron Removal from Titanium Ore Using Selective Chlorination and Effective Utilization of Chloride Waste*", Master thesis, The University of Tokyo, 2005.

Table 1-1 Physical and chemical properties of Ti, Ti-6Al-4V, Fe and Al.[1-6]

	Titanium	Ti-6Al-4V	Aluminum	Iron
Common symbol	Ti	Ti-6Al-4V	Al	Fe
Melting Temp., T_m / K	1943	-	934	1811
Density[1], ρ_d / g·cm^{-3}	4.507	4.430	2.699	7.870
Tensile strength[1], σ / MPa	235	900[2]	40 – 50	265
Elongation[1], el / %	54	10	50 – 70	43 – 48
Coefficient of linear thermal expansion[1], α / μm·(m·K)$^{-1}$	8.41	8.6[7]	22.8	11.8
Thermal conductivity[1], k / W·(m·K)$^{-1}$	11.4	6.6 – 6.8	247	80.4
Corrosion rate[3,4], r_{corr} / mpy	≈ 0	-	0.039 – 0.197	-
Corrosion rate, r_{corr} / mpy	0.394[5]	0.591[5]	0.747[6]	5.03[6]
Clarke No.[8]	9	-	3	4

1: Physical properties at room temperature.
2: Mechanical properties given for the annealed condition; may be solution treated and aged to increase strength.
3: mpy is mils per year (1/1000 inches per year).
4: Corrosion rate for metals in stagnant or slowly flowing seawater.
5: 5 % HCl + 0.1% FeCl$_3$, temperature = boiling temperature.
6: Average in seawater (New York harbor, Hudson river near New York, Miami (Florida), Haifa (Israel)).
7: Temperature ranges from 293 K to 373 K.
8: Orders in composition of element to be existing in upper crust of the earth.

Table 1-2 Advantages and disadvantages of the selected Ti metal production processes (reprinted in the doctoral thesis of Zheng[32]).

Process	Advantages	Disadvantages
Kroll process	◎ High-purity titanium obtainable ◎ Easy metal/salt separation ○ Established chlorine circulation ○ Efficient Mg electrolysis	× Complicated process × Slow production speed × Batch-type process
FFC process	◎ Simple process ○ Semi-continuous process	× Difficult metal/salt separation × Reduction and electrolysis must be simultaneously carried out △ Carbon and iron contamination △ Low current efficiency
OS process	◎ Simple process ○ Semi-continuous process	× Difficult metal/salt separation △ Carbon and iron contamination △ Low current efficiency
EMR/MSE process	◎ Resistant to iron and carbon contamination ○ Semi-continuous process ○ Reduction and electrolysis operation can be independently carried out	× Difficult metal/salt separation × Complicated cell structure △ Complicated process

Table 1-3 Comparison of physical and chemical properties of various kinds of the
white pigments.[73-74]

		Titania (rutile)	Titania (anatase)	Zinc sulfide[1]	Zinc oxide
Chemical formula		TiO_2	TiO_2	ZnS	ZnO
Density, ρ_d / g·cm^{-3}		4.21	4.06	4.08	5.65 – 5.68
Refractive index		2.70	2.55	2.37	1.95 – 2.10
Mohs hardness		6.5 – 7.0	5.5	3	4.0 – 4.5
Crystal structure		Tetragonal	Tetragonal	Hexagonal, Cubic	Hexagonal
Chemical stability	HCl	Insoluble	Insoluble	Soluble[2]	Soluble
	HNO$_3$	Insoluble	Insoluble	Soluble[2]	Soluble
	NaOH	Insoluble	Insoluble	Insoluble[2]	Soluble

1: Normally, the mixture of ZnS and BaSO$_4$ called the lithopone is used as white pigment.
   reaction for production of the lithopone: $ZnSO_4 + BaS = ZnS + BaSO_4$
2: Chemical stability of the lithopone.

Table 1-4 Advantages and disadvantages of the sulfate process and chloride process.

Process	Advantages	Disadvantages
Sulfate process	○ Level of difficulty is not high ◎ Low-grade Ti ore can be used ○ Capital cost is low ○ Energy consumption is low	× Multiple steps for removing iron × Slow production speed × Generation of a large amount of iron waste × Generation of a large amount of acid waste solution × Batch-type process × Quality of titania pigment is not good enough.
Chloride process	○ Relative small amount of chloride waste is produced ○ Semi-continuous process ◎ Quality of titania pigment is very good	△ Little effective method for recycling the chloride waste produced × Use of Cl_2 gas as chlorinating agent × Capital cost is high

Table 1-5 Classification of various types of titanium minerals by chemical formula and its TiO_2 content.

Ti mineral		Chemical formula	TiO_2 content, C_{TiO_2} (mass %)
Oxides	Ilmenite	$FeTiO_3$	$30 - 65$
	Leucoxene	$FeTiO_3 \cdot n\, TiO_2$	> 65
	Rutile	TiO_2	≥ 95
	Anatase	TiO_2	≥ 95
	Brookite	TiO_2	≥ 95
	Perovskite	$CaTiO_3$	$58 - 59$
	Magetite	$(Fe, Ti)_2O_3$	$0 - 34$
Silicates	Sphene (titanite)	$CaTiSiO_5$	$40 - 41$
	Melanitic garnet	$Ca_3Fe_2Si_3O_{12}$	$0 - 17$
	Augite	$Ca(Mg, Fe)(Si, Al)_2O_6$	$0 - 9$

Table 1-6 Advantages and disadvantages of the Becher, the Benilite, and
the slag and UGS processes.

Process	Advantages	Disadvantages
Becher process	○ Use of various types of Ti ore ○ Aeration is cost-effective method	× Multiple steps for removing iron × Relative high energy consumption × Acid leaching is required for high-grade TiO_2 × Generation of large amount of acid waste solution × Iron is dumped out as waste
Benilite process	○ Relative simple process ○ Removal of impurities from Ti ore is favorable	× Acid leaching is required for high-grade TiO_2 × Generation of large amount of acid waste solution × Iron is dumped out as waste
Slag & UGS processes	○ Iron is removed as pig iron ○ Large scale and high speed process	× Low purity of the product by the slag process × Consumption of high amount of energy (high temperature) × Acid leaching is required for high-grade TiO_2 in UGS process × Generation of large amount of acid waste solution × Multiple steps for removing iron

Table 1-7 Selective chlorination processes using pyrometallurgical method developed in the past.

Author	Chlorinating agent	Reducing agent	Temp., T/K	Composition of Ti ore, C_i (mass%)					After selective chlorination		Notes
				TiO$_2$	Fe$_2$O$_3$	FeO	Ti¶	Fe§	TiO$_2$ purity, p_{TiO_2} (mass%)	Fe removal, R_{Fe} (%)	
Doraiswamy et al.[1]	Cl$_2$	CO	1173	62.6	23.4	11.0	(60.1)	(39.9)	-	97.0*	-
Dunn[2]	Cl$_2$	CO	1173	-	-	-	-	-	97.0	-	-
Lakshmanan et al.[3]	Cl$_2$	CO	1173	59.3	24.9	10.8	(55.0)	(45.0)	-	83.2*	-
Rhee and Sohn[4]	Cl$_2$	CO	1123	37.5	18.5	33.7	(36.5)	(63.5)	-	94.0#	-
Fukushima and Kimura[5]	Cl$_2$	C	1223	53.4	19.5	19.9	(52.4)	(47.6)	87.5	(85.9)+¶¶	Roasted Ti ore, pilot
Fuwa et al.[6]	Cl$_2$	C	1153	53.4	19.7	20.2	(52.1)	(47.9)	-	99.0#	Roasted Ti ore
Neurgaonkar et al.[7]	Cl$_2$	C	1273	61.1	23.3	9.6	(60.7)	25.2 (39.3)	94.0	96.9*	O$_2$ supply, Cl$_2$:O$_2$=8:1
Deventer[8]	Cl$_2$	C	1243	49.7	-	-	-	35.9	94.0	$\approx$ 90.0#	-
Rhee and Sohn[9]	Cl$_2$	C	973	20.2	44.6	21.4	(20.2)	(79.8)	-	$\approx$ 90.0#	-
Ichimura et al.[10]	Cl$_2$	TiO$_x$	1123	84.7	0.2	11.1	(85.3)	8.8 (14.7)	93.0	97.4+	TiO$_x$ (0 < x < 2)
Athavale and Altekar[11]	Cl$_2$ + H$_2$ (HCl)	(H$_2$)	1073	61.5	36.0	-	(59.4)	(40.6)	-	90.0&	98% HCl generated
Othmer[12]	TiCl$_4$	C	-	-	-	-	-	-	-	-	No actual data
Matsuoka and Okabe[13]	MgCl$_2$	-	1123	-	-	-	44.5	48.4	(76.6)¶¶	48.2+	Carbon crucible
Zheng and Okabe[14]	CaCl$_2$ + H$_2$O	-	1293	-	-	-	43.8	51.3	(80.6)¶¶	67.4+	Carbon crucible

1: Ref.[32], 2: Composition of Ti ore was not provided in the ref.[131], 3: Ref.[132], 4: Results of the composition of Ti ore are average values written in the ref.[140], 5: Ref.[135],
6: Ref.[137], 7: Ref.[138], 8: Exact result of percent of iron removal was not provided as the value in the ref.[139] Values are roughly estimated based on result graph,
9: Exact result of percent of iron removal was not provided as the value in the ref.[141] Values are roughly estimated based on result graph, 10: Ref.[142], 11: Ref.[133],
12: Ref.[134,136], 13: Ref.[143], 14: Ref.[32],
*: Removal percentage of Fe$_2$O$_3$ calculated by residual weight of the ore when all iron oxides present in the ore are assumed as Fe$_2$O$_3$.
#: Removal percentage of iron from the ore as total Fe.
&: Removal percentage of iron oxide. Form of iron oxide was not provided.
+: Removal percentage of iron (%) = 100×(w_{Fe} in feed − w_{Fe} in residue) / w_{Fe} in feed.
¶: Total Ti composition excluding gaseous elements. Values in parenthesis are calculated by the authors assuming pseudo-binary TiO$_2$ − FeO$_x$ system.
§: Total Fe composition excluding gaseous elements. Values in parenthesis are calculated by the authors assuming pseudo-binary TiO$_2$ − FeO$_x$ system.
¶¶: Values in parenthesis are calculated by the authors assuming TiO$_2$ − FeO$_x$ − MO$_x$ system given by authors.
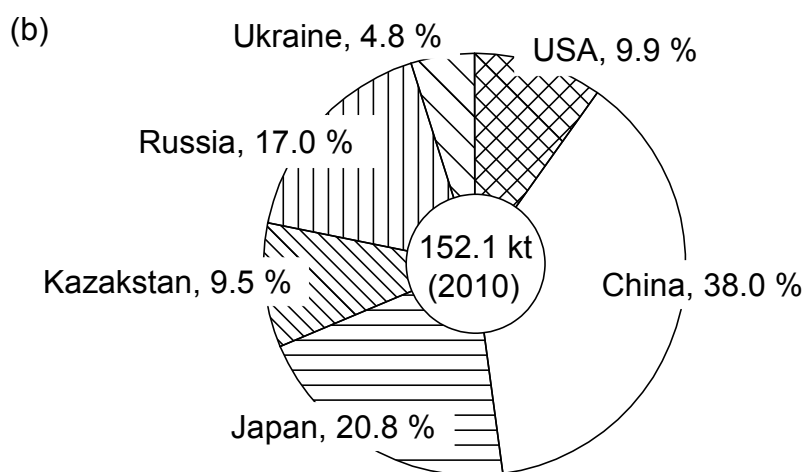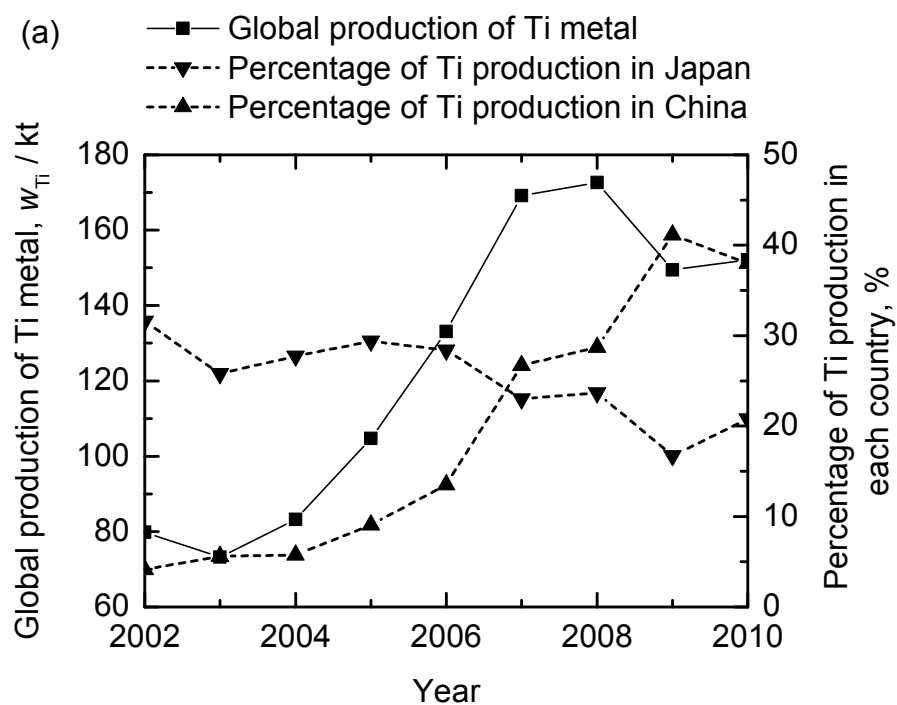
Figure 1-1 (a) Global titanium metal production from 2002 to 2010 and
percentage of titanium metal production in Japan and China and
(b) global titanium metal production in several countries in 2010.[7-16]

49
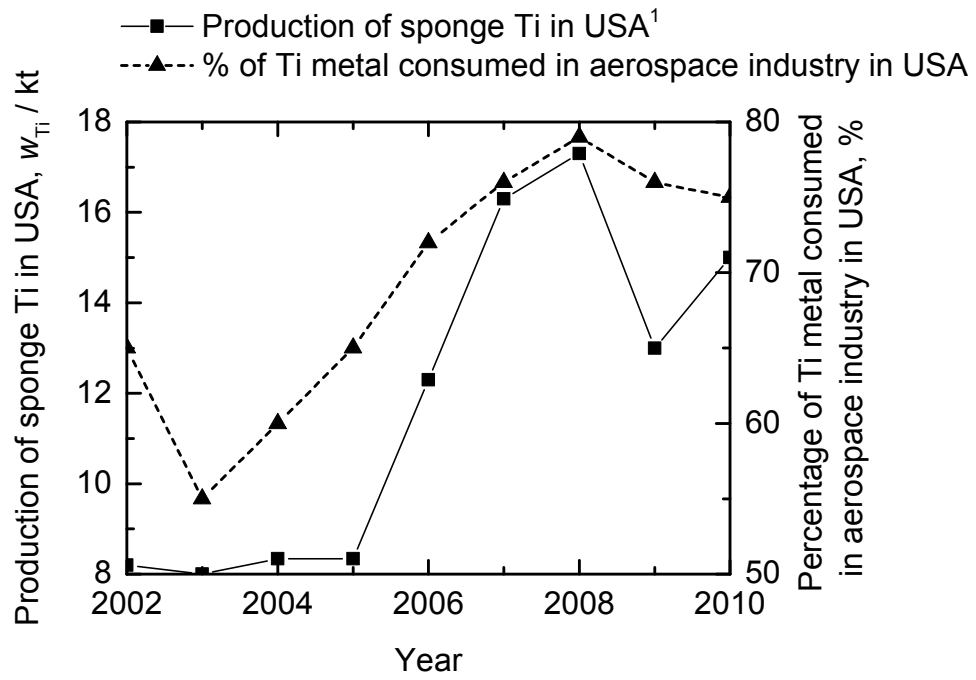
Figure 1-2 Production of titanium metal and the estimated percentage
of titanium metal consumed in aerospace industry in USA
from 2002 to 2010.[7-16]
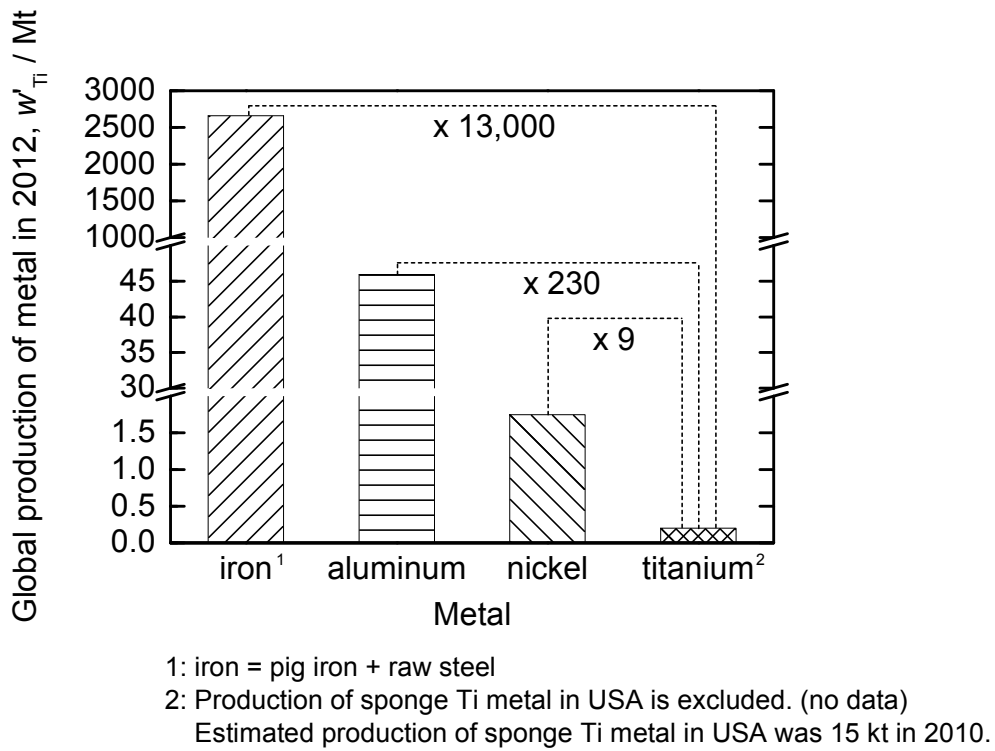
Figure 1-3 Global production of iron, aluminum, nickel, and titanium in 2012.[19-22]
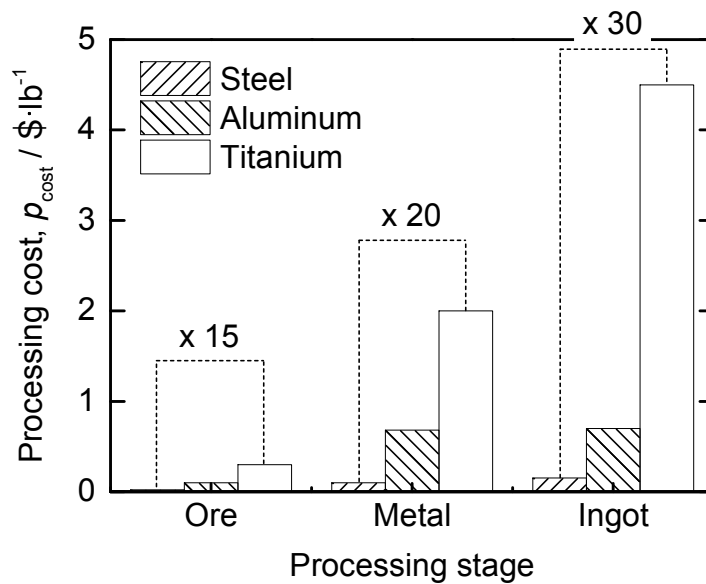
Figure 1-4 Comparison for processing costs of steel, aluminum, and titanium from ore to ingot.[24,25]

High-grade TiO$_2$ (s)　C (s)　　　　Cl$_2$ (g)

Carbo-chlorination

Crude TiCl$_4$ (g)　CO$_x$ (g)　Chloride waste (I)

FeCl$_x$, AlCl$_3$ ···

Additives

H$_2$S ···

Distillation

TiCl$_4$ (l)　　　Chloride waste (II)

VOCl$_x$, SiCl$_4$, SnCl$_4$ ···

Mg (l)

Magnesiothermic reduction

Ti (s) (+ Mg, MgCl$_2$)　　MgCl$_2$ (l)

Vacuum distillation　　　**Electrolysis**

Mg, MgCl$_2$　　Ti (s, sponge)　Cl$_2$ (g)　Mg (l)

Crushing · Melting

Ti (s, ingot)
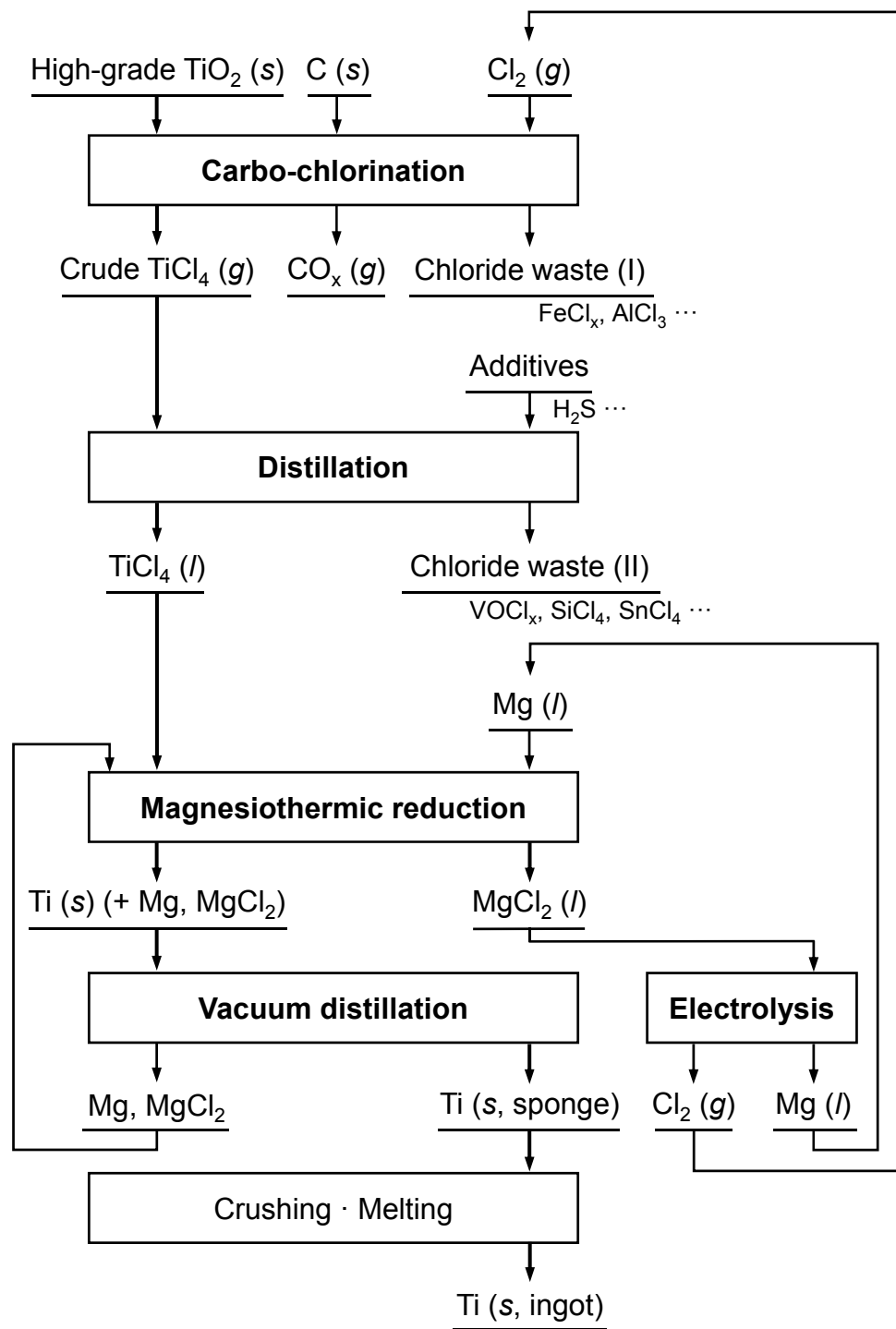
Figure 1-5 Flowchart of the Kroll process for titanium metal production.[23,26,42,43]
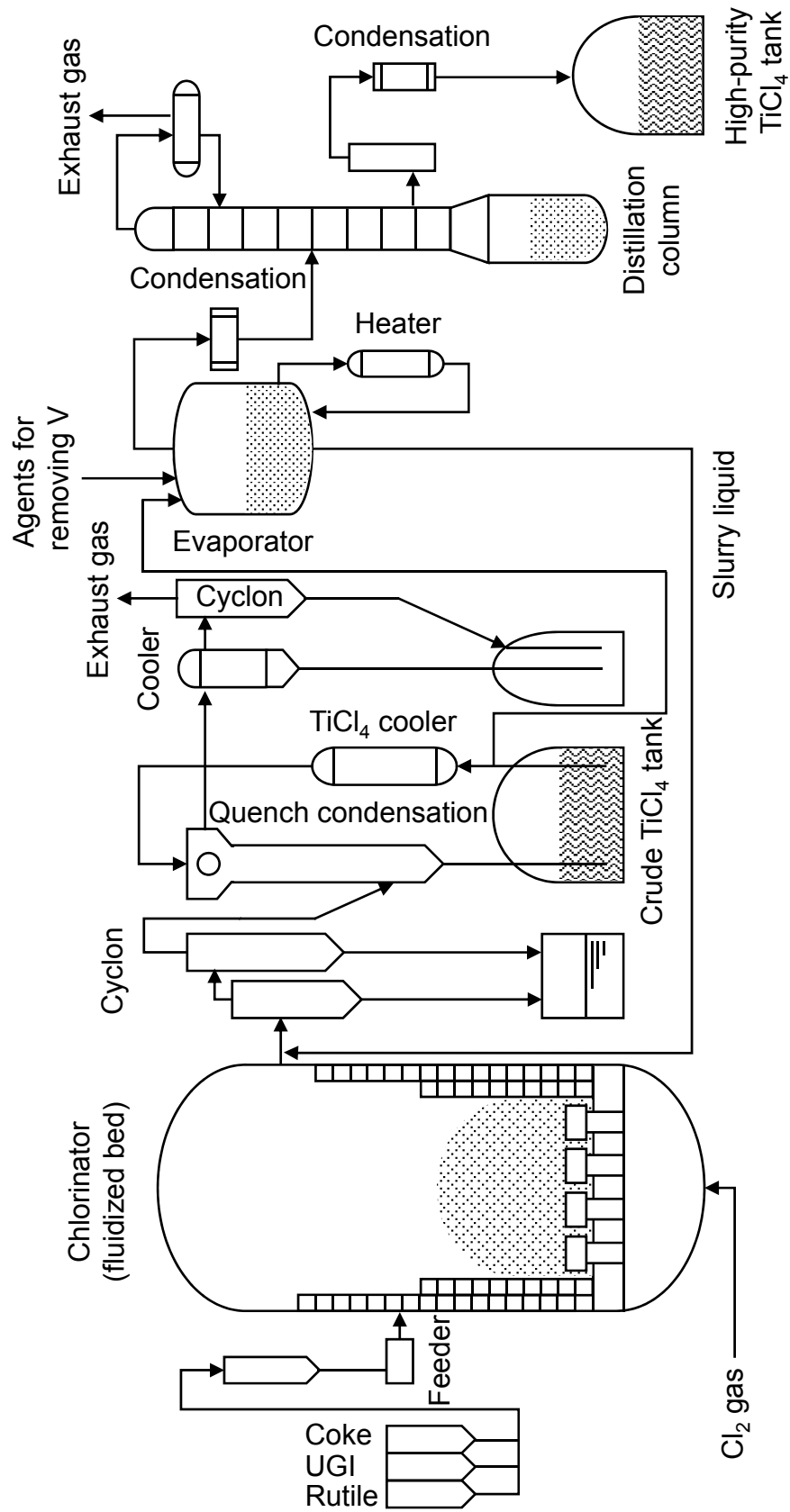
Figure 1-6 Schematic of the carbo-chlorination process that the fluidized bed and distillation equipment are integrated.[43,44]
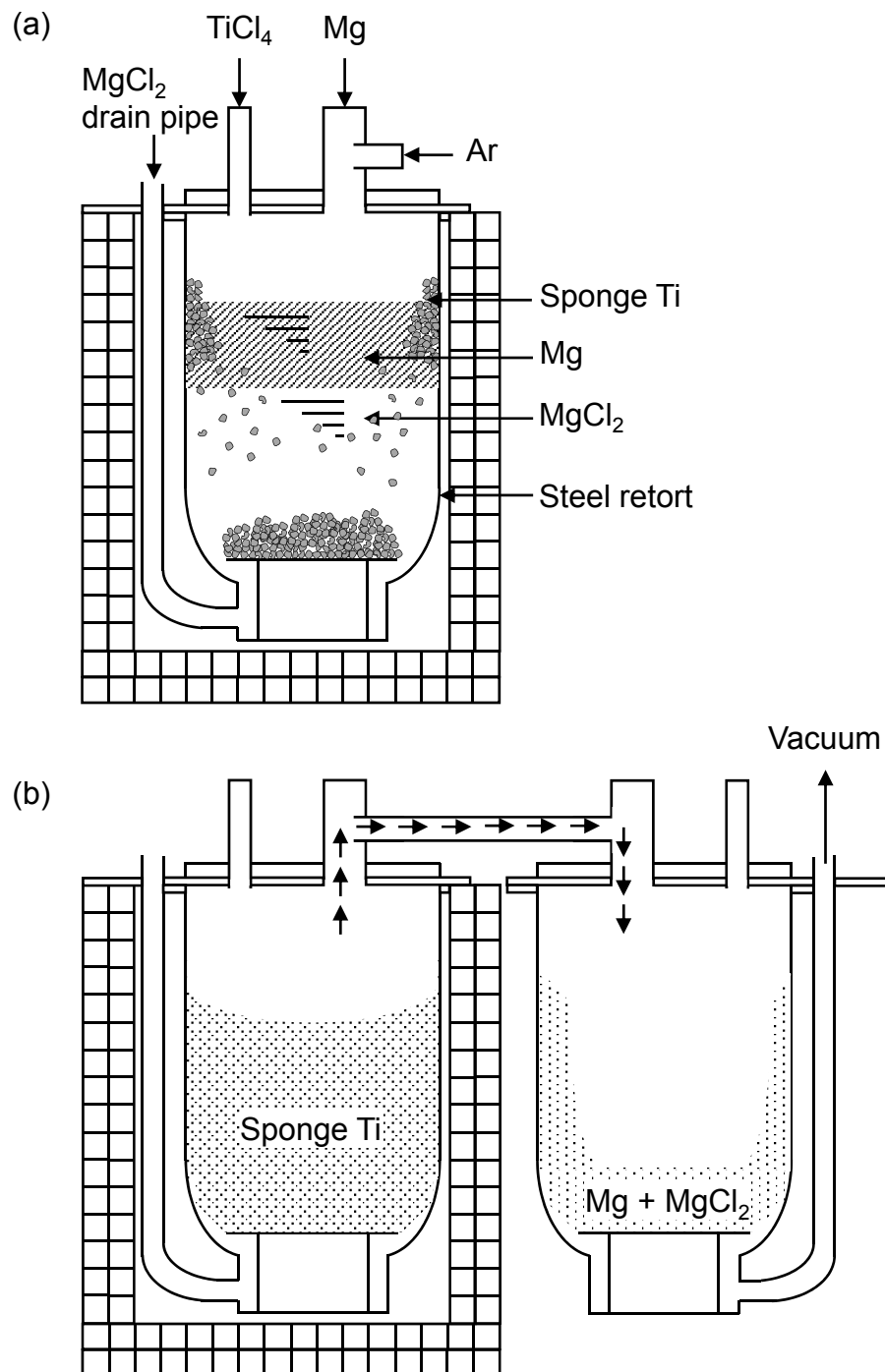
Figure 1-7 (a) Schematic of the magnesiothermic reduction and
(b) schematic of the vacuum distillation after the reduction
in the Kroll process.[43]
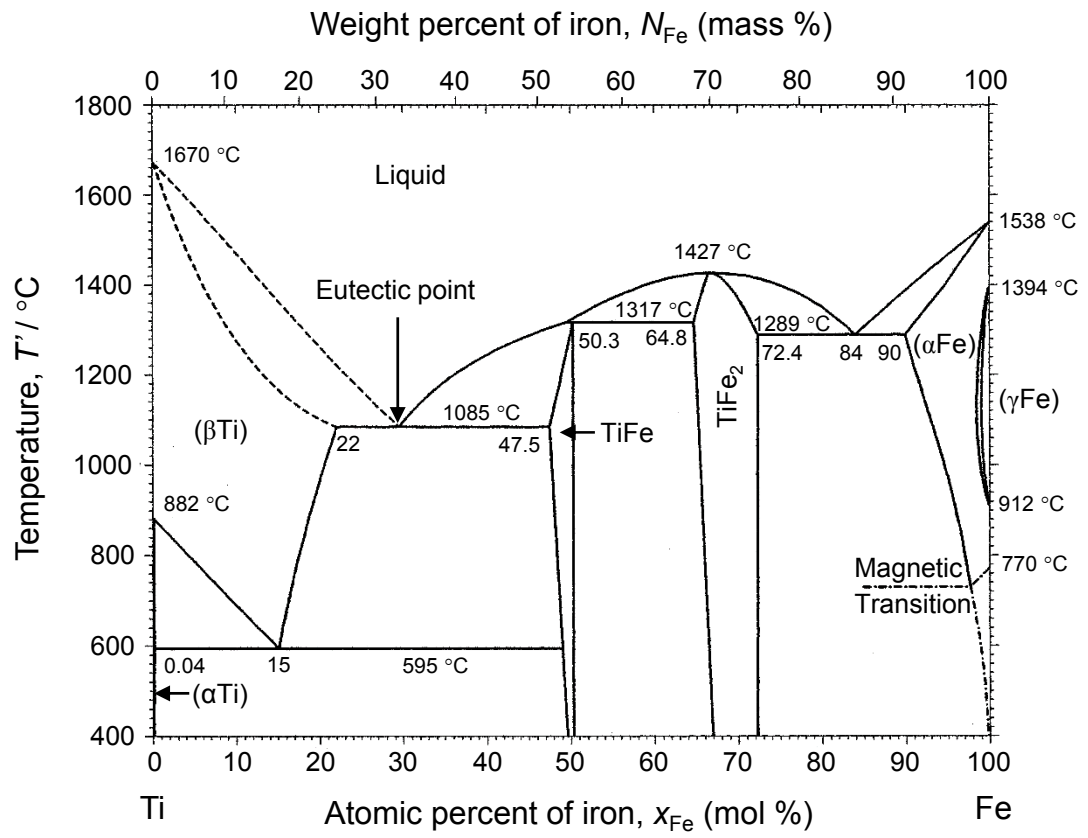
Figure 1-8 Binary phase diagram of the Ti-Fe system.[48]
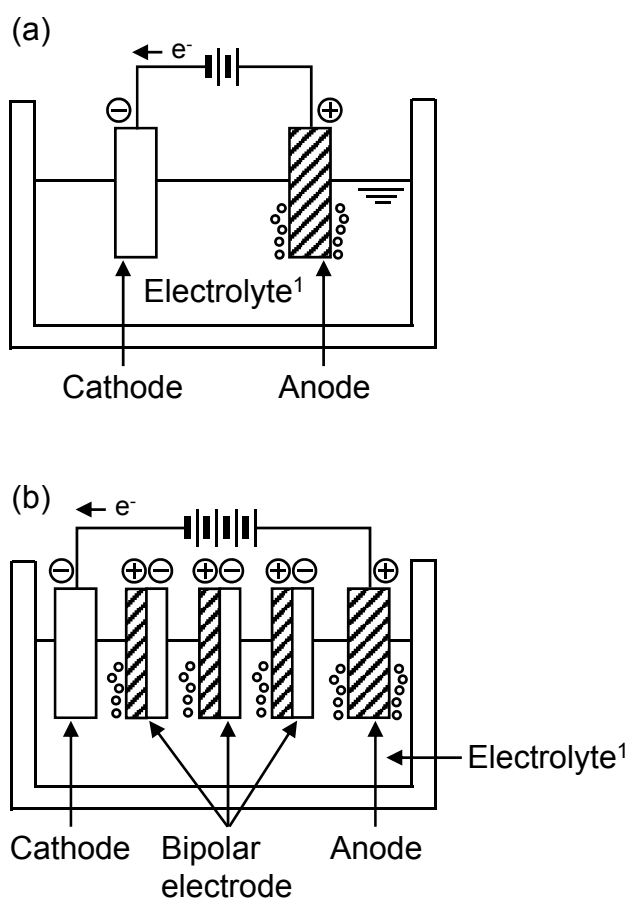
Figure 1-9 (a) Single electrochemical cell for $MgCl_2$ electrolysis and (b) four electrochemical cells for $MgCl_2$ electrolysis utilizing bipolar electrodes.[51]
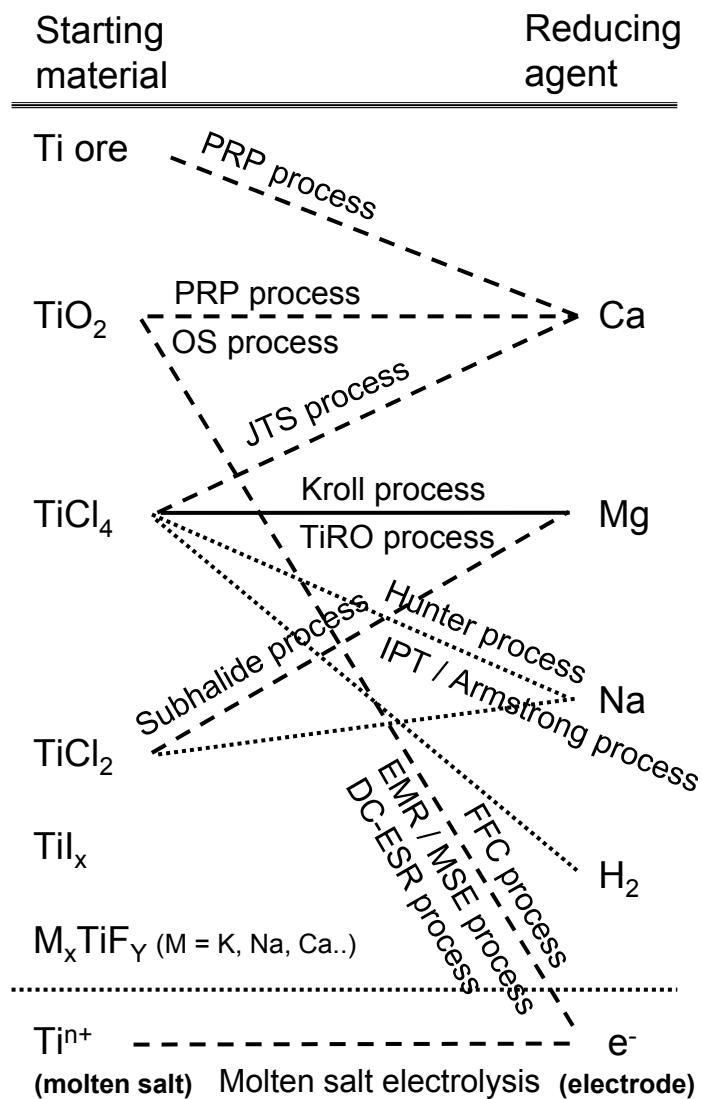
Figure 1-10 Relationship between starting materials and reducing
agents of several reduction process (reprinted in the chapter
of book written by Okabe and Kang[23]).

(a) FFC process (Fray *et al.*)

Anode: $C + x\,O^{2-} = CO_x + 2x\,e^-$
Cathode: $TiO_2 + 4\,e^- = Ti + 2\,O^{2-}$

Cathode   Anode
: TiO_2 prefrom   : carbon
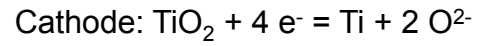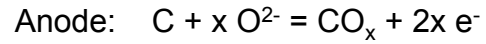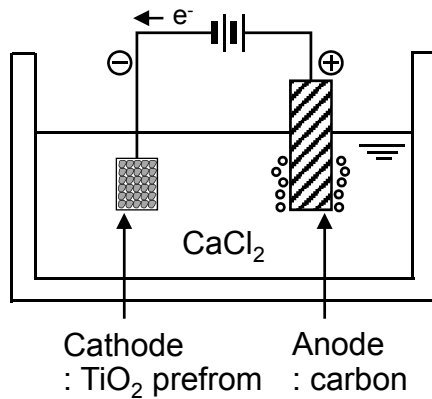
(b) OS process (Ono and Suzuki)

TiO_2 powder

Anode: $C + x\,O^{2-} = CO_x + 2x\,e^-$
Cathode: Ca^{2+} (salt) $+ 2\,e^- = Ca$

Metallothermic reduction
: $TiO_2 + 2\,Ca = Ti + 2\,O^{2-} + 2\,Ca^{2+}$
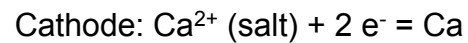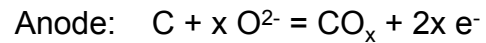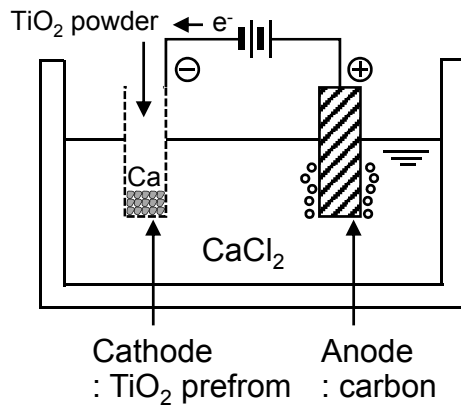
Cathode   Anode
: TiO_2 prefrom   : carbon
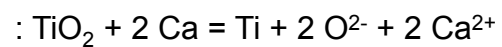
(c) EMR/MSE process (Okabe *et al.*)

Current monitor / controller

MSE
Anode: $C + x\,O^{2-} = CO_x + 2x\,e^-$
Cathode: Ca^{2+} (salt) $+ 2\,e^- = Ca$ (alloy)

EMR
Anode: $2\,Ca$ (alloy) $= 2\,Ca^{2+} + 4\,e^-$
Cathode: $TiO_2 + 4\,e^- = Ti + 2\,O^{2-}$

Cathode Ca alloy Anode
: TiO_2 : carbon
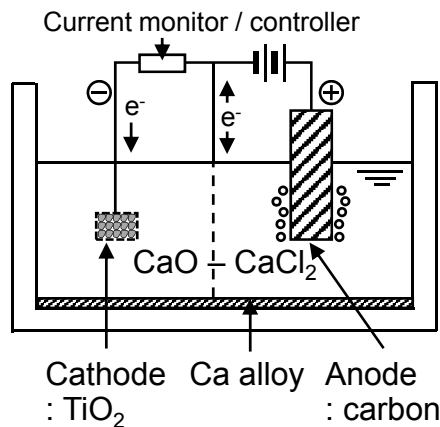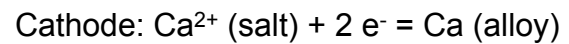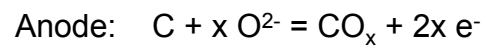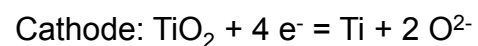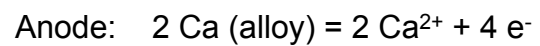
Figure 1-11 Comparison of various titanium reduction processes.[53-65]
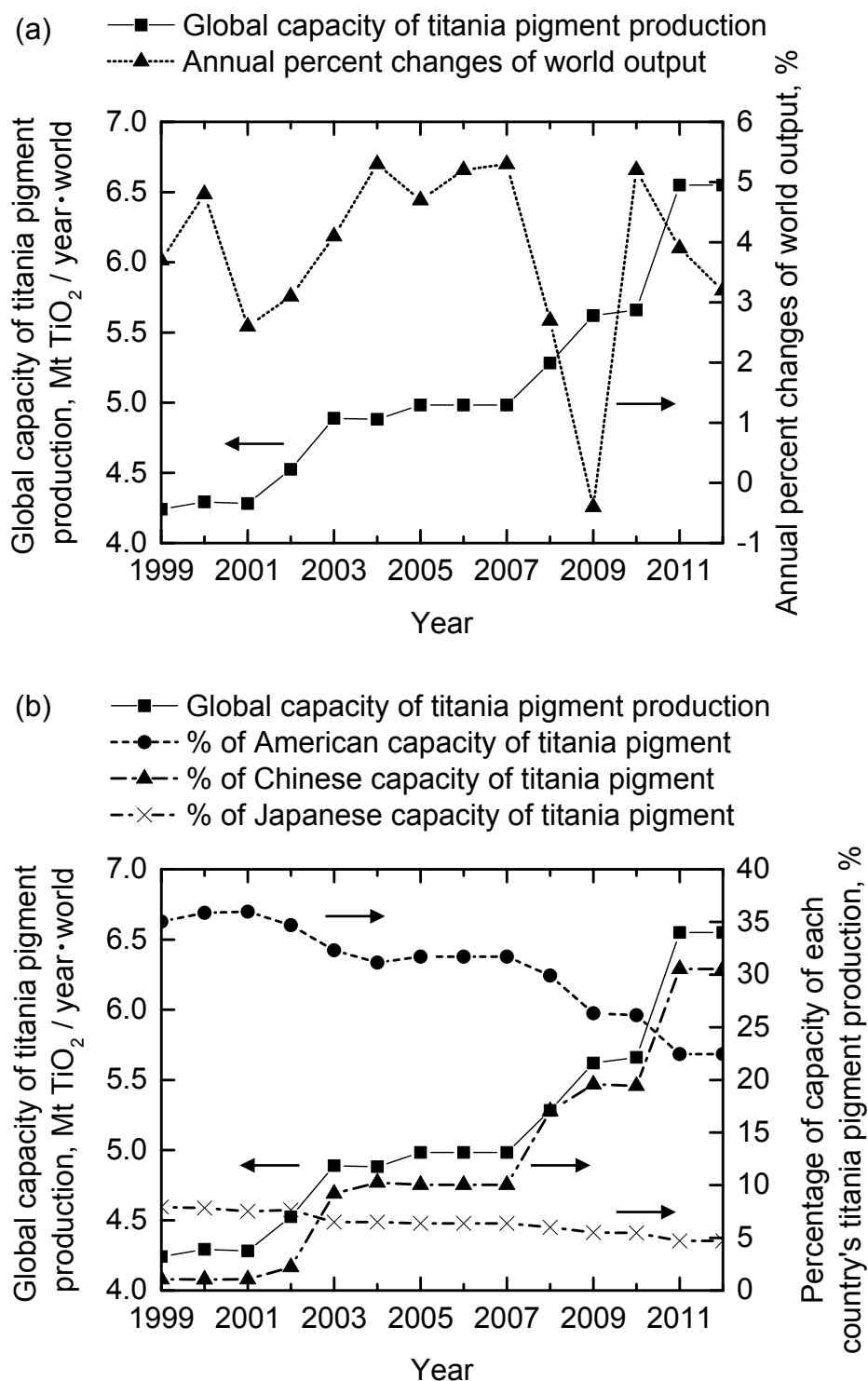
Figure 1-12 (a) Trend of the global capacity of titania pigment production and annual percent changes of world output and (b) trend of the global capacity of titania pigment production and percentage of capacity of each country's titania pigment production in global production.[7-15,18,19,75-81]
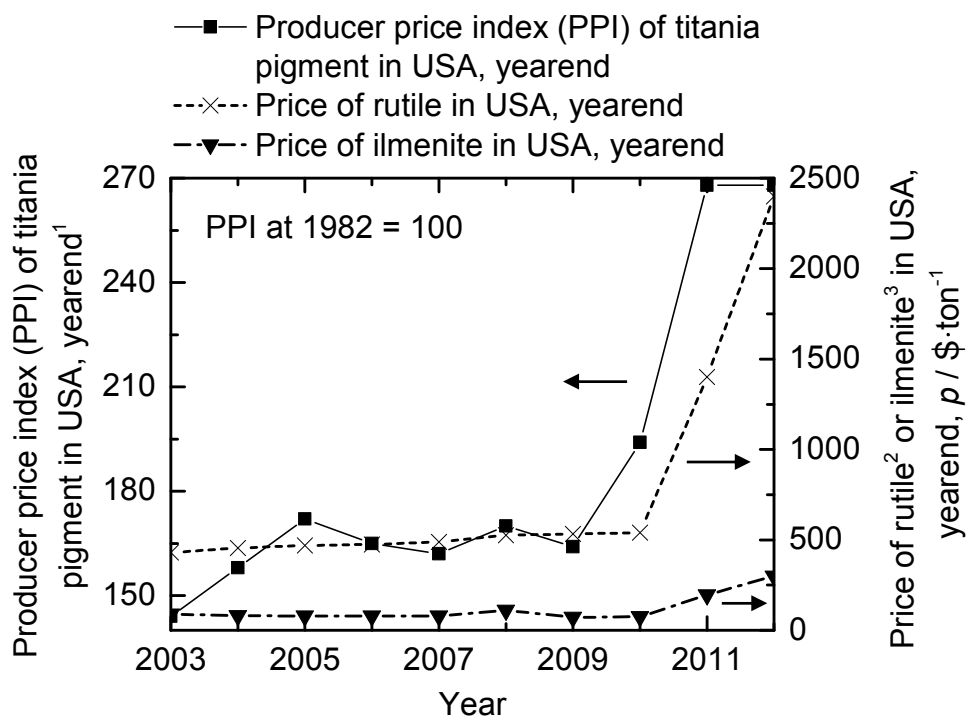
Figure 1-13 The trend of producer price index (PPI) of titania pigment in the USA and the trend of price of rutile and ilmenite in the USA.[83-87]
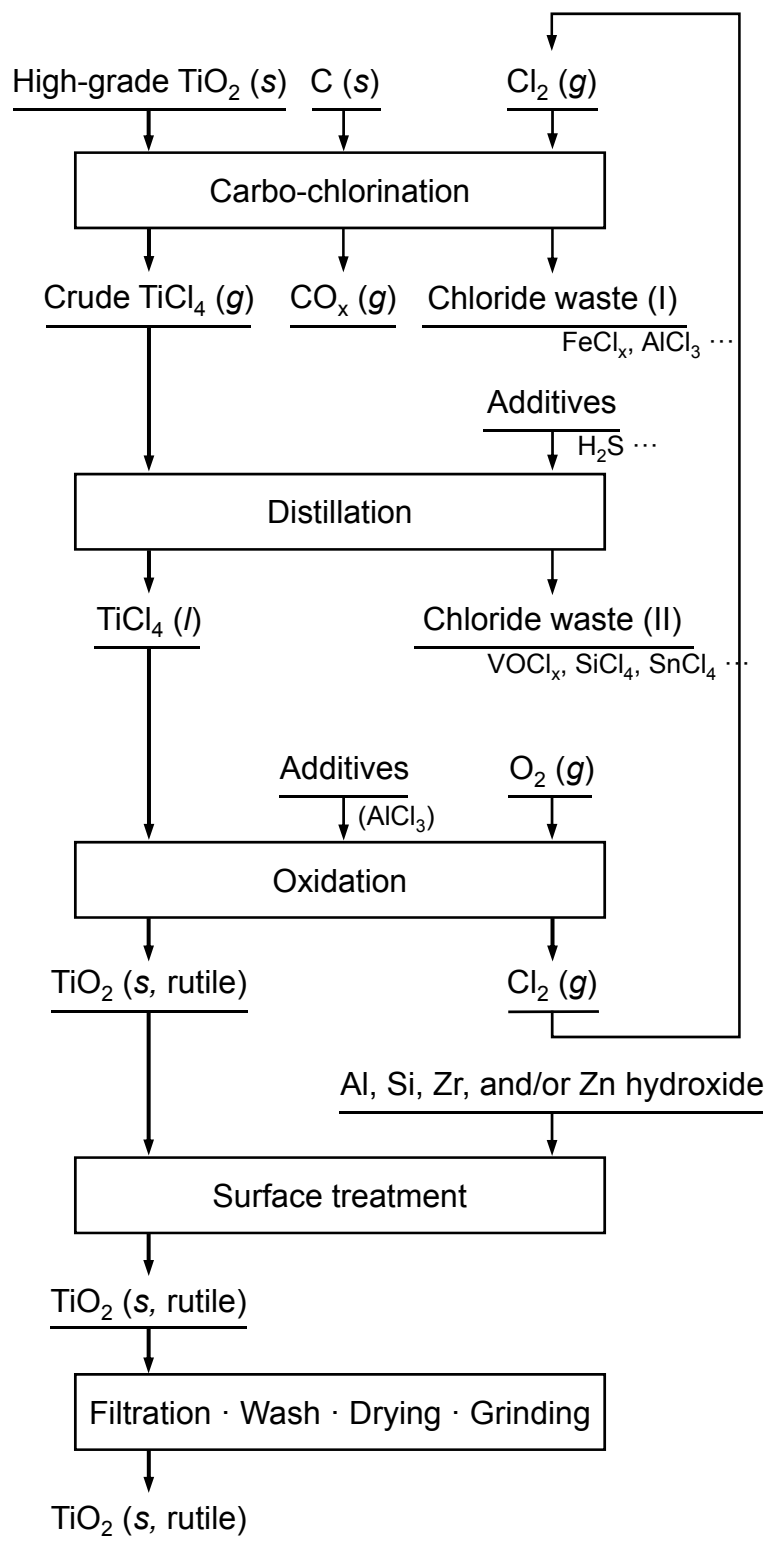
Figure 1-14 Flowchart of the chloride process for production of titania pigment.[27,88-95]

Ilmenite, Titania slag   Reductant[3] H_2SO_4 (*l*)

Digestion[4]

L   S → Unreacted ilmenite

$TiOSO_4$ (*l*) + $FeSO_4$ (*l*) + H_2SO_4 (*l*)

Crystallization

L   S → $FeSO_4 \cdot 7H_2O$ (*s*)

$TiOSO_4$ (*l*) + H_2SO_4 (*l*)   Seed H_2O (*l*)

Hydrolysis

$TiO(OH)_2$ (*s*) + H_2SO_4 (*l*)   Dilute acid   Al / Zn

Purification (Filtration · Bleaching)

S   L → Waste acid

$TiO(OH)_2$ (*s*)

Calcination

TiO_2 (*s*) H_2O (*g*)
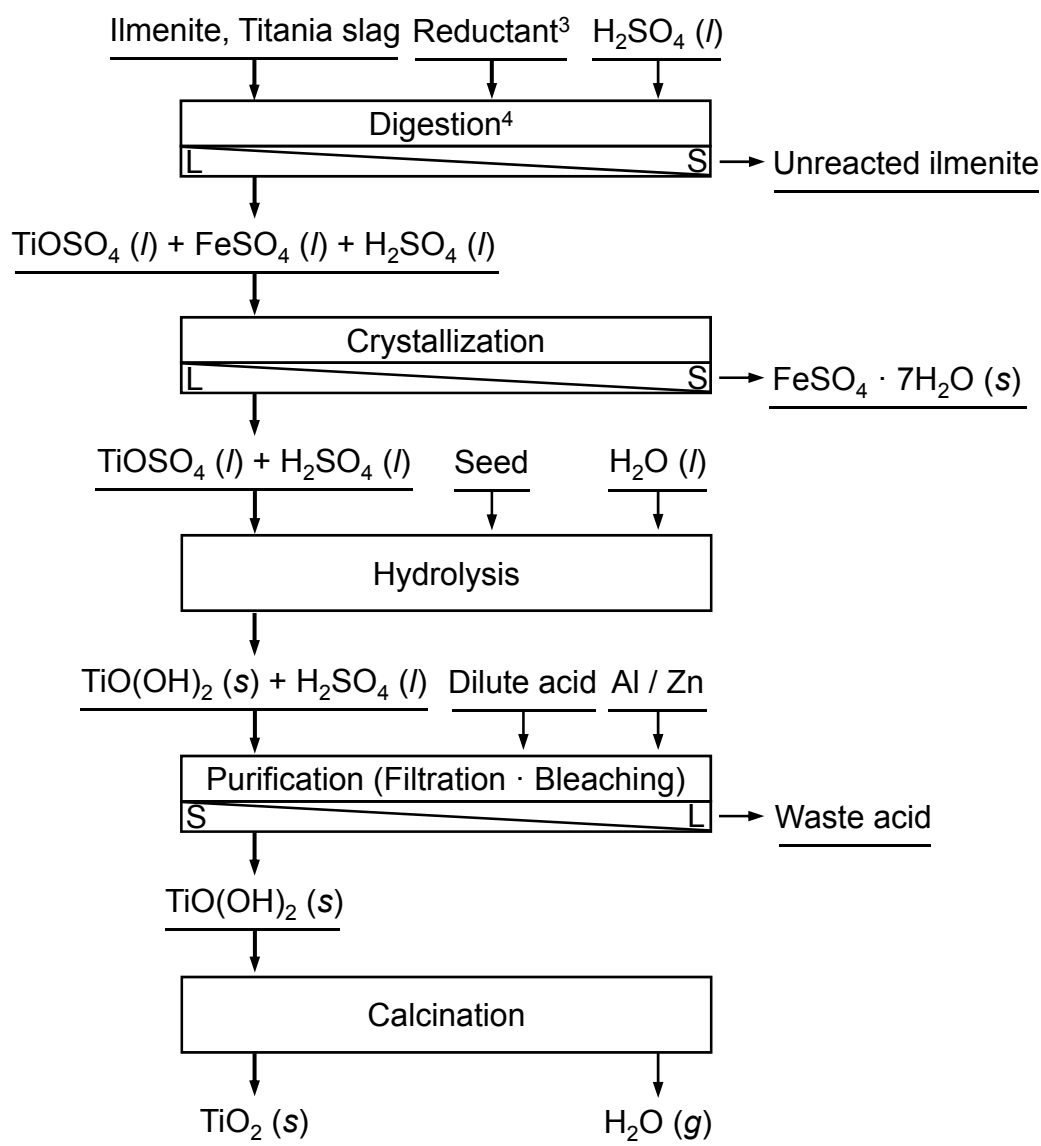
1: Reduction is performed in the Ishihara Sangyo process.
2: Drying and grinding (ca. 40 µm) are performed before digestion.
3: For example, iron scrap is used as reducing agent.
4: In some cases, additives are used for accelerating leaching reaction.

Figure 1-15 Flowchart of the sulfate process for production of titania pigment.[27,44,74,97,98]
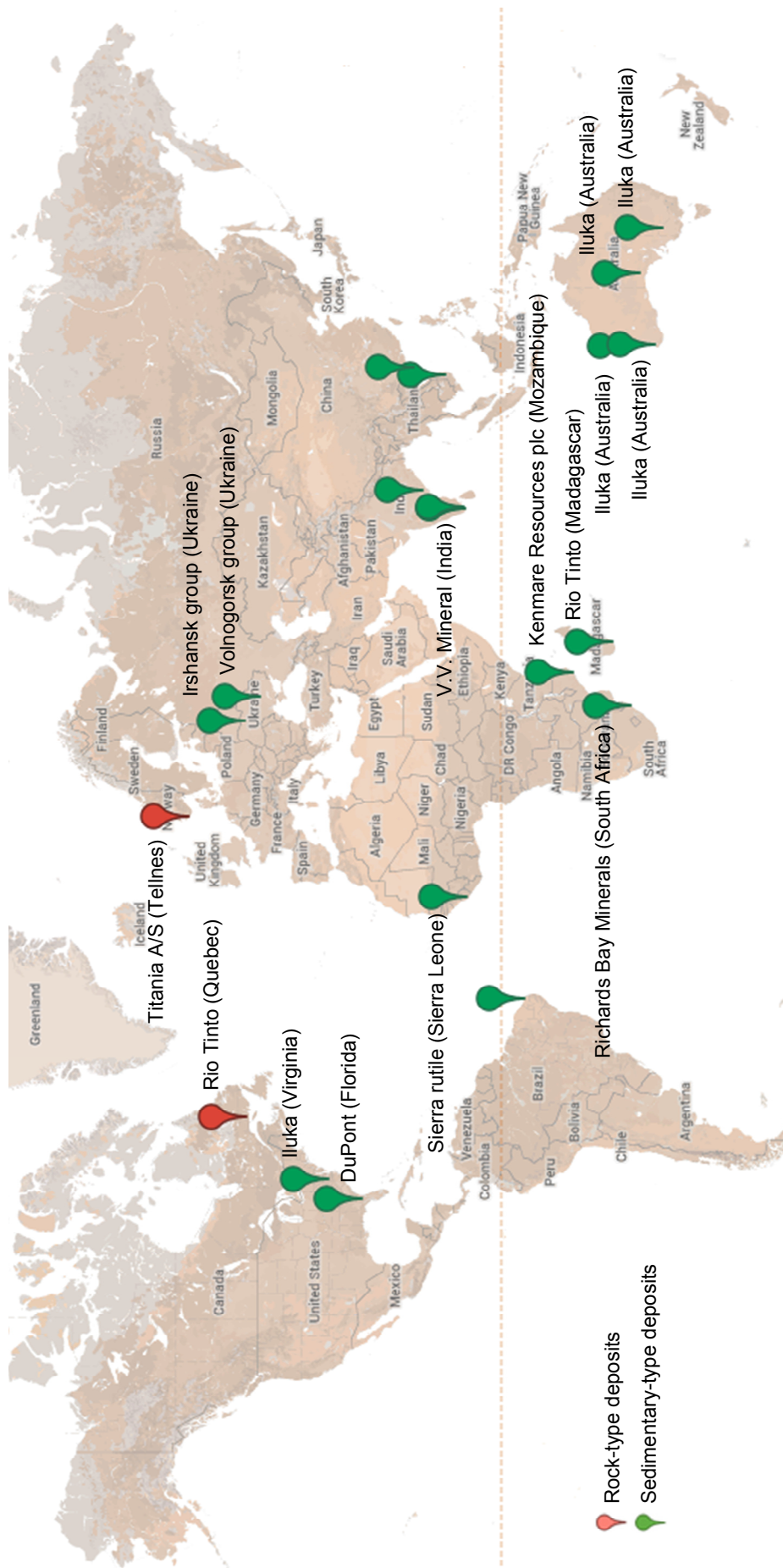
Figure 1-16 Examples of the important titanium mineral mine sites in the world.[100,103]

63

(a)
- ■— Global production of ilmenite
- ▲--- Global production of rutile
- -×-- Percentage of ilmenite production in total production

90% line

(b)
- ■— Global ilmenite reserves
- ▲-- Global rutile reserves
- -×-- Percentage of ilmenite reserves in total reserves
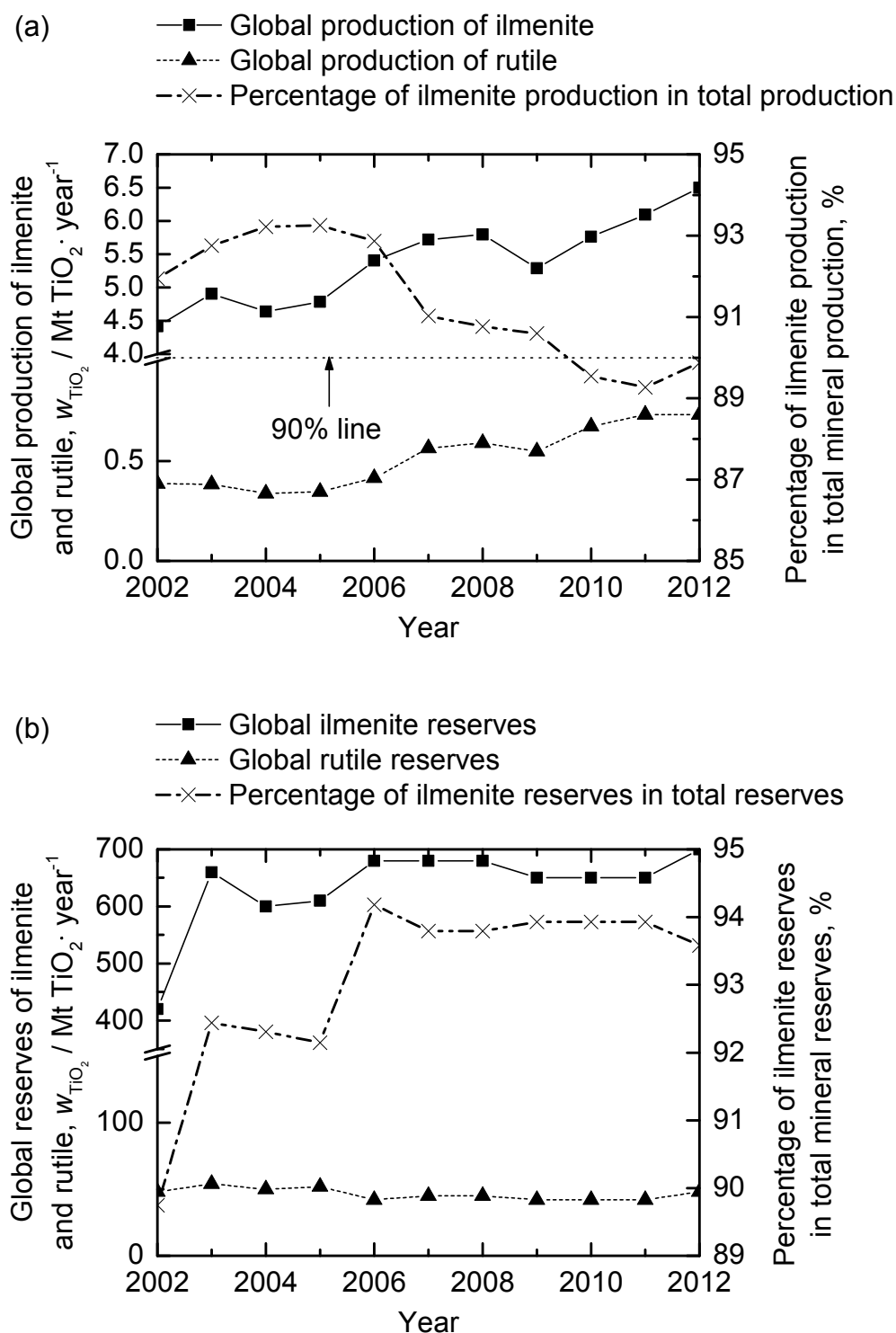
Figure 1-17 (a) The global production of ilmenite and rutile and (b) the global reserves of ilmenite and rutile.[104-114]
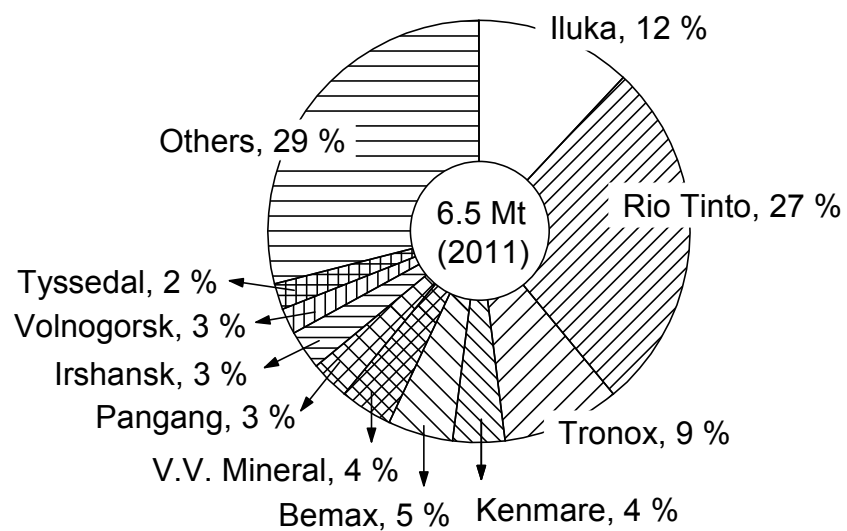
Iluka reported that the production of Ti feedstock in 2011 was 6.5 TiO_2 Mt.

Figure 1-18 The global production of titanium feedstock in 2011 by various companies.[82]

Mineral sands ⟶

Composition		Percent, %
Slimes / Clay		15
Oversize		2
Heavy mineral	Zircon	1.44
	Rutile	0.48
	Ilmenite	7.92
	Non-valuable	2.16
Quartz		71

Screening

Big particles ≥ 150 mm   Mineral sands (Slurry form)

Hydrocyclones

Slimes / Clay < 63 μm   Mineral sands

Spiral separation

Quartz   Heavy minerals

Magnetic separation (WHIMS)[1]

Ilmenite-rich   Heavy minerals[2]

Wet Concentrator Plant (WCP)

Magnetic separation (RE drum)[3]

Heavy minerals   Ilmenite (Magnetic)

Electrostatic · Magnetic separation

Heavy minerals (Nonconductor)   Rutile   Ilmenite (Conductor, Non-magnetic)

Gravity · Electrostatic · Magnetic separations

Quartz, garnet, etc.   Zircon

Nonconductor, Nonmagnetic

Mineral Separation Plant (MSP)

1: Wet high intensity magnets.
2: Attritioning and secondary concentration are conducted After WHIMS.
3: Rare earth drum magnets.

Figure 1-19 Flowchart of titanium ore deposits processing for separating valuable heavy minerals such as ilmenite, rutile, or zircon.[115,116]
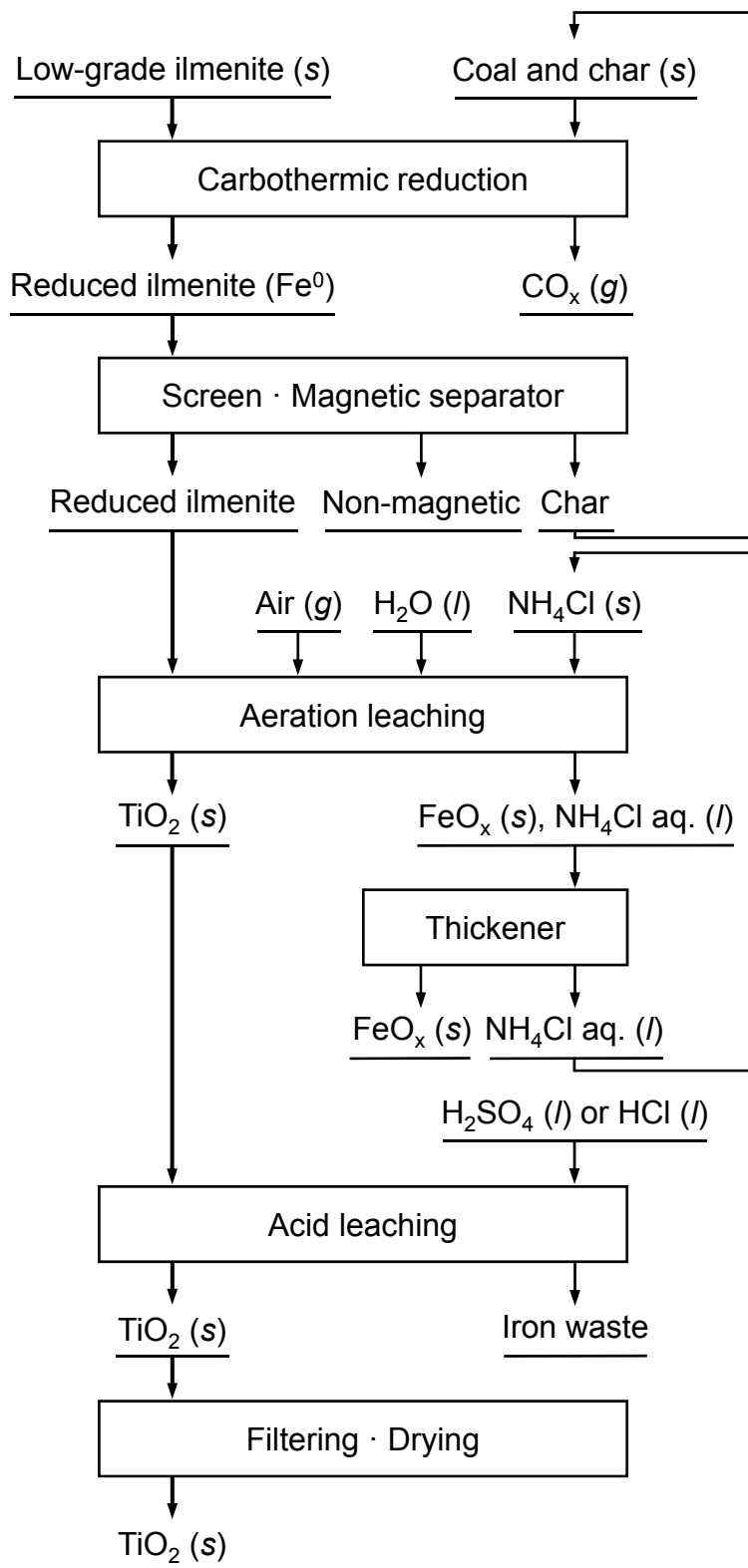
Figure 1-20 Flowchart of the Becher process for upgrading low-grade titanium ore.[72,117-121]
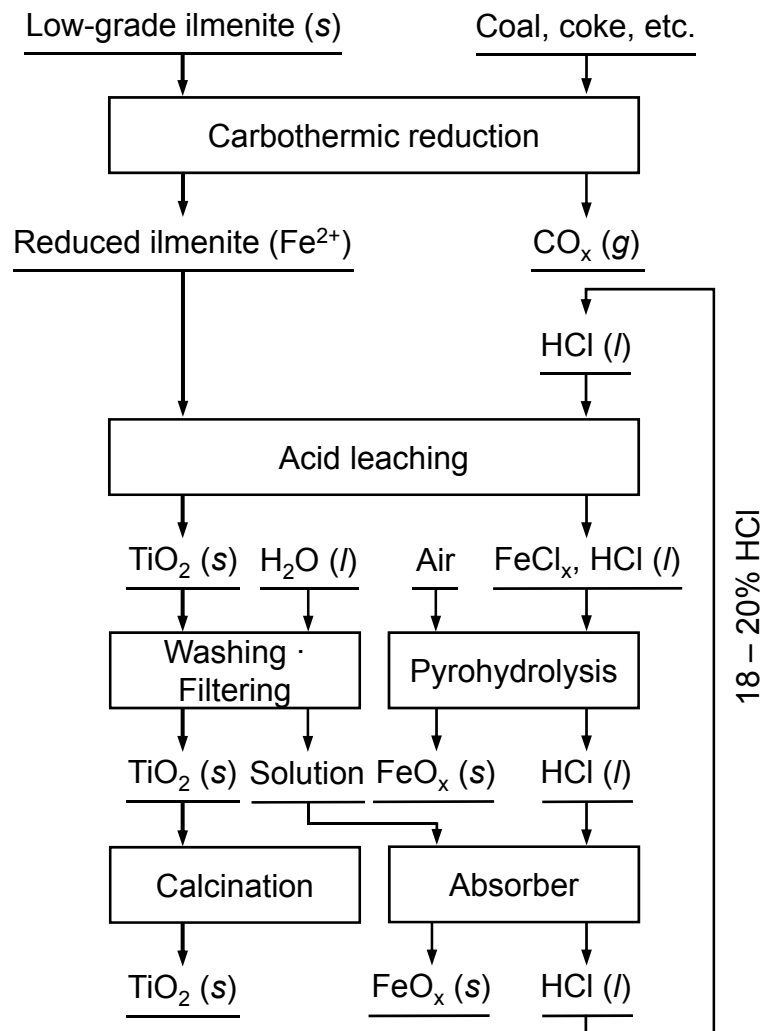
Figure 1-21 Flowchart of the Benilite process for upgrading
low-grade titanium ore.[123-125]
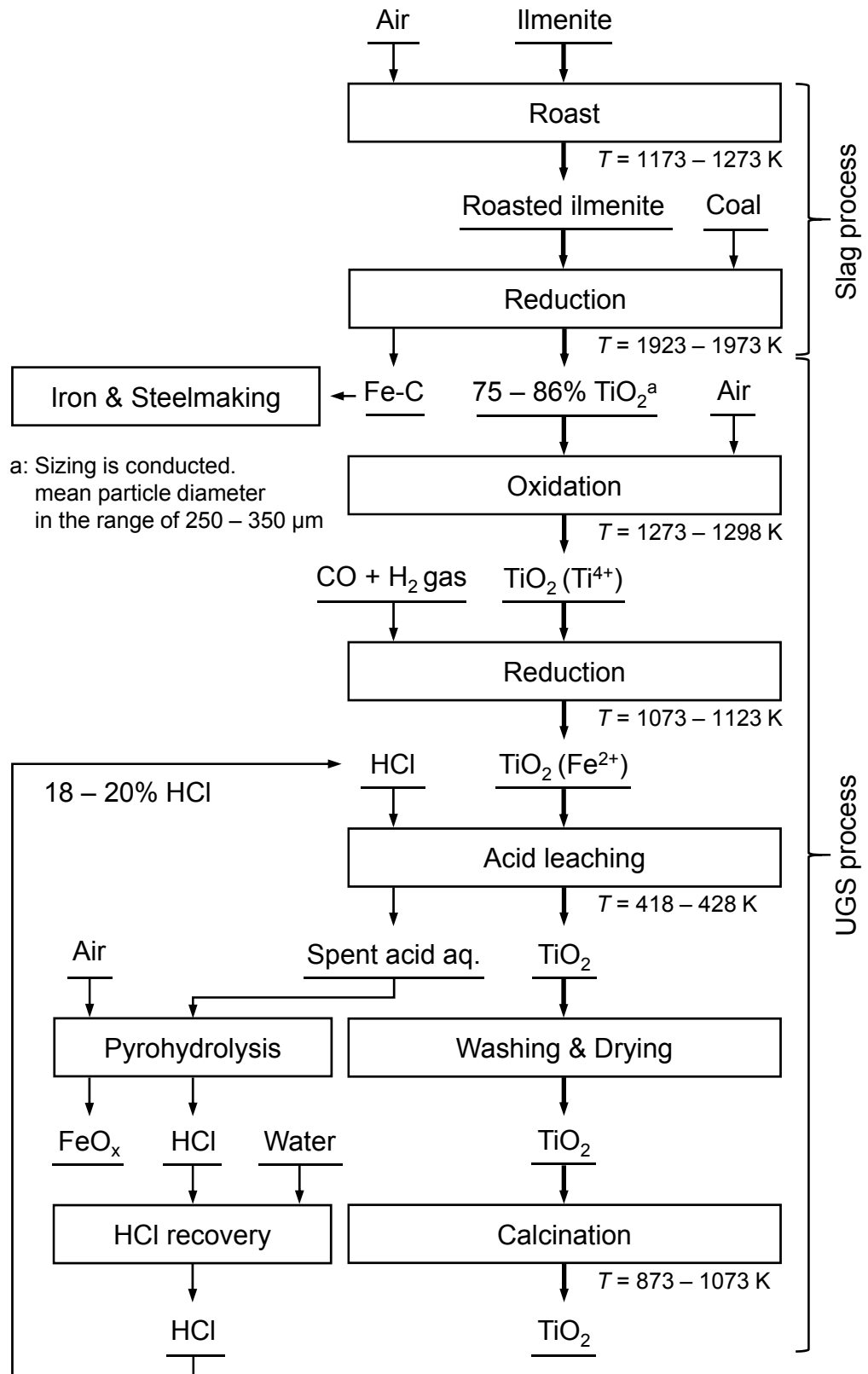
Figure 1-22 Flowchart of the slag and UGS processes for upgrading
low-grade titanium ore.[72,126-128]
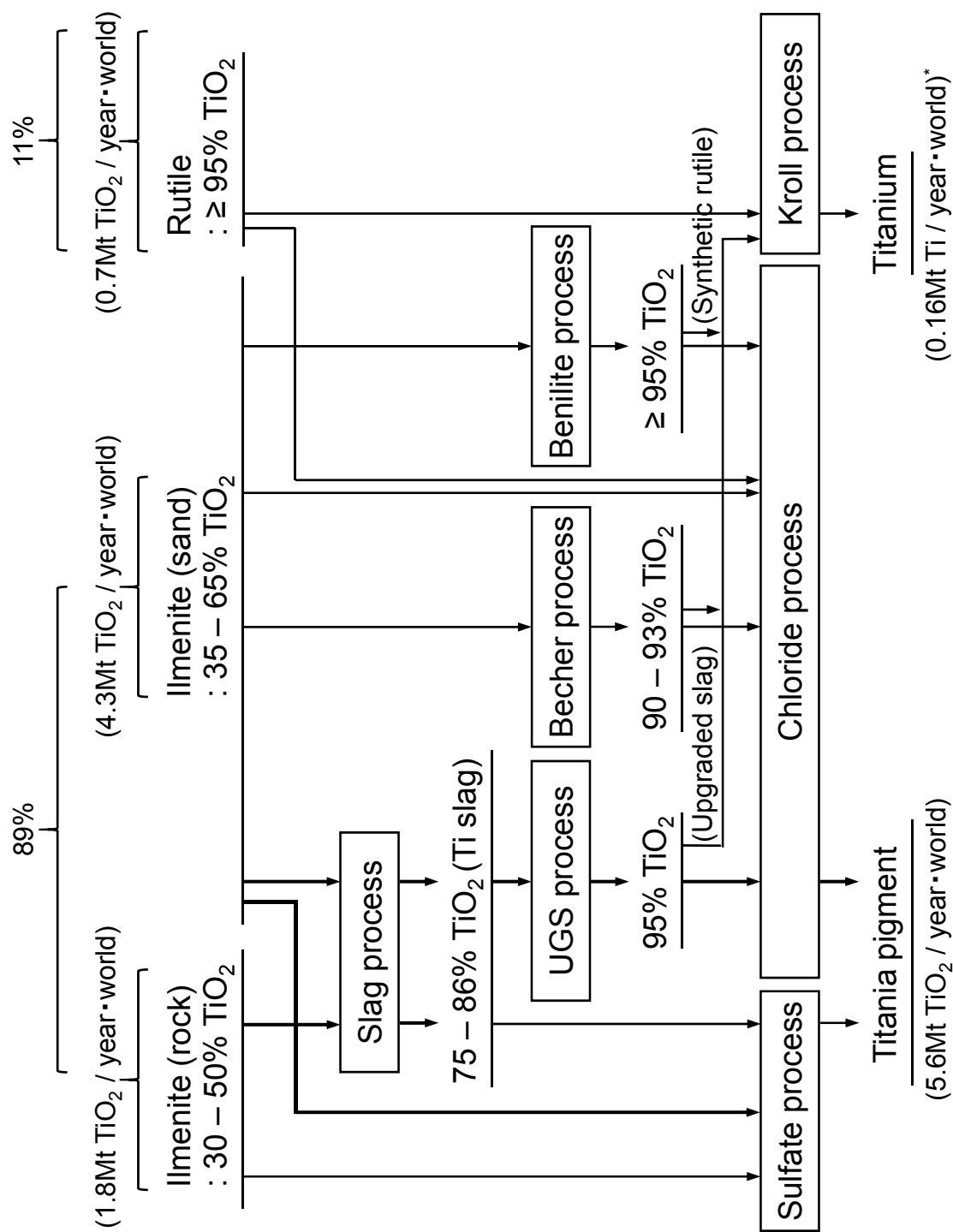
Figure 1-23 The current flowchart of titanium from titanium ore to titanium metal and titania pigment.

*: Ti produced in USA is excluded. The estimated Ti production in USA in 2010 was 0.015 Mt Ti / year

70
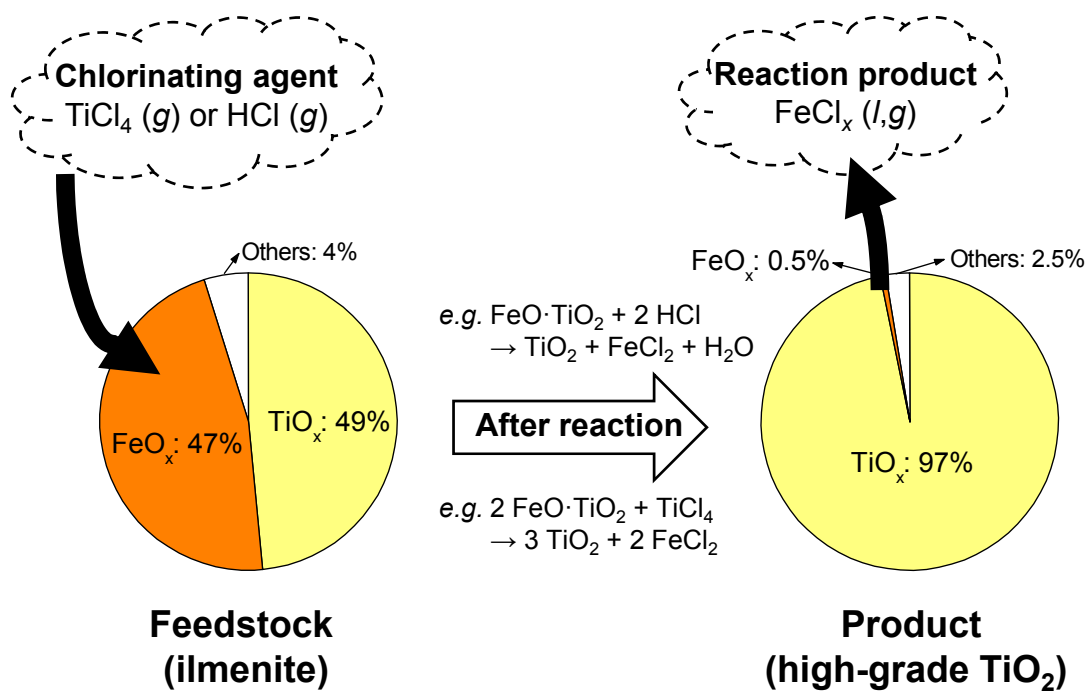
Figure 1-24 Schematic of the concept of the selective chlorination.
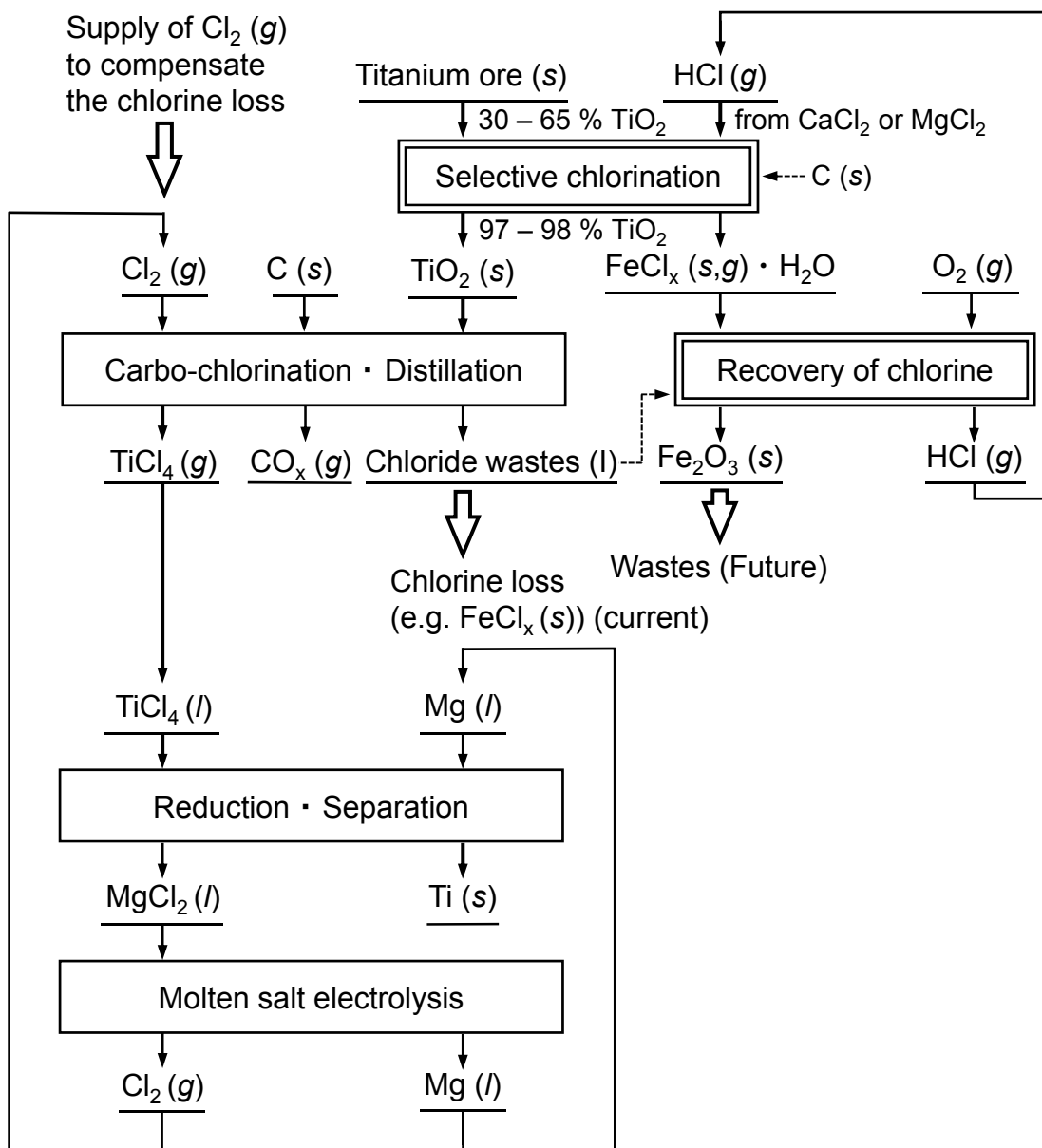
Figure 1-25 Flowchart of the novel selective chlorination process using CaCl$_2$ or MgCl$_2$ as chlorinating agent for upgrading titanium ore and the Kroll process from the viewpoint of circulation of chlorine gas and chloride waste.

Titanium ore (*s*)　　　Carbon (*s*)

↓ 30 – 65 % TiO_2　　　↓

Ti slag production

Oversea, or mining
on-site operation

↓　　　↓　　　↓

Ti slag (*l*)　Fe-C (*l*)　CO_x (*g*)

⇧

Supply of Cl_2 (*g*)
to compensate
the chlorine loss

Ti slag (*s*)　　　$TiCl_4$ (*g*) ◄── ☆ From carbo-
chlorination

↓ 75 – 86% TiO_2　　　↓

Selective chlorination ◄┈┈ (C (*s*), Cl_2 (*g*))

⇩

↓ 95 – 98 % TiO_2　　　↓

Cl_2 (*g*)　　C (*s*)　　TiO_2 (*s*)　　$FeCl_x$ (*s,g*)　　O_2 (*g*)

↓　　↓　　↓　　↓　　↓

Carbo-chlorination · Distillation　　　Recovery of chlorine

↓　　↓　　↓　　↓　　↓

$TiCl_4$ (*g*)　CO_x (*g*)　Chloride wastes (l)┈┤├─ Cl_2 (*g*)　　Fe_2O_3 (*s*)

↓ → ☆
To selective
chlorination

⇩

⇩

Chlorine loss (e.g. $FeCl_x$ (*s*))
(current)

Wastes
(future)

$TiCl_4$ (*l*)　　　　Mg (*l*)

↓　　　　　　↓

Reduction · Separation

↓　　　　　　↓

$MgCl_2$ (*l*)　　　　Ti (*s*)

↓

Molten salt electrolysis

↓　　　　　　↓

Cl_2 (*g*)　　　　Mg (*l*)

Figure 1-26 Flowchart of the novel environmentally friendly
selective chlorination process using $TiCl_4$ as chlorinating
agent for upgrading titanium ore and the Kroll process from
the viewpoint of circulation of chlorine gas and chloride waste.

Chapter 2 Thermodynamic consideration of the removal of iron from low-grade titanium ore through selective chlorination

As discussed in chapter 1, if high-grade TiO_2 feed can be produced directly from low-grade titanium (Ti) ore using a pyrometallurgical process, it can be used as a feedstock for titanium smelting. Among many upgrading processes, the selective chlorination process is one of the most effective methods. For these reasons, in chapter 2, thermodynamic study of the chlorination reactions of metal or oxides such as titanium oxides and iron oxides at elevated temperatures was carried out in order to consider the removal of iron from Ti ore using selective chlorination method. This thermodynamic consideration results in the development of an efficient method of removing iron from Ti ore by selective chlorination. In this chapter, in particular, various chlorination reactions were analyzed by utilizing chemical potential diagrams, and the applicability and usefulness of this thermodynamic study for analyzing the selective chlorination of Ti ore were demonstrated. Furthermore, chlorination reactions using various types of chlorinating agents were discussed from different viewpoints.

2.1 Fundamentals of chlorination reactions for oxides

2.1.1 Thermodynamic parameters of chlorination reaction

When considering the treatment of Ti ore at a high temperature, the influence of oxygen and H_2O vapor in the atmosphere, carbon in the system, and impurities in the ore must be taken into account. Especially for the chlorination reactions in a complex reaction system such as the chlorination of an ore, it is necessary to consider the reactions involving HCl gas and other various reactions, as well as the chlorination reactions involving the chlorinating agent directly supplied into the system.

When chlorination reactions of metal elements such as titanium or iron in the Ti ore are analyzed, partial pressure of oxygen (p_{O_2}) has to be considered in addition to the existence form of the iron oxides, the activity of the species, and partial pressure of chlorine (p_{Cl_2}) in the reaction system. Under certain conditions, the chlorination-

evaporation reactions of titanium or iron are dominated by the partial vapor pressure of the water (p_{H_2O}) and hydrogen chloride (p_{HCl}) owing to the large influence of the H_2O on the chlorination reactions. In addition, some chlorination reactions of specific metal elements proceed when the activity of the products of the chlorination reactions is decreased by acid-base reactions of the oxides or sulfate. Practically, the influence of the coexisting elements, such as impurities in the ore, also must be considered.

Chlorination reactions of oxides do not proceed by simply increasing the concentration of the Cl_2 gas at high temperature. To control the chlorination reaction, other parameters must be considered in addition to the p_{Cl_2} and reaction temperature (T). Specifically, it is impossible to discuss the chlorination of oxides appropriately if p_{O_2} is not controlled. However, in some research conducted in the past, the amount of chloride products evaporated in the reactions between Ti ore and Cl_2 gas at high temperature was evaluated without controlling or analyzing the p_{O_2} or p_{H_2O} in the reaction system.

Therefore, in this chapter, a thermodynamic discussion of the chlorination of oxides at high temperature was conducted by considering parameters such as p_{O_2}, p_{H_2O}, or p_{HCl} of the reactions in order to understand the removal of iron from Ti ore through selective chlorination. Specifically, the selective chlorination of the iron in Ti ore was discussed by utilizing the chemical potential diagram to analyze the various types of chlorination reactions systematically.

The thermodynamic data used in this chapter are mainly taken from the *Thermochemical Data of Pure Substances*, 3rd ed., edited by Barin.[1] The data required to construct the chemical potential diagrams in this chapter for the thermodynamic consideration are shown in Tables 2-1 and 2-2.

2.1.2 Vapor pressures of metal chlorides

If the metal reacts with Cl_2 gas, metal chloride (MCl_x) is produced because many metal elements (M) are thermodynamically stable as chlorides. The standard Gibbs energy of formation ($\Delta G^\circ_{f, MCl_x}$) is greatly negative value for many metal chlorides. In particular, alkaline metals or alkaline earth metals are chemically stable because their $\Delta G^\circ_{f, MCl_x}$ are large negative values. Among them, $CaCl_2$ and $NaCl$ are extremely thermodynamically stable chlorides.

As shown in Fig. 2-1, many metal chlorides have high vapor pressures. Among them, chlorides of iron (Fe), aluminum (Al), and Ti have high vapor pressures, and temperatures of several hundred kelvin are enough to surpass the boiling points of these chlorides. Therefore, when chlorides such as $FeCl_3$, $AlCl_3$, or $TiCl_4$ are produced, they can be transported and separated efficiently as a gas from the reaction system at high temperature.

Meanwhile, chlorides such as $CaCl_2$ and $NaCl$ have low vapor pressures, and they are difficult to separate by evaporation at 1100 K. These chlorides play important roles in several reactions that occur in a high-temperature reactor by reacting with other oxides and chlorides, because they remain as a condensed phase in the furnace, even for high-temperature treatments.

Although alkaline metal or alkaline earth metal chlorides act as chlorinating agents for chlorination reactions of ores, these chlorides can clog and corrode pipes or damage the refractory materials of chlorinator in practical processes. Therefore, in many cases, the chloride process applied in industry uses ores that contain low concentrations of alkaline metal or alkaline earth metal impurities.

2.1.3   Chlorination reactions of metal oxides

Figs. 2-2 (a) and (b) show the $\Delta G^\circ_{r,\ (2\text{-}3)}$ of the reactions in Eq. 2-3, obtained by combining the standard Gibbs formation energies (ΔG°_f) of Eqs. 2-1 and 2-2, plotted with temperature as the abscissa. The reactions shown as dotted lines in Fig. 2-2 do not obey Eq. 2-3 because they involve oxidation or reduction reactions of the metal element. However, the chlorination reaction of suboxides or the oxidation reaction of subchlorides often proceeds in practical processes. Therefore, these reactions are shown in the figure for reference, because some of them are important when considering practical chlorination reactions.

$$M\ (s) + x\ Cl_2\ (g)\ \ = MCl_{2x}\ (s,l,g) \tag{2-1}$$

$$\Delta G^\circ_{f,\ MCl_{2x},\ (2\text{-}1)}$$

$$M\ (s) + x/2\ O_2\ (g) = MO_x\ (s,l,g) \tag{2-2}$$

$$\Delta G^\circ_{f,\ MO_x,\ (2\text{-}2)}$$

$$1/x\ MO_x\ (s) + Cl_2\ (g) = 1/x\ MCl_{2x}\ (s,l,g) + 1/2\ O_2\ (g) \tag{2-3}$$
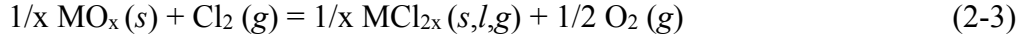
$$\Delta G^\circ_{r,\ (2\text{-}3)} = 1/x\ \Delta G^\circ_{f,\ MCl_{2x}} - 1/x\ \Delta G^\circ_{f,\ MO_x}$$

Because water vapor (H_2O) is one of the significant chemical species for the chlorination reactions in the practical processes, the chlorination reaction of water was also plotted in Fig. 2-2 and will be discussed later.

$$H_2O\ (g) + Cl_2\ (g) = 2\ HCl\ (g) + 1/2\ O_2\ (g) \tag{2-4}$$
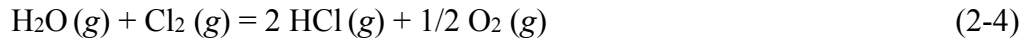
$$\Delta G^\circ_{r,\ (2\text{-}4)} = 2\ \Delta G^\circ_{f,\ HCl} - \Delta G^\circ_{f,\ H_2O}$$

As shown in Fig. 2-2, some oxides have a positive value for ΔG°_r for their chlorination reactions. In many cases, both oxides and chlorides are thermodynamically stable. However, as shown in Fig. 2-2, the difference in stability between the oxide and the chloride changes greatly depending on the metal element or its oxidation state. This analysis shows that metal elements can be effectively separated from each other if the formation reaction of chlorides or oxides is efficiently utilized by controlling the oxidation state of the metal elements.

Fig. 2-2 (a) shows that $FeCl_3$ or $TiCl_4$ are not produced by the reaction shown in Eq. 2-3, even though Fe_2O_3 or TiO_2 is placed in Cl_2 gas atmosphere at high temperatures ($\Delta G^\circ_{r,\ (2\text{-}3)} > 0$), respectively. Meanwhile, the figure also shows that chlorides are produced when oxides with low oxidation states of the metal elements (suboxides) such as FeO or TiO react with Cl_2 gas ($\Delta G^\circ_r < 0$). In addition, it is understood that subchlorides such as $TiCl_2$ can easily change into TiO_x by reacting with oxygen. The actual oxidation reaction of $TiCl_2$ is complex and can involve the production of $TiCl_4$ gas or metal oxychlorides; it is not limited to the production of Cl_2 gas.

2.1.4 Systematic consideration of the chlorination reactions of metal oxides

The stabilities of oxides and chlorides of iron and titanium at elevated temperatures calculated, and are shown in the chemical potential diagrams of the Fe-O-Cl and Ti-O-Cl systems in Figs. 2-3 and 2-4, respectively. These diagrams show the stability of the metal compounds when p_{Cl_2} is very high, at $p_{Cl_2} = 0.1$ atm, and are plotted with T as the abscissa and logarithm of p_{O_2} as the ordinate. Fe_2O_3 (s) and TiO_2 (s) are stable in the upper areas of the diagrams, where p_{O_2} is high. Therefore, even at a high p_{Cl_2}, the oxides of iron and titanium are stable, and the chlorination reactions by Cl_2 gas do not proceed if p_{O_2} is high.

Thus, the chlorination of oxides cannot be appropriately analyzed by only considering the p_{Cl_2}. The p_{O_2} in the reaction system, the activity (a_i) of the feed, and reaction products also have to be considered. As shown in Figs. 2-3 and 2-4, $FeCl_3$ (g) and $TiCl_4$ (g) are the stable chemical species when p_{Cl_2} is very high at 0.1 atm and p_{O_2} is low in the presence of carbon in the system. Therefore, the chlorination of the oxides by Cl_2 gas proceeds. The symbols ($\bigcirc, \triangle$) labeled with characters A or B in Figs. 2-3 and 2-4 correspond to the chemical potentials represented by the symbols labeled with A or B in Figs. 2-6 and 2-7, respectively, which will be discussed in the following section.

In industry, chlorination reactions are carried out under low p_{O_2} in the presence of carbon. For example, chlorination reactions in the chloride process or the Kroll process are carried out under low p_{O_2}. Specifically, chloride gases including $TiCl_4$ and $FeCl_3$ are produced by reacting Ti ore or an upgraded Ti ore with Cl_2 gas under a highly reducing atmosphere in the presence of graphite at an elevated temperature from 1073 K to 1273 K (carbo-chlorination).

From the examples mentioned above, for a systematic and reasonable consideration of the chlorination reactions of metal or oxides, it is convenient to utilize the chemical potential diagram plotted with the p_{O_2} and p_{Cl_2} as parameters.

Generally, when chemical reactions are considered, the chemical potentials of the reaction species, $\mu_i = \mu°_i + RT \ln a_i$ (or $\mu_i = \mu°_i + RT \ln p_i$), are used as the parameters for discussion. In this equation, R is the gas constant (8.314 J/mol·K). For instance, if $\mu_{O_2} = \mu°_{O_2} + RT \ln p_{O_2}$ is used as a parameter, then the physical quantity becomes the energy

scale with units of joules (J). This use of μ_i as parameter allows the driving force of the reactions to be compared with those in other reaction systems on an energy scale.

For an intuitive understanding of the absolute value of the chemical potential, a logarithmic partial pressure such as $\log p_{O_2}$ or $\log p_{Cl_2}$ is used as the parameter in this thesis. In addition, $\log p_{O_2}$ ($= \mu_{O_2}/2.303RT$) is standardized as the dimensionless value relative to oxygen gas in the standard state (oxygen gas at 1 atm), and this p_{O_2} is generally called the activity of oxygen (oxygen potential).

Furthermore, the p_{HCl} and p_{H_2O} have to be considered as parameters in some cases when the chlorination of oxides is discussed. When considering the reaction in Eq. 2-5, if $RT \ln (p_{HCl}^2 / p_{H_2O})$ is employed as a variable, the driving force for the chlorination of the oxide by HCl (g) can be systematically treated using the Gibbs energy change as the parameter. Fig. 2-5 (a) shows the MO_x (s)/MCl_{2x} (s,l,g) eq. described in Eq. 2-5 with $RT \ln (p_{HCl}^2 / p_{H_2O})$ as the ordinate and the linear temperature (T) as the abscissa.

$$1/x\ MO_x\ (s) + 2\ HCl\ (g) = 1/x\ MCl_{2x}\ (s,l,g) + H_2O\ (g) \tag{2-5}$$
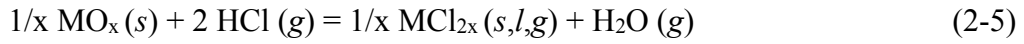
$$\Delta G^{\circ}_{r,\ (2\text{-}5)} = 1/x\ \Delta G^{\circ}_{f,\ MCl_{2x},\ (2\text{-}1)} + \Delta G^{\circ}_{f,\ H_2O} - 1/x\ \Delta G^{\circ}_{f,\ MO_x,\ (2\text{-}2)} - 2\ \Delta G^{\circ}_{f,\ HCl}$$

Chlorination of oxides by HCl gas is also discussed using $\log (p_{HCl}^2 / p_{H_2O})$ as a variable instead of $RT \ln (p_{HCl}^2 / p_{H_2O})$. Fig. 2-5 (b) plots the MO_x (s)/MCl_{2x} (s,l,g) eq. shown in Eq. 2-5 using $\log (p_{HCl}^2 / p_{H_2O})$ as the ordinate and the inverse temperature ($1/T$) as the abscissa. Figs. 2-5 (a) and (b) are essentially identical from the thermodynamic viewpoint. These figures (Figs. 2-5 (a) and (b)) show the driving force of the reactions for the MO_x (s)/MCl_{2x} (s,l,g) eq. in Eq. 2-3 with respect to the reactions for the H_2O (g)/HCl (g) eq. in Eq. 2-4 as the standard. Thermodynamically, the oxides in the lower region of the figure can be chlorinated by HCl gas, which acts as a reaction mediator, because p_{HCl} is higher for chlorides in the upper region than for chlorides in the lower region. If the vapor pressure of certain gas is below 0.001 atm, the reaction involving that gas as reactant is hard to proceed, because the amount of mass flux for the reaction is too low. Therefore, generally, if the value of $\log (p_{HCl}^2 / p_{H_2O})$ in Fig. 2-5 (b) is lower than -6, chlorination reaction by HCl gas is kinetically difficult owing to the low p_{HCl}. In addition, if the value of $\log (p_{HCl}^2 / p_{H_2O})$ is greater than -4, the H_2O (g)/HCl (g) eq. in the system controls the reactions in the system in some cases.

2.2 Consideration of chlorination methods utilizing the chemical potential diagram of oxygen and chlorine

In order to analyze the chlorination reactions of Ti ore using a simplified approach, reactions at constant temperature were considered in this section, with p_{Cl_2} and p_{O_2} as parameters.

2.2.1 Chlorination of iron oxides utilizing the chemical potential diagram of the Fe-O-Cl system

Fig. 2-6 shows the isothermal chemical potential diagram of the Fe-O-Cl system at 1100 K plotted with the logarithmic oxygen partial pressure (log p_{O_2}) as the ordinate and the logarithmic chlorine partial pressure (log p_{Cl_2}) as the abscissa. In addition, Fig. 2-7 shows the chemical potential diagram of the Ti-O-Cl system plotted for the identical temperature and with identical axes to those used for the Fe-O-Cl system. Details on the methods for construction of the chemical potential diagrams can be found in the references.[2-4]

In the vicinity of point A in Fig. 2-6, Fe_2O_3 (s) is thermodynamically stable (see point A in Fig. 2-3), where both p_{Cl_2} and p_{O_2} are high. This diagram also shows that when the p_{O_2} is high, chlorination of iron oxide does not proceed even when the pure Cl_2 gas was used.
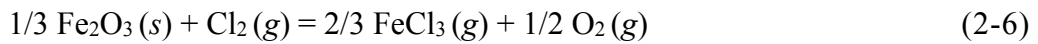
$$1/3\ Fe_2O_3\ (s) + Cl_2\ (g) = 2/3\ FeCl_3\ (g) + 1/2\ O_2\ (g) \qquad\qquad (2\text{-}6)$$
$$\Delta H^{\circ}_{r,\ (2\text{-}6)} = 95.1\ kJ,\ \Delta G^{\circ}_{r,\ (2\text{-}6)} = 24.4\ kJ\ at\ 1100\ K$$

Meanwhile, the vicinity of point B in Fig. 2-6 has high p_{Cl_2} and low p_{O_2}. If a strong chlorinating agent and carbon are both present in the system, the p_{O_2} in the system decreases to the p_{O_2} at point B in Fig. 2-6, and chlorination reactions occur (see point B in Fig. 2-3). In this case, the following chlorination reaction will proceed because $FeCl_3$ (g) is the thermodynamically stable chemical species, and Fe_2O_3 (s) is unstable.

$$1/3\ Fe_2O_3\ (s) + Cl_2\ (g) + C\ (s) = 2/3\ FeCl_3\ (g) + CO\ (g) \tag{2-7}$$
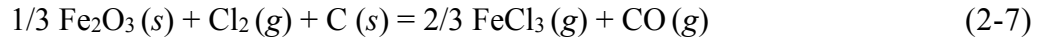
$\Delta H^{\circ}_{r,\ (2\text{-}7)} = -17.5$ kJ, $\Delta G^{\circ}_{r,\ (2\text{-}7)} = -184.7$ kJ at 1100 K

It is worth noting that the progress of the chlorination reaction of oxides becomes totally different depending on the p_{O_2} in the reaction system, even though pure Cl_2 gas is used.

2.2.2 Chlorination of titanium oxides utilizing the chemical potential diagram of the Ti-O-Cl system

A similar thermodynamic analysis can be conducted for titanium. The vicinity of point A in Fig. 2-7 has both high p_{Cl_2} and high p_{O_2}, and $TiO_2\ (s)$ is stable in this region; thus, there is no reaction with Cl_2 gas (see point A in Fig. 2-4). However, the stable phase is $TiCl_4\ (g)$ instead of $TiO_2\ (s)$ in the vicinity of point B in Fig. 2-7, where p_{O_2} is low. Therefore, if the p_{O_2} is low in the system because of the presence of carbon or another chemical species that lowers p_{O_2} in the reaction system, the following chlorination reaction will proceed:

$$1/2\ TiO_2\ (s) + Cl_2\ (g) + C\ (s) = 1/2\ TiCl_4\ (g) + CO\ (g) \tag{2-8}$$
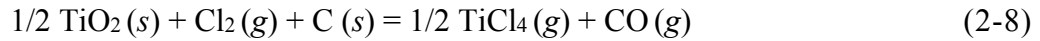
$\Delta H^{\circ}_{r,\ (2\text{-}8)} = -24.3$ kJ, $\Delta G^{\circ}_{r,\ (2\text{-}8)} = -151.9$ kJ at 1100 K

As mentioned before, the reactions in Eqs. 2-7 and 2-8 are utilized in industry and are called carbo-chlorination. Continuous chlorination reactions of titanium and iron oxides are conducted using a fluidized bed at a chemical potential in the vicinity of point B in Fig. 2-7.[5,6]

Although some stable oxides such as SiO_2 are not kinetically chlorinated, almost all oxides are chlorinated at the high p_{Cl_2} and low p_{O_2}. There are several interpretations of this reaction, but one representative explanation is as follows: it becomes easy for the oxides to react with Cl_2 gas because the activity of the metal (a_M) in the oxides is relatively increased under the low p_{O_2}.

It is possible to separate the chlorides produced by the chlorination reaction effectively by cooling the evolved gas, because the vapor pressures of chlorides are

different from each other depending on temperature, as shown in Fig. 2-1. Even though the boiling points of several chlorides such as $SnCl_4$ and $SiCl_4$ are close to the boiling point of $TiCl_4$, these chlorides can be separated through multi-step distillation. The processes using chlorides thus have the advantage of effective separation or purification, although they also have the disadvantage of high costs for processing facilities and maintenance, because the reaction environments become highly corrosive.

2.2.3   Consideration on chlorination reaction utilizing the chemical potential diagram of the H-O-Cl system

Fig. 2-8 shows the isothermal chemical potential diagram of the H-O-Cl system at 1100 K plotted with the log p_{O_2} as the ordinate and log p_{Cl_2} as the abscissa. If HCl gas exists in the reaction system, in some cases, chlorination of oxides proceeds according to the reaction in Eq. 2-5. In this case, analysis of the chlorination reactions occurring under the H_2O (g)/HCl (g) eq. in Fig. 2-8 becomes important, because the H_2O (g)/HCl (g) eq. determines the chemical potential in the system. The line of H_2O (g)/HCl (g) eq., which has a slope of 2 in the potential diagram, is located near the line connecting points A and C in the figure, and the potential region near this equilibrium is important for discussing the chlorination reactions in practical systems containing H_2O gas.

Chlorination of oxides proceeds under the H_2O (g)/HCl (g) eq. in many cases, because oxygen or hydrogen (or water) exists in the reaction system. In some cases, the chlorination reactions under the H_2O (g)/HCl (g) eq. are the dominant reactions in actual industrial processes under certain conditions. Therefore, the H_2O (g)/HCl (g) eq. is also plotted in the figures for iron (Fig. 2-6) and titanium (Fig. 2-7) that were previously discussed, because it is important in the consideration of the actual chlorination reactions.

2.3 Thermodynamic consideration of the reaction for the removal of iron from titanium ore using the selective chlorination method

2.3.1 Selective chlorination utilizing chemical potential diagram

Fig. 2-9 was constructed by overlapping the chemical potential diagrams of the Fe-O-Cl and Ti-O-Cl systems explained previously. (*see* Figs. 2-6 and 2-7) The hatched region in the figure is the chemical potential region where both $FeCl_x$ (x=2,3) and TiO_2 are stable. If the chemical potentials in the reaction system can be fixed in the hatched region in Fig. 2-9 or a region nearby, only iron will be chlorinated as iron chlorides, and titanium will remain as TiO_2 from compound that consists of oxides of iron and titanium. There are conditions under which the progress of the chlorination of oxides is retarded because the activity of FeO_x (a_{FeO_x}) is lowered in the system owing to the formation of complex oxides by a reaction between FeO_x and TiO_x. However, it is not inappropriate to consider FeO_x and TiO_x separately for chlorination reactions, because the $\Delta G°$ of the mixture for reaction between FeO_x and TiO_x is a small negative value. Table 2-3 lists the Gibbs energy changes of reactions in the Fe-Ti-O system from 1000 K to 1200 K.[1,7,8]

The vapor pressure of $FeCl_2$ is high, 0.09 atm, at 1100 K (*see* Fig. 2-1), while the vapor pressure of TiO_2 is very small and can be neglected.[1] Therefore, thermodynamically, iron can be selectively removed from Ti ore as chloride gas through chlorination reactions. In general, this reaction is called selective chlorination.

2.3.2 Selective chlorination of titanium ore by HCl

Fig. 2-9 shows the H_2O (*g*)/HCl (*g*) eq. that was shown in Fig. 2-8. This equilibrium line passes through a region in the vicinity of the hatched region mentioned above, where selective chlorination of iron proceeds. Therefore, if a compound ($FeO_x \cdot TiO_2$) that consists of iron and titanium oxides reacts with HCl (*g*) at 1100 K, chlorination of iron will proceed according to the following reaction.

$$FeO_x \cdot TiO_2 \, (s) + 2x \, HCl \, (g) = FeCl_{2x} \, (l) + TiO_2 \, (s) + x \, H_2O \, (g) \tag{2-9}$$
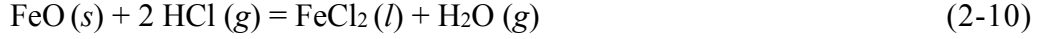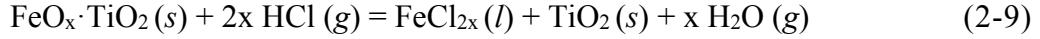
$$FeO \, (s) + 2 \, HCl \, (g) = FeCl_2 \, (l) + H_2O \, (g) \tag{2-10}$$
$\Delta H^\circ_{r, \, x=1, \, (2\text{-}10)} = -77.6$ kJ, $\Delta G^\circ_{r, \, x=1, \, (2\text{-}10)} = 3.72$ kJ at 1100 K[1]
$\Delta H^\circ_{r, \, x=1, \, (2\text{-}10)} = -77.2$ kJ, $\Delta G^\circ_{r, \, x=1, \, (2\text{-}10)} = 0.76$ kJ at 1100 K[8]
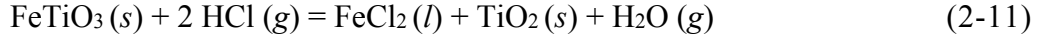
$$FeTiO_3 \, (s) + 2 \, HCl \, (g) = FeCl_2 \, (l) + TiO_2 \, (s) + H_2O \, (g) \tag{2-11}$$
$\Delta H^\circ_{r, \, x=1, \, (2\text{-}11)} = -56.9$ kJ, $\Delta G^\circ_{r, \, x=1, \, (2\text{-}11)} = 14.7$ kJ at 1100 K[1]

As shown in Eqs. 2-10 and 2-11, from the thermodynamic analysis, when HCl is used as a chlorinating agent, it is expected that the iron in low-grade Ti ore will be selectively chlorinated and removed as gaseous $FeCl_2$ owing to the high vapor pressure at 1100 K, and TiO_2 (s) will be produced after selective chlorination.

2.3.3   Selective chlorination of titanium ore by CaCl₂

Fig. 2-10 shows the chemical potential diagram of the Ca-O-Cl system at 1100 K. The chemical equilibrium corresponding to the CaO (s)/$CaCl_2$ (l) eq. is located at the low p_{Cl_2} side at an identical p_{O_2} to that of the H_2O (g)/HCl (g) equilibrium. As a result, $CaCl_2$ has less chlorinating power than HCl when the activity of CaO (a_{CaO}) is unity. However, if the a_{CaO} decreases to a very small value, the equilibrium line corresponding to CaO (s)/$CaCl_2$ (l) eq. in the figure shifts to the high p_{Cl_2} side. This chemical potential shifts sometimes occur when CaO reacts with an acidic oxide to form stable complex compounds.

For example, complex compounds such as $CaTiO_3$ are produced by the reaction between CaO and TiO_2 when a large excess amount of TiO_2 is present in the system. Thermodynamically, the a_{CaO} is very low when TiO_2 and $CaTiO_3$ coexist, and it becomes about $a_{CaO} = 6.6 \times 10^{-5}$ at 1100 K.

The chemical potential line of the TiO_2 (s)/$CaTiO_3$ (s)/$CaCl_2$ (l) eq. is also shown in Fig. 2-10. This chemical potential line is located at almost the same position as the line for the H_2O (g)/HCl (g) eq. discussed above. In other words, $CaCl_2$ works along with HCl as chlorinating agent according to the reaction shown in Eq. 2-12, for example, if the a_{CaO}

decreases to 6.6×10^{-5} in the reaction system. In addition, the vapor pressure of $FeCl_2$ (l) at 1100 K is 0.09 atm[1], which is high enough that the $FeCl_2$ (l) will evaporate. As a result, $FeCl_2$ (l) is removed as $FeCl_2$ (l,g) at 1100 K. Under some conditions, the activity of $FeCl_2$ (l) will decrease because the majority of the vaporized $FeCl_2$ (l) will solidify at the low temperature part of the reactor. Therefore, the reaction shown in Eq. 2-12 will proceed, and the thermodynamic analysis shows that when $CaCl_2$ is used as a chlorinating agent in a reaction system containing a large amount of TiO_2 at 1100 K, iron in the low-grade Ti ore will be removed as $FeCl_2$ (l,g) and $CaTiO_3$ (s) will be produced.

$$FeO\ (s) + TiO_2\ (s) + CaCl_2\ (l) = FeCl_2\ (l) + CaTiO_3\ (s) \qquad (2\text{-}12)$$
$$\Delta H°_{r,\ (2\text{-}12)} = 26.7\ kJ,\ \Delta G°_{r,\ (2\text{-}12)} = 8.3\ kJ\ at\ 1100\ K^{[1]}$$
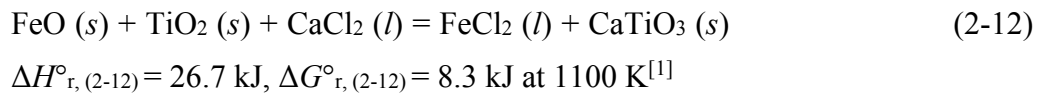
$CaCl_2$ is a hygroscopic chloride, which means that it adsorbs H_2O strongly. Practically, a large amount of H_2O is contained in the commercially available $CaCl_2$. Therefore, from Fig. 2-10, it is expected that HCl can be produced from $CaCl_2 \cdot (H_2O)_n$ when the a_{CaO} is sufficiently lowered in the reaction system. For example, the formation of $CaTiO_3$ described in Eq. 2-13 accelerates the generation of HCl gas by the reaction between $CaCl_2$ and H_2O. This suggests that the HCl (g) produced from the $CaCl_2$ can also be used as a chlorinating agent for the selective removal of iron from low-grade Ti ore to produce high-grade TiO_2 feed. The detailed thermodynamic analysis for the selective chlorination of low-grade TiO_2 using $CaCl_2$ will be discussed with some experimental results in chapter 3.

$$CaCl_2\ (l) + H_2O\ (g) + TiO_2\ (s) = 2\ HCl\ (g) + CaTiO_3\ (s) \qquad (2\text{-}13)$$
$$\Delta H°_{r,\ (2\text{-}13)} = 104.3\ kJ,\ \Delta G°_{r,\ (2\text{-}13)} = 4.6\ kJ\ at\ 1100\ K^{[1]}$$
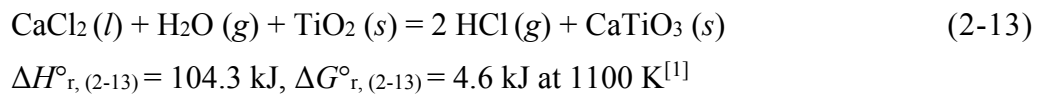
2.3.4 Selective chlorination of titanium ore by $MgCl_2$

Based on these thermodynamic calculation results, $MgCl_2$ can also be used as a chlorinating agent for selective chlorination, because the position of the line corresponding to the MgO (s)/$MgCl_2$ (l) eq. is almost identical to that of the H_2O (g)/ HCl (g) eq. as shown in Fig. 2-11. In addition, Fig. 2-11 shows that when $MgCl_2$ is used

as a chlorinating agent, iron in the low-grade Ti ore can be removed as iron chloride regardless of the activity of the MgO (a_{MgO}) produced by the reaction shown in Eq. 2-14.

$$FeO\ (s,\ in\ ore) + MgCl_2\ (l) = FeCl_2\ (l) + MgO\ (s) \qquad (2\text{-}14)$$

$$\Delta G°_{r,\ (2\text{-}14)} = -23\ kJ\ at\ 1000\ K^{[1]}$$
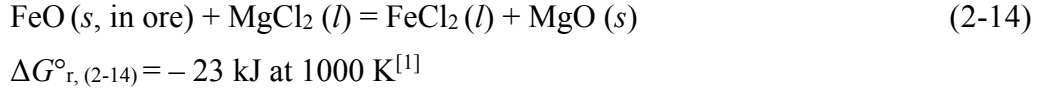
MgCl$_2$ is also a hygroscopic chloride. As a result, it is expected that when MgCl$_2$ is used as the chlorinating agent, HCl can be generated from the MgCl$_2$ regardless of a_{MgO}, as shown in Eq. 2-15, because the MgO (s)/MgCl$_2$ (l) eq. is located at right side of the H$_2$O (g)/HCl (g) eq. under an identical p_{O_2}. The HCl (g) produced from the MgCl$_2$ can also be used as a chlorinating agent for the selective removal of iron from low-grade Ti ore to produce high-grade TiO$_2$ feed. If CaCl$_2$ is used as a chlorinating agent, a large amount of HCl (g) will be produced even without intentional introduction of water vapor into the system, because CaCl$_2$ contains a large amount of H$_2$O as an impurity. However, if high-purity MgCl$_2$ is used as the chlorinating agent, introduction of H$_2$O gas into the reaction system is required in order to accelerate the HCl gas production. A detailed thermodynamic analysis of the selective chlorination of low-grade TiO$_2$ using MgCl$_2$ will be discussed with some experimental results in chapter 5.

$$MgCl_2\ (l) + H_2O\ (g) = 2\ HCl\ (g) + MgO\ (s) \qquad (2\text{-}15)$$

$$\Delta G°_{r,\ (2\text{-}15)} = -19\ kJ\ at\ 1000\ K^{[1]}\ under\ a_{MgO} = 1$$
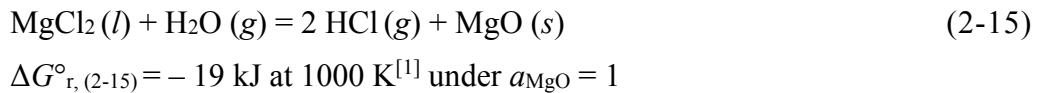
2.3.5   Selective chlorination of titanium ore by TiCl$_4$

On a basis of the thermodynamic analysis, as shown in Fig. 2-12, it is anticipated that TiCl$_4$ will also work as a chlorinating agent for FeO$_x$. In this case, it is expected that iron oxides in Ti ore will be directly chlorinated according to the following reaction, for example:

$$FeO_{3/2}\ (s,\ in\ ore) + 3/4\ TiCl_4\ (g) = FeCl_3\ (g) + 3/4\ TiO_2\ (s) \qquad (2\text{-}16)$$
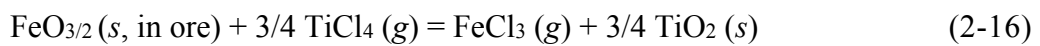
$$\Delta H°_{r,\ (2\text{-}16)} = 10.2\ kJ,\ \Delta G°_{r,\ (2\text{-}16)} = -49.1\ kJ\ at\ 1100\ K^{[1]}$$

$$FeO\ (s,\ in\ ore) + 1/2\ TiCl_4\ (g) = FeCl_2\ (l) + 1/2\ TiO_2\ (s) \qquad (2\text{-}17)$$
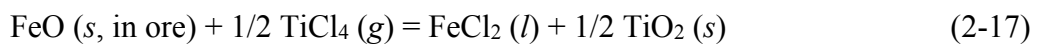
$$\Delta H^\circ_{r,\,(2\text{-}17)} = -\,106.6\ \text{kJ},\ \Delta G^\circ_{r,\,(2\text{-}17)} = -\,69.1\ \text{kJ at 1100 K}^{[1]}$$

Generally, chlorination reaction of the FeO_x is conducted under a low p_{O_2} atmosphere in the presence of carbon. However, the chlorination reaction by $TiCl_4$ shown in Eq. 2-16 does not necessarily have to be conducted under a low p_{O_2} atmosphere. As shown in Fig. 2-12, this chlorination reaction of the FeO_x by $TiCl_4$ in the potential region for oxidation-selective-chlorination proceeds under a high partial pressure of oxygen (high p_{O_2}), for example, p_{O_2} of about 10^{-5} atm (where C or CO does not exist).

Furthermore, reactions shown in Eqs. 2-16 and 2-17 are p_{Cl_2} independent reactions, which do not involve any redox reactions of chlorides. When the chemical potential in the system is fixed by the chemical equilibrium corresponding to the TiO_2 (*s*)/$TiCl_4$ (*g*)/CO (*g*)/CO_2 (*g*) eq. (point D in Fig. 2-12), selective chlorination of FeO (*s*) by $TiCl_4$ (*g*) is feasible. This carbo-selective-chlorination by $TiCl_4$ (*g*) in the presence of carbon can also be applied for upgrading Ti ore. A detailed thermodynamic analysis of the selective chlorination of low-grade TiO_2 using $TiCl_4$ under reducing and oxidative atmospheres will be introduced and discussed in chapters 6 and 7, respectively, along with some experimental results.

Currently, in the Ti smelting process used in industry, a large amount of $TiCl_4$ is circulated in the system, and oxide feeds are supplied to the chlorinator, and mixed with carbon. Therefore, it is easy to use $TiCl_4$ as a chlorination agent. When $TiCl_4$ reacts with a mixture of carbon and low-grade Ti ore containing a large amount of iron, the high-grade TiO_2 and $FeCl_x$ produced as reaction products are obtained simultaneously. Treatment of the large amount of $FeCl_x$ produced and recovery of the chlorine are the problems that must be solved in the future. However, as an option for using low-grade Ti ore as a feedstock for Ti smelting without producing aqueous waste solutions, the selective chlorination process by $TiCl_4$ discussed in this section has the potential to be developed into a practical process in the future.

2.3.6　Chlorination of titanium ore by CCl_4

Generally, CCl_4 is considered a strong chlorinating agent, as well. Therefore, this section provides a thermodynamic consideration of the chlorination of low-grade Ti ore

using CCl4. Fig. 2-13 shows the chemical potential diagram of the C-O-Cl system at 700 K. As shown in Fig. 2-13, the CO_2 (*g*)/CCl_4 (*g*) eq. is located at the far right side of the FeO_x (*s*)/$FeCl_y$ (*s,g*) eq. and TiO_2 (*s*)/$TiCl_4$ (*g*) eq. Therefore, when the chlorination of low-grade Ti ore using CCl_4 is conducted at elevated temperature, it is expected that the iron and titanium in the ore will be chlorinated simultaneously by the reactions shown in Eqs. 2-18 and 2-19, respectively. From thermodynamic viewpoint, these reactions are identical to carbo-chlorination of $FeTiO_x$ (or FeO_x – TiO_2 mixture) by Cl_2 in the presence of carbon. In other words, CCl_4 cannot be used as a chlorinating agent for the selective removal of iron from low-grade Ti ore.
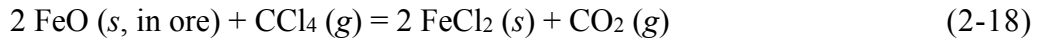
$$2 \text{ FeO } (s, \text{ in ore}) + CCl_4 \text{ } (g) = 2 \text{ FeCl}_2 \text{ } (s) + CO_2 \text{ } (g) \tag{2-18}$$
$$\Delta H^\circ_{r, (2\text{-}18)} = -430.7 \text{ kJ}, \Delta G^\circ_{r, (2\text{-}18)} = -446.3 \text{ kJ at 700 K}^{[1]}$$
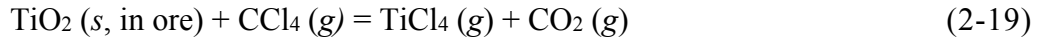
$$TiO_2 \text{ } (s, \text{ in ore}) + CCl_4 \text{ } (g) = TiCl_4 \text{ } (g) + CO_2 \text{ } (g) \tag{2-19}$$
$$\Delta H^\circ_{r, (2\text{-}19)} = -117.5 \text{ kJ}, \Delta G^\circ_{r, (2\text{-}19)} = -254.8 \text{ kJ at 700 K}^{[1]}$$

As explained in chapter 1, high-grade TiO_2 feed is chlorinated by Cl_2 gas in the presence of carbon for the production of $TiCl_4$ in the carbo-chlorination process of the chloride process or the Kroll process. However, the thermodynamic analysis results show that CCl_4 can also be used as a chlorinating agent for the carbo-chlorination process. In addition, it is expected that some other impurities in the low-grade Ti ore can also be chlorinated by CCl_4, because the chemical potentials established by CCl_4 (*g*) injected into the reaction system locate at the high p_{Cl_2} and low p_{O_2} region, as shown in Fig. 2-13.

2.3.7   Conditions for chlorination of iron oxides and titanium oxides

On the basis of the discussion so far, Table 2-4 summarizes the conditions for chlorination of iron oxides and titanium oxides based on the thermodynamic calculations. As shown in the table, for chlorination of oxides at high temperature, the effective chlorination reaction does not proceed when only p_{Cl_2} is controlled, and it is important to control p_{O_2} in the reaction system, as well. In addition, if p_{Cl_2} and p_{O_2} are precisely and simultaneously controlled, a particular metal element can be selectively chlorinated.

If the chemical potential diagrams of two metal elements are overlapped, as in Fig. 2-9, a chemical potential region in which only one type of metal element is chlorinated can be found, because the standard Gibbs formation energies of chlorides ($\Delta G^\circ_{f, MCl_x}$) and oxides ($\Delta G^\circ_{f, MO_y}$) are unique value for each element. Therefore, only one type of metal element can be selectively chlorinated and separated if the chemical potentials of p_{Cl_2} and p_{O_2} are properly controlled and maintained simultaneously in a potential region where just one type of metal element is chlorinated in the reaction system.

However, practically, the chemical potential regions that can be realized for industrial processes with inexpensive methods are limited. Specifically, the conditions of $p_{Cl_2} = 0.1 - 1$ atm, $p_{O_2} = 0.1 - 1$ atm, the H_2O/HCl eq., the C/CO_x eq., the CO/CO_2 eq., the MO_x/MCl_y eq., and so on are economically feasible. In addition, the chemical potential in the system can be controlled by equilibrium such as the CaO (in $CaTiO_3$)/$CaCl_2$ eq., as previously discussed. The chlorination reaction also proceeds under the MO_x(in compound)/MCl_y eq. in actual industrial processes. For example, when the products (MO_x) of the chlorination reaction are nonvolatile stable complex oxides and also chlorides with high vapor pressures, the selective chlorination reaction proceeds preferentially.

Fig. 2-14 shows the chemical potentials of some representative metal chlorides that can potentially act as chlorinating agents specifically for the selective chlorination reactions. The chemical potentials determined by the $MO_x/MCl_y/C/CO$ eq. are shown using ◆ symbols in the figure. As shown in figure, p_{Cl_2} is greatly changed in the reaction system under the coexistence of different salt species.

2.4 Summary

In chapter 2, thermodynamic study of the chlorination reactions of metal or oxides at elevated temperature was carried out in order to consider the removal of iron directly from Ti ore through selective chlorination. In particular, various chlorination reactions were analyzed by utilizing the chemical potential diagrams, which are found to be applicable and useful for analyzing the selective chlorination of Ti ore. Furthermore, chlorination reactions with various types of chlorinating agents were discussed from various viewpoints. It was shown that the selective chlorination of iron from Ti ore is

thermodynamically feasible and effective for upgrading Ti ore with HCl gas, $CaCl_2$, or $MgCl_2$ as the chlorinating agent. Further thermodynamic analysis showed that under certain conditions, $TiCl_4$ is applicable as a chlorinating agents for directly removing and separating the iron in the ore as iron chlorides by chlorination. The results shown in this study give useful information for developing a process for upgrading low-grade Ti ore through dry method that does not produce any aqueous waste solution, and this dry process could be applied as an upgrading process to produce feed for Ti smelting.

References

[1]   I. Barin: "*Thermochemical Data of Pure Substances*", 3rd ed., VCH Verlagsgesellschaft mbH, Weinheim, Germany, 1995.

[2]   T.H. Okabe and T. Oishi: "*Basic and Application of Thermodynamics and Reaction Kinetics for Materials Processing*", The Mining and Materials Processing Institute of Japan, Kyoto, Japan, 2004. (in Japanese)

[3]   D.R. Gaskell: "*Introduction to the Thermodynamics of Materials*", 3rd ed., Taylor & Francis, Washington, USA, 1995.

[4]   M. Takahashi and N. Masuko: Soda Chlor., 2003, vols. 11–12, pp. 276–294. (in Japanese)

[5]   F. Habashi: "*Handbook of Extractive Metallurgy*", VCH Verlagsgesellschaft mbH–A Wiley, Weinheim, 1997.

[6]   J.H. Braun, A. Baidins, and R.E. Marganski: "*TiO_2 pigment technology: a review*", Prog. Org. Coat., 1992, vol. 20, pp. 105–138.

[7]   A. Roine: "*HSC Chemistry® 6.1 Outokumpu HSC Chemistry for Windows*", version 6.1, Outokumpu Research Oy Information Center, Finland, 2006.

[8]   A. Roine et al.: "*HSC Chemistry® version 7.11*", Outotec Oy Information Center, Finland, 2011.

[9]   J. Kang and T.H. Okabe: "*Thermodynamic Consideration of the Removal of Iron from Titanium Ore by Selective Chlorination*", Metall. Trans. B, 2014 (in print)

[10]   J. Kang and T.H. Okabe: "*Upgrading Titanium Ore Through Selective Chlorination Using Calcium Chloride*", Metall. Trans. B, 2013, vol. 44B (3), pp. 516-527.

[11]   J. Kang and T.H. Okabe: "*Removal of Iron from Titanium Ore through Selective Chlorination Using Magnesium Chloride*", Meter. Trans., 2013, vol. 54 (8), pp. 1444-1453.

[12]   J. Kang and T.H. Okabe: "*Production of Titanium Dioxide Directly from Titanium Ore Through Selective Chlorination Using Titanium Tetrachloride*", Meter. Trans., 2014, vol. 55 (3), pp. 591-598.

[13]   J. Kang and T.H. Okabe: "*Removal of Iron from Titanium Ore by $TiCl_4$ under High Oxygen Potential*", International Journal of Mineral Processing, 2014 (submitted).

[14]   T.H. Okabe and J. Kang: "*Thermodynamic Study on Chlorination Reactions of Oxides at Elevated Temperatures*", Molten Salts, 2013, vol. 56 (1), pp. 15-26. (in Japanese)

Table 2-1 Thermodynamic properties of selected oxides at 1100 K.[1]

Species	State	$\Delta H^{\circ}{}_{f}$ / kJ·mol^{-1}	$\Delta S^{\circ}{}_{f}$ / J·(mol·K)$^{-1}$	$\Delta G^{\circ}{}_{f}$ / kJ·mol^{-1}
Al_2O_3	s (α)	-1692.711	-331.426	-1328.142
CO	g	-112.619	87.670	-209.056
CO_2	g	-394.837	0.983	-395.918
CaO	s	-634.486	-103.365	-520.784
FeO	s	-270.332	-63.294	-200.709
Fe_3O_4	s	-1091.822	-299.515	-762.355
Fe_2O_3	s	-808.651	-247.883	-535.980
H_2O	g	-248.461	-55.721	-187.168
MgO	s	-608.783	-115.932	-481.258
Na_2O	s	-412.431	-131.976	-267.257
SiO_2	s	-902.349	-172.277	-712.844
TiO	s	-537.296	-91.037	-437.155
TiO_2	s (rutile)	-938.413	-175.910	-744.912
$FeTiO_3$	s	-1229.486	-248.071	-956.608

[1] : I. Barin, Thermochemical Data of Pure Substances, 3rd ed.,
      (Weinheim, Federal Republic of Germany, VCH Verlagsgesellschaft mbH, 1995).

Table 2-2 Thermodynamic properties of selected chlorides at 1100 K.[1]

Species	State	ΔH°_{f} / kJ·mol^{-1}	ΔS°_{f} / J·(mol·K)$^{-1}$	ΔG°_{f} / kJ·mol^{-1}
AlCl$_3$	g	-598.963	-65.223	-527.218
CaCl$_2$	l	-758.481	-117.612	-629.108
	g	-478.519	16.945	-497.158
FeCl$_2$	l	-288.657	-69.098	-212.649
	g	-151.279	36.006	-190.886
FeCl$_3$	g	-261.633	-27.444	-231.445
HCl	g	-94.594	6.199	-101.413
MgCl$_2$	l	-595.010	-112.599	-471.151
	g	-405.724	8.345	-414.904
NaCl	l	-377.392	-60.656	-310.670
	g	-192.461	45.735	-242.769
SiCl$_4$	g	-658.959	-128.175	-517.967
TiCl$_2$	s	-504.277	-149.128	-340.236
	g	-241.244	18.970	-262.111
TiCl$_4$	g	-761.788	-119.190	-630.679

[1] : I. Barin, Thermochemical Data of Pure Substances, 3rd ed.,
     (Weinheim, Federal Republic of Germany,VCH Verlagsgesellschaft mbH, 1995).

Table 2-3 The Gibbs energy changes of reactions
in the Fe-Ti-O system from 1000 K to 1200 K.

Reaction	Gibbs energy change of reaction, ΔG°_r / kJ·mol^{-1}			Ref.
	1000 K	1100 K	1200 K	
$FeO\ (s) + TiO_2\ (s) = FeTiO_3\ (s)$	-11.9	-11.0	-10.1	Barin[1]
$Fe_2O_3\ (s) + TiO_2\ (s) = Fe_2TiO_5\ (s)$	-1.4	-1.9	-2.4	HSC 6.1[7]
	1.8	1.3	0.8	HSC 7.1[8]
$2\ FeO\ (s) + TiO_2\ (s) = Fe_2TiO_4\ (s)$	-19.3	-18.4	-17.5	Barin[1]
	-25.4	-25.1	-24.9	HSC 7.1[8]
$FeO\ (s) + 2\ TiO_2\ (s) = FeTi_2O_5\ (s)$	76.5	101.7	128.8	HSC 7.1[8]

Table 2-4 Various conditions for the chlorination of iron oxides and titanium oxide at elevated temperatures.[9-14]

Feed materials	Chlorinating agent				
	Cl_2	$Cl_2 + C$	$TiCl_4$	HCl	MCl_x (M = **Ca, Mg,** ⋯)
Symbols in Figs. 2-3 – 2-10, 2-12, 2-14	O	△	▨	☆	◆
FeO_x	× ($\Delta G^{\circ} > 0$)	◎ ($\Delta G^{\circ} << 0$) Current $TiCl_4$ production process	◎ ($\Delta G^{\circ} << 0$)	O ($\Delta G^{\circ} \sim 0$)	O ($\Delta G^{\circ} \sim 0$)
			Selective chlorination of iron is feasible		
TiO_2	× ($\Delta G^{\circ} > 0$)	◎ ($\Delta G^{\circ} << 0$)	× ($\Delta G^{\circ} > 0$)	× ($\Delta G^{\circ} > 0$)	× ($\Delta G^{\circ} >> 0$)
Notes	high p_{Cl_2} high p_{O_2}	high p_{Cl_2} low p_{O_2}	$p_{Cl_2}{}^2/p_{O_2}$ = const	$p_{Cl_2}{}^2/p_{O_2}$ = const	$p_{Cl_2}{}^2/p_{O_2}$ = const
		Employed in Kroll process and Chloride process (Dupont)	Chapter 6-8	Chapter 3, 5	Chapter 3-5

Figure 2-1 Temperature dependence of the vapor pressures
of some selected metal chlorides.

Temp. discussed in Figs. 2-6 - 2-10, 2-12, 2-14 (1100 K)

(a)

Temperature, T' / °C
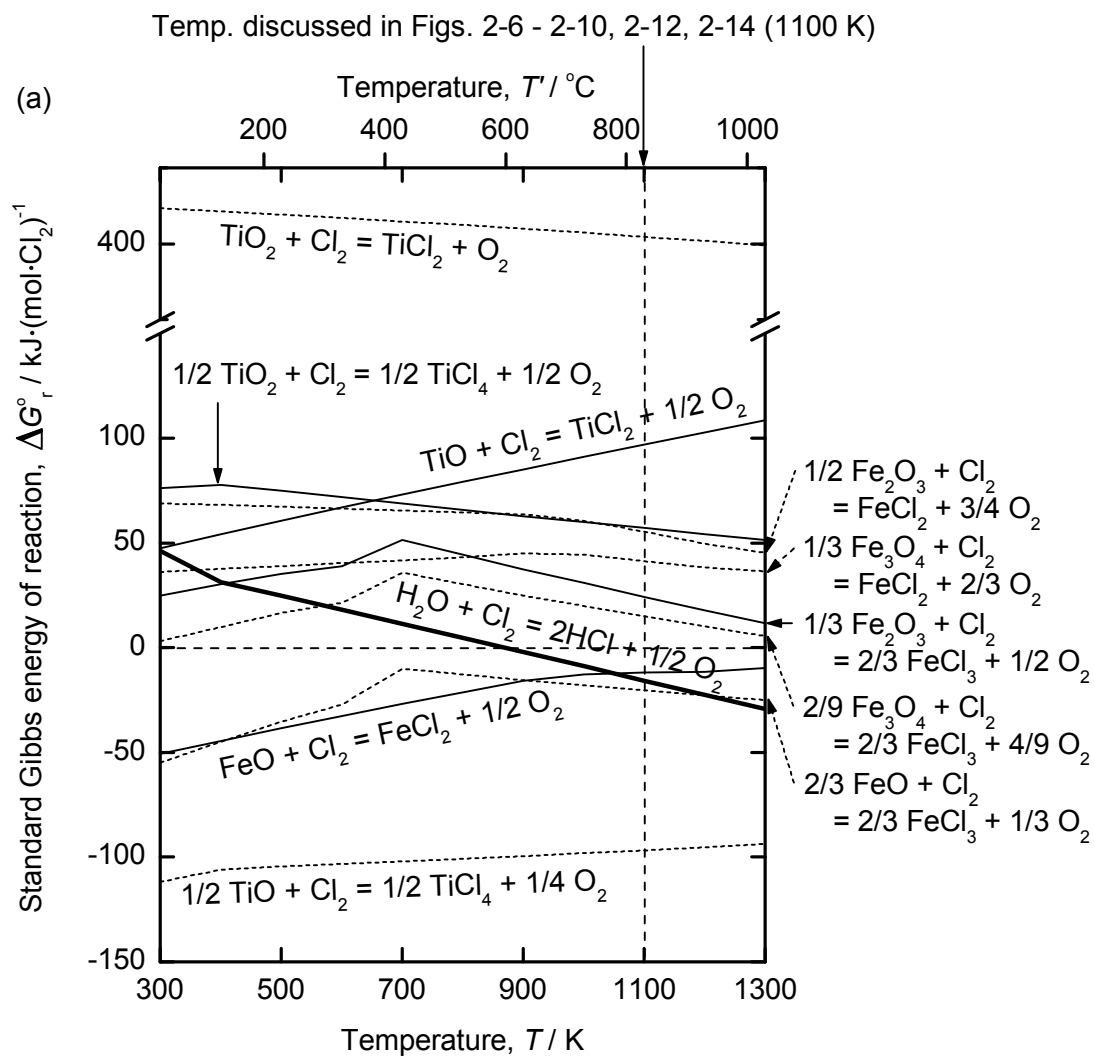
Figure 2-2 (a) Standard Gibbs energy of reaction (ΔG°_{r}) for Ti and Fe compounds.

Temp. discussed in Figs. 2-6 - 2-10, 2-12, 2-14 (1100 K)
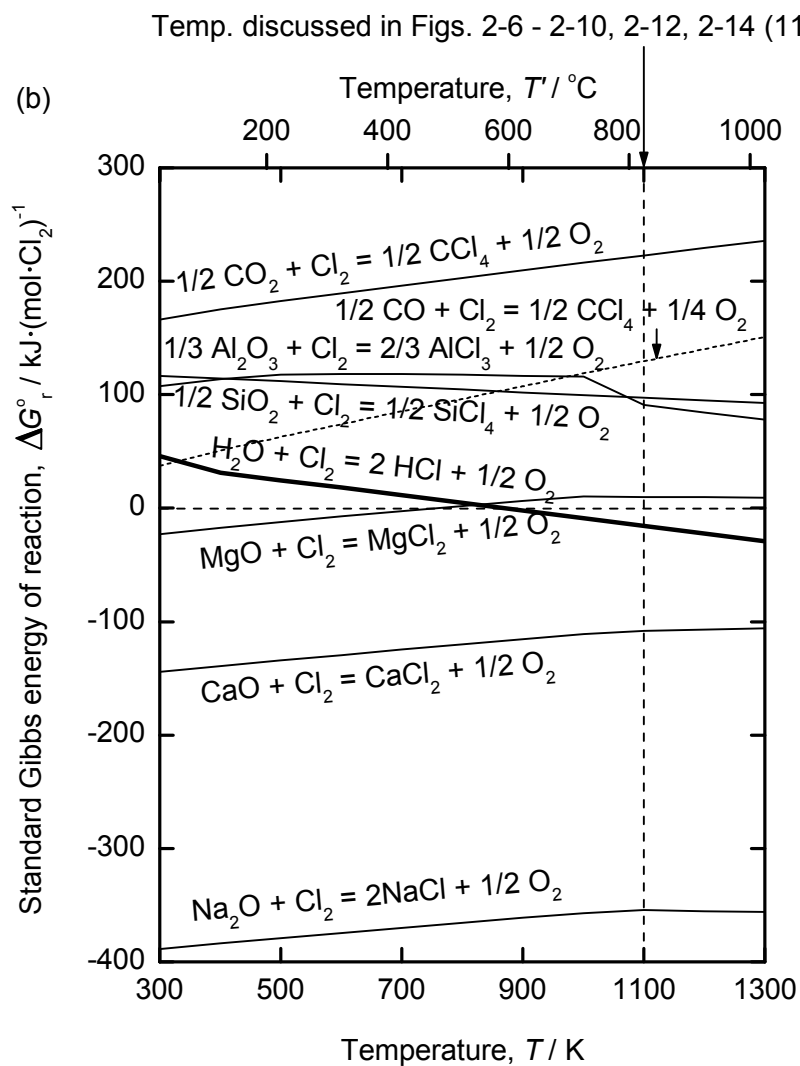
Figure 2-2 (b) Standard Gibbs energy of reaction (ΔG°_r)
for selected compounds.

Fe-O-Cl system, p_{Cl_2} = 0.1 atm
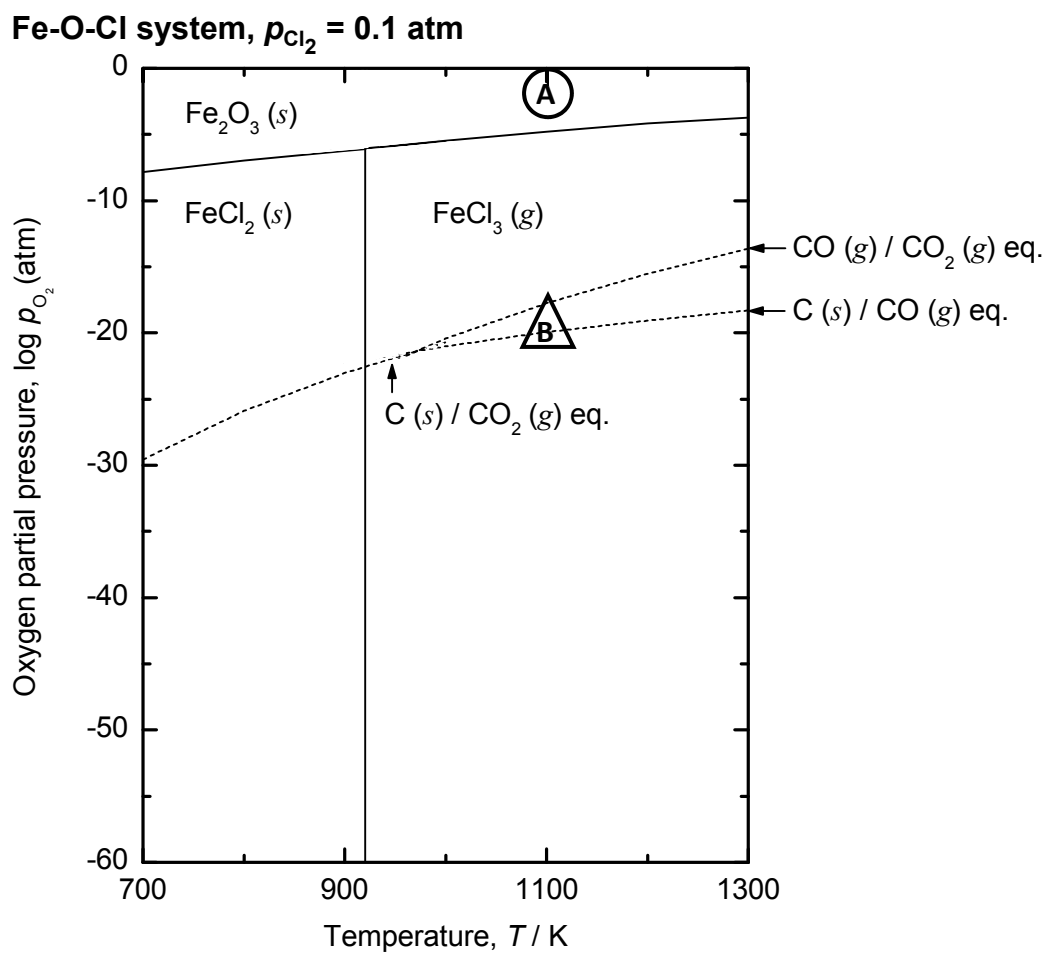
Figure 2-3 Chemical potential diagram for the Fe-O-Cl system
under high chlorine partial pressure (p_{Cl_2} = 0.1 atm).

Ti-O-Cl system, p_{Cl_2} = 0.1 atm
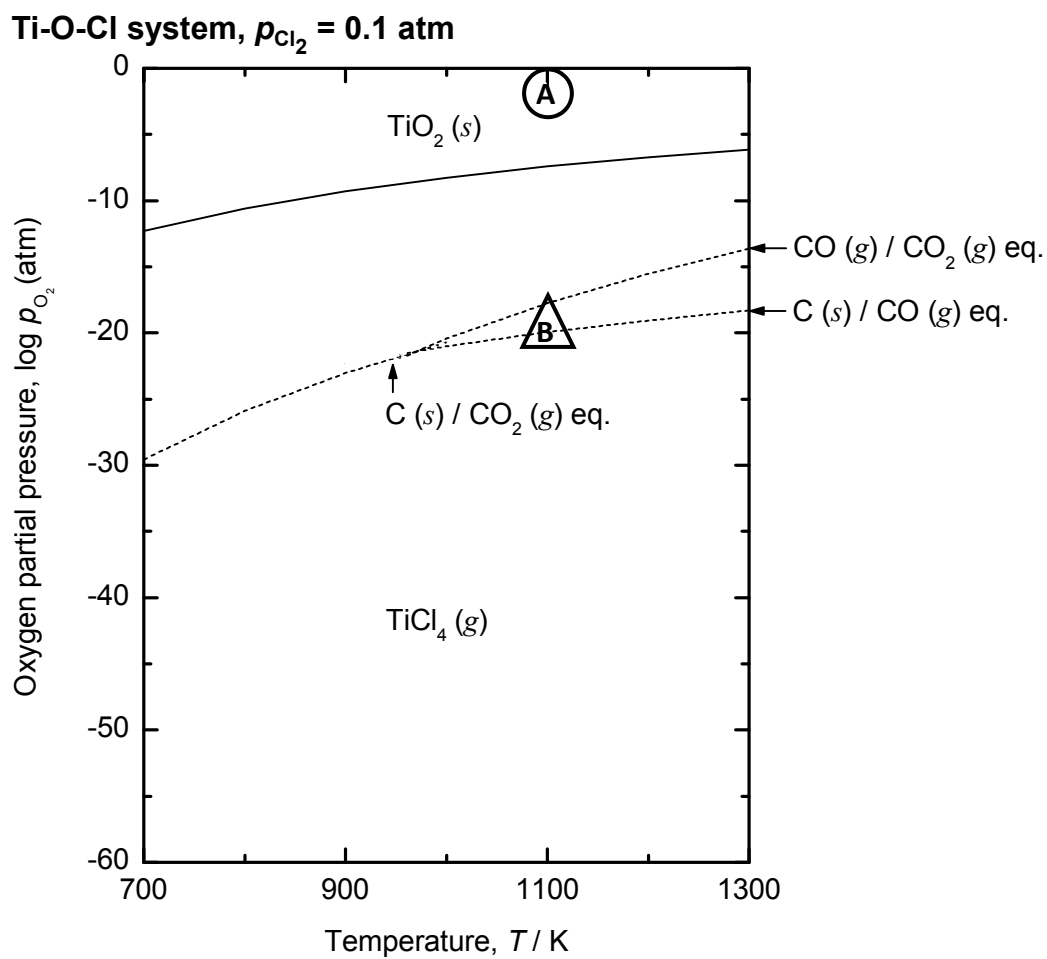
Figure 2-4 Chemical potential diagram for the Ti-O-Cl system
under high chlorine partial pressure (p_{Cl_2} = 0.1 atm).
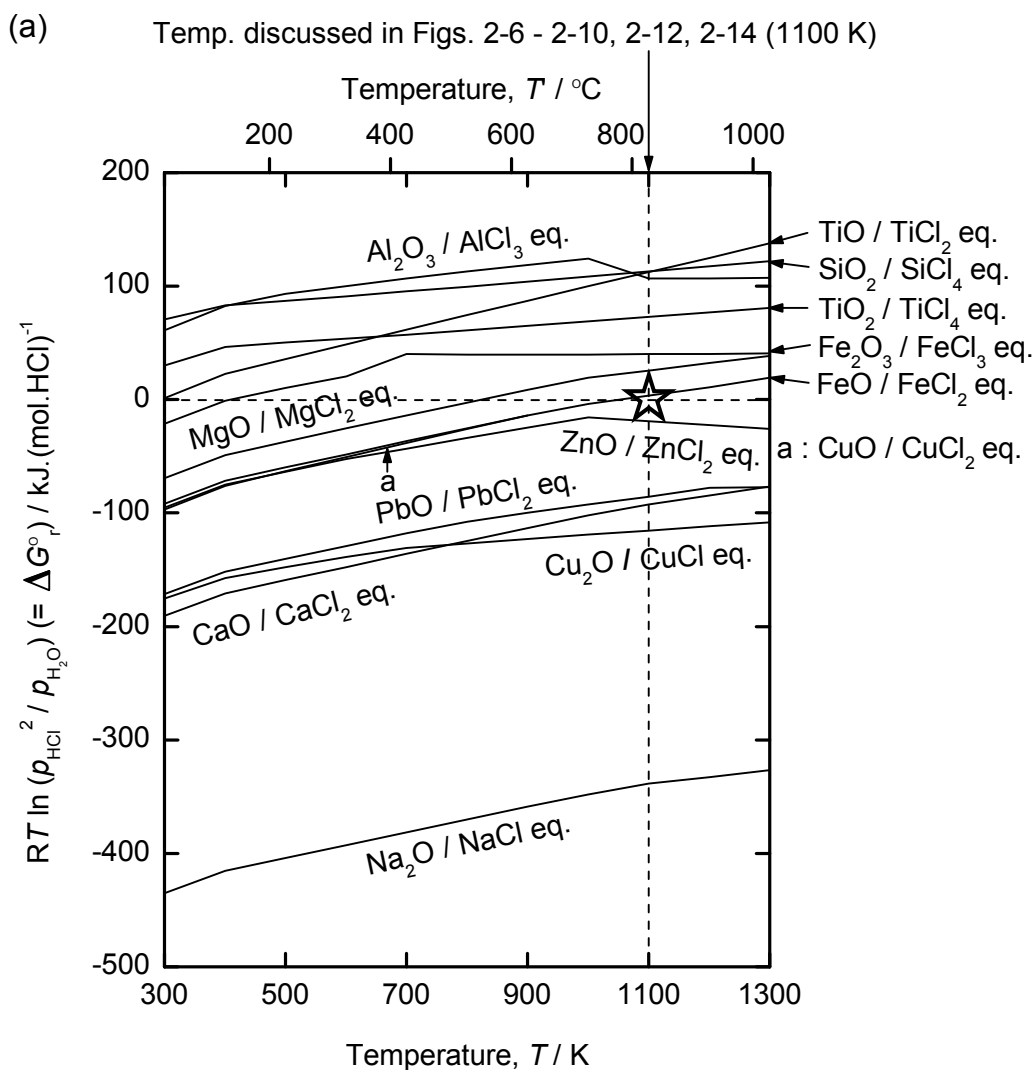
Figure 2-5 (a) Temperature dependence of $RT \ln (p_{HCl}^2 / p_{H_2O})$
under various MO_x (s) / MCl_{2X} (s, l, g) eq.

(b) Temp. discussed in Figs. 2-6 - 2-10, 2-12, 2-14 (1100 K)
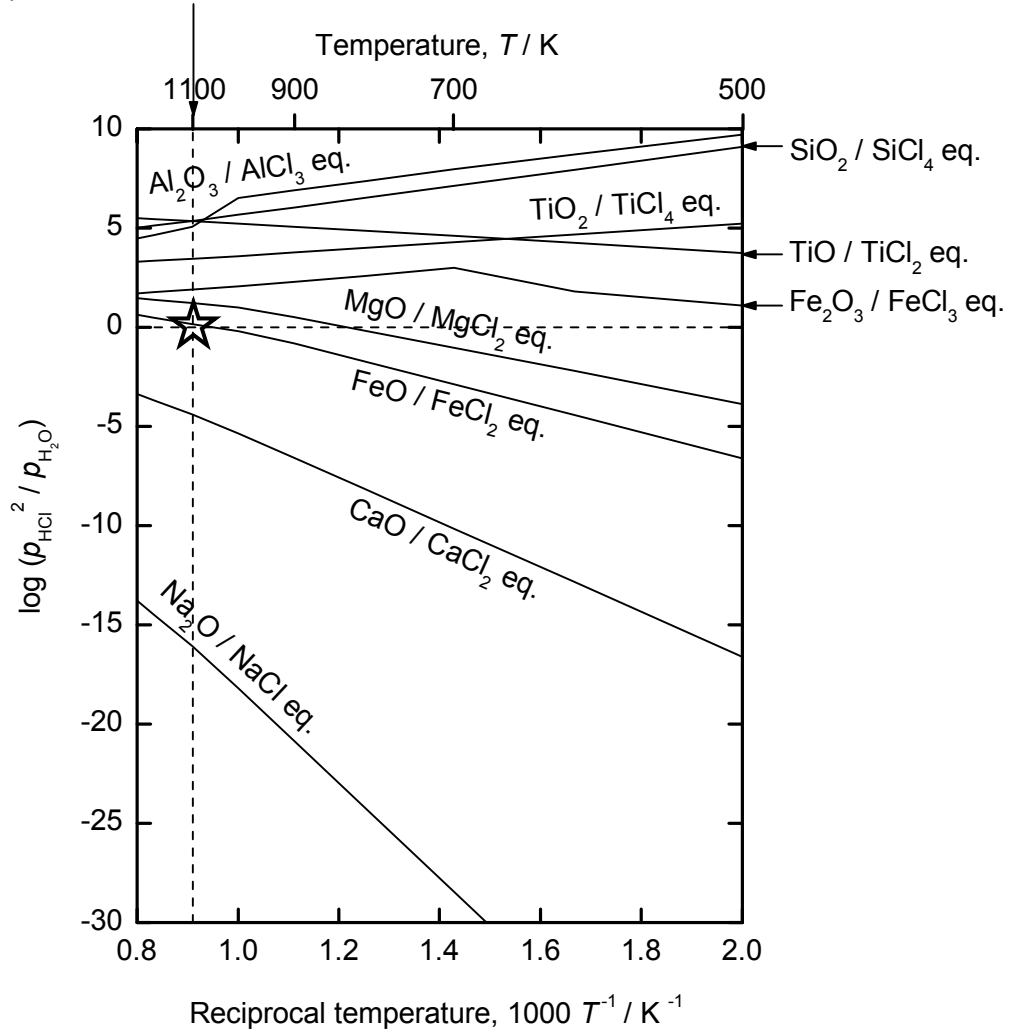
Figure 2-5 (b) Reciprocal temperature dependence of log (p_{HCl}^2 / p_{H_2O}) under various MO_x (s) / MCl_{2x} (s, l, g) eq.

103

Fe-O-Cl system, *T* = 1100 K
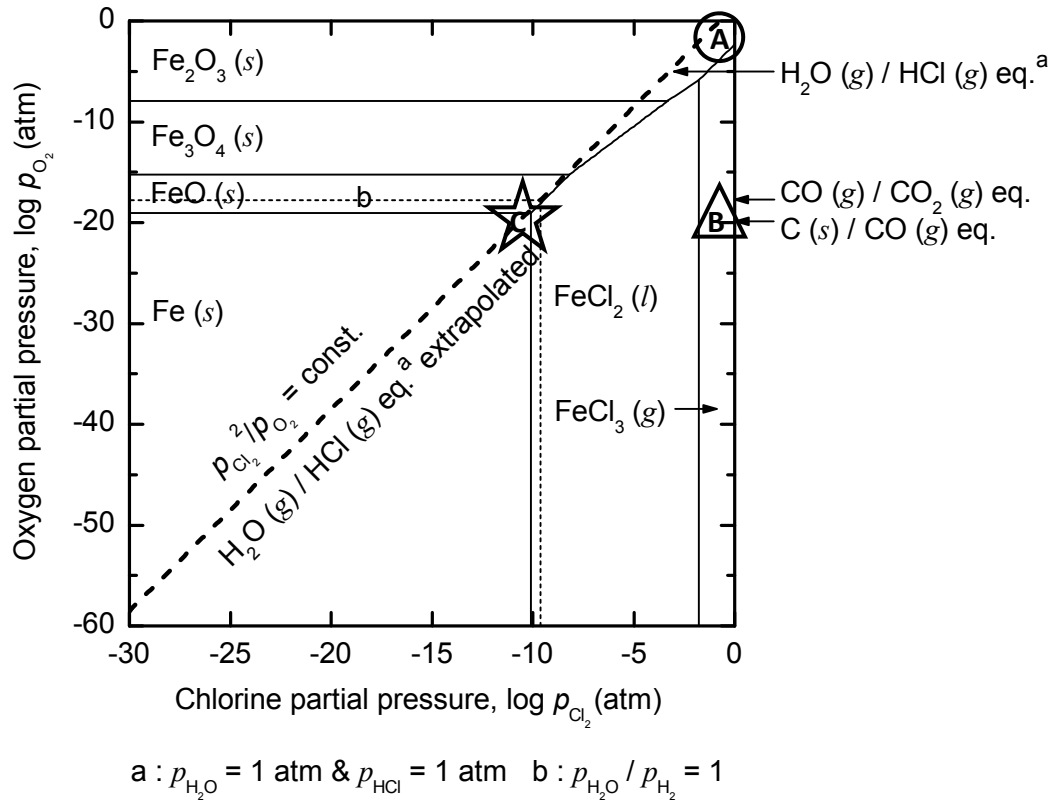
Figure 2-6 Chemical potential diagram of the Fe-O-Cl system at 1100 K.

Figure 2-7 Chemical potential diagram of the Ti-O-Cl system at 1100 K.

Figure 2-8 Chemical potential diagram of the H-O-Cl system at 1100 K.

Fe-O-Cl system,

Ti-O-Cl system, *T* = 1100 K

a : p_{H_2O} = 1 atm & p_{HCl} = 1 atm   b : p_{H_2O} / p_{H_2} = 1

-- Ti-O-Cl   — Fe-O-Cl
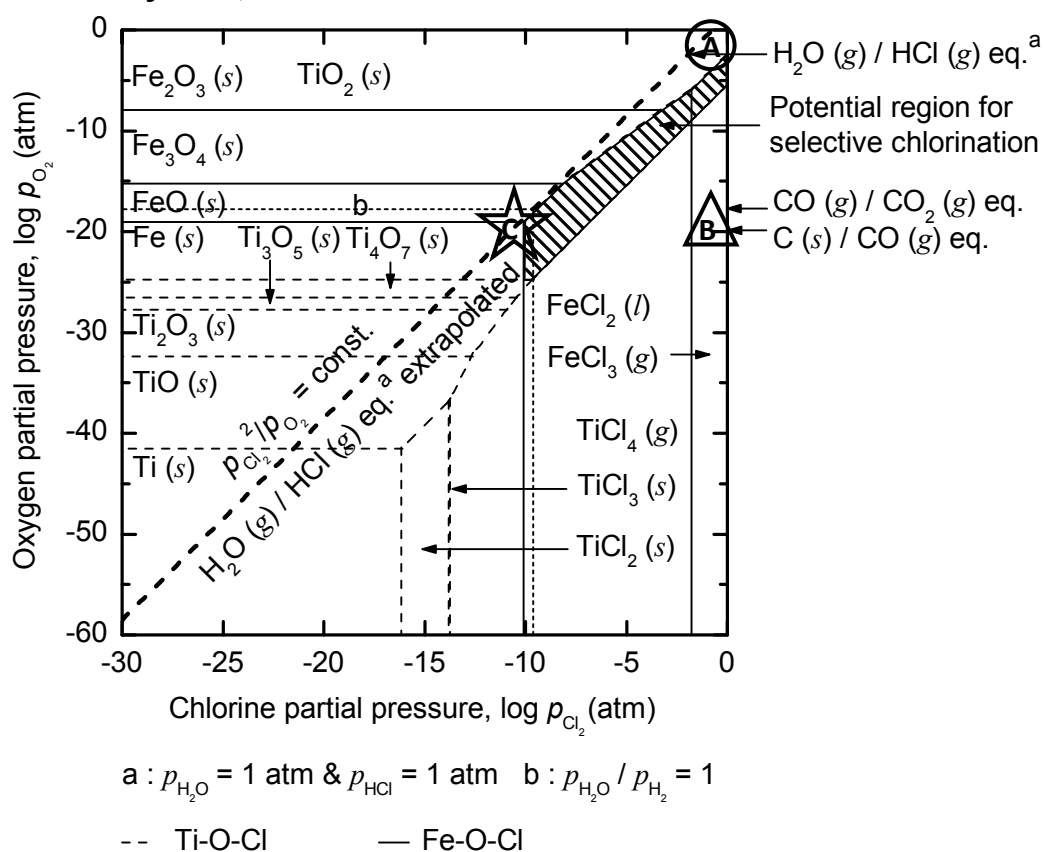
Figure 2-9 Combined chemical potential diagram of the Fe-O-Cl and
　　　　　Ti-O-Cl systems at 1100 K. See Figs. 2-6 and 2-7 for reference
　　　　　(The hatched area is the potential region for the selective
　　　　　chlorination of iron).

Ca-O-Cl system, *T* = 1100 K

a : p_{H_2O}= 1 & p_{HCl}= 1   b : p_{H_2O} / p_{H_2} = 1
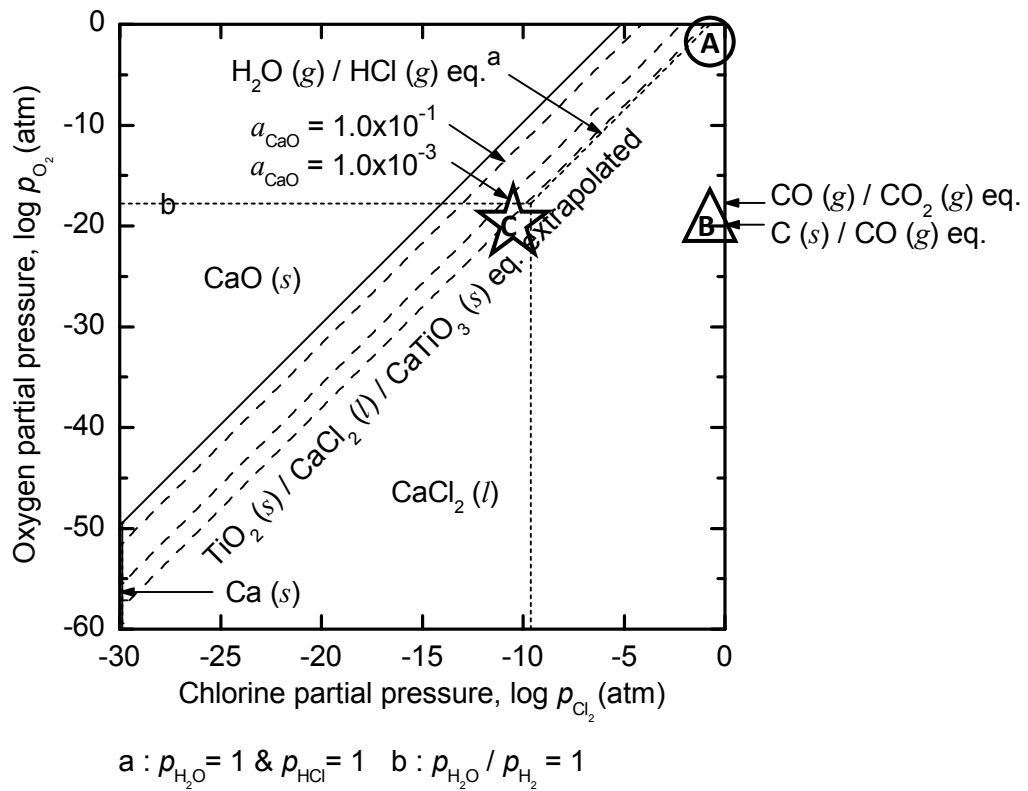
Figure 2-10 Chemical potential diagram of the Ca-O-Cl system at 1100 K.

Mg-O-Cl system, *T* = 1000 K
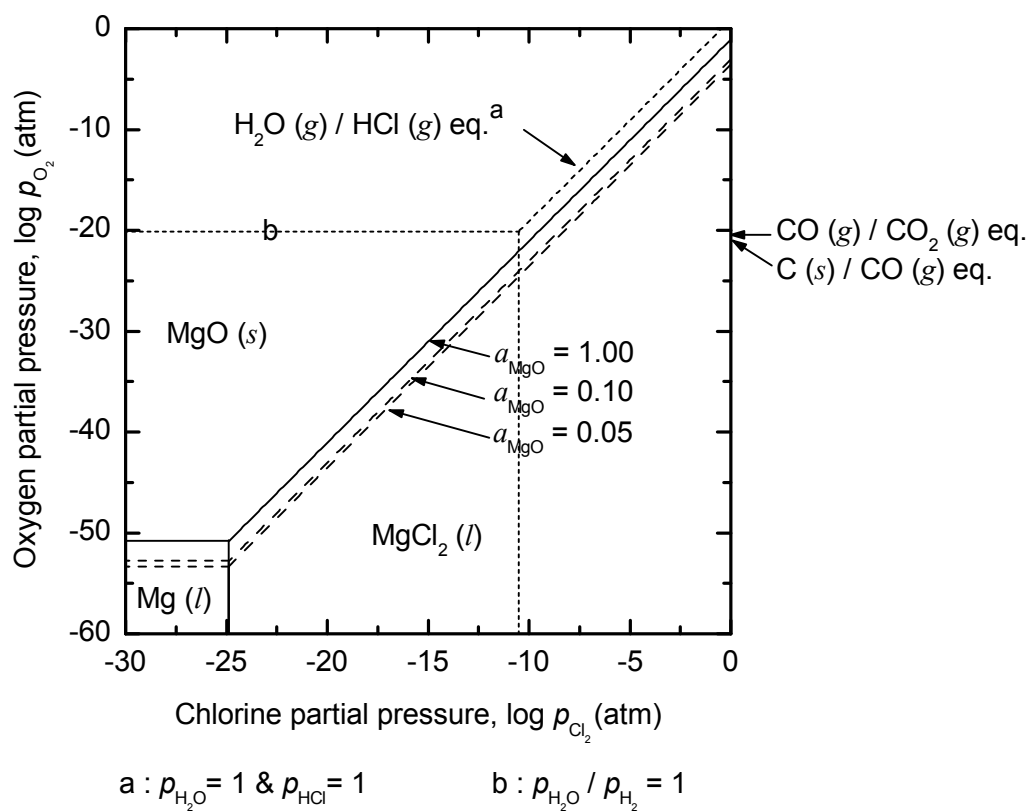
Figure 2-11 Chemical potential diagram of the Mg-O-Cl system at 1000 K.

109
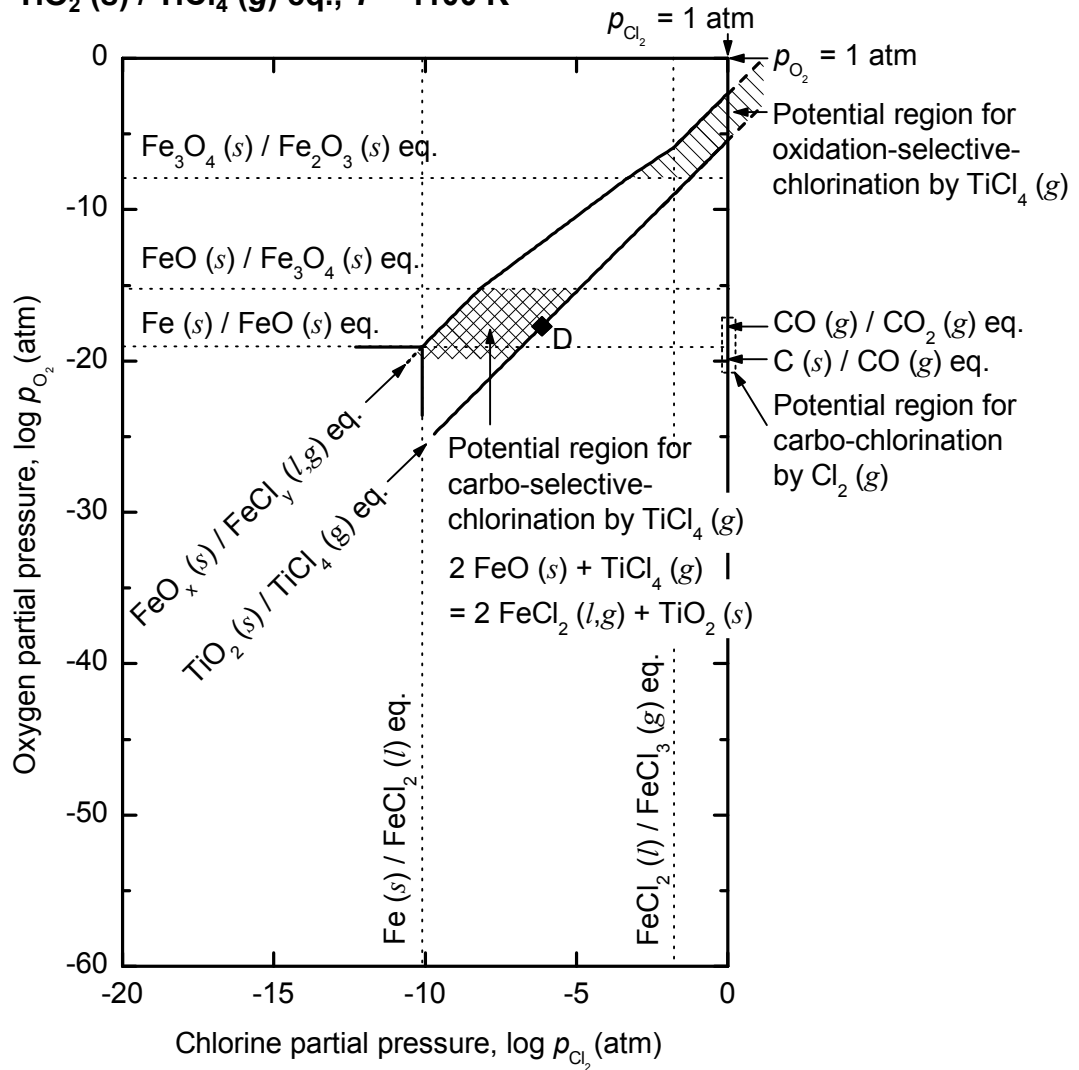
Figure 2-12 Comparison of potential regions for oxidation-selective-chlorination
by $TiCl_4$ (g), carbo-selective-chlorination by $TiCl_4$ (g), and
carbo-chlorination by Cl_2 (g) using modified chemical potential
diagram of the Fe-O-Cl system and the Ti-O-Cl system at 1100 K.

(a)
C-O-Cl system, _T_ = 700 K

(b)
C-O-Cl system, _T_ = 700 K (Enlarged diagram of (a))
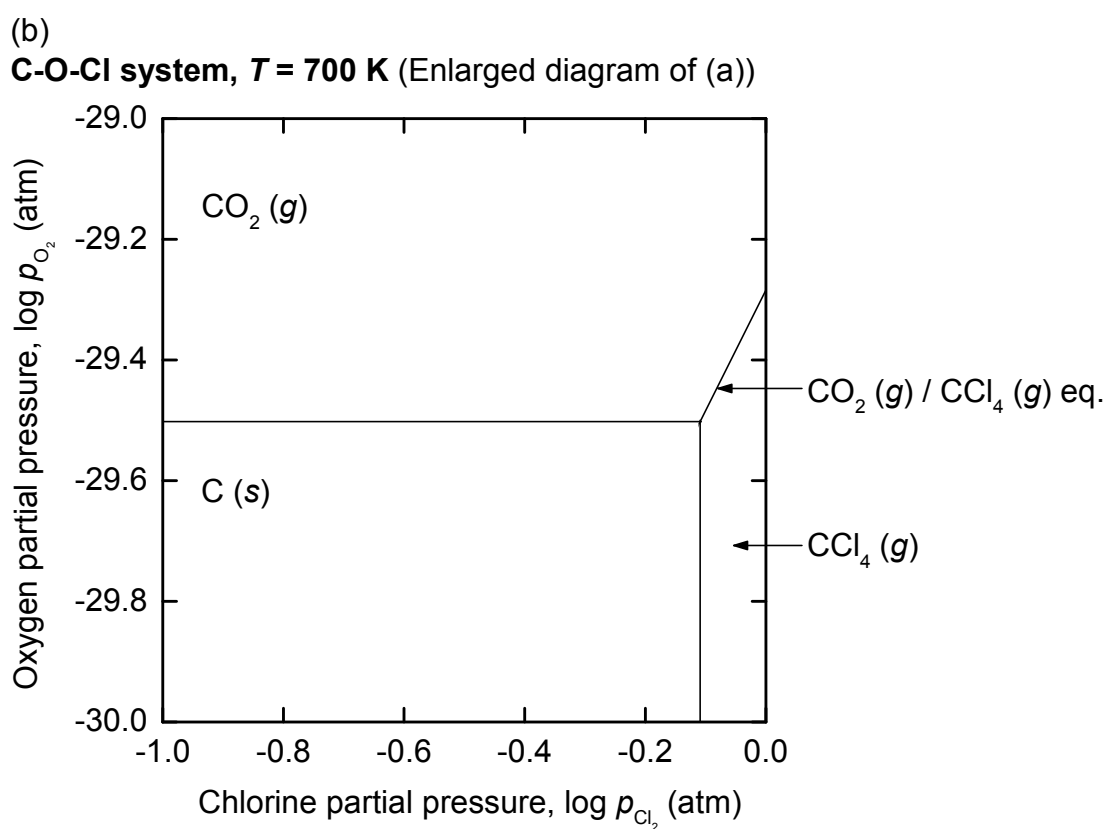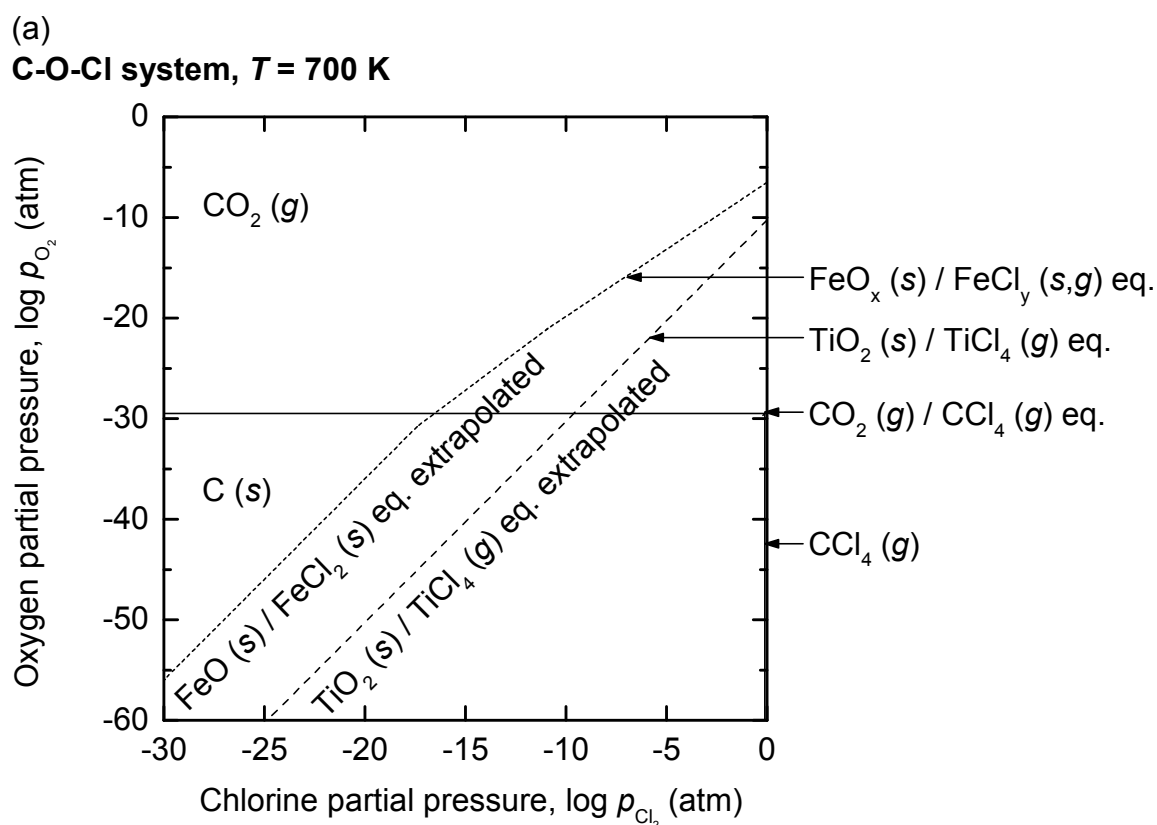
Figure 2-13 (a) Chemical potential diagram of the C-O-Cl system at 700 K and (b) enlarged diagram of (a).
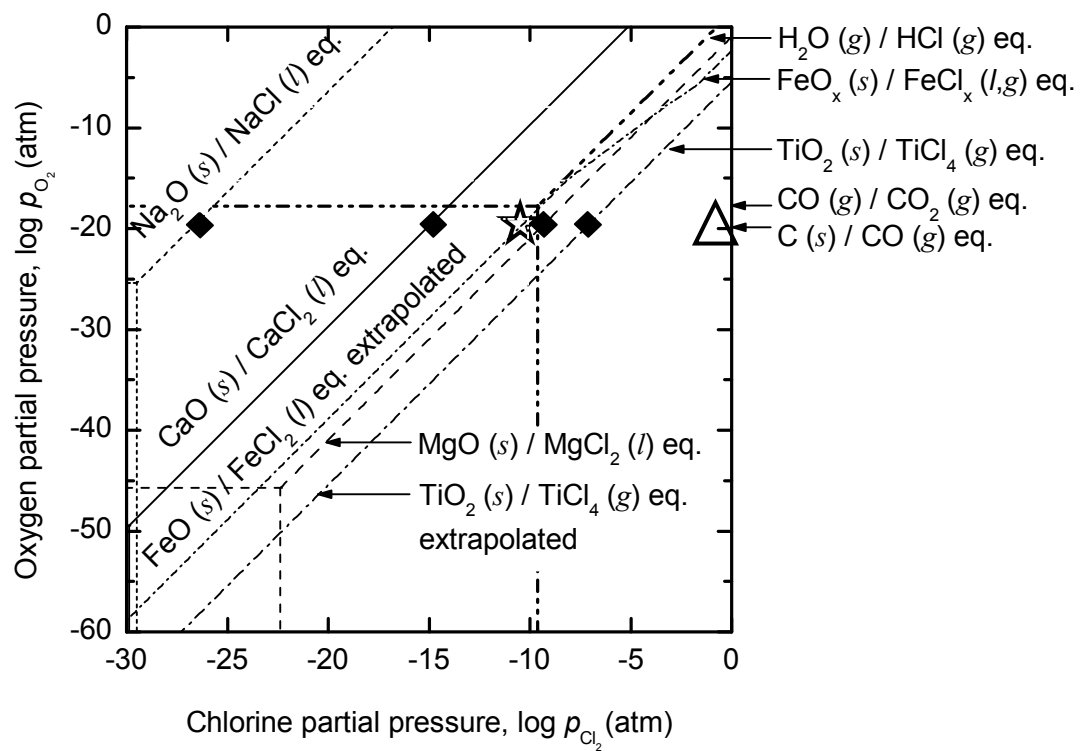
Figure 2-14 Chemical potential diagram of the M-O-Cl
(M = Na, Ca, Mg, Fe, Ti) and H-O-Cl systems at 1100 K.

112

Chapter 3　Selective chlorination of low-grade titanium ore using calcium chloride

3.1　Introduction

Currently, the high-grade TiO_2 with a purity of above 90 % called UGI (Up-Graded Ilmenite) or synthetic rutile is used as a feedstock for the Kroll process, the current titanium metal production process.[1] This is because if the low-grade titanium ore (ilmenite, mainly $FeTiO_3$) containing 30 % – 65 % TiO_2 is used as a feedstock for the Kroll process, large amount of chloride waste is produced and chlorine loss increases during processing.[2] The generation of large amount of chloride waste results in operating problems such as the clogging of pipes in the chlorinator.[1,2] In addition, the chloride waste treatment cost and environmental burden increase significantly in some countries having strict environmental regulations such as Japan.[1,3]

Industrial processes for upgrading titanium ore are the Becher process[4-8], the Benilite process[9-11], and the slag and UGS processes.[12-13] However, there are several disadvantages to these processes as shown in Table 1-6 in chapter 1. For example, in the case of the Becher and the slag and UGS processes, multiple steps are required to yield high-grade TiO_2. In the Benilite process, highly concentrated 18 % – 20 % HCl is required.

In order to mitigate these disadvantages, much research has been carried out, and selective chlorination has been found to be promising for upgrading low-grade Ti ore. However, most of the investigated selective chlorination processes were carried out under chlorine gas (Cl_2) in the presence of carbon or under a mixture of CO and Cl_2.[14-22] This could be a disadvantage, because the use of Cl_2 gas has safety and environmental problems. Recently, Okabe's group developed a new process utilizing metal chlorides such as $CaCl_2$ as the chlorine source for selective removal of iron from titanium ore under Ar or N_2 atmospheres.[23,27] However, even in the best result of their study, which was conducted under a mixed atmosphere of N_2 and H_2O at 1293 K for 12 h using $CaCl_2$, 16.7 mass% iron remained.[23]

To improve these results, this study aims to develop a simple and effective process for upgrading low-grade titanium ore. In particular, a novel selective chlorination process that uses $CaCl_2$ as the chlorinating agent is applied to selectively remove iron

from the titanium ore. A flow diagram of this process is shown in Fig. 3-1. The overall chlorination process investigated in this study consists of two selective chlorination processes. One process uses $CaCl_2$ as a chlorinating agent to remove iron from the titanium ore, as suggested by Okabe's group, and the $CaTiO_3$ produced by this process has a possibility to be used as a feedstock for titanium metal production such as the FFC process in the future. The other process suggested in this study uses the HCl gas produced from $CaCl_2$ to remove iron from the titanium ore. This second process leads to better recovery of the chlorine source. The selective chlorination process investigated in this study has the following advantages: (1) it does not require the handling of highly concentrated HCl or Cl_2 gas for the chlorination, (2) high-grade titanium dioxide can be obtained in a single step through a simple and scalable process, and (3) various ilmenites can be used as the starting materials.

3.2   Experimental

Fig. 3-2 shows a schematic and a photograph of the experimental apparatus, and the experimental conditions are listed in Table 3-1. In this study, natural ilmenite ore, natural rutile ore, and titania slag were used as starting materials. In addition, $CaCl_2$ (anhydrous; purity > 95.0 %; powder; Kanto Chemicals, Inc.) was used as the starting material for the chlorinating agent. The compositions of the titanium ores used in this study are shown in Tables 3-2, 3-3, and 3-4.

Titanium ore was placed in the quartz crucible ($\phi = 31$ mm, I.D.; $d = 13$ mm, depth), and a mixture of titanium ore and $CaCl_2$ was placed in the molybdenum-lined quartz crucible (quartz crucible: $\phi = 26$ mm, I.D.; $d = 24$ mm, depth; molybdenum lining: $t = 0.1$ mm, thickness; $w = 10$ mm, width; $l = 10$ mm, length; $d = 25$ mm, depth). These crucibles were then positioned in the gas-tight quartz tube ($\phi = 41.5$ mm, I.D.; $l = 545$ mm, length), which was subsequently positioned in the horizontal furnace.

The $CaCl_2$ was dried under vacuum for more than 3 days at 473 K in a vacuum dryer (EYELA, VOS-201SD) prior to use. The $CaCl_2$ was premelted two times in the molybdenum-lined quartz crucible before the titanium ore was added to it under vacuum at 1100 K in order to prevent the overflow of the $CaCl_2$ from the crucible. In each premelting step, half of the total weight of $CaCl_2$ was premelted for 5 min. After the

114

premelting of $CaCl_2$ was finished, titanium ore was placed in both the quartz crucible and the molybdenum-lined quartz crucible.

Table 3-1 shows the experimental conditions used in this study. When the experiments were carried out under vacuum, the quartz tube was sealed with a silicone rubber plug and evacuated two times for 5 min each before the experiments. The quartz tube was then introduced into the horizontal furnace, which was already heated to 1100 K. This temperature was then maintained for 5 h, 7 h, or 13 h.

When the experiments were carried out under an Ar gas (purity > 99.9995%) atmosphere, the sealing and evacuation procedure were identical to those used when the experiments were conducted under vacuum. The Ar gas atmosphere was added using two methods. In the first method, the quartz tube was filled with Ar gas until the internal pressure was 0.31 atm or 0.41 atm. These values were chosen by considering the increase in the internal pressure caused by heat expansion when the quartz tube was introduced into the furnace. The internal pressure was maintained at 1 atm during the experiments carried out for 5 h, 7 h, and 11 h at 1100 K. In the second method, Ar gas was flowed through the quartz tube at a rate of 50 sccm controlled using a MFC (mass flow controller, Aera Japan LTD., Model: RO-100). In this case, the internal pressure was also maintained at 1 atm during the experiment carried out for 5 h at 1100 K.

After the completion of the reactions, the quartz tube was immediately removed from the furnace and allowed to cool gradually to room temperature. Leaching was not conducted for the residues in the quartz crucible, while the residues in the molybdenum-lined quartz crucible were dissolved in deionized water for at least 12 h and sonication was performed for at least 1 h at room temperature. The chemical compositions of the residues obtained in the quartz crucible and in the molybdenum-lined quartz crucible were determined using X-ray fluorescence spectroscopy (XRF: JEOL, JSX-3100RII), their microstructures and compositions were analyzed using scanning electron microscopy / energy dispersive X-ray spectroscopy (SEM/EDS: JEOL, JSM-6510LV), and their crystalline phases were identified using X-ray diffraction (XRD: RIGAKU, RINT 2500, RINT 2000, Cu-Kα radiation) analysis.

3.3   Thermodynamic analysis of selective chlorination using CaCl$_2$

From a thermodynamic viewpoint, titanium ore can be considered to be a mixture of FeO and TiO$_2$, because the standard Gibbs energy of the reaction shown in Eq. 3-1 is small at 1100 K. This makes it possible to carry out thermodynamic calculations for titanium ore by considering FeO and TiO$_2$ separately, and not FeTiO$_3$. Therefore, the conditions for selective removal of iron from the titanium ore can be considered in terms of the chemical potential diagrams of the Fe-O-Cl system and the Ti-O-Cl system.

$$FeO \ (s) + TiO_2 \ (s) = FeTiO_3 \ (s) \tag{3-1}$$
$$\Delta G^\circ_r = -11.0 \text{ kJ at } 1100 \text{ K}^{[24]}$$

Figs. 3-3 and 3-4 show the chemical potential diagrams of the Fe-O-Cl system and the Ti-O-Cl system, respectively, at 1100 K, plotted with p_{Cl_2} as the abscissa and p_{O_2} as the ordinate. First, the case of both a high oxygen and a high chorine chemical potential should be considered. As shown in Fig. 3-3, when the oxygen chemical potential is high (for example, at p_{O_2} = 0.1 atm), Fe$_2$O$_3$ (s) is thermodynamically stable even when the chlorine chemical potential is very high (for example, at p_{Cl_2} = 0.1 atm). Therefore, it is impossible to chlorinate Fe$_2$O$_3$ (s) with chlorine gas even at 1 atm under high p_{O_2}. In addition, TiO$_2$ (s) cannot be chlorinated under these conditions either, as shown in Fig. 3-4. Therefore, selective chlorination process cannot proceed even at very high p_{Cl_2} when p_{O_2} is high.

However, iron oxides will be chlorinated in the presence of carbon in this system under a high chlorine chemical potential (for example, at p_{Cl_2} = 0.1 atm), because the oxygen chemical potential is fixed by the C (g)/CO (g) eq. or CO (g)/CO$_2$ (g) eq. (both at p_{Cl_2} = 0.1 atm), as shown in Fig. 3-3. In addition, titanium oxides can also be chlorinated under these low p_{O_2} conditions, as shown in Fig. 3-4. For this reason, these conditions are employed in industrial processes (e.g., the Kroll process) to achieve direct chlorination and produce TiCl$_4$ gas from upgraded titanium ore.

As shown in Fig. 3-3, the ratio between the oxygen chemical potential and the chlorine chemical potential ($p_{O_2}/p_{Cl_2}{}^2$) of the Fe-O-Cl system can be determined by considering the relevant equilibrium reactions, such as the H$_2$O (g)/HCl (g) eq. and

CaO (s)/CaCl$_2$ (l) eq. in this system. The lines corresponding to the H$_2$O (g)/HCl (g) eq.[e] and the CaO (s, CaTiO$_3$)/CaCl$_2$ (l) eq.[a] in Fig. 3-3 pass through the vicinity of the FeCl$_2$ (l) stability region. Thus, FeO (s) can be chlorinated as FeCl$_2$ (l) by HCl (g), or by CaCl$_2$ (l) if the lines corresponding to H$_2$O (g)/HCl (g) eq.[e] and CaO (s, CaTiO$_3$)/CaCl$_2$ (l) eq.[a] pass through (or near) the FeCl$_2$ (l) stability region. Even when the H$_2$O (g)/HCl (g) eq.[e] line does not pass through the FeCl$_2$ (l) stability region, the chlorination reaction could be achieved by a slight alteration of thermodynamic parameters or experimental conditions. In addition, the lines corresponding to the H$_2$O (g)/HCl (g) eq.[e] and the CaO (s, CaTiO$_3$)/CaCl$_2$ (l) eq.[a] do not pass through any region of titanium chlorides (TiCl$_2$ (s), TiCl$_3$ (s), or TiCl$_4$ (g)) stability region, as shown in Fig. 3-4. The line corresponding to the H$_2$O (g)/HCl (g) eq.[e] is located a few magnitudes of p_{O_2} above the TiCl$_x$ (x = 2, 3, 4) stability region. Thus, this thermodynamic analysis indicates that the selective chlorination of FeO (s) from titanium ore can take place under conditions in which equilibrium reactions of the H$_2$O (g)/HCl (g) eq.[e] and the CaO (s, CaTiO$_3$)/CaCl$_2$ (l) eq.[a] are established.

The line corresponding to the H$_2$O (g)/HCl (g) eq.[e] in Fig. 3-3 can be calculated from Eq. 3-2, because it is expected that in the actual experiments the dried CaCl$_2$ will absorb H$_2$O from the air while being prepared. The Gibbs energy of the reaction shown in Eq. 3-2 can be calculated using Eq. 3-3.
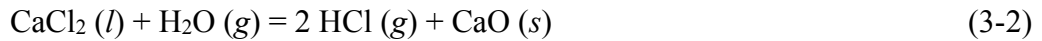
$$CaCl_2 \ (l) + H_2O \ (g) = 2 \ HCl \ (g) + CaO \ (s) \tag{3-2}$$
$$\Delta G^{\circ}_r = 92.7 \text{ kJ at } 1100 \text{ K}^{[24]}$$
$$\Delta G_r = 4.6 \text{ kJ at } 1100 \text{ K}^{[24]} \text{ under } a_{CaO} = 6.58 \times 10^{-5}$$

$$\Delta G_r = \Delta G^{\circ}_r + RT \ln \ \{(p_{HCl}{}^2 \cdot a_{CaO}) \ / \ (a_{CaCl_2} \cdot p_{H_2O})\} \tag{3-3}$$

When H$_2$O is present in the system during the premelting of the CaCl$_2$, it reacts with the CaCl$_2$ (l) to produce CaO (s) and HCl (g) in the molybdenum-lined quartz crucible. Because of the low partial pressure of HCl (g) in the system, this reaction proceeds even though the standard Gibbs energy of the reaction in Eq. 3-2 is positive. Then, when the titanium ore is added to the molybdenum-lined quartz crucible, the CaO (s) in the premelted CaCl$_2$ reacts with the TiO$_2$ (s) in the titanium ore. As a result,

the activity of CaO (a_{CaO}) decreases as the reaction shown in Eq. 3-4 proceeds. Eq. 3-3 shows that if the activity of CaO decreases or/and the partial pressure of HCl (g) decreases, the reaction shown in Eq. 3-2 can progress. Therefore, the reaction shown in Eq. 3-2 will take place during the experiments, and the line corresponding to the H_2O (g)/HCl (g) eq.[e] in Fig. 3-3 can be determined according to Eq. 3-2. In addition, if the activity of CaO is much lower than the activity calculated from Eq. 3-4, the line corresponding to the H_2O (g)/HCl (g) eq.[e] in Fig. 3-3 will pass through a $FeCl_2$ (l) stability region. The line corresponding to the CaO (s, $CaTiO_3$)/$CaCl_2$ (l) eq.[a] in Fig. 3-3 can be also determined from the activity of CaO, which is lowered by the production of $CaTiO_3$ (s).

$$CaO \ (s) + TiO_2 \ (s, FeTiO_3) = CaTiO_3 \ (s) \qquad\qquad (3\text{-}4)$$
$$a_{CaO} = 6.58 \times 10^{-5} \text{ at 1100 K}^{[24]} \text{ when } a_{TiO_2} = 1 \text{ and } a_{CaTiO_3} = 1$$
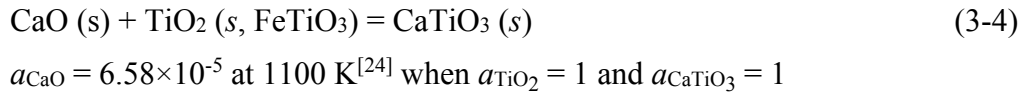
Eq. 3-5 shows the reaction between the titanium ore and $CaCl_2$. The vapor pressure of $FeCl_2$ (l) at 1100 K is 0.09 atm[24], which is high enough that the $FeCl_2$ (l) will evaporate. As a result, $FeCl_2$ (l) is removed as $FeCl_2$ (l,g) at 1100 K. Under the experimental conditions employed in this study, the activity of $FeCl_2$ (l) will decrease because the majority of the vaporized $FeCl_2$ (l) will solidify at the low temperature part of the quartz tube. As a result, the reaction shown in Eq. 3-5 proceeds and the FeO (s) in the titanium ore is removed as $FeCl_2$ (l,g) in the molybdenum-lined quartz crucible, even though the standard Gibbs energy of the reaction for the formation of $FeCl_2$ (l) shown in Eq. 3-5 has a small positive value. Therefore, thermodynamic analysis suggests that the line corresponding to the CaO (s, $CaTiO_3$)/$CaCl_2$ (l) eq.[a] in Fig. 3-3 will pass through a $FeCl_2$ (l) stability region under these experimental conditions.

$$FeO \ (s) + TiO_2 \ (s) + CaCl_2 \ (l) = FeCl_2 \ (l) + CaTiO_3 \ (s) \qquad\qquad (3\text{-}5)$$
$$\Delta G^{\circ}_r = 8.3 \text{ kJ at 1100 K}^{[24]}$$
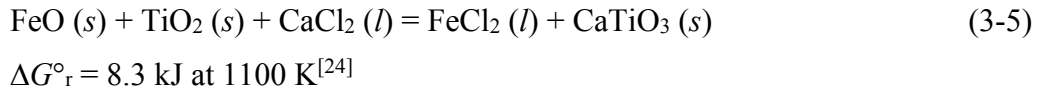
The HCl (g) produced by the reaction shown in Eq. 3-2 reacts with the FeO (s) present in the titanium ore placed in the quartz crucible, and this FeO (s) is also removed as $FeCl_2$ (l,g). The standard Gibbs energy of the reaction shown in Eq. 3-6 is close to zero and could be either a small positive or a small negative depending on the reference

consulted. As a result, depending on the reference, the line corresponding to the H_2O (*g*)/HCl (*g*) eq.[e] in Fig. 3 may pass through the $FeCl_2$ (*l*) stability region. Therefore, it is expected that under certain conditions the FeO (*s*) will be removed from the titanium ore and TiO_2 (*s*) will be produced in the quartz crucible.

FeO (*s*) + 2 HCl (*g*) = $FeCl_2$ (*l*) + H_2O (*g*)   (3-6)
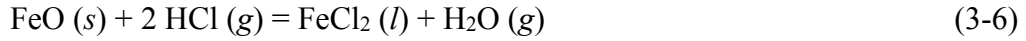
$\Delta G°_r$ =   3.7 kJ at 1100 K[24], based on I.Barin

$\Delta G°_r$ = − 4.1 kJ at 1100 K[25], based on HSC 6.1

3.4 Results and discussion

3.4.1 Verification of selective chlorination using $CaCl_2$

Fig. 3-5 shows photographs of the low temperature part of the quartz tube, the residues in the quartz crucible, and the residues in the molybdenum-lined quartz crucible after the experiment. During the experiment, as shown in Fig. 3-5 (a), a white powder was deposited at the low temperature part of the quartz tube. In addition, the black color of the titanium ore was changed to the bright gray color of the residues after the experiment, as shown in Fig. 3-5 (b).

Fig. 3-6 shows the XRD patterns of the white residues that condensed inside the low temperature part of the quartz tube. XRD analysis showed that the main crystalline phases of the white residues were $FeCl_2 \cdot (H_2O)_2$ and $FeCl_2$. It is expected that H_2O adhered to the $FeCl_2$ during the experiment or during the sample preparation for the XRD measurements. In addition, $FeCl_3 \cdot 6H_2O$ was also found; the detailed reason for this $FeCl_3 \cdot 6H_2O$ production is still being investigated. Fig. 3-7 shows SEM images of the microstructure of a titanium ore particle before the experiment and of the residues obtained in the quartz crucible after the experiment. As shown in Fig. 3-7, microstructural pores were formed on the surfaces of the residues even though the leaching was not conducted after the experiment. These experimental results imply that the iron present in the titanium ore was removed mainly in the form of $FeCl_2$ (*l,g*), as expected from the thermodynamic analysis.

3.4.2 Influence of particle size of titanium ore

Table 3-2 lists the analytical results for the residues obtained in the quartz crucible and in the molybdenum-lined quartz crucible after the experiments. Figs. 3-8 (a) and 3-8 (b) show the XRD patterns of the residues obtained in the quartz crucible and in the molybdenum-lined quartz crucible, respectively, when the experiments were conducted under vacuum on Vietnamese titanium ore with various particle size ranges. The XRF and XRD results show that a purity of about 96 % to 97 % TiO_2 (s) was obtained in the quartz crucible when the particle size range was from 44 μm to 297 μm, and a purity of about 94 % TiO_2 (s) was obtained in the quartz crucible when the particle size range was from 297 μm to 510 μm.

However, 18.1 % to 32.6 % of the iron in the titanium ore remained in the residues in the molybdenum-lined quartz crucible, even though 17.1 % to 31.6 % of the iron present in the titanium ore was removed in the form of $FeCl_x$ (l,g) (x = 2, 3). In addition, XRD analysis indicated that $CaTiO_3$ (s) was the main crystalline phase in the molybdenum-lined quartz crucible, as shown in Fig. 3-8 (b).

Fig. 3-9 shows an SEM image and the EDS results found for a cross section of a titanium ore particle obtained from the molybdenum-lined quartz crucible. As shown in Fig. 3-9, $CaTiO_3$ (s) was produced at the outer part of the titanium ore particle from the reaction between $CaCl_2$ and the titanium ore particle. However, the iron present at the inner part of the titanium ore particle could not physically react with $CaCl_2$ because of this formation of $CaTiO_3$ (s) at the outer part of the titanium ore particle. Therefore, $CaTiO_3$ (s) hindered the progress of the chlorination of the iron in the titanium ore, although the formation of $CaTiO_3$ (s) is preferable for the production HCl (g) from $CaCl_2$ (l) by lowering the activity of CaO (s).

It has been demonstrated that there is no influence of the particle size of the titanium ore on the ability of the selective chlorination process to produce high purity TiO_2 when the titanium ore is upgraded by the HCl gas produced from $CaCl_2$. Therefore, it is anticipated that the costs for sieving and crushing to select a particular particle size can be reduced.

3.4.3   Influence of various types of titanium ores

Table 3-3 lists the analytical results for the residues obtained in the quartz crucible and in the molybdenum-lined quartz crucible after the experiments. Figs. 3-10 (a) and 3-10 (b) show the XRD patterns of the residues obtained in the quartz crucible and in the molybdenum-lined quartz crucible, respectively, when the experiments were conducted using natural ilmenite produced in China and Australia and natural rutile produced in South Africa.

As shown in Table 3-3, Fig. 3-10 (a), and Fig. 3-10 (b), a purity of about 91 % TiO_2 (*s*) was obtained in the quartz crucible and $CaTiO_3$ (*s*) was the main crystalline phase in the molybdenum-lined quartz crucible when the Chinese titanium ore was used as feedstock. In addition, a purity of about 95 % TiO_2 (*s*) was obtained in the quartz crucible when the Australian titanium ore and South African rutile were used as feedstock, and $CaTiO_3$ (*s*) and TiO_2 (*s*), respectively, were the main crystalline phases in the molybdenum-lined quartz crucible. The purity of the TiO_2 (*s*) obtained in the quartz crucible when the Chinese titanium ore was used was slightly lower than that obtained when the Vietnamese ore was used. This is because compared to the titanium ore produced in Vietnam, the Chinese titanium ore contains higher amounts of minor impurities such as Al and Si that cannot be chlorinated by HCl gas.

The minor impurities contained in the titanium ores produced in Vietnam, Australia, and China include Al, Si, Mn, and so on. Among these impurities, Al, Si, and Mn are the most abundant. It is difficult to chlorinate Al and Si with HCl gas, whereas Mn can be chlorinated by HCl gas through the reactions shown in Eqs. 3-7 – 3-9. Therefore, it is expected that the purity of the TiO_2 (*s*) obtained in the quartz crucible when the Chinese titanium ore is used will be slightly lower, because about 4.6 % of minor impurities that cannot be chlorinated were already present in the Chinese titanium ore.

$$1/6\ Al_2O_3\ (s) + HCl\ (g) = 1/3\ AlCl_3\ (g) + 1/2\ H_2O\ (g) \qquad\qquad (3\text{-}7)$$
$$\Delta G^\circ_r = 53.4\ kJ\ at\ 1100\ K^{[24]}$$

$$1/4 \ SiO_2 \ (s) + HCl \ (g) = 1/4 \ SiCl_4 \ (g) + 1/2 \ H_2O \ (g) \tag{3-8}$$

$\Delta G°_r = 56.5$ kJ at 1100 K[24]

$$1/2 \ MnO \ (s) + HCl \ (g) = 1/2 \ MnCl_2 \ (l) + 1/2 \ H_2O \ (g) \tag{3-9}$$
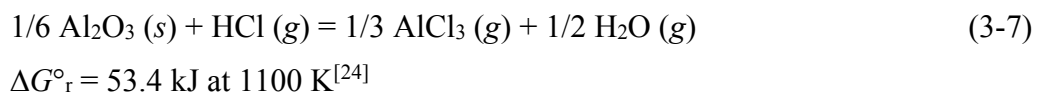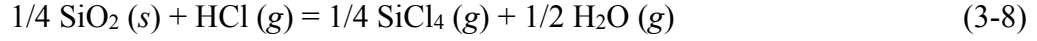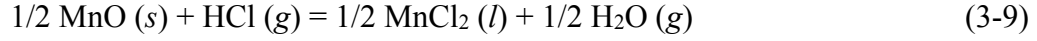
$\Delta G°_r = -13.0$ kJ at 1100 K[24]

As shown in Fig. 3-11, the main crystalline phase of the Canadian slag feedstock was $FeTi_2O_5$ (s). This is a different phase from those in the other Vietnamese, Australian, and Chinese titanium ores, which have $FeTiO_3$ (s) as the main crystalline phase. Thermodynamically, $FeTi_2O_5$ (s) disassociates into $FeTiO_3$ (s) and TiO_2 (s) at 1100 K, as shown in Eq. 3-10. As a result, the concentration of titanium increased from 76.7 % to 89.1 % in the quartz crucible when the experiment was conducted for 13 h.

$$FeTi_2O_5 \ (s) = FeTiO_3 \ (s) + TiO_2 \ (s) \tag{3-10}$$

$\Delta G°_r = -53.7$ kJ at 1100 K[25]

However, the purity of the TiO_2 (s) obtained in the quartz crucible was just below 90 %, which is the criterion for the practically minimum purity of the feedstock that can be used for the Kroll process. The reason for this low purity is probably that the total concentration of minor impurities in the Canadian slag that cannot be chlorinated by HCl gas is about 5.9 %, which is much higher than that of the Chinese titanium ore.

When the experiment was conducted for 13 h, the main product produced in the quartz crucible was TiO_2 (s), and TiO_2 (s) and $CaTiO_3$ (s) were the main products in the molybdenum-lined quartz crucible. In addition, Fe_2TiO_5 (s) was found in both the quartz crucible and the molybdenum-lined quartz crucible, as shown in Fig. 3-11. However, a detailed explanation for this is still being investigated.

3.4.4 Influence of atmosphere in the reaction system

Table 3-4 lists the analytical results for the residues obtained in the quartz crucible and in the molybdenum-lined quartz crucible after the experiments. Figs. 3-12 (a) and 3-12 (b) show the XRD patterns of the residues obtained in the quartz crucible

and in the molybdenum-lined quartz crucible, respectively, when the experiments were conducted under an Ar gas atmosphere. As shown in Table 3-4, Fig. 3-12 (a), and Fig. 3-12 (b), when the experiment was conducted under a static Ar gas atmosphere for 11 h, a purity of about 97 % TiO_2 (s) was obtained in the quartz crucible and mainly $CaTiO_3$ (s) was obtained in the molybdenum-lined quartz crucible. However, compared to the reactions conducted under vacuum, the reactions performed in a static Ar gas atmosphere required 6 more hours to completely remove the iron from the titanium ore. In addition, the iron present in the titanium ore was not selectively chlorinated in the quartz crucible when the experiment was conducted under an Ar gas flow.

Eq. 3-11 describes the reaction establishing the line corresponding to the H_2O (g)/HCl (g) eq. shown in Fig. 3-3. If Ar gas is introduced into the quartz tube, the total pressure of the quartz tube is increased compared to that when the experiments were conducted under vacuum because of the increase in the total number of molecules. As a result, the partial pressure of H_2O (g) and HCl (g) decreases.

$$\log p_{O_2} = 2 \log p_{Cl_2} + 2 \log p_{H_2O} - 4 \log p_{HCl}$$
$$+ 4 \log K_f(HCl) - 2 \log K_f(H_2O) \qquad (3\text{-}11)$$

However, it is expected that the line corresponding to the H_2O (g)/HCl (g) eq. in Fig. 3-3 still locates inside the area where iron oxide can be chlorinated in the scale of Fig. 3-3 when the experiments are conducted under a static Ar gas atmosphere. In addition, it is expected that it took 11 h to remove the iron from the titanium ore because the amount of mass flux for the reaction was decreased or because the probability of collision between the produced HCl gas and the surface of the titanium ore was decreased. When the Ar gas was flowed through the quartz tube, the partial pressures of H_2O (g) and HCl (g) were greatly decreased from those obtained when the quartz tube was simply filled with Ar gas because the Ar gas was forcibly introduced. Therefore, because the mass flux of the produced HCl gas was below the minimum mass flux required for the reactions to proceed, the iron present in the titanium ore was not chlorinated.

3.4.5 Influence of activity of CaO on selective chlorination

Table 3-5 lists the analytical results for residues obtained in the quartz crucible and the molybdenum-lined quartz crucible when the titanium ore was or was not placed in the molybdenum-lined quartz crucible. As shown in Table 3-5, when the titanium ore was placed in the molybdenum-lined quartz crucible, the amount of iron in the titanium ore in the quartz crucible decreased from 49.7 % to 0.27 % and high-grade TiO_2 was produced. However, when the titanium ore was not placed in the molybdenum-lined quartz crucible, the amount of iron in the titanium ore in the quartz crucible decreased from 49.7 % to 26.3 %.

These results show that even though titanium ore is not used in the molybdenum-lined quartz crucible, a portion of the iron in the titanium ore in the quartz crucible can be selectively removed by the HCl produced from $CaCl_2$. It is expected that a certain amount of HCl was produced, because the activity of the CaO was decreased owing to the high solubility of CaO in $CaCl_2$ at 1100 K of about 18 mol%.[26] However, high-grade TiO_2 was not produced in the quartz crucible. On the contrary, when titanium ore was placed in the molybdenum-lined quartz crucible, high-grade TiO_2 was produced in the quartz crucible under identical conditions. Therefore, as expected from the thermodynamic analysis, the excess amount of TiO_2 in the molybdenum-lined quartz crucible helped to generate a sufficient amount of the HCl from $CaCl_2$ for the selective removal of iron from the titanium ore in the quartz crucible to produce high-grade TiO_2.

3.5 Summary

With the purpose of establishing a novel, simple, and effective process for upgrading low-grade titanium ore based on selective chlorination, fundamental studies of the process were conducted and its feasibility was demonstrated. The iron present in the titanium ore was completely removed as $FeCl_x$ (l,g) (x = 2, 3) via a reaction between the titanium ore and HCl (g) produced from $CaCl_2$ (l) at 1100 K. In result, a high purity of TiO_2 (s) was obtained. In addition, the iron present in the titanium ore was also partially removed as $FeCl_x$ (l,g) (x = 2, 3) via the reaction between the titanium ore and $CaCl_2$ (l)

at 1100 K, and $CaTiO_3$ (s) was mainly obtained. However, the formation of $CaTiO_3$ (s) hinders the selective chlorination reaction in the titanium ore.

It was demonstrated that when the Vietnamese titanium ore with particle sizes in the range of 44 μm to 510 μm was used as feedstock under vacuum at 1100 K for 5 h, a purity of about 94 % to 97 % TiO_2 (s) was obtained. In addition, when the titanium ores produced in China, Australia, and South Africa were used, a purity of about 91 % to 97 % TiO_2 (s) was obtained when the experiments were conducted under vacuum at 1100 K for 5 h. However, when the Canadian slag was used, a purity of about 89 % TiO_2 (s) was obtained. Moreover, a purity of about 97 % TiO_2 (s) was obtained when the experiment was conducted under an Ar gas atmosphere at 1100 K for 11 h.

References

[1]   T.H. Okabe and J. Kang: "*The Latest Technological Trend of Rare Metals*", CMC Publishing Co. LTD., Tokyo, 2012, Chap. 6-1, pp. 83-94. (in Japanese)

[2]   J. Kang and T.H. Okabe: "*Thermodynamic Consideration of the Removal of Iron from Titanium Ore by Selective Chlorination*", Metall. Trans. B, 2014 (in print).

[3]   T. Wako: "*Industrial Wastewater Management in Japan*", Conference of WEPA Dialogue in Sri Lanka, 2012.
        http://www.env.go.jp/en/focus/docs/files/20120801-51.pdf.

[4]   K.S. Geetha and G.D. Surender: "*Experimental and modelling studies on the aeration leaching process for metallic iron removal in the manufacture of synthetic rutile*", Hydrometallurgy, 2000, vol. 56 (1), pp. 41-62.

[5]   R.G. Becher, R.G. Canning, B.A. Goodheart, and S. Uusna: "*A new process for upgrading ilmenitic mineral sands*", Proceeding of the Australasian Institute of Mining and Metallurgy, 1965, vol. 21, pp. 21-44.

[6]   S. Jayasekera, Y. Marinovich, J. Avraamides, and S.I. Bailey: "*Pressure leaching of reduced ilmenite: electrochemical aspects*", Hydrometallurgy, 1995, vol. 39 (1), pp. 183-199.

[7]   W. Hoecker: "*Process for the production of synthetic rutile*", United States Patent 5601630, 1997.

[8]   J.B. Farrow, I.M. Ritchie, P. Mangano: "*The reaction between reduced ilmenite and oxygen in ammonium chloride solutions*", Hydrometallurgy, 1987, vol. 18 (1), pp. 21-38.

[9]   J.H. Chen: "*Beneficiation of Titaniferous Ores*", United States Patent 3825419, 1974.

[10]   J.H. Chen and L.W. Huntoon: "*Beneficiation of ilmenite ore*", United States Patent 4019898, 1977.

[11]   J.H. Chen: "*Pre-leaching or reduction treatment in the beneficiation of titaniferous iron ores*", United States Patent 3967954, 1976.

[12]   M. Gueguin and F. Cardarelli: "*Chemistry and mineralogy of titania-rich slags. Part 1-hemo-ilmenite, sulphate, and upgraded titania slags*", Miner. Process. Extr. Metall. Rev., 2007, vol. 28, pp. 1–58.

[13]   K. Borowiec, A.E. Grau, M. Gueguin, and J-F. Turgeon: "*Method to upgrade titania slag and resulting product*", United States Patent 5830420, 1998.

[14]   L.K. Doraiswamy, H.C. Bijawat, and M.V. Kunte: "*Chlorination of ilmenite in a fluidized bed*", Chemical Engineering Progress, 1959, vol. 55 (10), pp. 80-88.

[15]   W.E. Dunn: "*High-temperature chlorination of TiO₂ bearing minerals*", Transactions of the Metallurgical Society of AIME, 1960, vol. 218 (1), pp. 6-12.

[16]   C.M. Lakshmanan, H.E. Hoelscher, and B. Chennakesavan: "*The kinetics of ilmenite beneficiation in a fluidised chlorinator*", Chemical Engineering Science, 1965, vol. 20 (12), pp. 1107-1113.

[17]   S. Fukushima and E. Kimura: "*Ilmenite Upgrading: Particularly Concerning Mitsubishi Process*", Titanium·Zirconium, 1975, vol. 23 (2), pp. 67-74. (in Japanese)

[18]   A. Fuwa, E. Kimura, and S. Fukushima: "*Kinetics of Iron Chlorination of Roasted Ilmenite Ore, Fe₂TiO₅ in a Fluidized-Bed Reactor*", Metallurgical Transactions B, 1978, vol. 9B (4), pp. 643-652.

[19]   V.G. Neurgaonkar, A.N. Gokarn, and K. Joseph: "*Beneficiation of ilmenite to rutile by selective chlorination in a fluidised bed*", Journal of Chemical Technology and Biotechnology, 1986, vol. 36 (1), pp. 27-30.

[20]   J.S.J. Van Deventer: "*Kinetics of the selective chlorination of ilmenite*", Thermochimica Acta, 1988, vol. 124, pp. 205-215.

[21]   K.I. Rhee and H.Y. Sohn: "*The selective chlorination of iron from llmenite ore by CO-Cl₂ mixtures: Part I. intrinsic kinetics*", Metallurgical Transactions B, 1990, vol. 21B (2), pp. 321-330.

[22]   K.I. Rhee and H.Y. Sohn: "*The selective carbochlorination of iron from titaniferous magnetite ore in a fluidized bed*", Metallurgical Transactions B, 1990, vol. 21B (2), pp. 341-347.

[23]   H. Zheng: "*Development of a Novel Titanium Production Process Using Selective Chlorination*", Doctoral Thesis, The University of Tokyo, 2007.

[24]   I. Barin: "*Thermochemical Data of Pure Substances*", 3rd ed., VCH Verlagsgesellschaft mbH, Weinheim, Germany, 1995.

[25]   A. Roine: "*HSC Chemistry® 6.1 Outokumpu HSC Chemistry for Windows*", version 6.1, Outokumpu Research Oy Information Center, Finland, 2006.

[26]   D. A. Wenz, I. Johnson and R. D. Wolson: "*Binary alloy phase diagrams 2nd ed. plus updates*", version 1.0, ASM International, USA, 1996.

[27]   R. Matsuoka and T.H. Okabe: "*Iron removal from titanium ore using selective chlorination and effective utilization of chloride waste*", Proceedings of the Symposium on Metallurgical Technology for Waste Minimization (134th TMS Annual Meeting), 2005, San Francisco, United States. http://www.okabe.iis.u-tokyo.ac.jp/japanese/for_students/parts/pdf/050218_ TMS_proceedings_matsuoka.pdf.

Table 3-1 Experimental conditions used in this study.

Exp. No.[a]	Source country of Ti ore	Atmosphere	Reaction time, $t_r\text{'}$ / h	Quartz crucible Particle size, d_{ore} / μm	Weight of ore, w_{ore} / g	Mo-lined Use of Ti ore
120409	Vietnam	Vacuum	5	44 – 74	0.10	O
120510	Vietnam	Vacuum	5	74 – 149	0.10	O
120511	Vietnam	Vacuum	5	149 – 210	0.10	O
120514	Vietnam	Vacuum	5	210 – 297	0.10	O
120611	Vietnam	Vacuum	5	297 – 510	0.10	O
120423	China	Vacuum	5	44 – 74	0.10	O
120424	Australia	Vacuum	5	44 – 74	0.10	O
120426	Canada	Vacuum	5	44 – 74	0.10	O
120501	Canada	Vacuum	7	44 – 74	0.10	O
120824	Canada	Vacuum	13	44 – 74	0.10	O
120427	South Africa	Vacuum	5	44 – 74	0.10	O
120419	Vietnam	Ar gas filled[b]	5	44 – 74	0.10	O
120420	Vietnam	Ar gas filled[c]	7	44 – 74	0.10	O
120421	Vietnam	Ar gas filled[c]	11	44 – 74	0.10	O
120417	Vietnam	Ar gas flow[d]	5	44 – 74	0.10	O
120411	Vietnam	Vacuum	5	44 – 74	0.14	O
120413	Vietnam	Vacuum	5	44 – 74	0.14	X

a : Experimental conditions;
    Weight of titanium ore used in the Mo-lined quartz crucible, w_{ore} = 0.25 g.
    Weight of $CaCl_2$ used in the Mo-lined quartz crucible, w_{CaCl_2} = 3.00 g.
    Particle size used in the Mo-lined quartz crucible, d_{ore} = 74 – 149 μm.
    Reaction temperature, T = 1100 K.
b : After evacuating the quartz tube, the quartz tube was filled with an Ar gas.
    $p_{initial}$ = 0.41 atm. $p_{during\ experiment}$ = 1.00 atm.
c : After evacuating the quartz tube, the quartz tube was filled with an Ar gas.
    $p_{initial}$ = 0.31 atm. $p_{during\ experiment}$ = 1.00 atm.
d : After evacuating the quartz tube, an Ar gas was flowed through the quartz tube
    at a rate of 50 sccm via MFC. $p_{during\ experiment}$ = 1.00 atm.

Table 3-2 Analytical results for residues obtained in the quartz crucible and
the molybdenum-lined quartz crucible:
Influence of particle size of Ti ore on selective chlorination at 1100 K.

Exp. no.[b]		Ore size, d_{ore} / μm	Concentration of element i, C_i (mass%)[a]					
			Ti	Fe	Ca	Mn	Si	Al
Feedstock (Vietnam)			45.0	49.7	0.04	3.47	0.57	0.33
120409	Quartz	44 – 74	96.8	0.27	0.08	0.04	0.76	0.21
	Mo-lined	74 – 149	49.2	30.9	17.8	1.37	0.07	N.D
120510	Quartz	74 – 149	96.7	0.54	0.04	0.10	0.66	0.15
	Mo-lined	74 – 149	52.5	18.1	28.0	0.54	0.03	N.D
120511	Quartz	149 – 210	95.8	0.23	0.05	0.04	0.62	0.58
	Mo-lined	74 – 149	56.9	20.1	21.3	0.50	0.09	N.D
120514	Quartz	210 – 297	95.9	0.33	0.02	0.05	0.54	0.55
	Mo-lined	74 – 149	53.9	18.9	25.7	0.52	0.07	0.13
120611	Quartz	297 – 510	93.7	0.29	0.03	0.03	0.74	0.62
	Mo-lined	74 – 149	51.0	32.6	13.8	1.18	0.49	N.D

a : Determined by XRF analysis (excluding oxygen and other gaseous elements),
  N.D: Not Detected. Below the detection limit of the XRF (< 0.01 %),
  Values are determined by average of analytical results of five samples.

b : Experimental conditions;
  Weight of titanium ore used in the quartz crucible, w_{ore} = 0.10 g.
  Weight of titanium ore used in the Mo-lined quartz crucible, w_{ore} = 0.25 g.
  Weight of CaCl$_2$ used in the Mo-lined quartz crucible, w_{CaCl_2} = 3.00 g.
  Reaction time, t_r' = 5 h.
  Reaction temperature, T = 1100 K.
  Source country of titanium ore: Vietnam.
  Experiments were conducted under vacuum.

Table 3-3 Analytical results for residues obtained in the quartz crucible and the
molybdenum-lined quartz crucible:
Various kinds of Ti ores produced in different countries at 1100 K.

Exp. no.[b]		Source country of Ti ore	Reaction time, t_r' / h	Concentration of element i, C_i (mass%)[a]					
				Ti	Fe	Ca	Mn	Si	Al
Feedstock		China		47.2	45.4	0.21	2.79	1.65	1.41
		Australia		48.5	46.7	0.07	1.69	1.00	1.02
		Canada		76.7	17.1	0.68	0.35	1.60	0.86
		South Africa		93.7	1.46	N.D	N.D	1.27	0.50
120423	Quartz	China	5	91.2	2.37	0.25	0.10	1.28	0.83
	Mo-lined			58.9	20.8	17.2	0.39	0.13	0.65
120424	Quartz	Australia	5	95.1	0.62	0.12	0.06	0.92	0.65
	Mo-lined			59.2	25.1	13.6	0.24	0.07	0.49
120426	Quartz	Canada	5	87.0	6.28	0.59	0.34	1.46	1.29
	Mo-lined			83.4	6.48	4.03	0.22	0.60	0.82
120501	Quartz	Canada	7	88.3	5.41	0.61	0.33	1.31	1.26
	Mo-lined			83.8	5.72	4.29	0.22	0.88	0.77
120824	Quartz	Canada	13	89.1	2.40	0.75	0.29	1.68	1.28
	Mo-lined			83.7	3.04	6.66	0.18	0.65	0.74
120427	Quartz	South Africa	5	95.9	0.06	0.15	0.04	0.72	0.69
	Mo-lined			95.9	0.05	1.20	N.D	N.D	0.05

a : Determined by XRF analysis (excluding oxygen and other gaseous elements),

   N.D : Not Detected. Below the detection limit of the XRF (< 0.01%),

   Values are determined by average of analytical results of five samples.

b : Experimental conditions;

   Weight of titanium ore used in the quartz crucible, w_{ore} = 0.10 g.

   Weight of titanium ore used in the Mo-lined quartz crucible, w_{ore} = 0.25 g.

   Weight of $CaCl_2$ used in the Mo-lined quartz crucible, w_{CaCl_2} = 3.00 g.

   Particle size used in the quartz crucible, d_{ore} = 44 – 74 μm.

   Particle size used in the Mo-lined quartz crucible, d_{ore} = 74 – 149 μm.

   Reaction temperature, T = 1100 K.

   Experiments were conducted under vacuum.

Table 3-4 Analytical results for residues obtained in the quartz crucible and the
molybdenum-lined quartz crucible:
Influence of atmosphere on selective chlorination at 1100 K.

Exp. no.[e]		Atmosphere	Reaction time, t_r' / h	Concentration of element i, C_i (mass%)[a]					
				Ti	Fe	Ca	Mn	Si	Al
Feedstock (Vietnam)				45.0	49.7	0.04	3.47	0.57	0.33
120419	Quartz	Ar gas filled[b]	5	59.4	36.4	0.01	2.63	0.59	0.08
	Mo-lined			54.2	19.0	25.0	0.64	0.09	N.D
120420	Quartz	Ar gas filled[c]	7	73.9	22.9	0.05	1.61	0.41	0.15
	Mo-lined			55.5	17.0	26.1	0.53	0.02	N.D
120421	Quartz	Ar gas filled[c]	11	96.7	0.16	0.06	0.05	0.35	0.18
	Mo-lined			60.5	23.2	13.9	0.73	N.D	N.D
120417	Quartz	Ar gas flow[d]	5	46.8	48.8	0.05	3.58	0.13	N.D
	Mo-lined			53.3	18.7	26.3	0.64	0.04	N.D

a : Determined by XRF analysis (excluding oxygen and other gaseous elements),
   N.D : Not Detected. Below the detection limit of the XRF (< 0.01%),
   Values are determined by average of analytical results of five samples.
b : After evacuating the quartz tube, the quartz tube was filled with an Ar gas.
   $p_{initial}$ = 0.41 atm. $p_{during\ experiment}$ = 1.00 atm.
c : After evacuating the quartz tube, the quartz tube was filled with an Ar gas.
   $p_{initial}$ = 0.31 atm. $p_{during\ experiment}$ = 1.00 atm.
d : After evacuating the quartz tube, an Ar gas was flowed through the quartz tube
   at a rate of 50 sccm via MFC. $p_{during\ experiment}$ = 1.00 atm.
e : Experimental conditions;
   Weight of titanium ore used in the quartz crucible, w_{ore} = 0.10 g.
   Weight of titanium ore used in the Mo-lined quartz crucible, w_{ore} = 0.25 g.
   Weight of $CaCl_2$ used in the Mo-lined quartz crucible, w_{CaCl_2} = 3.00 g.
   Particle size used in the quartz crucible, d_{ore} = 44 – 74 μm.
   Particle size used in the Mo-lined quartz crucible, d_{ore} = 74 – 149 μm.
   Reaction temperature, T = 1100 K.
   Source country of titanium ore: Vietnam.

Table 3-5 Analytical results for residues obtained in the quartz crucible and
the molybdenum-lined quartz crucible:
Influence of the activity of CaO in molybdenum-lined quartz crucible on
selective chlorination at 1100 K.

Exp. no.[b]	Use of Ti ore in the Mo-lined quartz crucible		Concentration of element i, C_i (mass%)[a]			
			Ti	Fe	Ca	Mn
Feedstock (Vietnam)			45.0	49.7	0.04	3.47
120411	Quartz		97.0	0.27	N.D	0.04
	Mo-lined	O	52.0	26.3	20.3	0.69
120413	Quartz		55.6	39.8	0.04	3.03
	Mo-lined	X	-	-	-	-

a : Determined by XRF analysis (excluding oxygen and other gaseous elements),
N.D: Not Detected. Below the detection limit of the XRF (< 0.01 %),
Values are determined by average of analytical results of five samples.

b : Experimental conditions;
Weight of titanium ore used in the quartz crucible, w_{ore} = 0.14 g.
Weight of titanium ore used in the Mo-lined quartz crucible, w_{ore} = 0.25 g.
Weight of $CaCl_2$ used in the Mo-lined quartz crucible, w_{CaCl_2} = 3.00 g.
Particle size used in the quartz crucible, d_{ore} = 44 – 74 μm.
Particle size used in the Mo-lined quartz crucible, d_{ore} = 74 – 149 μm.
Reaction time, t_r' = 5 h.
Reaction temperature, T = 1100 K.
Source country of titanium ore: Vietnam.
Experiments were conducted under vacuum.
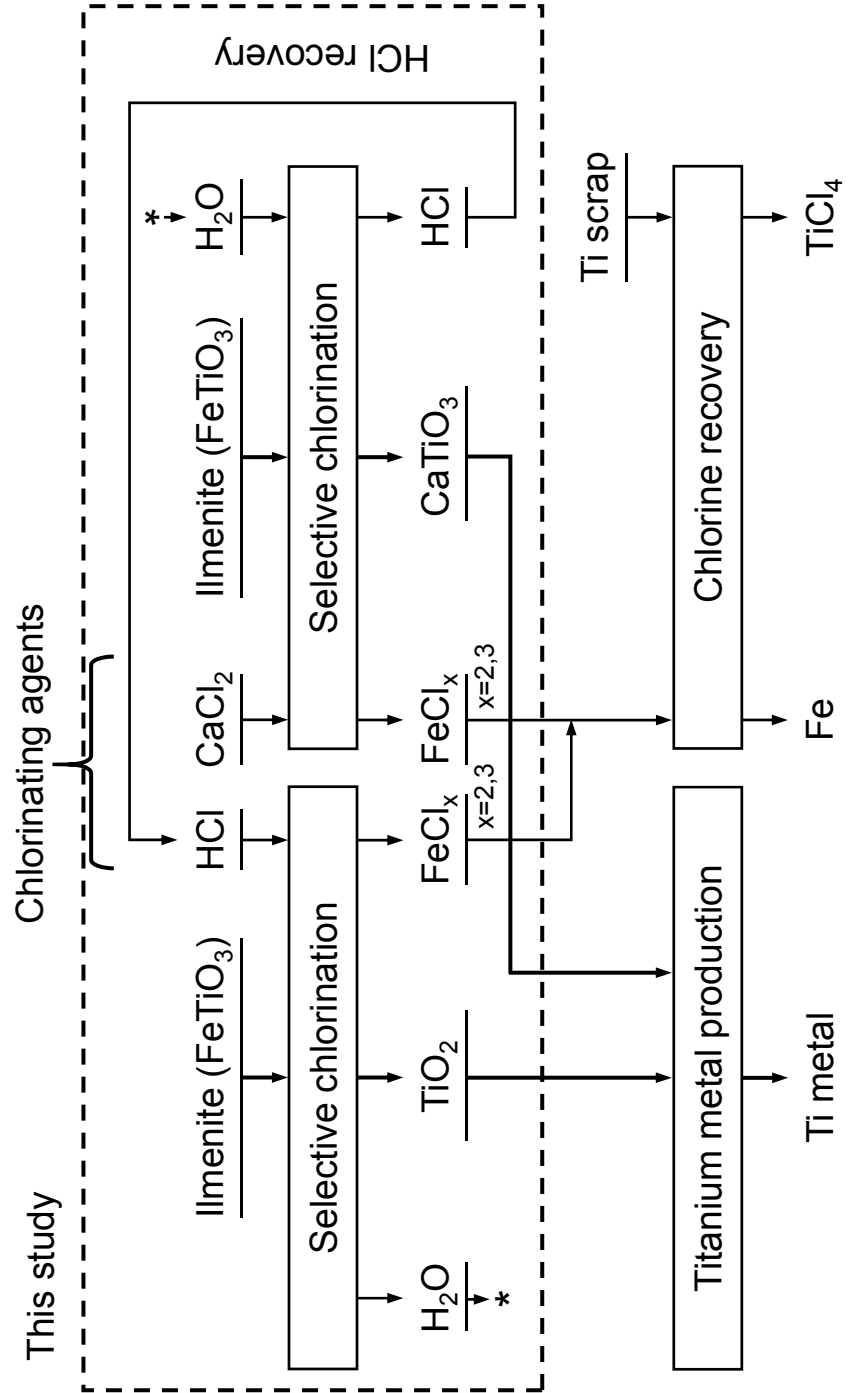
Figure 3-1 Flow diagram for the selective chlorination process investigated in this study.

133
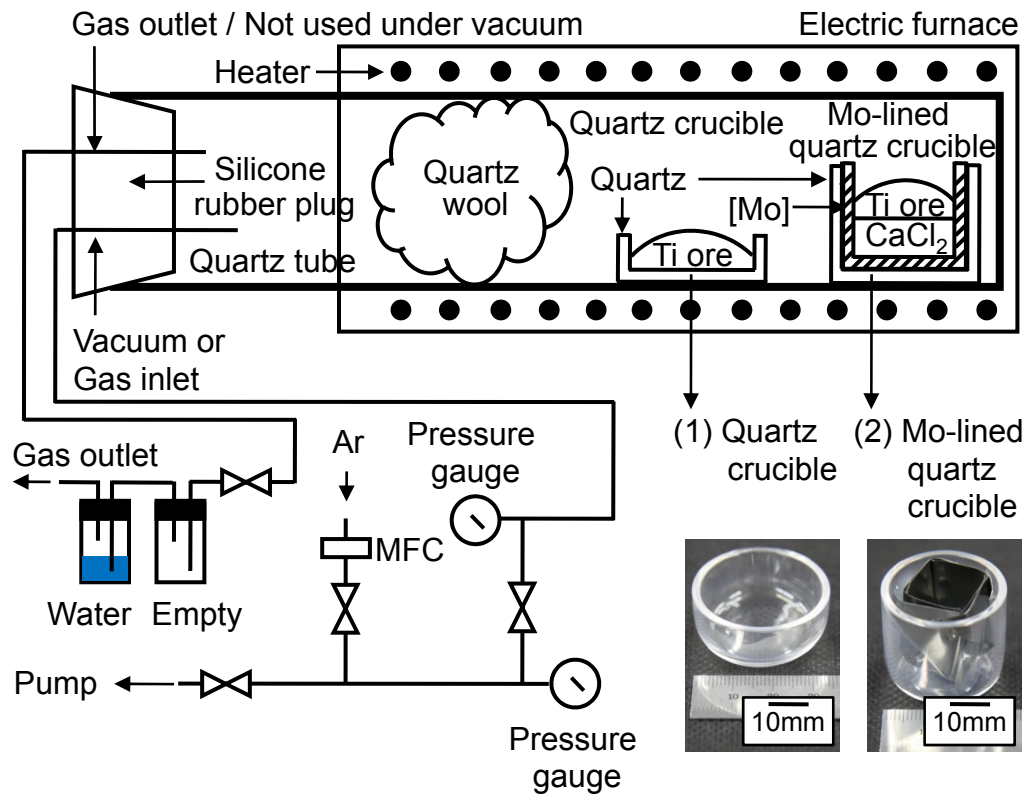
Figure 3-2 Schematic and photographs of the experimental apparatus
used in the study: (1) photograph of the quartz crucible,
(2) photograph of the molybdenum-lined quartz crucible,
and (3) photograph of the quartz tube.

134

Fe-O-Cl system, *T* = 1100 K

Figure 3-3 Chemical potential diagram of the Fe-O-Cl system at 1100 K.

Ti-O-Cl system, *T* = 1100 K
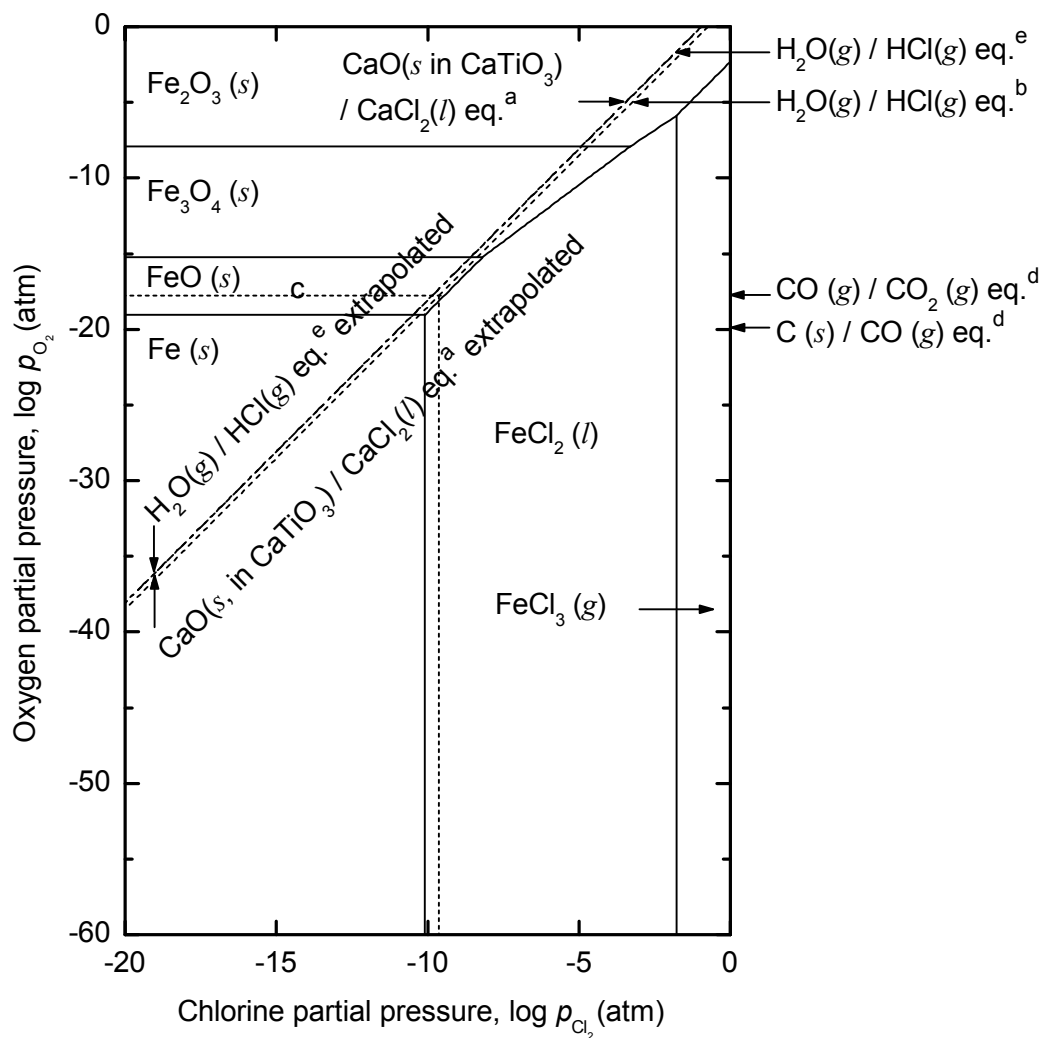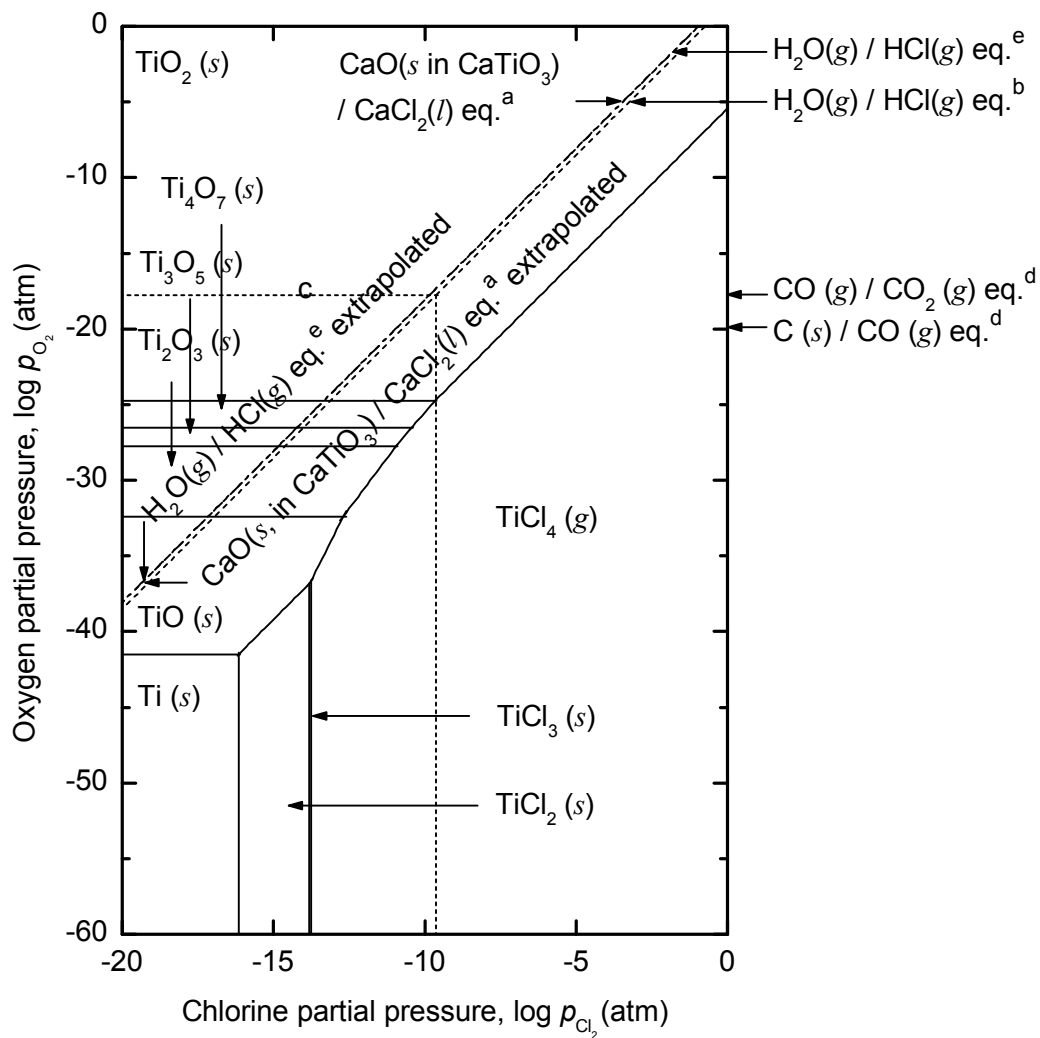
a : a_{CaCl_2} = 1 & a_{CaO} = 6.58x10^{-5} b : p_{H_2O} = 1 atm & p_{HCl} = 1 atm

c : p_{H_2O} / p_{H_2} = 1   d : p_{Cl_2} = 0.1 atm

e : p_{H_2O} / p_{HCl}^2 : Determined by $CaCl_2$ + H_2O = 2 HCl + CaO

under a_{CaO} = 6.58x10^{-5}

Figure 3-4 Chemical potential diagram of the Ti-O-Cl system at 1100 K.

(a)
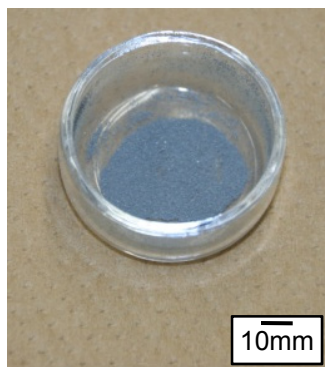
(b)   (c)
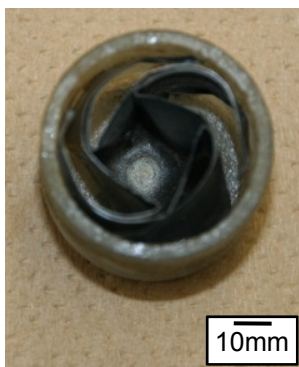
Figure 3-5 Representative photographs of the experimental apparatus
after the experiment: (a) white deposit at the low temperature
part of the quartz tube, (b) residue in the quartz crucible, and
(c) residue in the molybdenum-lined quartz crucible.
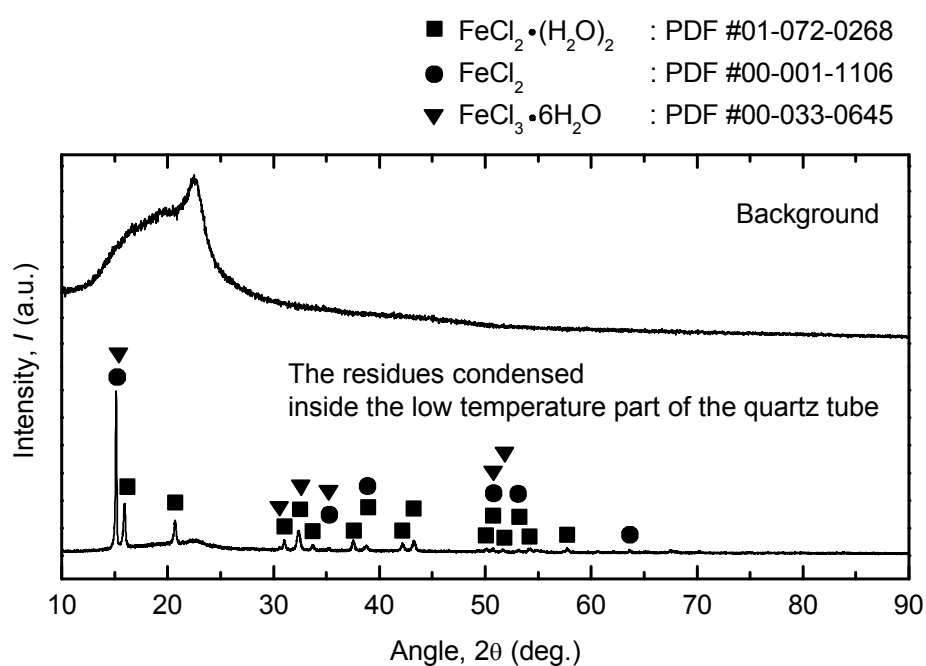
Figure 3-6 XRD patterns of the residues that condensed
inside the low temperature part of the quartz tube.
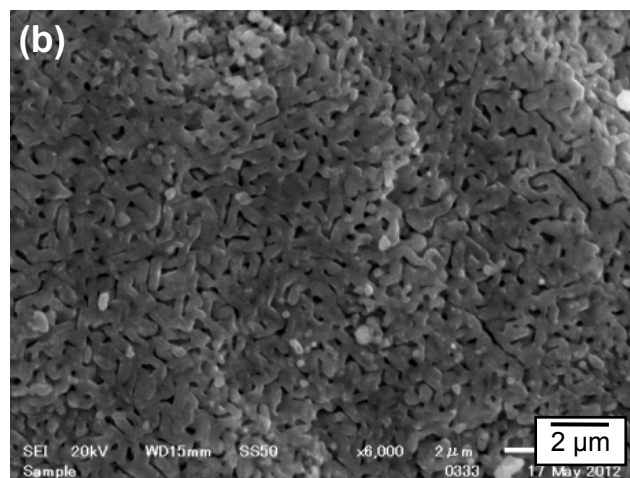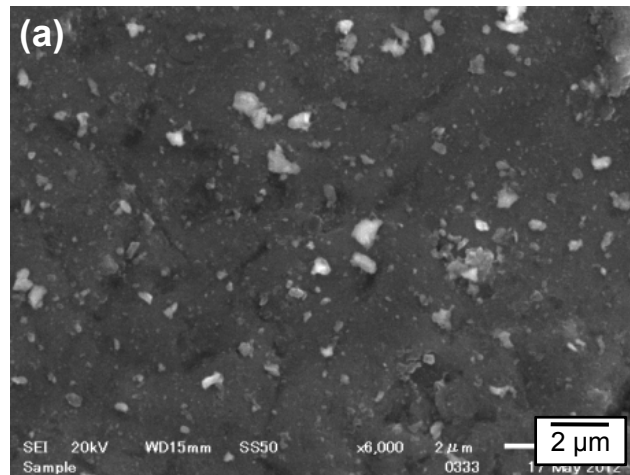
Figure 3-7 SEM images of the microstructure of the Vietnamese titanium
ore particles in the quartz crucible: (a) titanium ore particles with
sizes in the range of 74 μm to 149 μm before the experiment and
(b) titanium ore particles with sizes in the range of 74 μm to
149 μm after the experiment. (*see* Table 3-2)
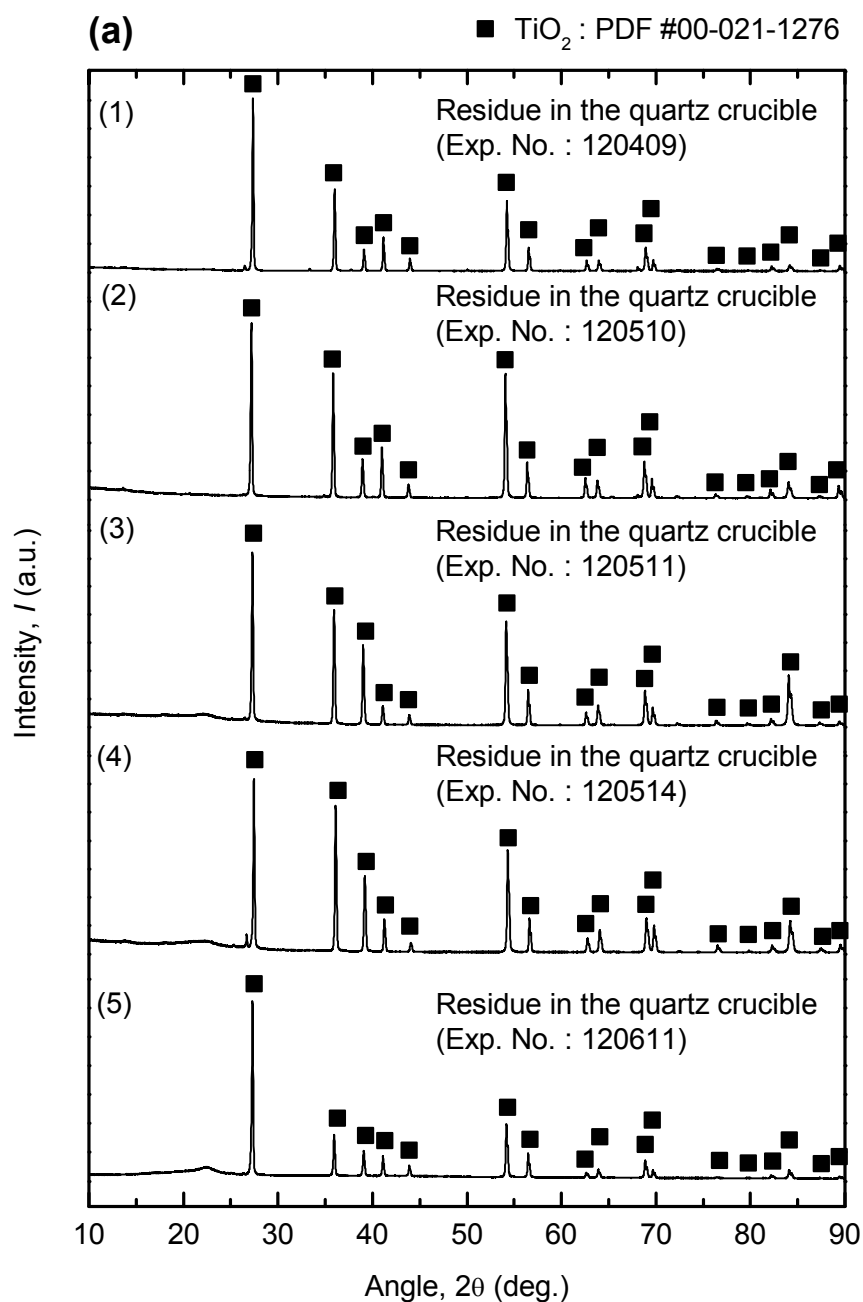
Figure 3-8 (a) XRD patterns of the residues obtained in the quartz crucible when several ore particle size ranges were used: (1) 44 – 74 μm, (2) 74 – 149 μm, (3) 149 – 210 μm, (4) 210 – 297 μm, and (5) 297 – 510 μm. (*see* Table 3-2)
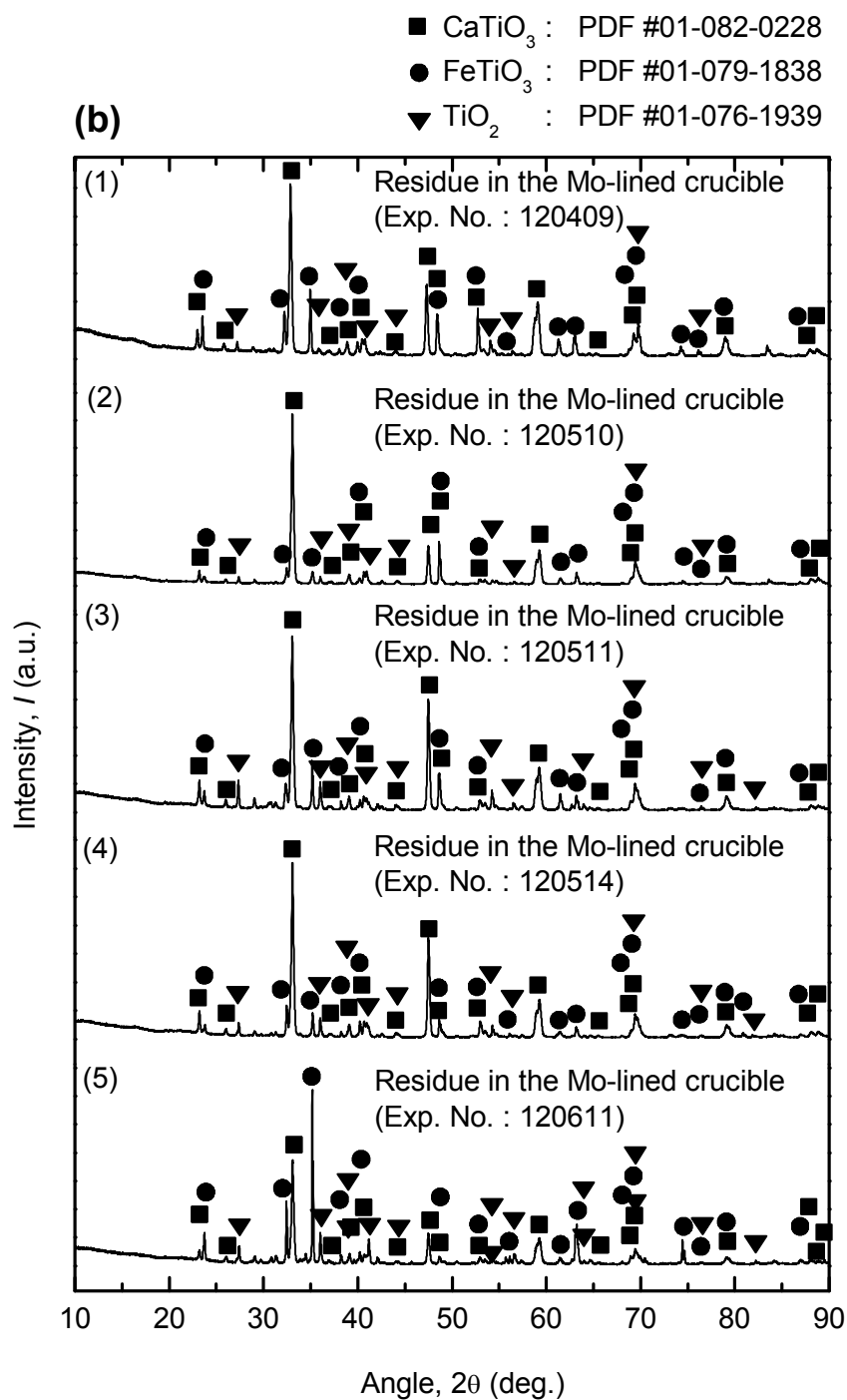
Figure 3-8 (b) XRD patterns of the residues obtained in the molybdenum-lined
quartz crucible when several ore particle size ranges were used:
(1) 44 – 74 μm, (2) 74 – 149 μm, (3) 149 – 210 μm,
(4) 210 – 297 μm, and (5) 297 – 510 μm. (*see* Table 3-2)
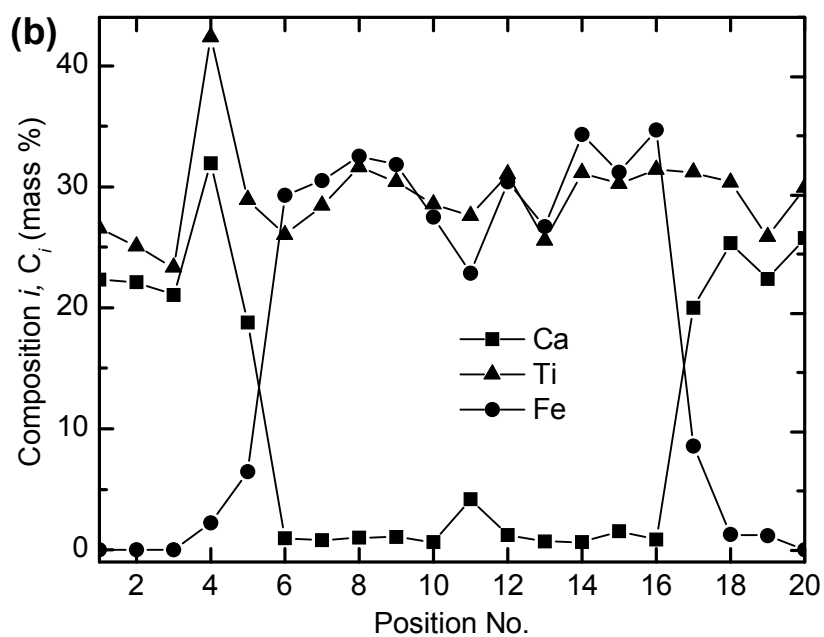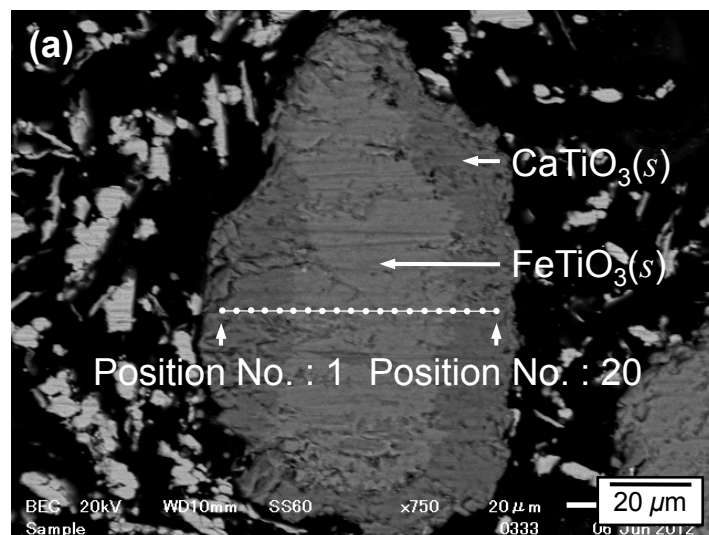
Figure 3-9 (a) SEM image of a cross section of a titanium ore particle obtained
from the molybdenum-lined quartz crucible (Exp. No. : 120409).
(b) EDS results from a cross section of a titanium ore particle
obtained from the molybdenum-lined quartz crucible
(Exp. No. : 120409). (*see* Table 3-2)
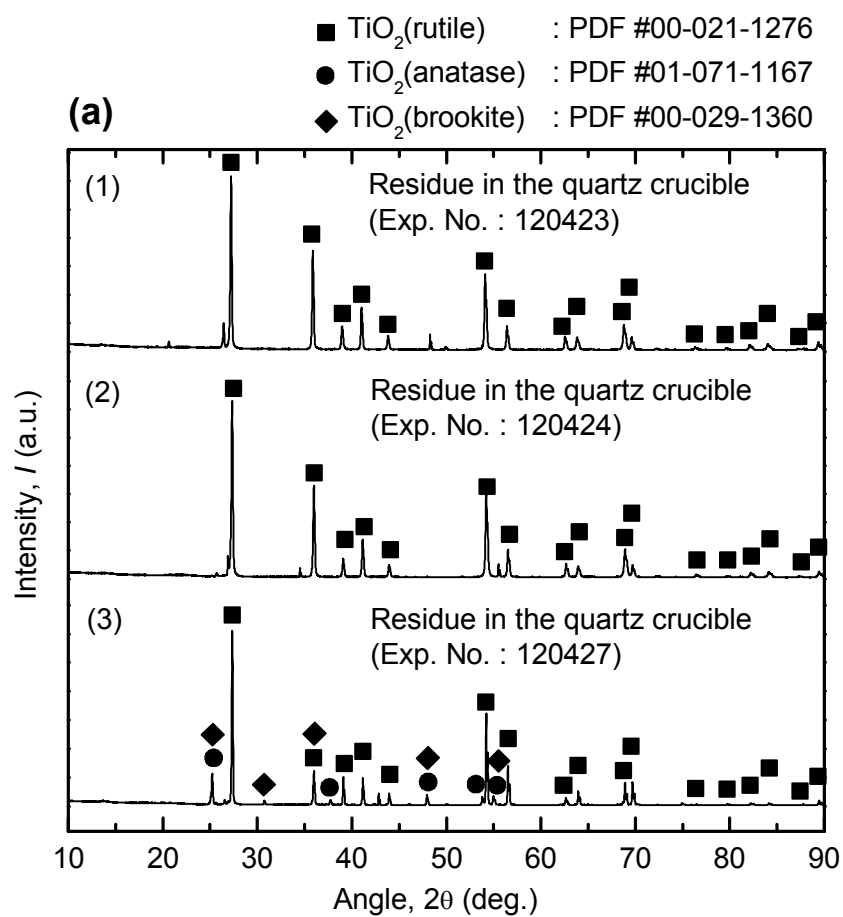
Figure 3-10 (a) XRD patterns of the residues obtained in the quartz crucible
when various kinds of Ti ore were used as feedstock:
(1) natural Chinese ilmenite, (2) natural Australian ilmenite,
and (3) natural rutile produced in South Africa. (*see* Table 3-3)
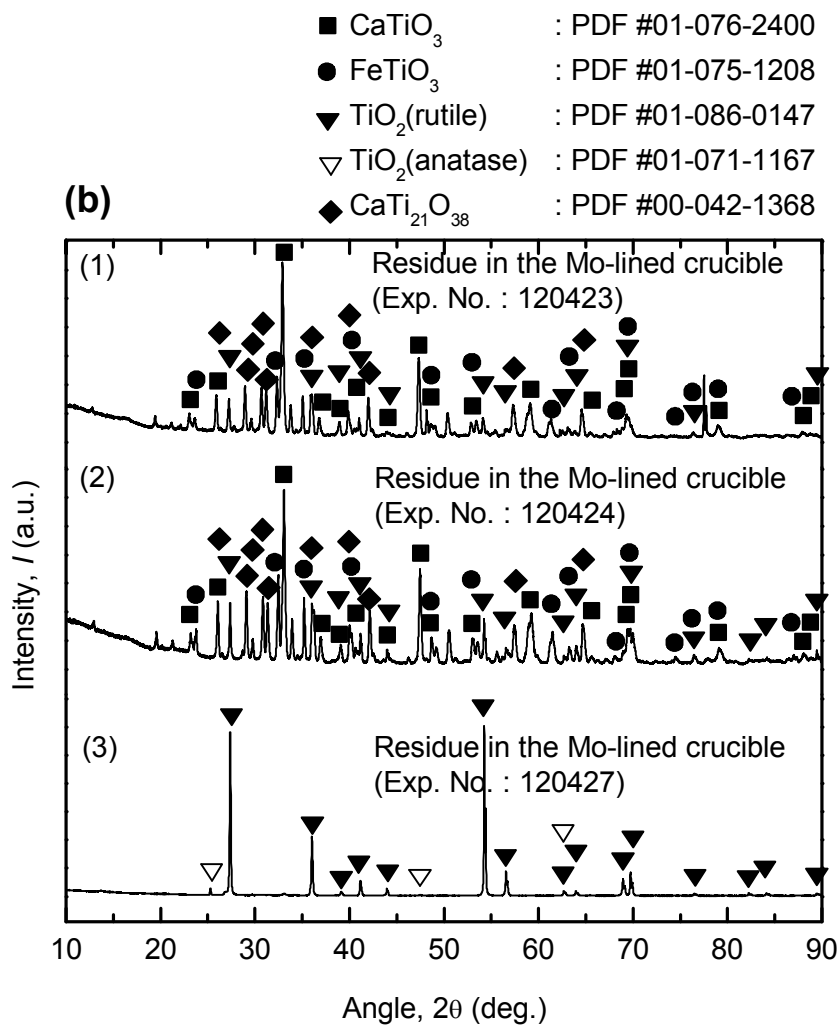
Figure 3-10 (b) XRD patterns of the residues obtained in the molybdenum-lined quartz crucible when various kinds of Ti ore were used as feedstock: (1) natural Chinese ilmenite, (2) natural Australian ilmenite, and (3) natural rutile produced in South Africa. (*see* Table 3-3)
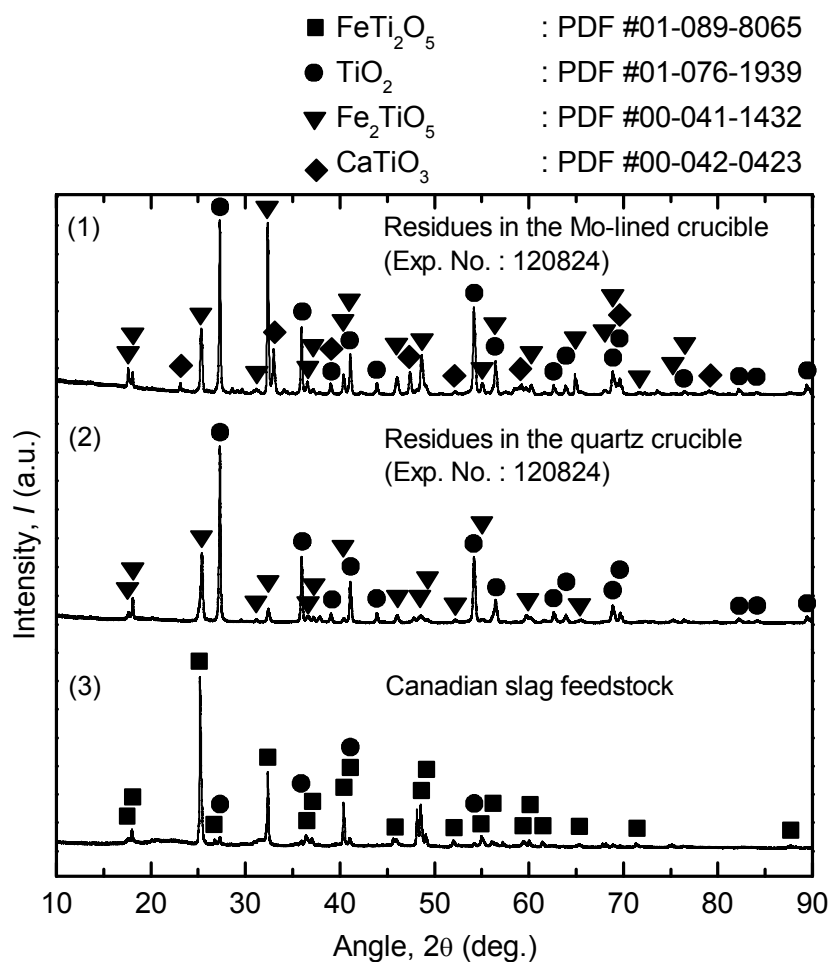
Figure 3-11 XRD patterns of the residues obtained in the quartz crucible and
the molybdenum-lined quartz crucible when the Canadian slag
was used as feedstock for 13 h: (1) residues in the molybdenum-
lined quartz crucible. (2) residues in the quartz crucible, and
(3) the Canadian slag used as a feedstock. (*see* Table 3-3)
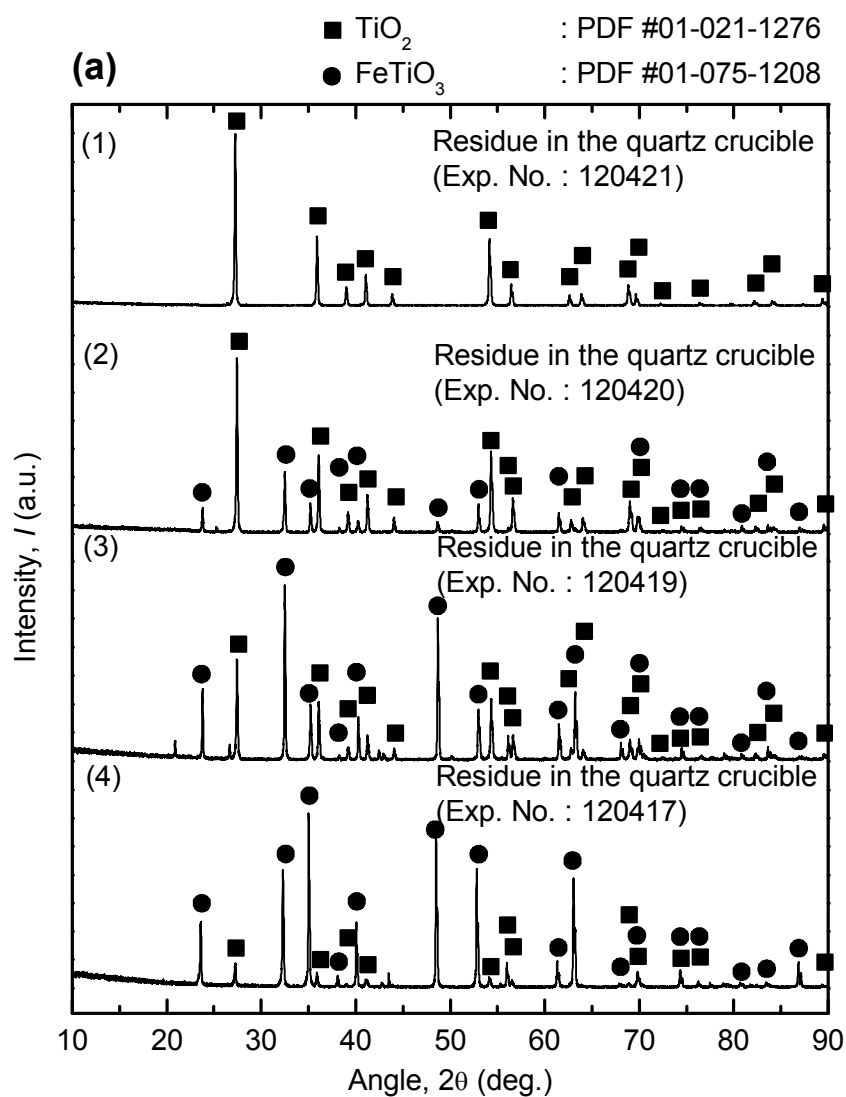
Figure 3-12 (a) XRD patterns of the residues obtained in the quartz crucible when the experiments were conducted under a static Ar gas atmosphere and under an Ar gas flow: (1) 11 h under a static Ar gas atmosphere, (2) 7 h under a static Ar gas atmosphere, (3) 5 h under a static Ar gas atmosphere, and (4) 5 h under an Ar gas flow. (*see* Table 3-4)
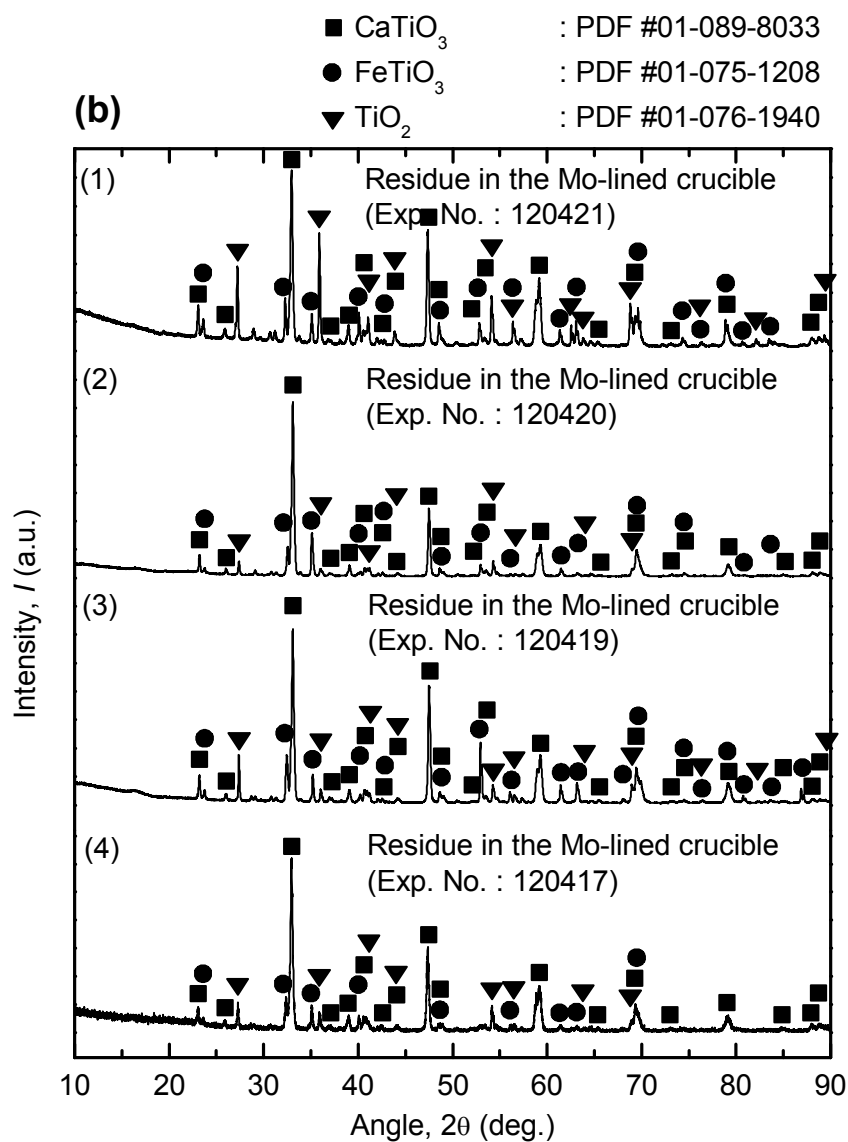
Figure 3-12 (b) XRD patterns of the residues obtained in the molybdenum-lined quartz crucible when the experiments were conducted under a static Ar gas atmosphere and under an Ar gas flow: (1) 11 h under a static Ar gas atmosphere, (2) 7 h under a static Ar gas atmosphere, (3) 5 h under a static Ar gas atmosphere, and (4) 5 h under an Ar gas flow. (*see* Table 3-4)

Chapter 4 Selective chlorination of low-grade titanium ore using calcium chloride for CaTiO₃ production

4.1 Introduction

Since the Kroll's invention in the 1940s, the Kroll process has become the commercial process for the production of titanium (Ti) metal.[1] However, the Kroll process is a low productivity process owing to its slow production speed and batch-type processing, and hence, the global production of titanium metal is much lower than that of iron (Fe) or aluminum (Al). For example, in 2012, the global production of iron and aluminum was about 13000 and 230 times larger than that of titanium, as shown in Fig. 1-3 in chapter 1. Therefore, in recent years, new titanium metal production processes such as the FFC process,[2-5] OS process,[6-11] and EMR/MSE process[12-13] have been proposed. Many studies have focused on increasing productivity by establishing a continuous process (or semi-continuous process) or through development of a high-speed process.

Among these new titanium metal production processes, the FFC and OS processes have been found to be promising for the production of titanium metal, because they are both simple and semi-continuous processes. In the FFC process, titanium metal can be obtained directly from TiO_2 by an electrochemical method using electrons as a reducing agent. In the OS process, titanium metal is produced through the calciothermic reduction of TiO_2 by regenerated calcium. One interesting aspect of these two processes is the possibility of the use of $CaTiO_3$ as a feedstock for titanium metal production. Chen and coworkers reported that perovskitization of TiO_2 ($CaTiO_3$) in $CaCl_2$ can increase the reduction speed and efficiency of the FFC process.[14] In addition, Suzuki and coworkers also reported the use of $CaTiO_3$ as a starting material for titanium metal production by the OS process.[7] These results imply that an effective process for the production of high-grade $CaTiO_3$ from low-grade titanium ore has the potential to be useful for titanium metal production in the future.

Recently, Zheng and Okabe developed a novel method for selective chlorination of low-grade titanium ore by using $CaCl_2$ as a chlorinating agent, and $CaTiO_3$ was mainly produced.[15] However, as shown in Table 1-7 in chapter 1, the iron in the titanium ore was only partially removed. Zheng reported that the iron concentration in the titanium ore

149

decreased from 51 % to 17 % at 1293 K. Very similar results were also obtained as shown in Table 3-2 in chapter 3. As shown in Table 3-2, the concentration of iron in the low-grade titanium ore decreased from 50 % to 18 % through the selective removal of iron by CaCl$_2$. Fig. 3-9 in chapter 3 showed that iron was partially removed from the titanium ore, because the CaTiO$_3$ was produced at the outermost parts of the titanium ore particles. Therefore, the reaction between the iron in the center parts of the titanium ore particles and CaCl$_2$ could not proceed.

In this study, the influence of the reaction temperature, reaction time, particle size of titanium ore, and types of titanium ore on the amount of iron removed from the titanium ore was investigated when CaCl$_2$ was reacted with the titanium ore through physical contact. In addition, after the effects of the various experimental parameters on selective chlorination were studied, an experiment was conducted to evaluate the feasibility of scaling up the selective chlorination process. Fig. 4-1 shows the flowchart of the selective chlorination process developed in this study. As shown in Fig. 4-1, iron in the titanium ore is directly and selectively removed as FeCl$_2$ by CaCl$_2$, and high-grade CaTiO$_3$ is produced in a single step. The selective chlorination process investigated in this study has the following advantages: (1) it does not require the handling of highly concentrated HCl or Cl$_2$ gas for the chlorination, (2) high-grade CaTiO$_3$ can be obtained in a single step through a very simple and scalable process, and (3) various types of low-grade titanium ore can be used as the starting materials.

4.2 Experimental

Fig. 4-2 shows the schematic and a photograph of the experimental apparatus, while Table 4-1 shows the experimental conditions used in this study. In the experiments, CaCl$_2$ (anhydrous; purity > 95.0 %; powder; Kanto Chemicals, Inc.) was used as the chlorinating agent. In addition, Vietnamese, Australian, and Chinese ilmenites were used as the starting materials, and the compositions of these titanium ores are shown in Table 4-2.

Prior to its use, CaCl$_2$ was dried for more than 3 days at 473 K in a vacuum dryer (EYELA, VOS-201SD). In preparation for the experiments, a half of the amount of dried CaCl$_2$ and the entire amount of titanium ore required for the reaction were uniformly

mixed in a molybdenum-lined nickel crucible (nickel crucible: $\phi = 36$ mm, I.D. of top part; $d = 36$ mm, depth; molybdenum lining: $t = 0.1$ mm, thickness). Thereafter, the remaining half amount of CaCl$_2$ required for the reaction was placed in the molybdenum-lined nickel crucible. For Exp. no. 130509 (in Tables 4-1 and 4-2), the preparation was the same as described above, with the exception of the molybdenum-lined nickel crucible, which had different dimensions (nickel crucible: $\phi = 60$ mm, I.D. of top part; $d = 59$ mm, depth; molybdenum lining: $t = 0.05$ mm, thickness). Subsequently, a top lid was loosely placed over the molybdenum-lined nickel crucible. After the CaCl$_2$ and titanium ore was prepared, the molybdenum-lined nickel crucible was placed inside a vertical stainless steel reactor, which was sealed with silicone rubber plugs.

Subsequently, the reactor was evacuated twice for 10 min each time, and Ar gas (purity > 99.9995 %) was flowed through the reactor until the internal pressure of the reactor reached 1 atm. During the experiments, the internal pressure of the reactor was maintained at 1 atm. Ar gas flow was set to 200 cc/min and controlled using a flow meter. The temperature of the reactor was increased at a rate of 4.9 K/min to the target reaction temperature. When the temperature reached the target temperature, the experiments were conducted for the designated reaction time.

After the completion of the reactions, the reactor was naturally cooled to room temperature, and the residues were obtained from the molybdenum-lined nickel crucible. The residues in the molybdenum-lined nickel crucible were dissolved in deionized water with sonication for at least 2 h at room temperature. Then, the residues were leached in 20 % HCl aqueous solution for 30 min with stirring at the rate of 300 rpm at room temperature. The chemical compositions of the residues were determined using X-ray fluorescence (XRF: JEOL, JSX-3100RII) spectroscopy, and their crystalline phases were identified by X-ray diffraction (XRD: RIGAKU, RINT 2500, RINT 2000, Cu-Kα radiation) analysis.

4.3   Thermodynamic analysis of selective chlorination using CaCl$_2$

Thermodynamically, titanium ore can be considered a mixture of FeO and TiO$_2$, because the standard Gibbs energy of the reaction is small at 1240 K, as shown in Eq. 4-1. Consequently, thermodynamic calculations for titanium ore can be performed by

considering FeO and TiO$_2$ separately. Therefore, thermodynamic analysis of the selective chlorination of titanium ore using CaCl$_2$ as a chlorinating agent can be carried out by utilizing the chemical potential diagrams of the Fe-O-Cl and Ti-O-Cl systems.

$$FeO\ (s) + TiO_2\ (s) = FeTiO_3\ (s) \hspace{3cm} (4\text{-}1)$$
$$\Delta G°_r = -17.1\ kJ\ at\ 1240\ K^{[16]}$$

Fig. 4-3 shows the combined chemical potential diagram of the Fe-O-Cl and Ti-O-Cl systems at 1240 K, plotted with chlorine partial pressure (p_{Cl_2}) as the abscissa and oxygen partial pressure (p_{O_2}) as the ordinate. In the hatched region in Fig. 4-3, FeCl$_x$ (l,g) (x=2,3) and TiO$_2$ (s) are stable compounds. This means that if p_{Cl_2} and p_{O_2} are located in the hatched region, the iron in the titanium ore will be transformed to FeCl$_x$ (l,g) (x=2,3) and the titanium in the titanium ore will be transformed to TiO$_2$ (s). In addition, under this condition, FeCl$_x$ (l,g) (x=2,3) will be removed as a gas because the vapor pressure of FeCl$_x$ (l,g) (x=2,3) at 1240 K is sufficient for it to evaporate while the vapor pressure of TiO$_2$ (s) is negligible. In particular, the vapor pressure of FeCl$_2$ (l) at 1240 K is 0.22 atm.[16] As a result, TiO$_2$ (s) can be obtained from the titanium ore by selective removal of iron from titanium ore. Therefore, the hatched region in Fig. 4-3 is called the potential region for selective chlorination.

In this study, the p_{Cl_2} and p_{O_2} of the reaction system were controlled by the CaO (s)/CaCl$_2$ (l) eq., because CaCl$_2$ was used as the chlorinating agent. In the presence of an excess amount of TiO$_2$ in the system, however, the CaO (s)/CaCl$_2$ (l) eq. shifts to the CaTiO$_3$ (s)/TiO$_2$ (s)/CaCl$_2$ (l) eq., which is identical to the CaO (s, in CaTiO$_3$)/ CaCl$_2$ (l) eq. shown in Fig. 4-3. This shift in the equilibrium line occurs because the activity of CaO in CaCl$_2$ is lowered by the formation of CaTiO$_3$, as shown in Eq. 4-2. Fig. 4-3 shows that the equilibrium line corresponding to the CaO (s, in CaTiO$_3$)/CaCl$_2$ (l) eq. (or CaTiO$_3$ (s)/TiO$_2$ (s)/CaCl$_2$ (l) eq.) passes through the vicinity of the FeCl$_2$ (l) stability region. If a slight alteration of thermodynamic parameters or experimental conditions is considered, the iron in the titanium ore is selectively removed as FeCl$_2$ (l) by its reaction between CaCl$_2$, and CaTiO$_3$ (s) is obtained as shown in Eq. 4-3.

$$CaO \ (s) + TiO_2 \ (s, \ FeTiO_3) = CaTiO_3 \ (s) \qquad\qquad (4\text{-}2)$$
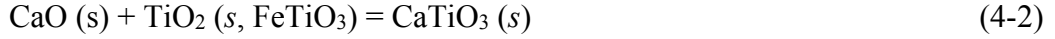
$a_{CaO} = 1.74 \times 10^{-4}$ at 1240 K[17] when $a_{TiO_2} = 1$ and $a_{CaTiO_3} = 1$

$$FeO \ (s) + TiO_2 \ (s) + CaCl_2 \ (l) = FeCl_2 \ (l) + CaTiO_3 \ (s) \qquad\qquad (4\text{-}3)$$
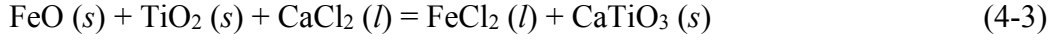
$\Delta G^\circ_r = 6.1$ kJ at 1240 K[17]

4.4   Results and discussion

4.4.1   Verification of selective chlorination using $CaCl_2$

Fig. 4-4 shows photographs of the low-temperature parts of the reactor and the residues in the molybdenum-lined nickel crucible after the experiment. As shown in Fig. 4-4 (a), the white deposits were condensed in the low-temperature regions of the furnace. These deposits were identified as $FeCl_2 \cdot (H_2O)_2$ and $FeCl_2 \cdot 4(H_2O)$ by XRD analysis, as shown in Fig. 4-5. Therefore, it can be claimed that the iron in the titanium ore was selectively removed as $FeCl_2$ as expected from the thermodynamic analysis of the selective chlorination using $CaCl_2$. In addition, the results of XRD analysis showed that H_2O was adhered to $FeCl_2$. It is expected that this H_2O adherence occurred through either or both of the following two routes: (1) H_2O in the air adhered when the top lid of the furnace was removed to collect the white deposits; (2) H_2O, adhered initially to the $CaCl_2$ during the preparation of experiments, was liberated when the reactor temperature was increased.

4.4.2   Influence of reaction temperature

Table 4-2 lists the analytical results for the residues obtained in the molybdenum-lined nickel crucible after the experiments. In this study, the degree of removal of iron from titanium ore is evaluated by the iron removal ratio, R, which was introduced by H. Zheng.[15] The iron removal ratio (R) is defined as follows:

$$R = 100 \times \{1 - (C_{Fe}^1/C_{Ti}^1) / (C_{Fe}^0/C_{Ti}^0)\} \tag{4-4}$$

C_{Fe}^0: the concentration of iron in the feedstock before the experiment,

C_{Fe}^1: the concentration of iron in the residue obtained after the experiment,

C_{Ti}^0: the concentration of titanium in the feedstock before the experiment,

C_{Ti}^1: the concentration of titanium in the residue obtained after the experiment.

When the Vietnamese titanium ore with particles of size under 44 μm was reacted with $CaCl_2$ at 1100 K, 1200 K, and 1240 K for 10 hours, the concentration of iron in the titanium ore decreased from 49.7 % to 14.2 %, 4.16 %, and 2.49 %, respectively. These results show that as the reaction temperature increased, more iron in the titanium ore was selectively removed. It is supposed that the reaction rate was increased by the increase in the reaction temperature. Therefore, it is concluded that iron removal ratio increased to 96 %, because almost all the iron in the titanium ore was selectively removed by $CaCl_2$ when the reaction temperature is 1240 K at least and the size of the particles are smaller than 44 μm.

4.4.3 Influence of reaction time

Table 4-2 also shows the influence of the reaction time on the amount of the iron removed from the titanium ore by selective chlorination. When selective chlorination of the Vietnamese titanium ore with particles of size under 44 μm was carried out using $CaCl_2$ as a chlorination agent at 1240 K for durations of 8, 6, 4, and 2 hours, the concentration of iron in the titanium ore decreased from 49.7 % to 1.87 %, 4.90 %, 4.13 %, and 8.25 %, respectively. Experimental results showed the tendency of a greater amount of iron being removed from the titanium ore with increasing time. In addition, these results showed when reaction times of over 8 hours are required to increase the iron removal ratio up to above 96 % by selective removal of the iron in the titanium ore feedstock at 1240 K when the particles are smaller than 44μm.

4.4.4　Influence of particle size of titanium ore

As shown in Table 4-2, when selective chlorination of the Vietnamese titanium ore with particle sizes in the ranges of 44 – 74 μm, 74 – 149 μm, 149 – 210 μm, and 210 – 297 μm was conducted at 1240 K for 10 hours using $CaCl_2$, the concentration of iron in the titanium ore decreased from 49.7 % to 1.79 %, 3.07 %, 14.4%, and 29.6 %, respectively. These results showed that as the particle size of the titanium ore increased, lesser amount of iron was selectively removed from the titanium ore. In addition, experimental results showed that the iron removal ratio increased to 97 % at most, because the iron in the titanium ore was removed when the particle size of the titanium ore used as a feedstock for the selective chlorination is smaller than 74 μm.

Fig. 4-6 shows the XRD analysis results of the residues obtained after experiments with titanium ore of various particle sizes. As shown in Figs. 4-6 and 4-7, when the size of the titanium ore particles was smaller than 74 μm, $CaTiO_3$ and TiO_2 were mainly obtained. Therefore, it can be concluded that the iron in the titanium ore was selectively removed as $FeCl_2$, and $CaTiO_3$ was produced as expected from the thermodynamic analysis. However, when the size of the titanium ore particles was larger than 74 μm, the presence of $FeTiO_3$ was identified by XRD analysis. It is expected that when titanium ore particles of sizes in the range of 74 – 297 μm were used, 3.07 – 29.6 % of the iron in the titanium ore remained because chlorination of the iron in the center parts of the titanium ore particles by $CaCl_2$ did not proceed owing to the production $CaTiO_3$.

4.4.5　Influence of the various types of titanium ores

The investigation of the influence of reaction temperature, reaction time, and particle size of the titanium ore on selective chlorination showed that the reaction temperature should be above 1240 K, reaction time should be above 8 hours, and the particle size of the titanium ore should be less than 74 μm for increasing the iron removal ratio up to 96 – 97 %. On the basis of these results, when selective chlorination was conducted at 1240 K for 10 hours using the Australian and Chinese titanium ores of particle sizes under 44 μm as feedstock, the concentrations of iron in the titanium ores decreased from 46.7 % to 1.59 % and from 45.4 % to 1.35 %, respectively.

Furthermore, Fig. 4-7 shows that $CaTiO_3$ and TiO_2 were mainly obtained after experiments when the Vietnamese, Australian, and Chinese titanium ores were used. It is thus concluded that selective chlorination using $CaCl_2$ for the production of high-grade $CaTiO_3$ can use various types of low-grade titanium ores as a feedstock. Moreover, the existence of $CaTiO_3$ and TiO_2 in the residues shows that the chemical potentials of oxygen and chlorine in the reaction system were controlled by the TiO_2 (*s*)/$CaTiO_3$ (*s*)/$CaCl_2$ (*l*) eq., as discussed in section 4.3.

Regarding the removal of impurities in the titanium ore, the experimental results showed that the concentration of Mn in the titanium ores was also decreased by selective chlorination. As shown in Table 4-2, when the Vietnamese, Australian, and Chinese titanium ores were used as feedstock, the concentrations of Mn in the titanium ores decreased from 3.47 % to 0.13 %, from 1.69 % to 0.06 %, and from 2.79 % to 0.11 %, respectively. It is expected that the Mn in the titanium ores was removed by the reaction shown in Eq. 4-5. The standard Gibbs energy of the reaction shown in Eq. 4-5 has a large positive value. Despite this, the reaction is expected to proceed, because the activity of CaO is lowered to 1.74×10^{-4} at 1240 K when the formation of $CaTiO_3$ is considered.

$$MnO\ (s) + CaCl_2\ (l) = MnCl_2\ (l) + CaO\ (s) \tag{4-5}$$
$$\Delta G^{\circ}_r = 65.5\ \text{kJ at 1240 K}^{[17]}$$
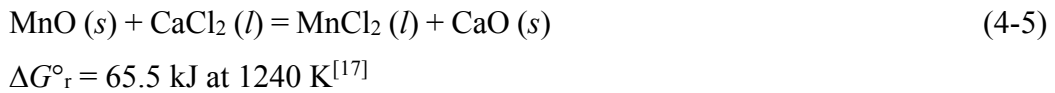
4.4.6   Influence of weight of titanium ore used

In order to check the feasibility of the scale-up of selective chlorination using $CaCl_2$ for the production of $CaTiO_3$, the weight of the titanium ore used was increased from 0.5 g to 3.0 g. The experiment was conducted using titanium ore with particles of size under 44 μm at 1240 K for 20 hours. Consequently, the concentration of iron decreased from 49.7 % to 2.22 % owing to the selective removal of iron from the titanium ore as shown in Table 4-2. In addition, the results of XRF analysis showed that Mn in the titanium ore was also removed from the titanium ore by the selective chlorination; the concentration of Mn decreased from 3.47 % to 0.25 %. These results show that selective chlorination using $CaCl_2$ for producing $CaTiO_3$ can be scaled up. However, it is supposed

that more research on the scaling up is required for improvement because it took 20 hours for upgrading 3.0 g of the low-grade titanium ore used for the experiment.

Table 4-3 lists the comparison of the results of the selective removal of iron from titanium ore obtained in this thesis and those obtained by Zheng *et al*.[15] As shown in Table 4-3, one of the important features of this study is that the feasibility of the scale-up of the selective chlorination using $CaCl_2$ for the production of high-grade $CaTiO_3$ was demonstrated. In addition, the iron removal ratio was 96 – 98 % in this study, while the iron removal ratio was 82 % for the experiments conducted by Zheng *et al*.

4.5   Summary

An effective selective chlorination using $CaCl_2$ as a chlorinating agent for upgrading low-grade titanium ore was investigated for the production of high-grade $CaTiO_3$. Experimental results showed that the iron was selectively removed directly as $FeCl_2$ from the various types of titanium ores studied, and that $CaTiO_3$ was produced in a single step. In this study, the influence of reaction temperature, reaction time, particle size of titanium ore, and types of titanium ore on the amount of iron removed from the titanium ore was investigated. The experimental results showed that amount of iron removed from the titanium ore increased with increasing reaction temperature and time and decreasing the particle size of the titanium ore.

When selective chlorination was conducted using Vietnamese titanium ore particles of size under 74 μm at 1240 K for above 8 hours, the concentration of iron in the titanium ore decreased from about 50 % to 1.8 %. In addition, the concentrations of iron in the Australian and Chinese titanium ores decreased from 47 % to 1.6 % and from 45 % to 1.4 %, respectively, when the experiments were conducted at 1240 K for 10 hours with particles of size under 44 μm. Furthermore, the feasibility of the scale-up of the selective chlorination process was also demonstrated. Therefore, the selective chlorination process using $CaCl_2$ is feasible for the production of high-grade $CaTiO_3$.

References

[1]   W. Kroll: "*The production of ductile titanium*", Transactions of the Electrochemical Society, 1940, vol. 78 (1), pp. 35-47.

[2]   G.Z. Chen, D.J. Fray, and T.W. Farthing: "*Direct electrochemical reduction of titanium dioxide to titanium in molten calcium chloride*", Nature, 2000, vol. 407 (6802), pp. 361-364.

[3]   D.J. Fray: "*Emerging molten salt technologies for metals production*", JOM, 2001, vol. 53 (10), pp. 26-31.

[4]   G.Z. Chen, T.W. Farthing, and D.J Fray: "*Removal of oxygen from metal oxides and solid solutions by electrolysis in a fused salt*", United States Patent 2004/0159559 A1, 2004.

[5]   K.S. Mohandas and D.J. Fray: "*FFC Cambridge process and removal of oxygen from metal-oxygen systems by molten salt electrolysis: an overview*", Trans. Indian Inst. Met., 2004, vol. 57 (6), pp. 579-592.

[6]   K. Ono and R.O. Suzuki: "*A new concept for producing Ti sponge: calciothermic reduction*", JOM, 2002, vol. 54 (2), pp. 59-61.

[7]   R.O. Suzuki and S. Inoue: "*Calciothermic reduction of titanium oxide in molten $CaCl_2$*", Metallurgical and Materials Transactions B, 2003, vol. 34B (3), pp. 277-285.

[8]   R.O. Suzuki, K. Ono, and K. Teranuma: "*Calciothermic reduction of titanium oxide and in-situ electrolysis in molten $CaCl_2$*", Metallurgical and Materials Transactions B, 2003, vol. 34B (3), pp. 287-295.

[9]   R.O. Suzuki and S. Fukui: "*Reduction of TiO_2 in Molten $CaCl_2$ by Ca Deposited during CaO Electrolysis*", Materials Transactions., 2004, vol. 45 (5), pp. 1665-1671.

[10]   R.O. Suzuki: "*Calciothermic reduction of TiO_2 and in situ electrolysis of CaO in the molten $CaCl_2$*", Journal of Physics and Chemistry of Solids, 2005, vol. 66 (2), pp. 461-465.

[11]   R.O. Suzuki: "*Direct reduction processes for titanium oxide in molten salt*", JOM, 2007, vol. 59 (1), pp. 68-71.

[12]   T.H. Okabe and Y. Waseda: "*Producing titanium through an electronically mediated reaction*", JOM, 1997. vol. 49 (6), pp. 28-32.

[13]   I. Park, T. Abiko, and T.H. Okabe: "*Production of titanium powder directly from TiO_2 in $CaCl_2$ through an electronically mediated reaction (EMR)*", Journal of Physics and Chemistry of Solids, 2005, vol. 66 (2) pp. 410-413.

[14]   K. Jiang, X. Hu, M. Ma, D. Wang, G. Qiu, X. Jin, and G.Z. Chen: "*Perovskitization‐Assisted Electrochemical Reduction of Solid TiO$_2$ in Molten CaCl$_2$*", Angewandte Chemie International Edition, 2006, vol. 45 (3) pp. 428-432.

[15]   H. Zheng: "*Development of a novel titanium production process using selective chlorination*", Doctoral Thesis, The University of Tokyo, 2007.

[16]   A. Roine et al.: "*HSC Chemistry$^®$ version 7.11*", Outotec Oy Information Center, Finland, 2011.

[17]   I. Barin: "*Thermochemical Data of Pure Substances*", 3rd ed., VCH Verlagsgesellschaft mbH, Weinheim, Germany, 1995.

Table 4-1 Experimental conditions used in this study.

Exp No.[a]	Source country for Ti ore	Reaction time, t_r' / h	Reaction Temp., T / K	Particle size of Ti ore, d_{ore} / μm	Weight of $CaCl_2$ used, w_{CaCl_2} / g	Weight of Ti ore used, w_{ore} / g
121022	Vietnam	10	1240	under 44	10.00	0.5
121024	Australia	10	1240	under 44	10.00	0.5
121028	China	10	1240	under 44	10.00	0.5
121127	Vietnam	10	1200	under 44	10.00	0.5
121113	Vietnam	10	1100	under 44	10.00	0.5
121029	Vietnam	10	1240	44 – 74	10.00	0.5
121031	Vietnam	10	1240	74 – 149	10.00	0.5
121101	Vietnam	10	1240	149 – 210	10.00	0.5
121106	Vietnam	10	1240	210 – 297	10.00	0.5
121210	Vietnam	8	1240	under 44	10.00	0.5
121211	Vietnam	6	1240	under 44	10.00	0.5
121213	Vietnam	4	1240	under 44	10.00	0.5
121219	Vietnam	2	1240	under 44	10.00	0.5
130509	Vietnam	20	1240	under 44	30.00	3.0

a: Experimental conditions;
  Ar gas flow controlled by flow meter, v_{Ar} = 200 cc / min.

Table 4-2 Analytical results of the feedstock and the residues obtained
in the molybdenum-lined nickel crucible after experiments.

Exp No.	Source country for Ti ore	Composition of element i, C_i (mass%)[a]				Iron removal ratio, R (%)[b]
		Ti	Fe	Ca	Mn	
Feedstock	Vietnam	45.0	49.7	0.04	3.47	
	Australia	48.5	46.7	0.07	1.69	
	China	47.2	45.4	0.21	2.79	
121022	Vietnam	57.2	2.49	39.3	0.13	96
121024	Australia	63.7	1.59	33.5	0.06	97
121028	China	61.5	1.35	35.0	0.11	98
121127	Vietnam	56.1	4.16	39.1	0.22	93
121113	Vietnam	52.8	14.2	31.9	0.34	76
121029	Vietnam	55.6	1.79	42.0	0.16	97
121031	Vietnam	55.1	3.07	41.1	0.20	95
121101	Vietnam	53.7	14.4	31.0	0.54	76
121106	Vietnam	49.7	29.6	18.9	1.36	46
121210	Vietnam	55.3	1.87	42.4	0.13	97
121211	Vietnam	56.6	4.90	37.7	0.23	92
121213	Vietnam	57.3	4.13	38.0	0.22	93
121219	Vietnam	55.5	8.25	35.6	0.23	87
130509	Vietnam	56.5	2.22	40.5	0.25	96

a: Determined by XRF analysis (excluding oxygen and other gaseous elements),
  N.D: Not Detected. Below the detection limit of the XRF (< 0.01 mass%),
  Values are determined by average of analytical results of five samples.
b: $R = 100 \times \{1 - (C_{Fe}^1/C_{Ti}^1) / (C_{Fe}^0/C_{Ti}^0)\}$
  C_{Fe}^0: the concentration of iron in the feedstock before the experiment,
  C_{Fe}^1: the concentration of iron in the residue obtained after the experiment,
  C_{Ti}^0: the concentration of titanium in the feedstock before the experiment,
  C_{Ti}^1: the concentration of titanium in the residue obtained after the experiment.

Table 4-3 Comparison of the results of the selective removal of iron from titanium ore obtained in this thesis and those obtained by Zheng *et al*.[15]

List	Kang *et al*. (this study)	Kang *et al*. (chapter 3)	Kang *et al*. (chapter 5)	Zheng *et al*. (2006)
Source country of feedstock (ilmenite)	Vietnam, Australia, China	Vietnam, Australia, China	Vietnam, Australia, China	Vietnam
Concentration of iron of the Vietnamese feedstock (mass%)	49.7	49.7	49.7	51.3
Concentration of iron after selective chlorination reaction (mass%)	2.22	0.27	1.24	16.7
Furnace type	Vertical	Horizontal	Horizontal	Vertical
Heating method	Electric resistance	Electric resistance	Electric resistance	R.F. induction
Atmosphere (H_2O bath Temp.)	Ar flow	Vacuum	$Ar + H_2O$ (303 K) flow	$N_2 + H_2O$ (298 K) flow
Chlorinating agent	$CaCl_2$	HCl produced from $CaCl_2$	HCl produced from $MgCl_2$	$CaCl_2$
Crucible	Mo-lined nickel	Mo-lined quartz	Mo-lined quartz	Ni-lined carbon
Reaction temperature, T / K	1240	1100	1000	1293
Reaction time, t_r' / h	20	5	7	12
Weight of Ti ore used, w_{ore} / g	3	0.1	0.1	3
Weight of MCl_2 used[a], w_{MCl_2} / g	30	3	3	2
Particle size of Ti ore, d_{ore} / μm	Under 44	44 – 74	44 – 74	Not divided
Product after experiment	$CaTiO_3$	TiO_2	TiO_2	$CaTiO_3$
Mechanism claimed	TiO_2 / $CaCl_2$ / $CaTiO_3$	HCl / H_2O under TiO_2 / $CaCl_2$ / $CaTiO_3$	HCl / H_2O under MgO / $MgCl_2$	TiO_2 / $CaCl_2$ / $CaTiO_3$ or HCl / H_2O under TiO_2 / $CaCl_2$ / $CaTiO_3$

a: M = Ca or Mg.

This study

Ilmenite (FeTiO$_3$)   CaCl$_2$

Selective chlorination

CaTiO$_3$ FeCl$_2$

Ti scrap

Chlorine recovery

Fe   TiCl$_4$

Calciothermic reduction
or electrochemical reduction

Ti metal
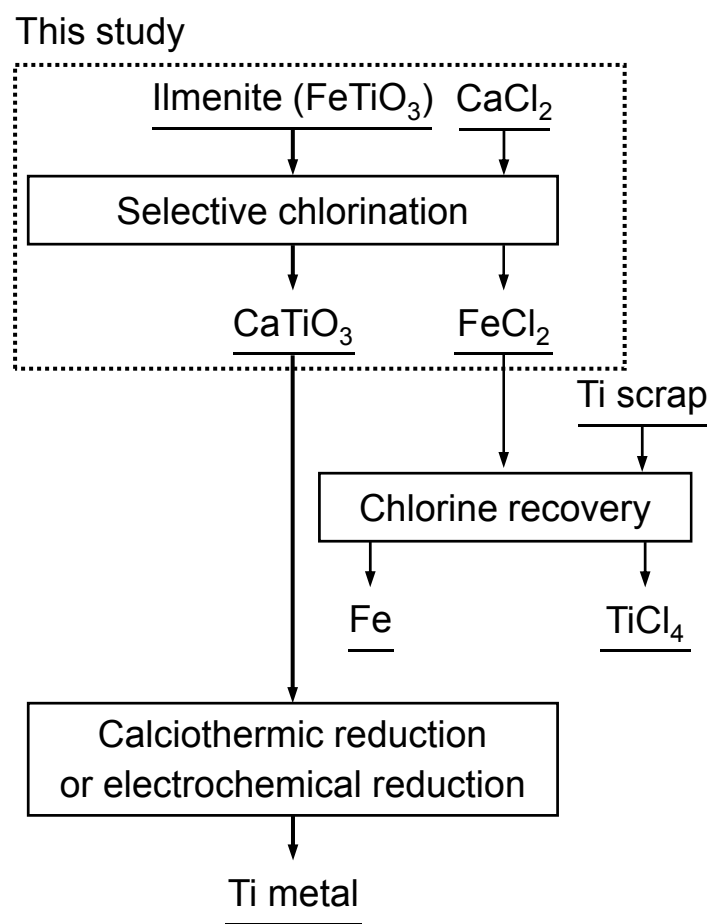
Figure 4-1 Flowchart of the selective chlorination process investigated
in this study.

(a)

Thermocouple

Exhaust gas out

Flow meter

Mg(ClO$_4$)$_2$

Silica gel

Ar gas in

Cooling chamber

600 mm

560 mm

[Mo]   [Ni]

Ti ore +CaCl$_2$

ϕ 103 mm

(b)

3cm
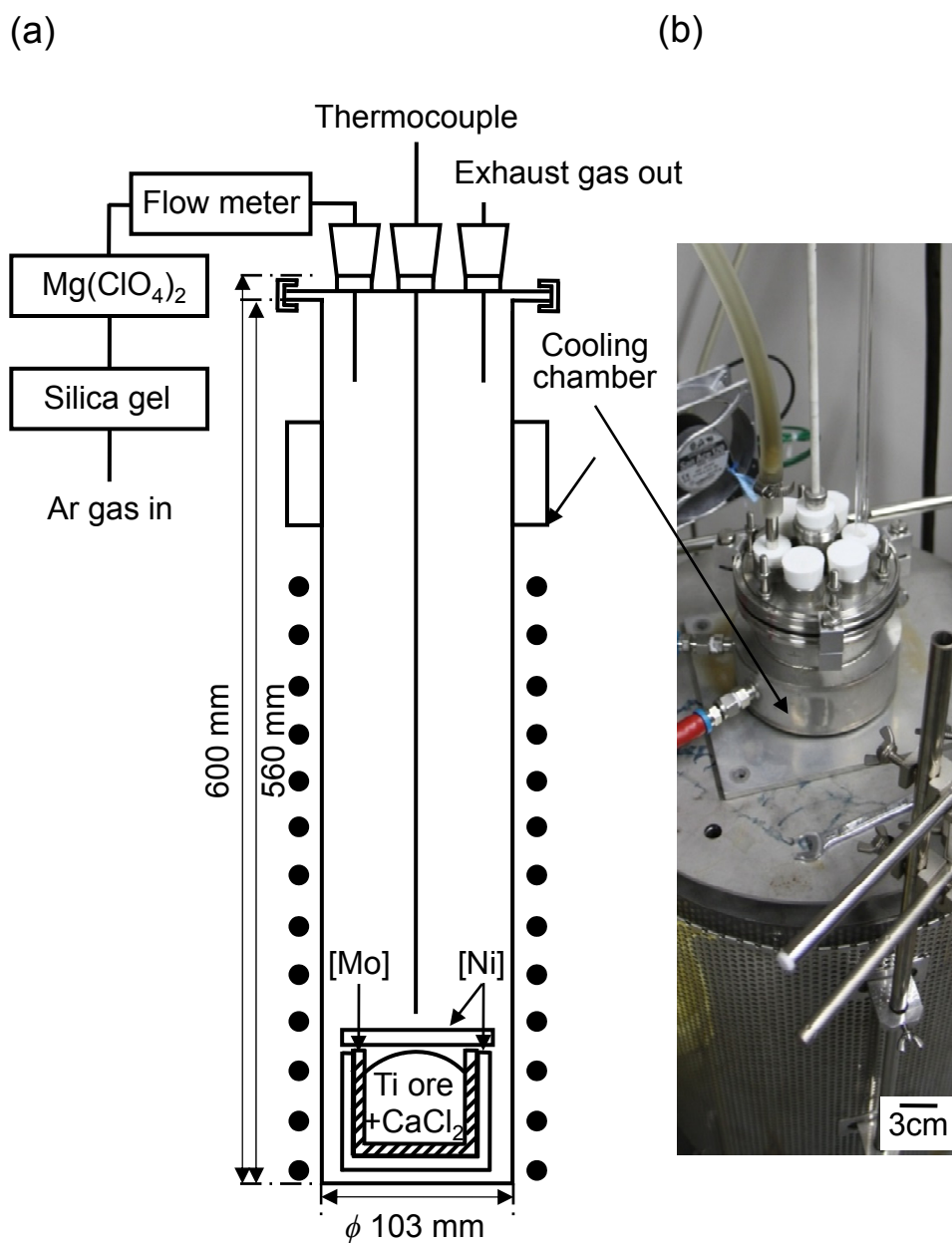
Figure 4-2 (a) Schematic of stainless stell reactor vessel and
(b) External view of the reaction vessel and electric furnace.

Ti-O-Cl system,

Fe-O-Cl system, *T* = 1240 K

Figure 4-3 Combined chemical potential diagram of the Fe-O-Cl system
(solid line) and the Ti-O-Cl system (dotted line) at 1240 K.

(a)

White deposit

20 mm

(b)   (c)

10 mm   140   150   1   10 mm
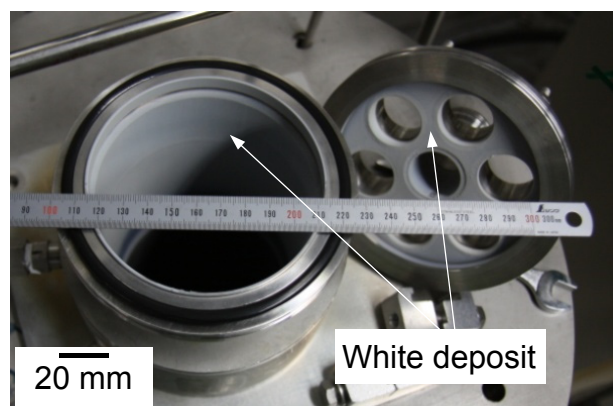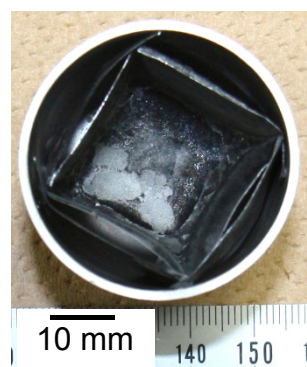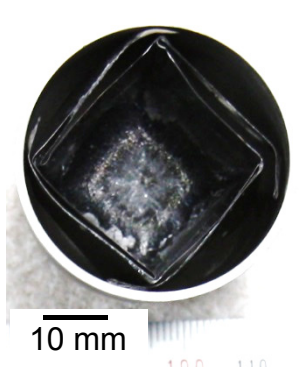
Figure 4-4 Photographs of the reactor and crucible after the experiment:
    (a) white deposit at the low temperature part of the furnace and
    residues in the molybdenum-lined nickel crucible
    (b) (Exp. no. 121024) and (c) (Exp. no. : 121101).
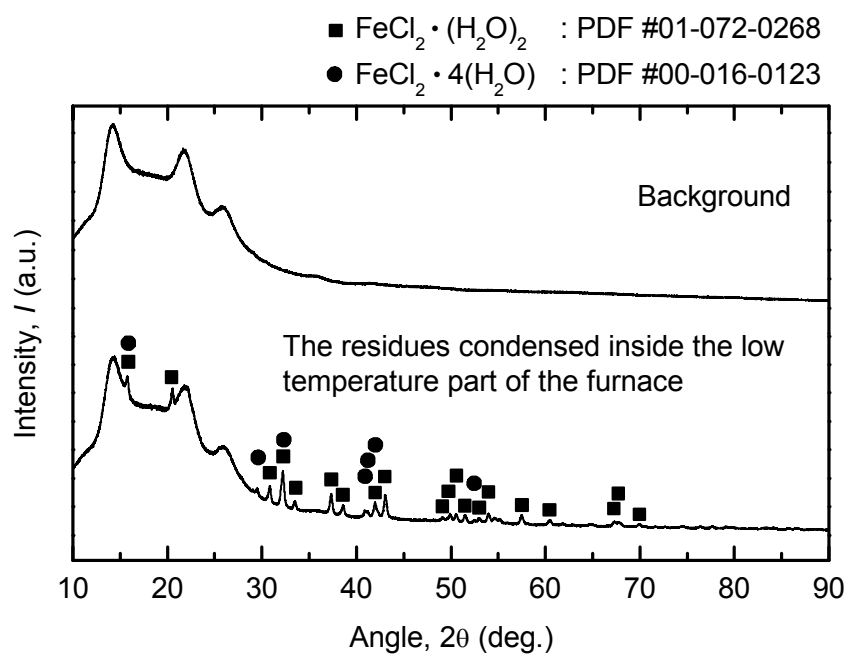
Figure 4-5 XRD patterns of the white deposits that condensed
inside the low-temperature part of the furnace
(Exp. no. 121029)
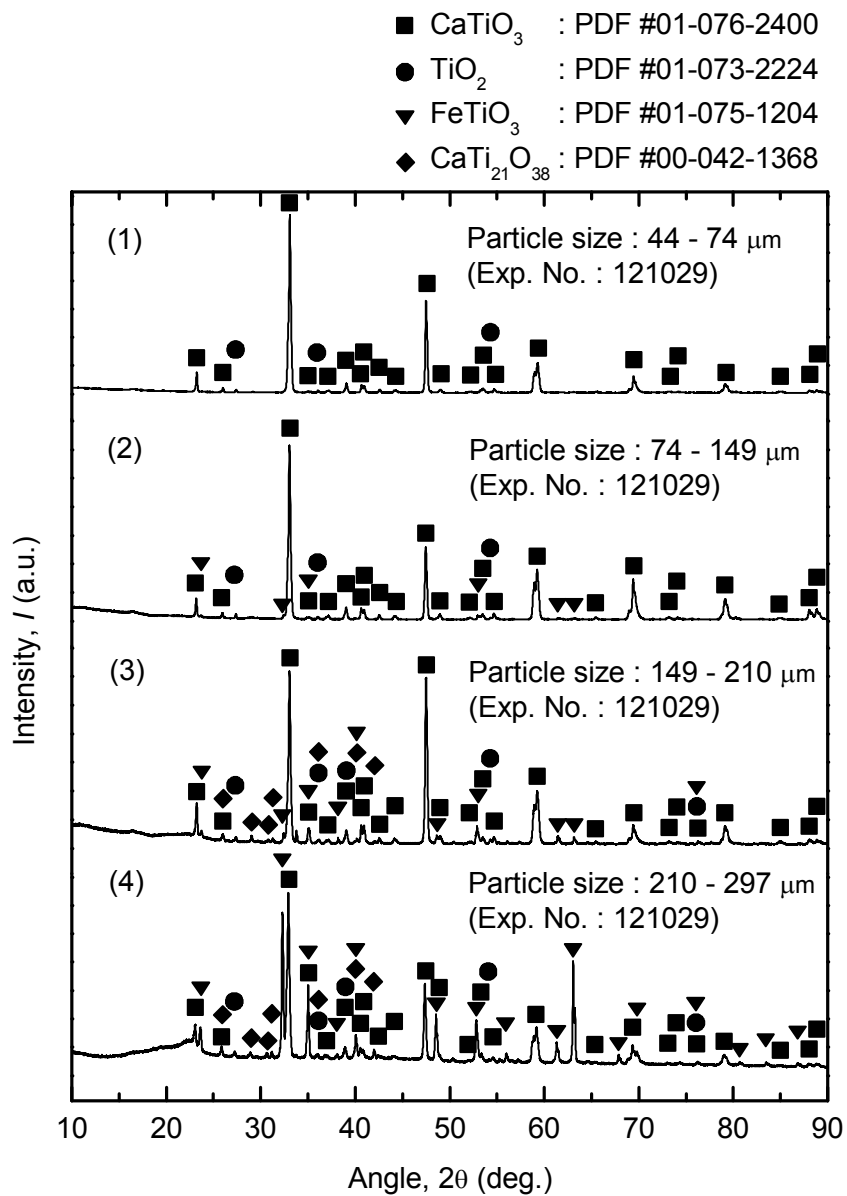
Figure 4-6 XRD results of the residues obtained after experiments
when Ti ore particles with various ranges of: (1) 44 – 74 μm,
(2) 74 – 149 μm, (3) 149 – 210 μm, and (4) 210 – 297 μm
were used. (*see* Table 4-2)
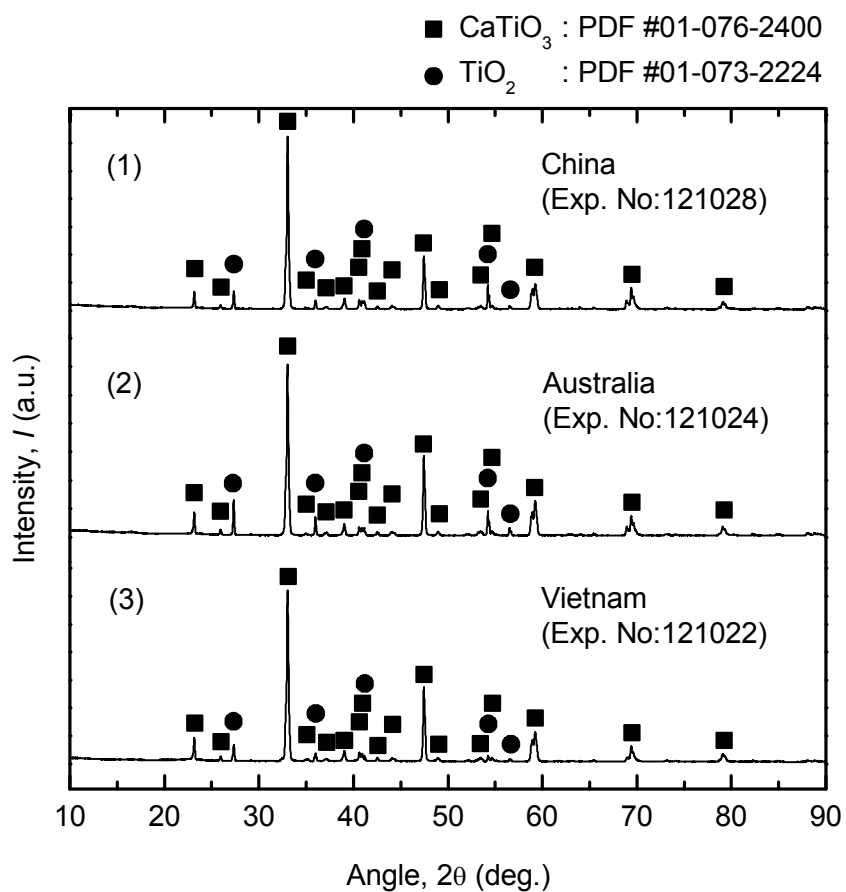
Figure 4-7 XRD results of the residues obtained after experiments
when various types of Ti ores were used as feedstock :
(1) natural Chinese ilmenite, (2) natural Australian ilmenite,
and (3) natural Vietnam ilmenite. (*see* Table 4-2)

Chapter 5   Selective chlorination of low-grade titanium ore using magnesium chloride

5.1   Introduction

Low-grade Ti ore is not used as a feedstock for the Kroll process to prevent operating problems such as clogging of pipes and chlorine loss in a chlorinator.[1] Therefore, as shown in Fig. 5-1, several processing stages are generally required for removing iron from the low-grade Ti ore to produce high-grade TiO_2 feed before use.[2] In many cases, ilmenite is upgraded by the Becher process,[3-7] the Benilite process,[8-10] or the slag and UGS processes.[11-12] In order to decrease the operating problems, many companies place a lower limit on the purity of TiO_2 feed before placing the feed into the chlorinator. Usually the feeds containing at least 90 % of TiO_2 are used.[1] Some countries including Japan have much more strict criteria for a purity of TiO_2 feed, and a minimum criteria for a purity of over 95 % TiO_2 is generally employed for the feed for the Kroll process. However, due to the increase in the price of the TiO_2 feed by, for example, the increase in the consumption of TiO_2 feed in China, recently, some companies in Japan have begun to use 90 % TiO_2 feed in order to reduce the cost of the feedstock.[13]

In the Becher process, various types of titanium ores are used as feedstock. However, multiple stages are required for treating iron, and a huge amount of iron compounds are dumped as wastes. In the Benilite process, processing of iron is simpler than the other processes. However, this process makes use of highly concentrated 18 – 20 % HCl aqueous solution. In the slag process, iron in the Ti ore is reduced to metal (Fe-C alloy) by a carbothermic reduction, and the slag containing titanium oxides and Fe-C alloy are separated. The scale of the slag process is large, and it is high speed process. However, TiO_2 with a low purity of 75 – 86 % is obtained. For obtaining high-grade titania slag, it is essential to employ additional upgrading process such as the UGS process, which entails multiple steps for the further removal of iron.

Extensive research has been conducted to improve the currently used upgrading processes of Ti ore. Among the various processes, selective chlorination has gained significant attention. In the selective chlorination process, iron is only removed directly from the Ti ore as iron chlorides and high-grade TiO_2 feed is obtained. The selective

chlorination processes investigated so far have entailed the use of chlorine gas (Cl_2) under carbon[14-18] or CO/Cl_2 mixture atmosphere,[19-22] or metal chlorides as the chlorine source. Among these processes, the first two processes require Cl_2 gas and installation of the reactor become costly and it also has environmental issue for operation.

The selective chlorination process that uses metal chlorides was recently developed by Okabe's group[23,27] In chapter 3, further improvement of the selective chlorination using calcium chloride ($CaCl_2$) as the chlorinating agent was investigated, and 97 % TiO_2 was successfully obtained directly from Ti ore containing 51 % TiO_2 in a single step.[24] However, because $CaCl_2$ was used as chlorinating agent, it was needed to decrease the activity of CaO by the production of complex oxides such as $CaTiO_3$ for producing HCl gas. In addition, high-grade TiO_2 feed could not be obtained when the experiment was conducted under Ar gas flow atmosphere.

Recently, on the basis of thermodynamic analysis, it was anticipated that extracting chlorine source such as HCl gas from $MgCl_2$ rather than $CaCl_2$ is easier because HCl gas can be produced even under standard state condition ($a_{MgO} = 1$), and is possible even at lower temperatures.[2,25] In this study, in the viewpoint of improvement of HCl gas production and the verification of feasibility for upgrading Ti ore by utilizing $MgCl_2$ for the selective chlorination, $MgCl_2$ was used as a chlorinating agent to remove iron directly from the Ti ore.

Fig. 5-2 shows the flow diagram of the process used in this study. As shown in Fig. 5-2, the process investigated in this study consists of two selective chlorination processes. One selective chlorination process uses $MgCl_2$ to chlorinate the iron in the Ti ore of the Ti ore/$MgCl_2$ mixture. The other selective chlorination process uses HCl gas produced from the Ti ore/$MgCl_2$ mixture to chlorinate the iron in the Ti ore. The selective chlorination investigated in this study has the following advantages; (1) it does not involve handling of highly concentrated HCl or Cl_2 gas, (2) high-grade TiO_2 feed is obtained directly from the Ti ore in one step by a simple scalable method under Ar atmosphere, and (3) various types of Ti ore can be used as a feedstock.

5.2　Experimental

Fig. 5-3 shows the schematic of the experimental apparatus used in this study. $MgCl_2$ (anhydrous; purity $\geq$ 97.0 %; granular; Wako Pure Chemical Industries, Ltd.) was dried in a vacuum dryer (EYELA, VOS-201SD) for more than 3 days at 473 K before use. In addition, natural ilmenite produced in Vietnam, Australia, and China were used as feedstocks. The compositions of the Ti ores are shown in Tables 5-2, 5-3, and 5-4. The particle of Ti ore sample was separated according to particle diameter using sieve before high temperature experiments. The particle size ranged from 44 μm to 149 μm was prepared by grinding and sieving the particle size ranged from 149 μm to 210 μm before the experiments.

Before the experiments were carried out, a mixture of $MgCl_2$ and Ti ore was placed in the molybdenum-lined quartz crucible (quartz crucible: ϕ = 26 mm, I.D.; d = 24 mm, depth). In addition, the Ti ore was placed in a quartz crucible (ϕ = 31 mm, I.D.; d = 13 mm, depth). After placing the samples in the two crucibles, both crucibles were placed into the quartz tube (ϕ = 41.5 mm, I.D.; l = 545 mm, length), and then an appropriate atmosphere was provided for the samples in each experiment. The quartz tube was then placed in a horizontal furnace that was heated to up to 1000 K.

Table 5-1 shows the experimental conditions used in the present study. When the experiments were conducted under vacuum, the quartz tube was evacuated twice for 10 min each before the experiments. Ar gas (purity > 99.9995 %) was filled into the quartz tube between the evacuations until the internal pressure was 1 atm.

When the experiments were conducted under Ar gas atmosphere, after evacuation (carried out as mentioned above), Ar gas was filled until the internal pressure of the quartz tube was 1 atm. After the internal pressure of the quartz tube became 1 atm, the quartz tube was flowed with Ar gas at the rate of 50 sccm via a mass flow controller (MFC), while maintaining the internal pressure of the quartz tube at 1 atm during experiments.

When the experiments were conducted under Ar + H_2O gas atmosphere, water in a bubbler was bubbled with Ar gas for 30 min to remove the dissolved oxygen. After pretreatment of the water, the quartz tube was filled with Ar gas until the internal pressure of the tube reached 1 atm after the evacuation procedure. Subsequently, Ar gas was injected through the water bubbler and the gas flow rate was maintained at 50 sccm by

the MFC, while the internal pressure of the quartz tube was maintained at 1 atm. The temperature of the water in the bubbler was controlled by using a mantle heater (Model No.: HF-200S, As One Co.) and maintained at 303 K.

After a preset reaction time, the quartz tube was instantly taken out of the furnace and cooled down at room temperature. The residues in the quartz crucible were analyzed without subjecting the samples to any leaching process. However, the residues in the molybdenum-lined quartz crucible were dissolved in deionized water for two hours by sonication at room temperature and then leached in 20 % HCl aqueous solution for 30 min with stirring at the rate of 300 rpm at room temperature.

The compositions of the residues obtained in both crucibles were analyzed using X-ray fluorescence spectroscopy (XRF: JEOL, JSX-3100RII), their microstructures and compositions were analyzed using scanning electron microscopy / energy dispersive X-ray spectroscopy (SEM/EDS: JEOL, JSM-6510LV), and their crystalline phases were identified using X-ray diffraction (XRD: RIGAKU, RINT 2500, Cu-Kα radiation) analysis.

5.3 Thermodynamic analysis of selective chlorination using MgCl$_2$

To understand the mechanism of the selective chlorination thermodynamically, FeTiO$_3$ is assumed as a mixture of FeO and TiO$_2$. This assumption is acceptable from a thermodynamic viewpoint and is used in several studies because the Gibbs energy of formation of FeTiO$_3$ is a small negative value as shown in Eq. 5-1.

$$FeO\ (s) + TiO_2\ (s) = FeTiO_3\ (s) \qquad\qquad (5\text{-}1)$$
$$\Delta G^\circ_r = -12\ \text{kJ at 1000 K}^{[26]}$$

Figs. 5-4 and 5-5 show the chemical potential diagrams of the Fe-O-Cl and the Ti-O-Cl systems at 1000 K, respectively, and the abscissa, p_{Cl_2}, is the chemical potential of chlorine gas and the ordinate, p_{O_2}, is the chemical potential of oxygen gas. In addition, Fig. 5-6 was constructed by overlapping the chemical potential diagram of Fe-O-Cl system and that of the Ti-O-Cl system shown in Figs. 5-4 and 5-5, respectively. Any point in the hatched area shown in Fig. 5-6 belongs to the stability region of TiO$_2$ (s) and

FeCl$_2$ (l), or TiO$_2$ (s) and FeCl$_3$ (g). The vapor pressure of FeCl$_2$ (l) at 1000 K is 0.02 atm,[26] which is high enough to evaporate FeCl$_2$ (l). As a result, thermodynamically, if the chemical potentials of oxygen and chlorine are positioned in the hatched area shown in the Fig. 5-6, the iron oxides can be removed as gaseous iron chlorides and solid titanium dioxide can be obtained as a result of the selective chlorination process.

In this study, MgCl$_2$ was used as the chlorinating agent. Even though MgCl$_2$ was dried in the vacuum oven prior to use, absorption of H$_2$O from air is expected to occur during experimental preparation owing to the hygroscopicity of the MgCl$_2$. Therefore, Eq. 5-2 is to be considered in this reaction system.

$$MgCl_2\ (l) + H_2O\ (g) = MgO\ (s) + 2\ HCl\ (g) \qquad (5\text{-}2)$$
$$\Delta G^{\circ}{}_r = -\ 19\ kJ\ at\ 1000\ K^{[26]}$$
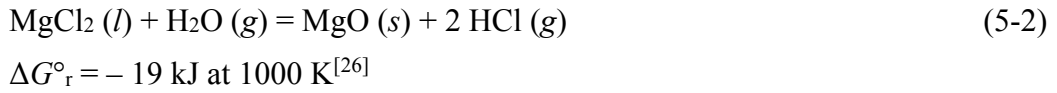
$$\log p_{O_2} = 2 \log p_{Cl_2} + 2 \log p_{H_2O} - 4 \log p_{HCl}$$
$$+ 4 \log K_f\ (HCl) - 2 \log K_f\ (H_2O) \qquad (5\text{-}3)$$

As shown in Eq. 5-2, if H$_2$O exists in the system, HCl gas can be produced from MgCl$_2$ installed in the molybdenum-lined quartz crucible at elevated temperature. In addition, it is easy to obtain HCl gas from MgCl$_2$ when H$_2$O is introduced in the reaction system. On the basis of this reason, a water bubbler was used in this study for intentionally introducing H$_2$O vapor into the quartz tube to accelerate the production of HCl gas according to the Eq. 5-2. The partial pressure of H$_2$O vapor introduced into the quartz tube could be fixed at 0.04 atm by using the water bubbler at 303 K.[26]

The lines corresponding to the H$_2$O (g)/HCl (g) eq.[d] and H$_2$O (g)/HCl (g) eq.[e] in Fig. 5-6 can be derived from Eq. 5-3 by considering the reaction shown in Eq. 5-2. If MgO remains as a solid in MgCl$_2$ (l) after the experiments, the activity of MgO (s) (a_{MgO}) is unity, and then H$_2$O (g)/HCl (g) eq.[e] under MgO (s)/MgCl$_2$ (l) eq.[a] dominates the reactions in the system. Meanwhile, if the solubility of MgO (s) in the MgCl$_2$ (l) at 1000 K is high enough, or if all of the MgO (s) reacts with TiO$_2$ (s) in Ti ore, the activity of MgO (s) is decreased by forming MgTiO$_3$ (s) as shown in Eq. 5-4, and H$_2$O (g)/ HCl (g) eq.[d] under TiO$_2$ (s)/MgTiO$_3$ (s)/MgCl$_2$ (l) eq. dominates the reactions in the system. If the activity of the reaction product MgO (s) is decreased in the system,

$MgCl_2$ becomes a stronger chlorinating agent. It is worth noting that both lines corresponding to the H_2O (*g*)/HCl (*g*) eq.[d] and H_2O (*g*)/HCl (*g*) eq.[e] in Fig. 5-6 pass through the stability region of $FeCl_2$ (*l*) in the hatched region. Therefore, iron in the Ti ore can be selectively removed from the ore directly as $FeCl_2$ (*l,g*) in the quartz crucible by the reaction shown in Eq. 5-5. In addition, the reaction shown in Eq. 5-2 proceeds further by the H_2O produced according to the reaction shown in Eq. 5-5. Both H_2O and HCl gas act as reaction mediators of chlorination when $MgCl_2$ (+H_2O) is used as the chlorinating agent.
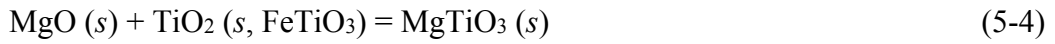
$$MgO\ (s) + TiO_2\ (s,\ FeTiO_3) = MgTiO_3\ (s) \tag{5-4}$$
$a_{MgO} = 0.054$ at 1000 K[26] when $a_{TiO_2} = 1$ and $a_{MgTiO_3} = 1$

$$FeO\ (s) + 2\ HCl\ (g) = FeCl_2\ (l) + H_2O\ (g) \tag{5-5}$$
$\Delta G°_r = - 3.8$ kJ at 1000 K[26]

$MgCl_2$ by itself can act as the chlorinating agent if it is used in reaction with the Ti ore through physical contact. Both lines corresponding to the MgO (*s*)/$MgCl_2$ (*l*) eq.[a] and TiO_2 (*s*)/$MgTiO_3$ (*s*)/$MgCl_2$ (*l*) eq. in Fig. 5-6 also pass through the stability region of $FeCl_2$ (*l*) in the hatched region. The line corresponding to the MgO (*s*)/$MgCl_2$ (*l*) eq.[a] considered the standard state, which means that the activity of MgO (*s*) produced in the molybdenum-lined quartz crucible is unity. The reaction under MgO (*s*)/$MgCl_2$ (*l*) eq.[a] is shown in Eq. 5-6. The line corresponding to the TiO_2 (*s*)/$MgTiO_3$ (*s*)/$MgCl_2$ (*l*) eq. considered $MgTiO_3$ (*s*) production during chlorination, and the reaction under TiO_2 (*s*)/$MgTiO_3$ (*s*)/$MgCl_2$ (*l*) eq. is shown in Eq. 5-7. In both cases, iron can be selectively removed from Ti ore directly as $FeCl_2$ (*l,g*) in the molybdenum-lined quartz crucible.

$$FeO\ (s) + MgCl_2\ (l) = FeCl_2\ (l) + MgO\ (s) \tag{5-6}$$
$\Delta G°_r = - 23$ kJ at 1000 K[26]
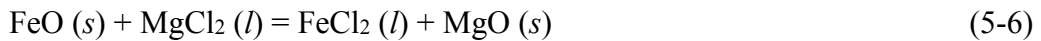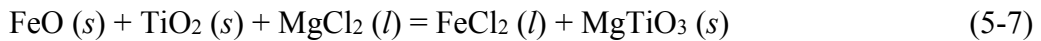
$$FeO\ (s) + TiO_2\ (s) + MgCl_2\ (l) = FeCl_2\ (l) + MgTiO_3\ (s) \tag{5-7}$$
$\Delta G°_r = - 47$ kJ at 1000 K[26]

5.4　Results and discussion

5.4.1　Verification of selective chlorination using $MgCl_2$

Fig. 5-7 shows the representative photographs of the experimental apparatus after the experiments. As shown in Fig. 5-7 (a), a white deposit was found inside the low temperature portion of the quartz tube. In addition, the black color of the reactant Ti ore changed to bright grey color in the product residues, as shown in Fig. 5-7 (b). The results of the XRD analysis of the white powder shown in Fig. 5-8 indicated that the white deposit was $FeCl_2$ and $FeCl_2 \cdot (H_2O)_2$, as expected from the thermodynamic calculations mentioned before. The vapor pressure of $FeCl_2$ (l) produced from the quartz crucible and molybdenum-lined quartz crucible is 0.02 atm at 1000 K,[26] which was sufficient to induce its evaporation. Therefore, $FeCl_2$ (l) evaporated from the both crucibles and solidified in the low temperature regions of the quartz tube. The H_2O adhered to the $FeCl_2$ might have originated from the H_2O produced in the quartz crucible or from the air when the silicone rubber plug was removed from the quartz tube during sample preparation for XRD analysis.

5.4.2　Influence of atmosphere in the reaction system

Table 5-2 shows the results of XRF analysis of the residues obtained in the quartz crucible and the molybdenum-lined quartz crucible. Figs. 5-9 and 5-10 show the XRD patterns of the residues obtained in the quartz crucible and the molybdenum-lined quartz crucible when the experiments were conducted under Ar gas or $Ar + H_2O$ gas atmosphere, respectively.

As shown in Table 5-2, Figs. 5-9 (a), and 5-10 (a), a purity of about 97 % TiO_2 was obtained in the quartz crucible when the experiments were conducted under Ar gas or $Ar + H_2O$ gas atmosphere for 11 h or 7 h, as expected from the thermodynamic analysis. A purity of TiO_2 was calculated by converting all elements in Table 5-2 to its nominal simple oxides. In addition, when the water bubbler was used in the experiments, the reaction time required for obtaining high-grade TiO_2 decreased. As shown in Table 5-2, the amount of iron removed from the Ti ore was greater when the experiments were

conducted under Ar + H_2O gas atmosphere than when the experiments were conducted under Ar atmosphere for equal reaction time. The reduction in the reaction time can be attributed to the active introduction of H_2O vapor into the reaction system by using water bubbler, which led to the accelerated production of HCl gas from the $MgCl_2$ in the molybdenum-lined quartz crucible.

Among the impurities present in the Ti ore, MnO (s) can be removed by HCl gas by the reaction shown in the Eq. 5-8. Table 5-2 shows that the concentration of Mn in the residues obtained in the quartz crucible decreased as the reaction time increased when the experiments were conducted under Ar gas or Ar + H_2O gas atmosphere. In addition, the concentration of Mg in the residues obtained in the quartz crucible could not be assessed for all cases. Although the vapor pressure of $MgCl_2$ at 1000 K is as low as 0.0003 atm,[26] $MgCl_2$ can evaporate depending on the atmosphere, such as in vacuum. Based on the results of the concentration of Mg listed in Table 5-2, it is supposed that there was no reaction through gas phase or negligible reaction between $MgCl_2$ in the molybdenum-lined quartz crucible and the Ti ore in the quartz crucible.

$$1/2 \text{ MnO } (s) + \text{HCl } (g) = 1/2 \text{ MnCl}_2 (l) + 1/2 \text{ H}_2\text{O } (g) \tag{5-8}$$
$$\Delta G°_r = - 17 \text{ kJ at 1000 K}^{[26]}$$
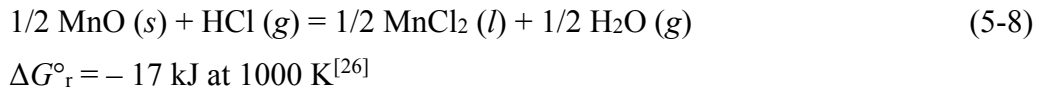
Fig. 5-11 shows the SEM images of the Vietnamese Ti ore before experiment and the residue obtained in the quartz crucible when the experiment was conducted under Ar gas atmosphere for 11 h. As shown in Fig. 5-11, pores were generated on the surface of the residue after the experiment. These results show that iron was selectively removed from Ti ore as $FeCl_2$ (l,g) leaving pores on the surface of the residues in the quartz crucible because of the high vapor pressure of $FeCl_2$ at 1000 K. As a result, it can be expected that the HCl gas produced from the $MgCl_2$ reacted with iron in the central portion of the Ti ore particle through the generated pores.

As shown in Figs. 5-9 (b) and 5-10 (b), the crystalline phases of the residues obtained in the molybdenum-lined quartz crucible were $MgTiO_3$ and MgO. Despite the presence of crystalline phase of $MgTiO_3$ in the residues revealed by the XRD analysis, the crystalline phase of MgO was also found in the residues present in the molybdenum-lined quartz crucible after the experiments. The most intense peak corresponded to MgO

in most cases. These results show that the lines corresponding to the H_2O (*g*)/HCl (*g*) eq.[e] and MgO (*s*)/$MgCl_2$ (*l*) eq.[a] dominated the reactions that occurred in the quartz crucible and molybdenum-lined quartz crucible, respectively, when the experiments were conducted under Ar gas or Ar + H_2O gas atmosphere.

Even though the iron was sufficiently removed leaving 1.2 % or 1.8 % in the Ti ore in the quartz crucible, about 18 % or 19 % of iron remained in the Ti ore present in the molybdenum-lined quartz crucible when the experiments were conducted under Ar gas or Ar + H_2O gas atmosphere for 11 h or 7 h, respectively.(*see* Table 5-2) Fig. 5-12 shows the SEM image and results of the EDS of a cross section of the residue obtained from the molybdenum-lined quartz crucible. As shown in Fig. 5-12, the reaction between $MgCl_2$ and the central portion of the Ti ore particle was hindered because of the production of $MgTiO_3$ at the outer portion of the Ti ore particle. Therefore, iron was partially removed from the Ti ore in the molybdenum-lined quartz crucible.

5.4.3   Influence of particle size of titanium ore

Table 5-3 shows the results of analyzing the residues obtained in the quartz crucible and the molybdenum-lined quartz crucible, and Figs. 5-13 (a) and 5-13 (b) show the XRD patterns of the residues obtained in the quartz crucible and the molybdenum-lined quartz crucible, respectively, when various sizes of Vietnamese Ti ore were used as a feedstock under vacuum.

As shown in Table 5-3 and Fig. 5-13 (a), a purity of about 97 % TiO_2 was obtained in the quartz crucible when the particle size ranged from 44 μm to 297 μm. It is certain that the HCl gas produced from the molybdenum-lined quartz crucible reacted with the entire volume of the Ti ore particle through the pores generated by the reaction between HCl gas and iron. Therefore, according to these results, the selective chlorination reaction that occurred in the quartz crucible did not depend on the particle size of the Ti ore.

It was also reconfirmed that the concentration of Mn in the residues obtained in the quartz crucible decreased because of the reaction shown in the Eq. 5-8 for all the particle size ranges. However, the concentration of 1.1 – 1.3 % Mg in the residues obtained in the quartz crucible was analyzed when the experiments were conducted under vacuum, while the concentration of Mg in the residues obtained in the quartz crucible

could not be detected when the experiments were conducted under Ar gas atmosphere. In addition, a weak intensity peak of $MgTiO_3$ was identified, as shown in Fig. 5-13 (a). These results show that even though the vapor pressure of the $MgCl_2$ is low as 0.0003 atm at 1000 K,[26] a portion of $MgCl_2$ evaporated from the molybdenum-lined quartz crucible reacted with the Ti ore in the quartz crucible under vacuum.

As shown in Table 5-3 and Fig. 5-13 (b), about 22 – 25 % of iron remained and MgO and $MgTiO_3$ were produced in the molybdenum-lined quartz crucible. It is expected that iron in the center of the Ti ore particle did not react with the $MgCl_2$ due to the formation of $MgTiO_3$ at the outer part of the Ti ore particle, similar to the case shown in the Fig. 5-12. In addition, MgO (s) found in the molybdenum-lined quartz crucible also shows that the lines corresponding to the H_2O (g)/HCl (g) eq.[e] and MgO (s)/$MgCl_2$ (l) eq.[a] dominated the reactions that occurred in the quartz crucible and molybdenum-lined quartz crucible, respectively.

5.4.4 Influence of various types of titanium ores

Table 5-4 shows the results of analyzing the residues obtained in the quartz crucible and the molybdenum-lined quartz crucible, and Figs. 5-14 (a) and 5-14 (b) show the XRD patterns of the residues obtained in the quartz crucible and the molybdenum-lined quartz crucible when the Australian Ti ore and the Chinese Ti ore were used as a feedstock, respectively.

As shown in Table 5-4 and Fig. 5-14 (a), a purity of about 92 % TiO_2 was obtained in the quartz crucible. The purity of TiO_2 obtained was lower than that obtained when the Vietnamese Ti ore was used as the feedstock. As shown in Eq. 5-8, Mn in the Ti ore can be removed by HCl gas produced from the molybdenum-lined quartz crucible. However, thermodynamically, it is difficult to remove other impurities such as Al, Si, Zr, and Nb in the Ti ore by HCl gas, as shown in Eqs. 5-9 and 5-10. The amount of these impurities in the Australian Ti ore and the Chinese Ti ore are larger than the amount of the impurities in the Vietnamese Ti ore as shown in Tables 5-3 and 5-4. When comparing the purity of residues obtained in the quartz crucible, the purity of the residue obtained from the Australian and the Chinese Ti ores (92 % and 92 % TiO_2) was lower than that of the residue obtained from the Vietnamese Ti ore (97 % TiO_2). In practice, this difference is

unimportant because a purity of 92 % TiO$_2$ is sufficient for application of the Kroll process.

$$1/6 \text{ Al}_2\text{O}_3 \ (s) + \text{HCl} \ (g) = 1/3 \text{ AlCl}_3 \ (l) + 1/2 \text{ H}_2\text{O} \ (g) \qquad\qquad (5\text{-}9)$$
$$\Delta G^\circ{}_r = 62 \text{ kJ at } 1000 \text{ K}^{[26]}$$

$$1/4 \text{ SiO}_2 \ (s) + \text{HCl} \ (g) = 1/4 \text{ SiCl}_4 \ (g) + 1/2 \text{ H}_2\text{O} \ (g) \qquad\qquad (5\text{-}10)$$
$$\Delta G^\circ{}_r = 54 \text{ kJ at } 1000 \text{ K}^{[26]}$$
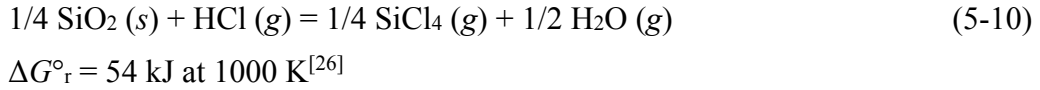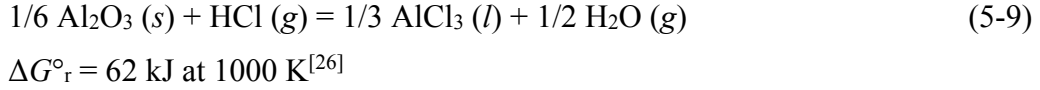
5.5 Summary

The use of MgCl$_2$ as the chlorinating agent was considered to develop a selective chlorination process for producing high-grade TiO$_2$ feed by upgrading low-grade Ti ore containing 51 % TiO$_2$. Iron was removed from the Ti ore as FeCl$_2$ (l,g) by the HCl gas produced from the MgCl$_2$/Ti ore mixture at 1000 K in the quartz crucible and TiO$_2$ with purity of 97 % was obtained when the experiments were conducted under Ar gas or Ar + H$_2$O gas atmosphere. The time required for the completion of the reaction was decreased when the experiments were conducted under Ar + H$_2$O gas atmosphere because of the accelerated production of HCl gas.

It was also demonstrated that 97 % TiO$_2$ feed was produced directly from the Vietnamese Ti ore that contained particles of sizes ranging from 44 μm to 297 μm by using the HCl gas produced from MgCl$_2$/Ti ore mixture. In addition, when the Australian or the Chinese Ti ores were used as the feedstock, 92 % TiO$_2$ feed was obtained. This was attributed to the presence of impurities like Al or Si in the Ti ore that were difficult to remove by HCl gas.

The iron present in the Ti ore was also removed as FeCl$_2$ (l,g) by the direct reaction between MgCl$_2$ and the Ti ore. However, when the MgCl$_2$ directly reacted with the Ti ore, 18 % – 25 % of iron remained in the Ti ore because of the formation of MgTiO$_3$ at the outer part of the titanium ore, which hindered further reaction between MgCl$_2$ and iron present at the central portion of the Ti ore particle, physically.

References

[1]   T.H. Okabe and J. Kang: "*The Latest Technological Trend of Rare Metals*", CMC Publishing Co. LTD., Tokyo, 2012, Chap. 6-1, pp. 83-94. (in Japanese)

[2]   J. Kang and T.H. Okabe: "*Thermodynamic Consideration of the Removal of Iron from Titanium Ore by Selective Chlorination*", Metall. Trans. B, 2014 (in print)

[3]   K.S. Geetha and G.D. Surender: "*Experimental and modelling studies on the aeration leaching process for metallic iron removal in the manufacture of synthetic rutile*", Hydrometallurgy, 2000, vol. 56 (1), pp. 41-62.

[4]   R.G. Becher, R.G. Canning, B.A. Goodheart, and S. Uusna: "*A new process for upgrading ilmenitic mineral sands*", Proceeding of the Australasian Institute of Mining and Metallurgy, 1965, vol. 21, pp. 21-44.

[5]   S. Jayasekera, Y. Marinovich, J. Avraamides, and S.I. Bailey: "*Pressure leaching of reduced ilmenite: electrochemical aspects*", Hydrometallurgy, 1995, vol. 39 (1), pp. 183-199.

[6]   W. Hoecker: "*Process for the production of synthetic rutile*", United States Patent 5601630, 1997.

[7]   J.B. Farrow, I.M. Ritchie, P. Mangano: "*The reaction between reduced ilmenite and oxygen in ammonium chloride solutions*", Hydrometallurgy, 1987, vol. 18 (1), pp. 21-38.

[8]   J.H. Chen: "*Beneficiation of Titaniferous Ores*", United States Patent 3825419, 1974.

[9]   J.H. Chen and L.W. Huntoon: "*Beneficiation of ilmenite ore*", United States Patent 4019898, 1977.

[10]   J.H. Chen: "*Pre-leaching or reduction treatment in the beneficiation of titaniferous iron ores*", United States Patent 3967954, 1976.

[11]   M. Gueguin and F. Cardarelli: "*Chemistry and mineralogy of titania-rich slags. Part 1-hemo-ilmenite, sulphate, and upgraded titania slags*", Miner. Process. Extr. Metall. Rev., 2007, vol. 28, pp. 1–58.

[12]   K. Borowiec, A.E. Grau, M. Gueguin, and J-F. Turgeon: "*Method to upgrade titania slag and resulting product*", United States Patent 5830420, 1998.

[13]   The Japan Titanium Society: Titanium Japan, 2013, vol. 61, pp. 84. (in Japanese)

[14]   S. Fukushima and E. Kimura: "*Ilmenite Upgrading: Particularly Concerning Mitsubishi Process*", Titanium·Zirconium, 1975, vol. 23 (2), pp. 67-74. (in Japanese)

[15]   A. Fuwa, E. Kimura, and S. Fukushima: "*Kinetics of Iron Chlorination of Roasted Ilmenite Ore, Fe_2TiO_5 in a Fluidized-Bed Reactor*", Metallurgical Transactions B, 1978, vol. 9B (4), pp. 643-652.

[16]   V.G. Neurgaonkar, A.N. Gokarn, and K. Joseph: "*Beneficiation of ilmenite to rutile by selective chlorination in a fluidised bed*", Journal of Chemical Technology and Biotechnology, 1986, vol. 36 (1), pp. 27-30.

[17]   J.S.J. Van Deventer: "*Kinetics of the selective chlorination of ilmenite*", Thermochimica Acta, 1988, vol. 124, pp. 205-215.

[18]   K.I. Rhee and H.Y. Sohn: "*The selective carbochlorination of iron from titaniferous magnetite ore in a fluidized bed*", Metallurgical Transactions B, 1990, vol. 21B (2), pp. 341-347.

[19]   L.K. Doraiswamy, H.C. Bijawat, and M.V. Kunte: "*Chlorination of ilmenite in a fluidized bed*", Chemical Engineering Progress, 1959, vol. 55 (10), pp. 80-88.

[20]   W.E. Dunn: "*High-temperature chlorination of TiO_2 bearing minerals*", Transactions of the Metallurgical Society of AIME, 1960, vol. 218 (1), pp. 6-12.

[21]   C.M. Lakshmanan, H.E. Hoelscher, and B. Chennakesavan: "*The kinetics of ilmenite beneficiation in a fluidised chlorinator*", Chemical Engineering Science, 1965, vol. 20 (12), pp. 1107-1113.

[22]   K.I. Rhee and H.Y. Sohn: "*The selective chlorination of iron from llmenite ore by $CO-Cl_2$ mixtures: Part I. intrinsic kinetics*", Metallurgical Transactions B, 1990, vol. 21B (2), pp. 321-330.

[23]   H. Zheng: "*Development of a Novel Titanium Production Process Using Selective Chlorination*", Doctoral Thesis, The University of Tokyo, 2007.

[24]   J. Kang and T.H. Okabe: "*Upgrading Titanium Ore Through Selective Chlorination Using Calcium Chloride*", Metallurgical and Materials Transactions B, 2013, vol. 44B (3), pp. 516-527.

[25]   T.H. Okabe and J. Kang: "*Thermodynamic Study on Chlorination Reactions of Oxides at Elevated Temperatures*", Molten Salts, 2013, vol. 56 (1), pp. 15-26. (in Japanese)

[26]   I. Barin: "*Thermochemical Data of Pure Substances*", 3rd ed., VCH Verlagsgesellschaft mbH, Weinheim, Germany, 1995.

[27]   R. Matsuoka and T.H. Okabe: "*Iron removal from titanium ore using selective chlorination and effective utilization of chloride waste*", Proceedings of the Symposium on Metallurgical Technology for Waste Minimization (134th TMS Annual Meeting), 2005, San Francisco, United States.
       http://www.okabe.iis.u-tokyo.ac.jp/japanese/for_students/parts/pdf/050218_

TMS_proceedings_matsuoka.pdf.

Table 5-1 Experimental conditions used in the present study.

Exp. No.[a]	Source country of Ti ore	Reaction time, t_r' / h	Atmosphere		H$_2$O bubbler		Particle size in the quartz crucible, d_{ore} / μm
			Gas	Flow, f / sccm	Use	Temp., T_{bub} / K	
121017	Vietnam	5	Vacuum	-	-	-	44 – 74
121030	Vietnam	5	Vacuum	-	-	-	74 – 149
121031	Vietnam	5	Vacuum	-	-	-	149 – 210
121101	Vietnam	5	Vacuum	-	-	-	210 – 297
121020	Australia	5	Vacuum	-	-	-	44 – 74
121029	China	5	Vacuum	-	-	-	44 – 74
121119	Vietnam	3	Ar	50	-	-	44 – 74
121118	Vietnam	5	Ar	50	-	-	44 – 74
121117	Vietnam	7	Ar	50	-	-	44 – 74
121114	Vietnam	9	Ar	50	-	-	44 – 74
121113	Vietnam	11	Ar	50	-	-	44 – 74
121216	Vietnam	1	Ar	50	O	303	44 – 74
121215	Vietnam	3	Ar	50	O	303	44 – 74
121212	Vietnam	5	Ar	50	O	303	44 – 74
121211	Vietnam	7	Ar	50	O	303	44 – 74

a : Experimental conditions;
 Weight of titanium ore used in the quartz crucible, w_{ore} = 0.10 g.
 Weight of titanium ore used in the Mo-lined quartz crucible, w_{ore} = 0.25 g.
 Weight of MgCl$_2$ used in the Mo-lined quartz crucible, w_{MgCl_2} = 3.00 g.
 Particle size used in the Mo-lined quartz crucible, d_{ore} = 74 – 149 μm.
 Reaction temperature, T = 1000 K.

Table 5-2 Analytical results of the residues obtained in the quartz crucible and
the molybdenum-lined quartz crucible: Influence of atmosphere on selective
chlorination at 1000 K. (*see* Figs. 5-9 and 5-10)

Exp. no.[b]		H₂O bubbler		Reaction time, t_r' / h	Concentration of element i, C_i (mass%)[a]					
		Use	Temp., T_{bub} / K		Ti	Fe	Mg	Mn	Si	Al
Feedstock (Vietnam)					45.0	49.7	N.D	3.47	0.57	0.33
121119	Quartz	-	-	3	73.0	23.4	N.D	2.30	0.66	N.D
	Mo-lined				61.3	18.0	18.3	1.25	N.D	N.D
121118	Quartz	-	-	5	83.2	13.9	N.D	1.47	0.50	N.D
	Mo-lined				58.5	19.3	19.8	1.14	0.21	N.D
121117	Quartz	-	-	7	92.1	5.88	N.D	0.70	0.46	N.D
	Mo-lined				58.4	19.8	19.3	0.98	N.D	N.D
121114	Quartz	-	-	9	94.4	3.67	N.D	0.44	0.43	0.14
	Mo-lined				62.5	19.1	15.3	1.96	N.D	N.D
121113	Quartz	-	-	11	96.7	1.77	N.D	0.14	0.31	0.24
	Mo-lined				63.4	18.1	15.5	1.12	0.13	N.D
121216	Quartz	O	303	1	61.0	35.1	N.D	2.94	0.53	N.D
	Mo-lined				57.8	26.6	12.7	1.61	0.34	N.D
121215	Quartz	O	303	3	77.7	19.6	N.D	1.94	0.27	N.D
	Mo-lined				55.9	23.4	18.0	1.24	N.D	N.D
121212	Quartz	O	303	5	90.9	7.23	N.D	0.98	0.32	N.D
	Mo-lined				56.6	20.7	19.9	1.23	N.D	N.D
121211	Quartz	O	303	7	97.2	1.24	N.D	0.13	0.32	N.D
	Mo-lined				57.1	19.4	20.5	1.25	N.D	N.D

a : Determined by XRF analysis (excluding oxygen and other gaseous elements),
 N.D : Not Detected. Below the detection limit of the XRF (< 0.01 %),
 Values are determined by average of analytical results of five samples.

b : Experimental conditions;
 Weight of titanium ore used in the quartz crucible, w_{ore} = 0.10 g.
 Weight of titanium ore used in the Mo-lined quartz crucible, w_{ore} = 0.25 g.
 Weight of MgCl₂ used in the Mo-lined quartz crucible, w_{MgCl_2} = 3.00 g.
 Particle size used in the quartz crucible, d_{ore} = 44 – 74 μm.
 Particle size used in the Mo-lined quartz crucible, d_{ore} = 74 – 149 μm.
 Reaction temperature, T = 1000 K.
 Source country of titanium ore : Vietnam.
 Ar gas was flowed through the quartz tube at a rate of 50 sccm via mass flow controller
  while the internal pressure of the quartz tube was maintained at 1 atm during the experiments.

Table 5-3 Analytical results of residues obtained in the quartz crucible and the molybdenum-lined quartz crucible: Influence of the particle size of the Ti ore on selective chlorination at 1000 K. (*see* Fig. 5-13)

Exp. no.[b]		Ore size, d_{ore} / μm	Concentration of element i, C_i (mass%)[a]					
			Ti	Fe	Mg	Mn	Si	Al
Feedstock (Vietnam)			45.0	49.7	N.D	3.47	0.57	0.33
121017	Quartz	44 – 74	96.8	0.60	1.12	0.06	0.42	0.09
	Mo-lined	74 – 149	54.1	21.9	21.0	1.15	0.01	N.D
121030	Quartz	74 – 149	96.9	0.53	1.11	0.07	0.30	0.04
	Mo-lined	74 – 149	53.9	24.6	18.6	1.56	N.D	N.D
121031	Quartz	149 – 210	96.9	0.61	1.16	0.08	0.09	0.13
	Mo-lined	74 – 149	50.2	24.2	22.6	1.49	0.04	N.D
121101	Quartz	210 – 297	96.6	0.59	1.28	0.06	0.28	0.32
	Mo-lined	74 – 149	53.2	23.0	20.7	1.47	0.01	N.D

a : Determined by XRF analysis (excluding oxygen and other gaseous elements),

   N.D : Not Detected. Below the detection limit of the XRF (< 0.01 %),

   Values are determined by average of analytical results of five samples.

b : Experimental conditions;

   Weight of titanium ore used in the quartz crucible, w_{ore} = 0.10 g.

   Weight of titanium ore used in the Mo-lined quartz crucible, w_{ore} = 0.25 g.

   Weight of MgCl$_2$ used in the Mo-lined quartz crucible, w_{MgCl_2} = 3.00 g.

   Reaction time, t_r' = 5 h.

   Reaction temperature, T = 1000 K.

   Source country of titanium ore : Vietnam.

   Experiments were conducted under vacuum.

Table 5-4 Analytical results of residues obtained in the quartz crucible and
the molybdenum-lined quartz crucible: Various types of the Ti ores produced
in several countries at 1000 K. (*see* Fig. 5-14)

Exp. no.[e]		Source country of Ti ore	Concentration of element i, C_i (mass%)[a]					
			Ti	Fe	Mg	Mn	Si	Al
Feedstock		Australia	48.5	46.7	N.D	1.69	1.00	1.02
		China	47.2	45.4	N.D	2.79	1.65	1.41
121020	Quartz	Australia	92.2	2.27	1.80	0.14	1.17	0.74
	Mo-lined		62.8	21.1	13.2	0.54	0.34	0.29
121029	Quartz	China	91.7	2.62	1.47	0.10	1.21	0.93
	Mo-lined		50.9	19.1	25.5	0.72	0.71	0.76

a : Determined by XRF analysis (excluding oxygen and other gaseous elements),
   N.D : Not Detected. Below the detection limit of the XRF (< 0.01 %),
   Values are determined by average of analytical results of five samples.

b : Experimental conditions;
   Weight of titanium ore used in the quartz crucible, w_{ore} = 0.10 g.
   Weight of titanium ore used in the Mo-lined quartz crucible, w_{ore} = 0.25 g.
   Weight of MgCl$_2$ used in the Mo-lined quartz crucible, w_{MgCl_2} = 3.00 g.
   Particle size used in the quartz crucible, d_{ore} = 44 – 74 μm.
   Particle size used in the Mo-lined quartz crucible, d_{ore} = 74 – 149 μm.
   Reaction temperature, T = 1000 K.
   Reaction time, t_r' = 5 h.
   Experiments were conducted under vacuum.
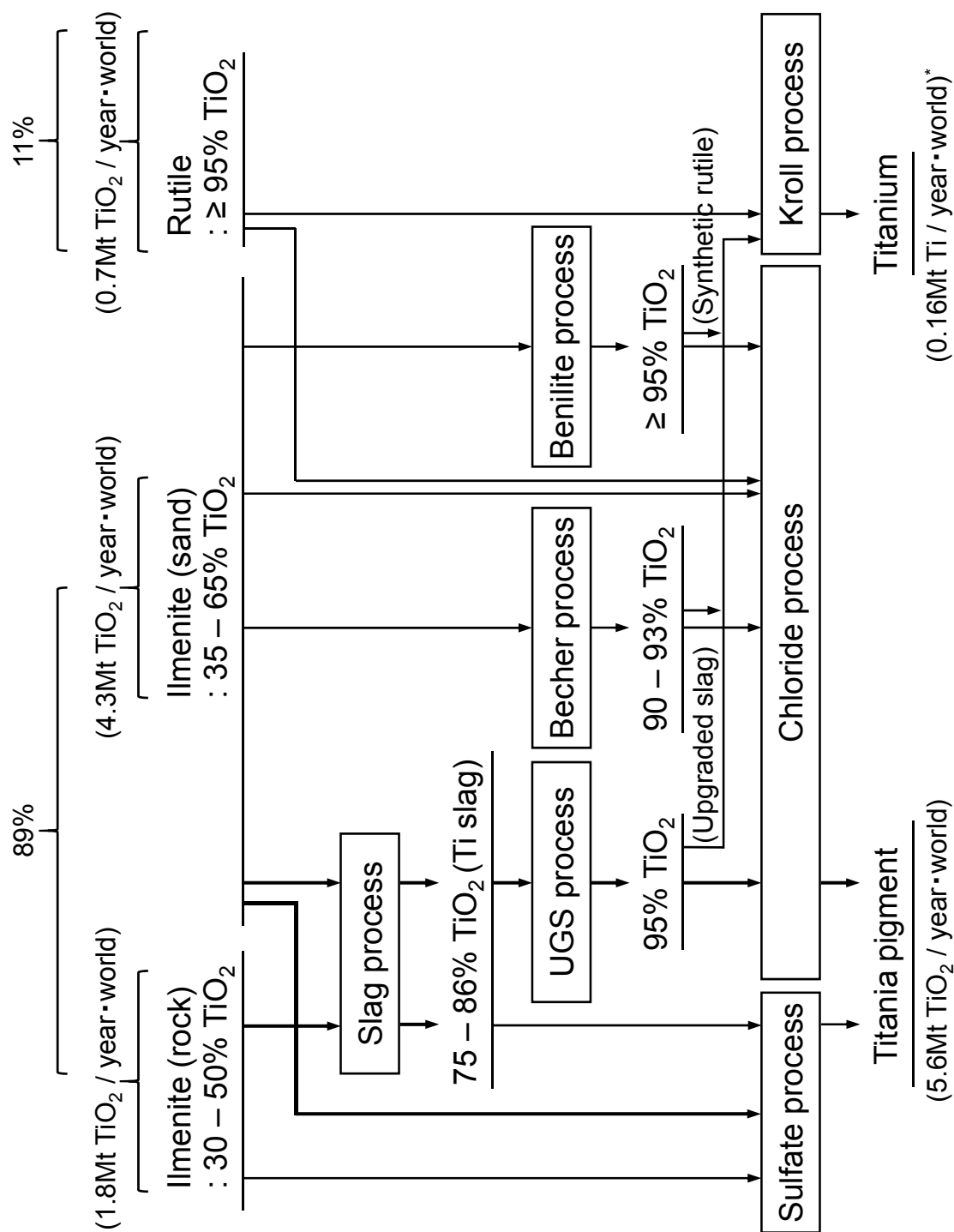
Figure 5-1 The current flowchart of Ti from Ti ore to Ti metal and titania pigment.

*: Ti produced in USA is excluded. The estimated Ti production in USA in 2010 was 0.015 Mt Ti / year

189
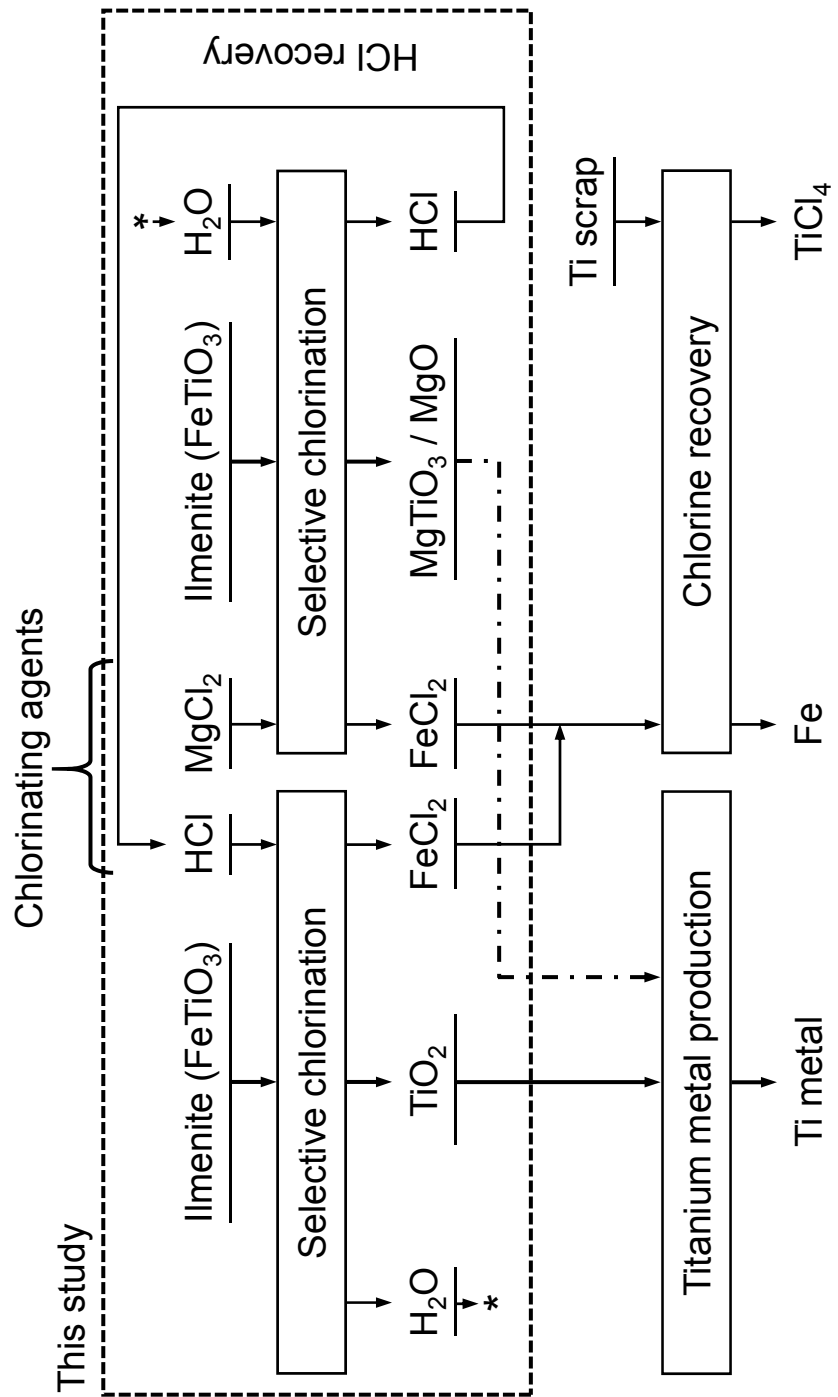
Figure 5-2 Flow diagram of the selective chlorination process investigated in the present study.
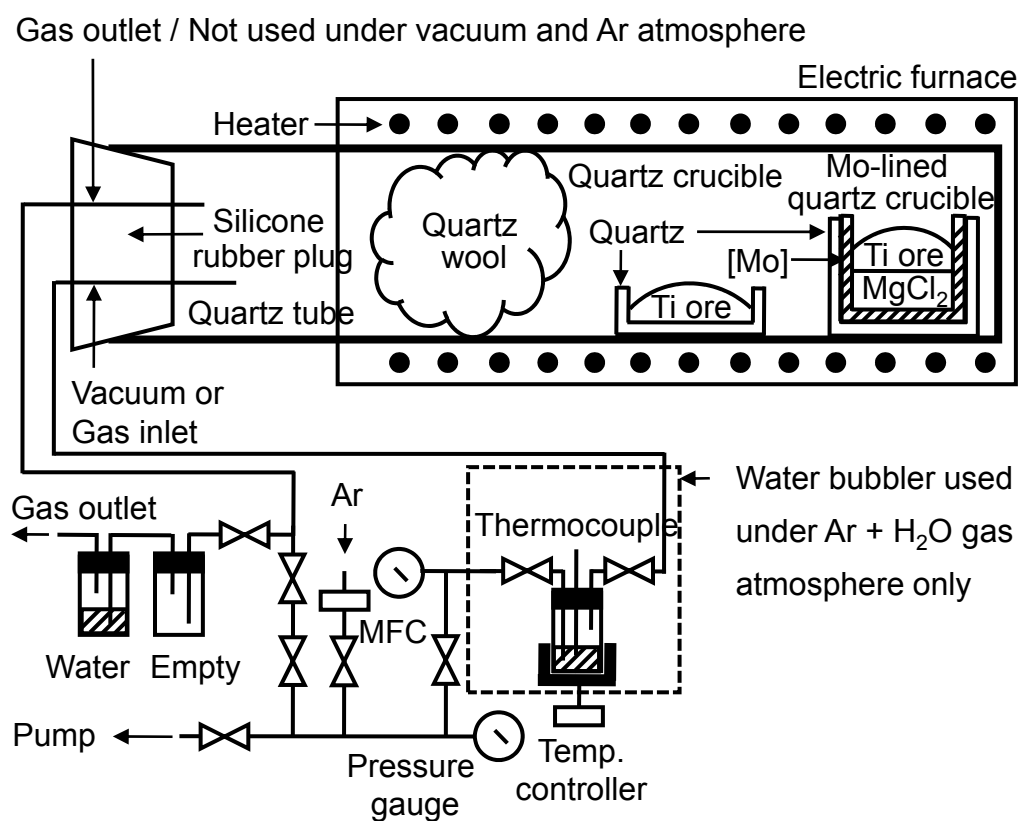
Figure 5-3 Schematic of the experimental apparatus used in the present study.

Fe-O-Cl system, *T* = 1000 K
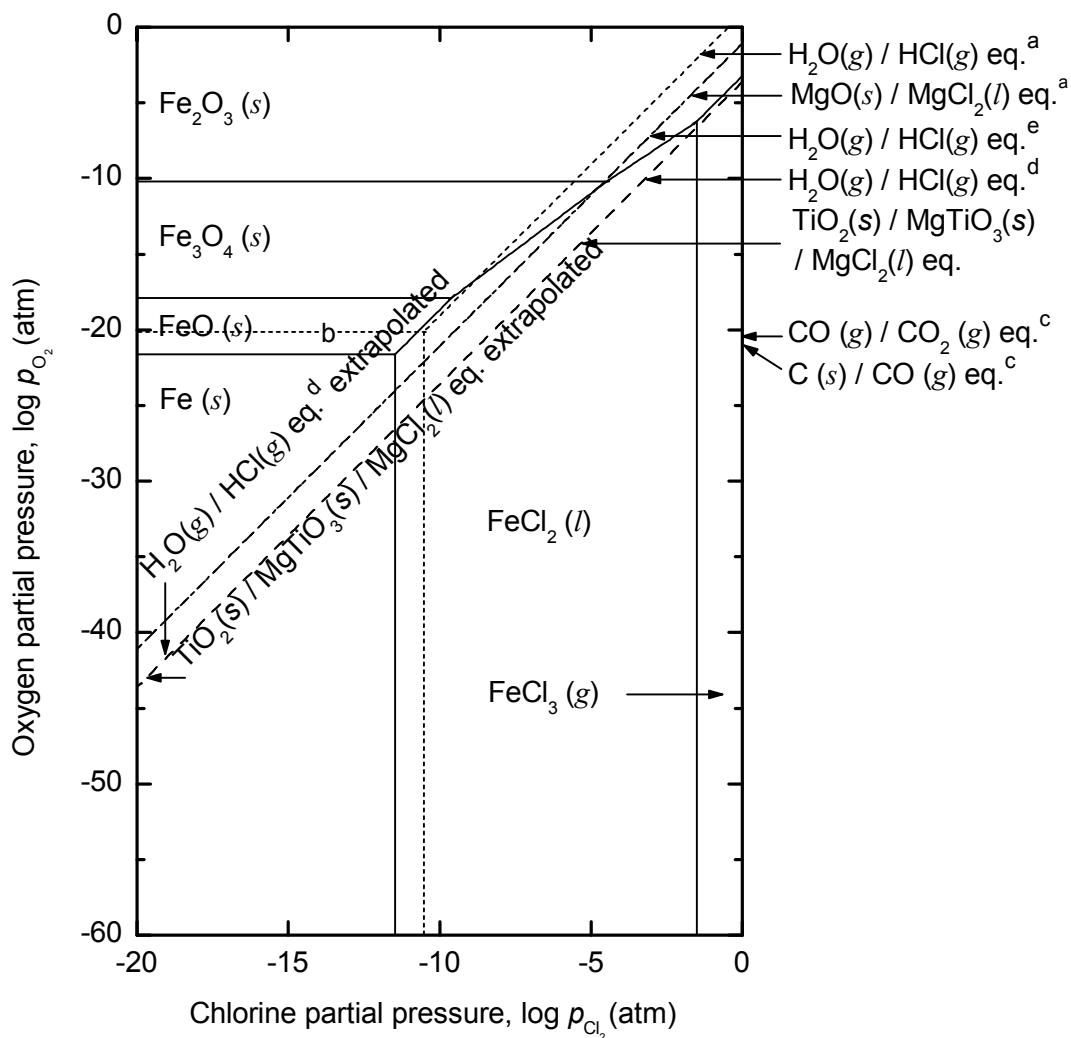
a : standard state   b : $p_{H_2O} / p_{H_2} = 1$

c : p_{Cl_2} = 0.1 atm

d : p_{H_2O} / p_{HCl}^2 : Determined by $MgCl_2 + H_2O = 2 HCl + MgO$

          in a_{MgO} = 0.054 (under $TiO_2(s)/MgTiO_3(s)$ eq.), and a_{MgCl_2} = 1

e : p_{H_2O} / p_{HCl}^2 : Determined by $MgCl_2 + H_2O = 2 HCl + MgO$ in a_{MgO} = 1, and a_{MgCl_2} = 1

Figure 5-4 Chemical potential diagram of the Fe-O-Cl system at 1000 K.

Ti-O-Cl system, T = 1000 K
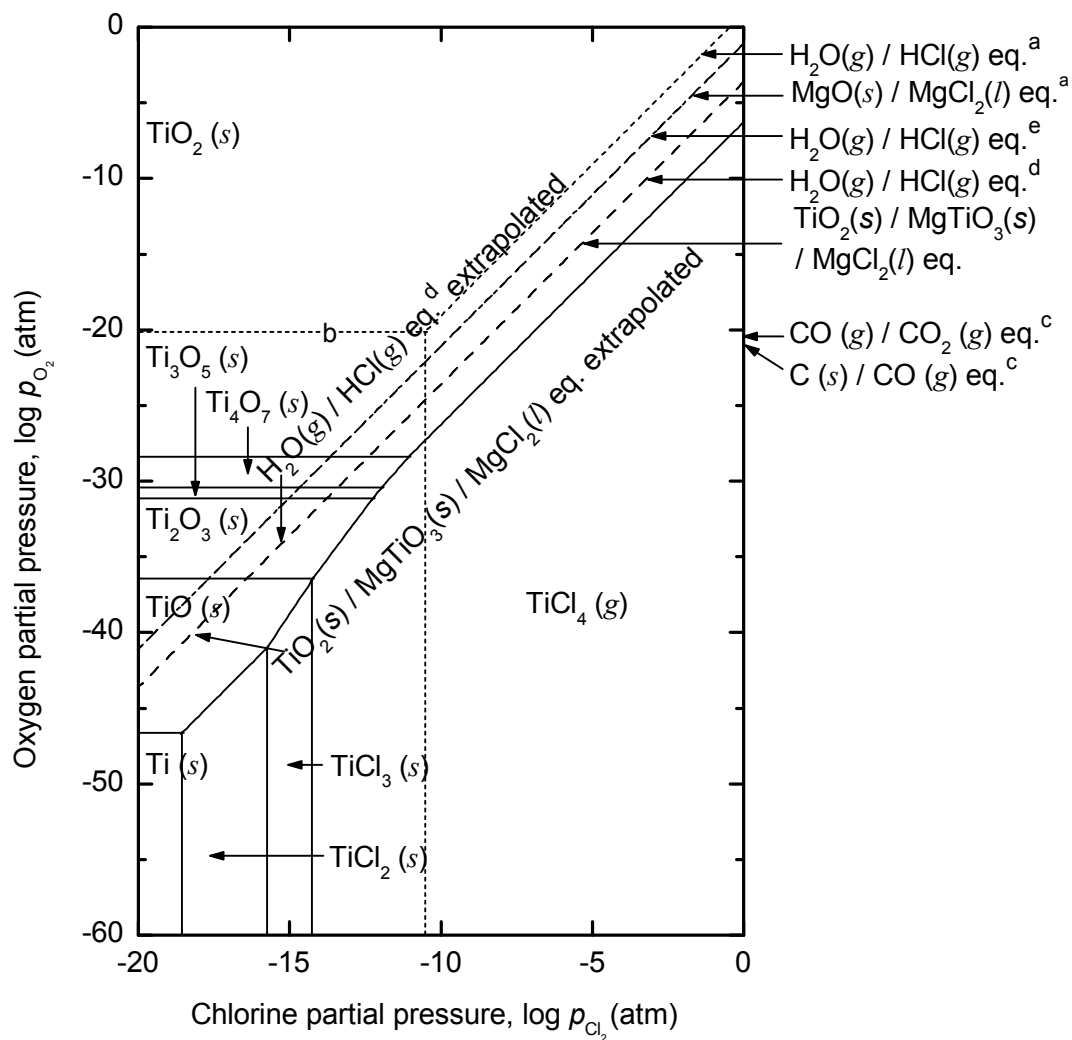
a : standard state   b : p_{H_2O} / p_{H_2} = 1

c : p_{Cl_2} = 0.1 atm

d : p_{H_2O} / p_{HCl}^2 : Determined by $MgCl_2 + H_2O = 2\ HCl + MgO$

in a_{MgO} = 0.054 (under $TiO_2(s)/MgTiO_3(s)$ eq.), and a_{MgCl_2} = 1

e : p_{H_2O} / p_{HCl}^2 : Determined by $MgCl_2 + H_2O = 2\ HCl + MgO$ in a_{MgO} = 1, and a_{MgCl_2} = 1

Figure 5-5 Chemical potential diagram of the Ti-O-Cl system at 1000 K.

Ti-O-Cl system,
Fe-O-Cl system, *T* = 1000 K
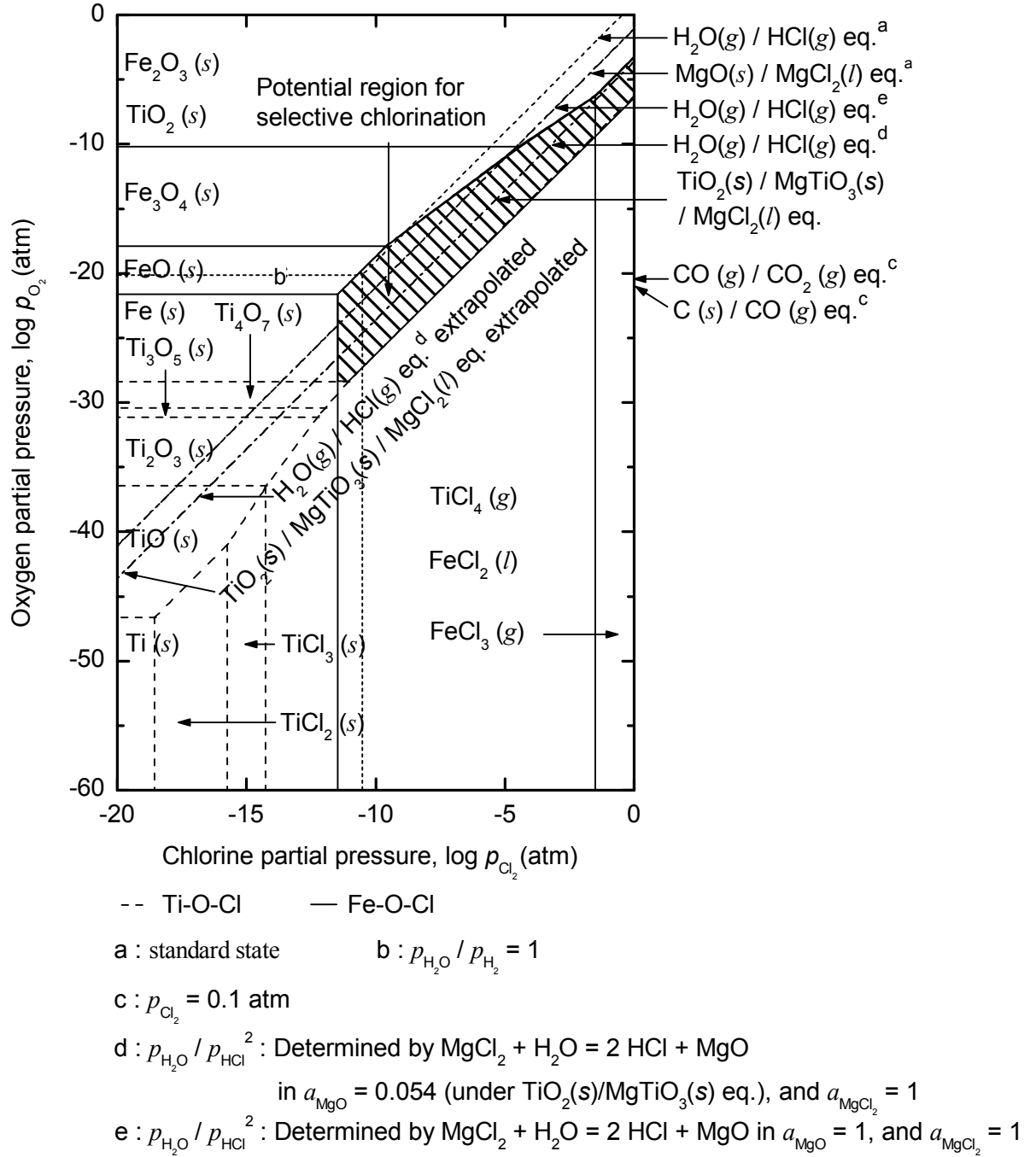
Figure 5-6 Combined chemical potential diagram of the Fe-O-Cl system
(solid line) and the Ti-O-Cl system (dotted line) at 1000 K.

(a)
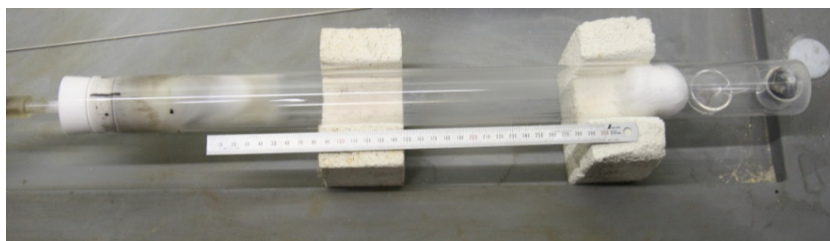
(b)

(c)

Figure 5-7 Photographs of the experimental apparatus after the experiment:
(a) the quartz tube (Exp. no. 121031), (b) residue in the quartz
crucible, and (c) residue in the molybdenum-lined quartz crucible.
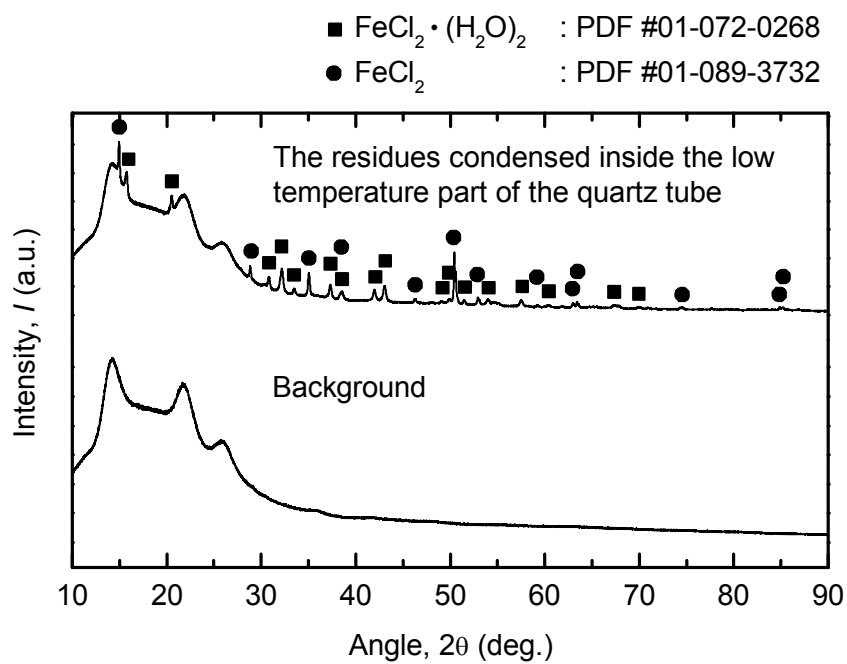
Figure 5-8 Results of the XRD analysis of the white deposit condensed
in the low temperature portion of the quartz tube.
(Exp. no. 121101)
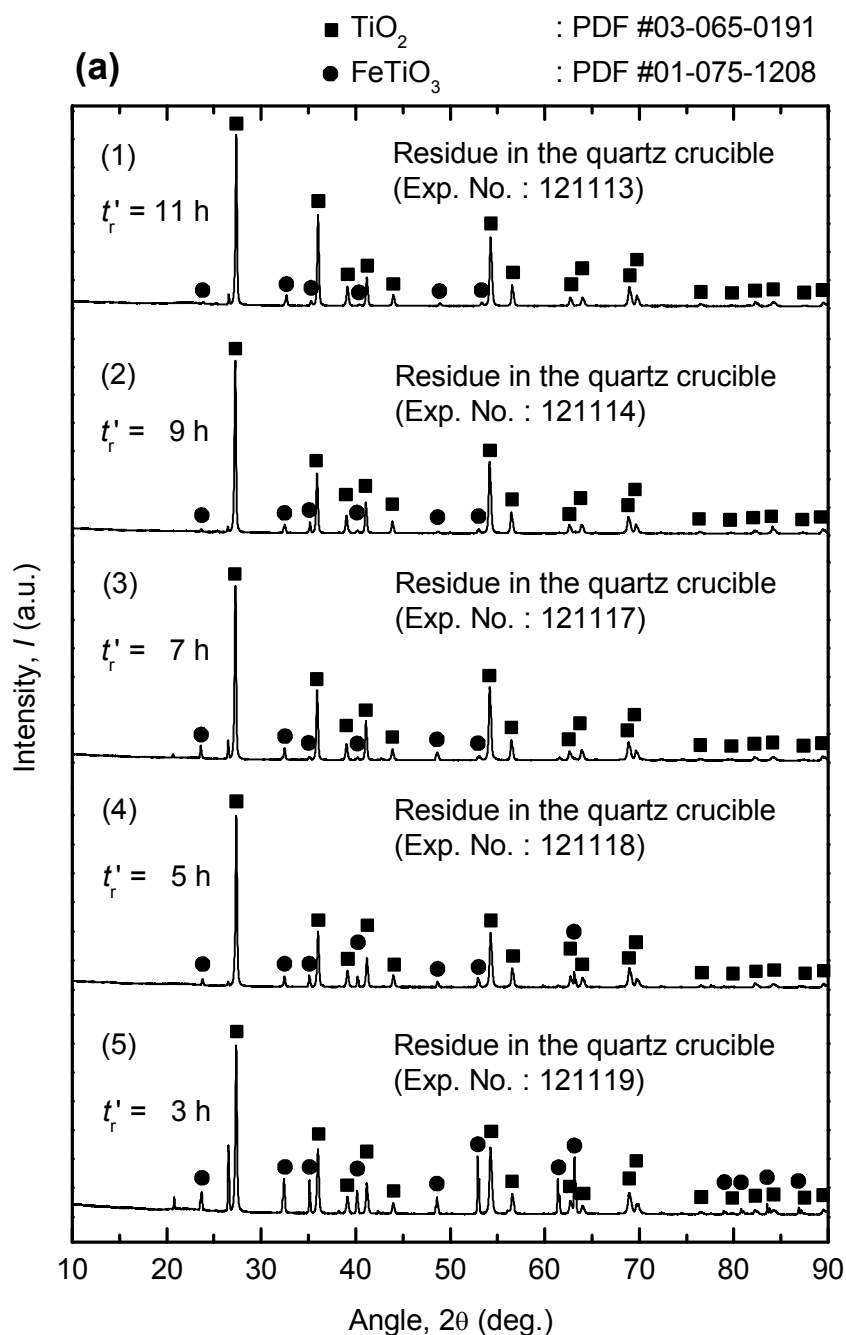
Figure 5-9 (a) XRD patterns of the residues obtained in the quartz crucible when the experiments were conducted under Ar gas atmosphere: (1) 11 h, (2) 9 h, (3) 7 h, (4) 5 h, and (5) 3 h. (*see* Table 5-2)
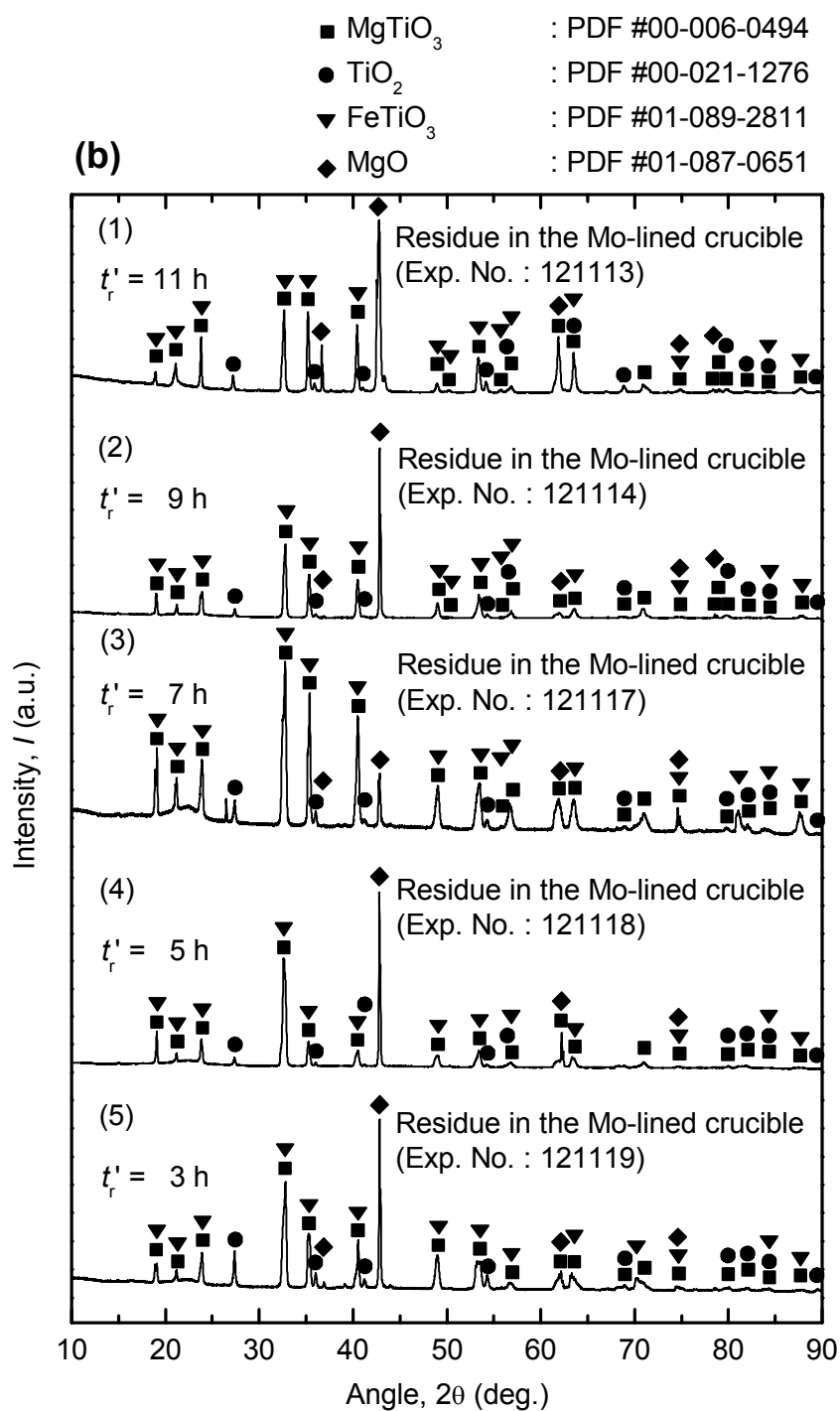
Figure 5-9 (b) XRD patterns of the residues obtained in the
molybdenum-lined quartz crucible when the
experiments were conducted under Ar gas atmosphere:
(1) 11 h, (2) 9 h, (3) 7 h, (4) 5 h, and (5) 3 h. (*see* Table 5-2)

198
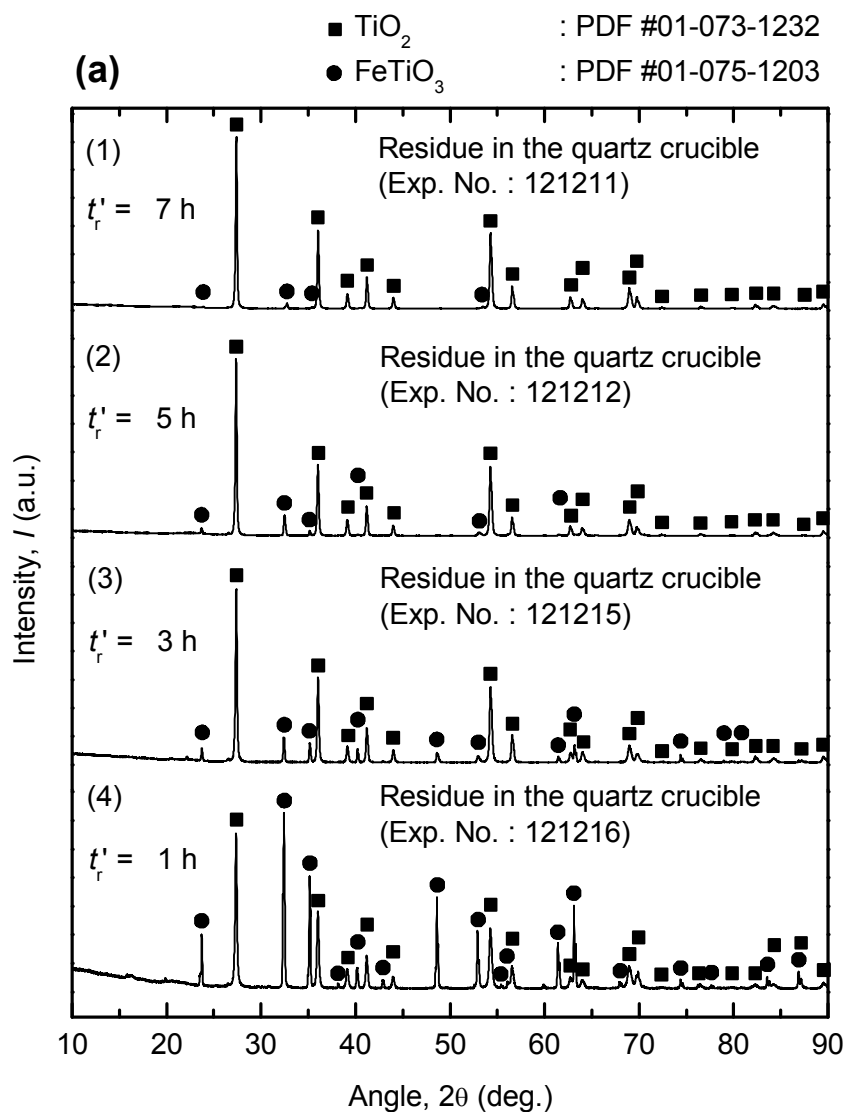
Figure 5-10 (a) XRD patterns of the residues obtained in the quartz
crucible when the experiments were conducted under
Ar + H$_2$O gas atmosphere: (1) 7 h, (2) 5 h, (3) 3 h, and
(4) 1 h. (*see* Table 5-2)
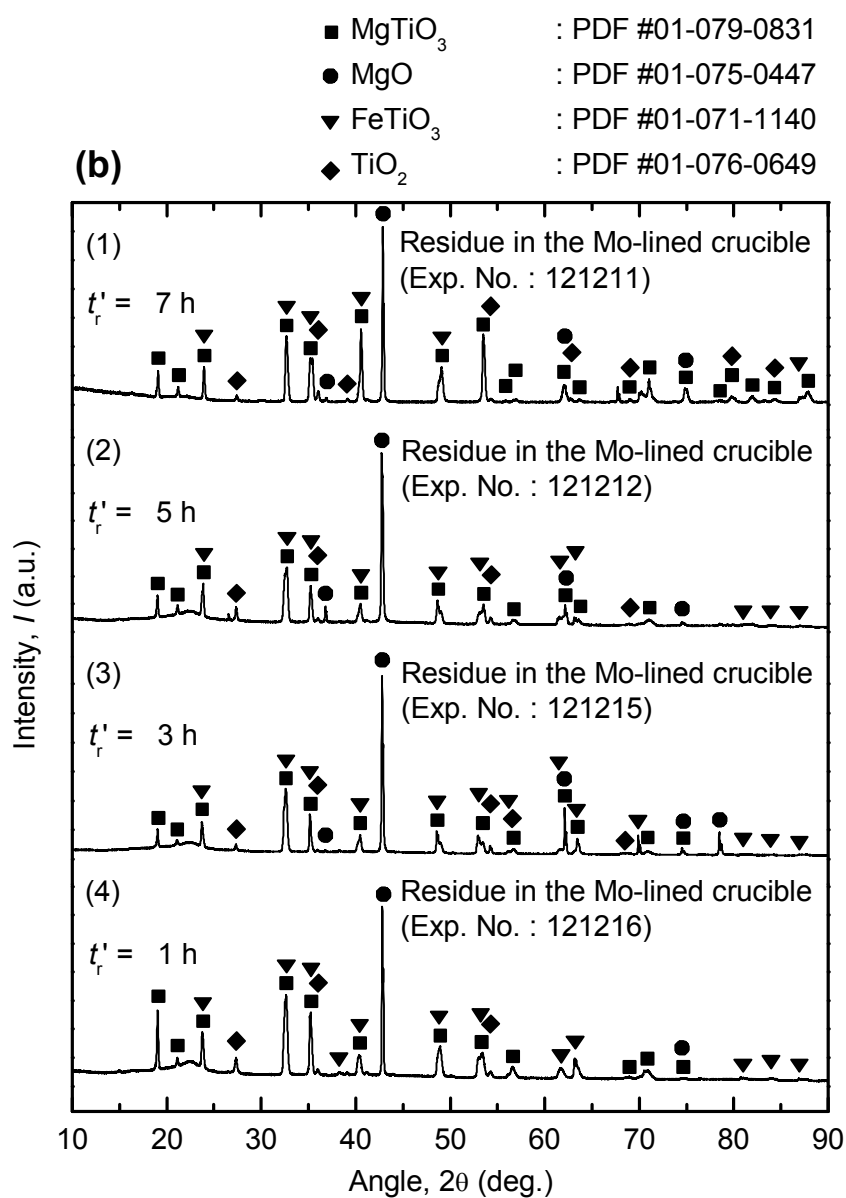
Figure 5-10 (b) XRD patterns of the residues obtained in the
molybdenum-lined quartz crucible when the experiments
were conducted under Ar + H_2O gas atmosphere:
(1) 7 h, (2) 5 h, (3) 3 h, and (4) 1 h. (*see* Table 5-2)

(a)

5µm

(b)

5µm
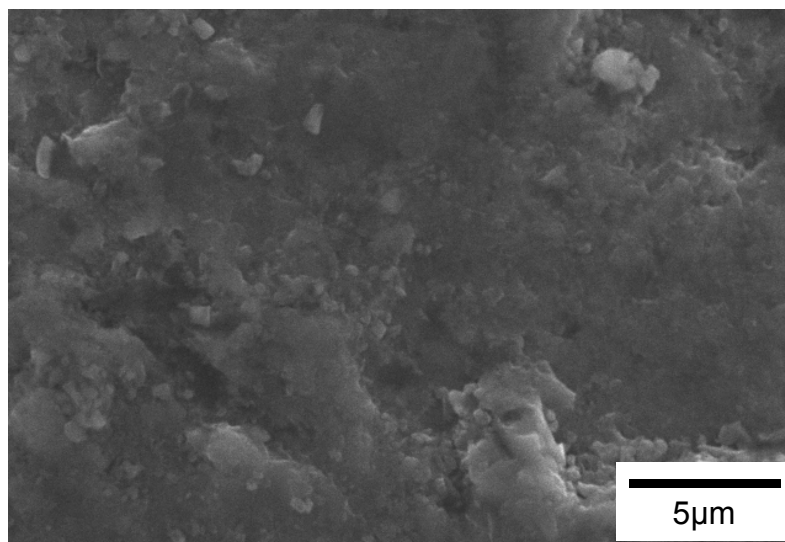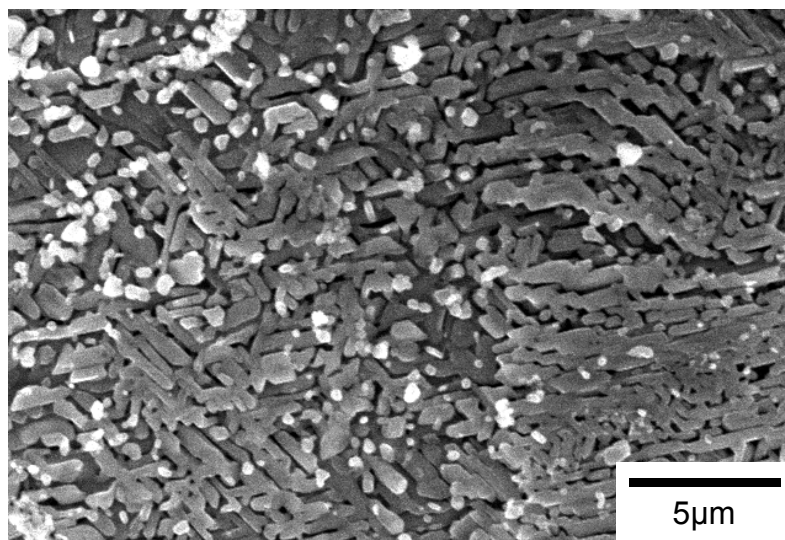
Figure 5-11 SEM images of the microstructure:
(a) the Vietnamese titanium ore before experiment, and
(b) the residue in the quartz crucible when the experiment
was conducted under Ar gas atmosphere. (Exp No.: 121113)
(*see* Table 5-2)

(a)

Position No. 1   Position No. 12

LG6

50 μm
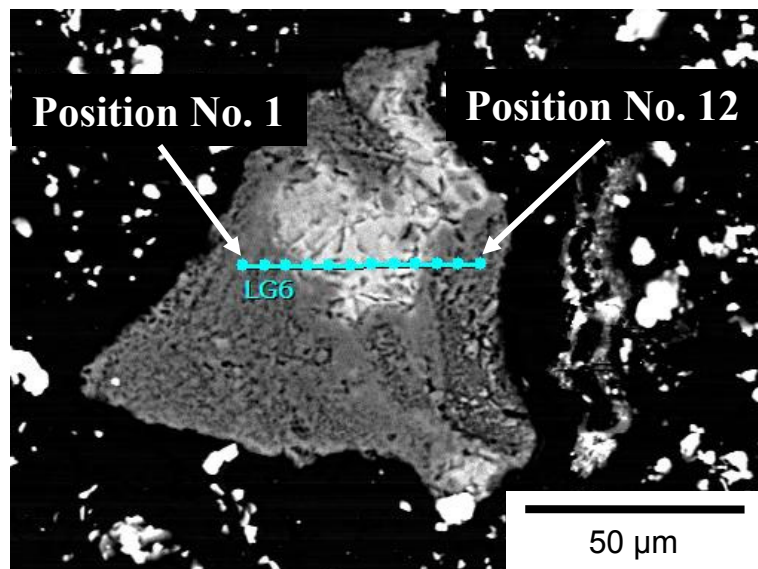
(b)
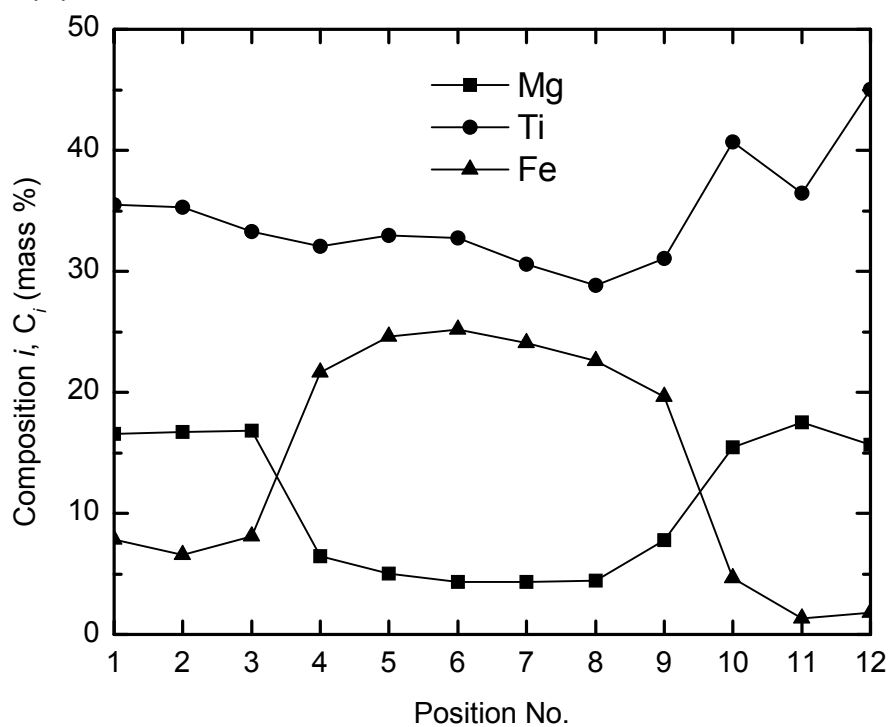
Figure 5-12 (a) SEM image of the cross section of the residue obtained
        from the molybdenum-lined quartz crucible (Exp. No. : 121117).
        (b) corresponding EDS results of the cross section of the residue
        obtained from the molybdenum-lined quartz crucible (Exp. No. : 121117).
        (*see* Table 5-2 and Figure 5-9)
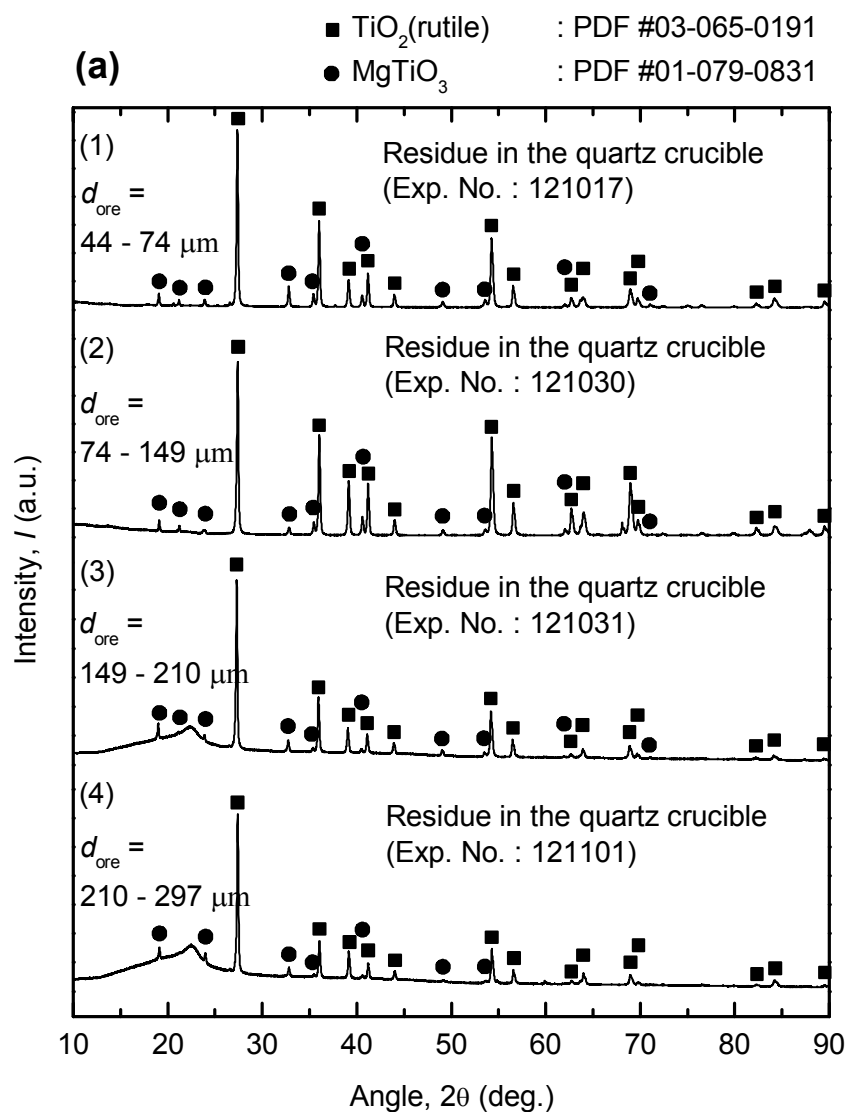
Figure 5-13 (a) XRD patterns of the residues obtained in the quartz crucible when the ore particle size was in the range: (1) 44 – 74 μm, (2) 74 – 149 μm, (3) 149 – 210 μm, and (4) 210 – 297 μm. (*see* Table 5-3)
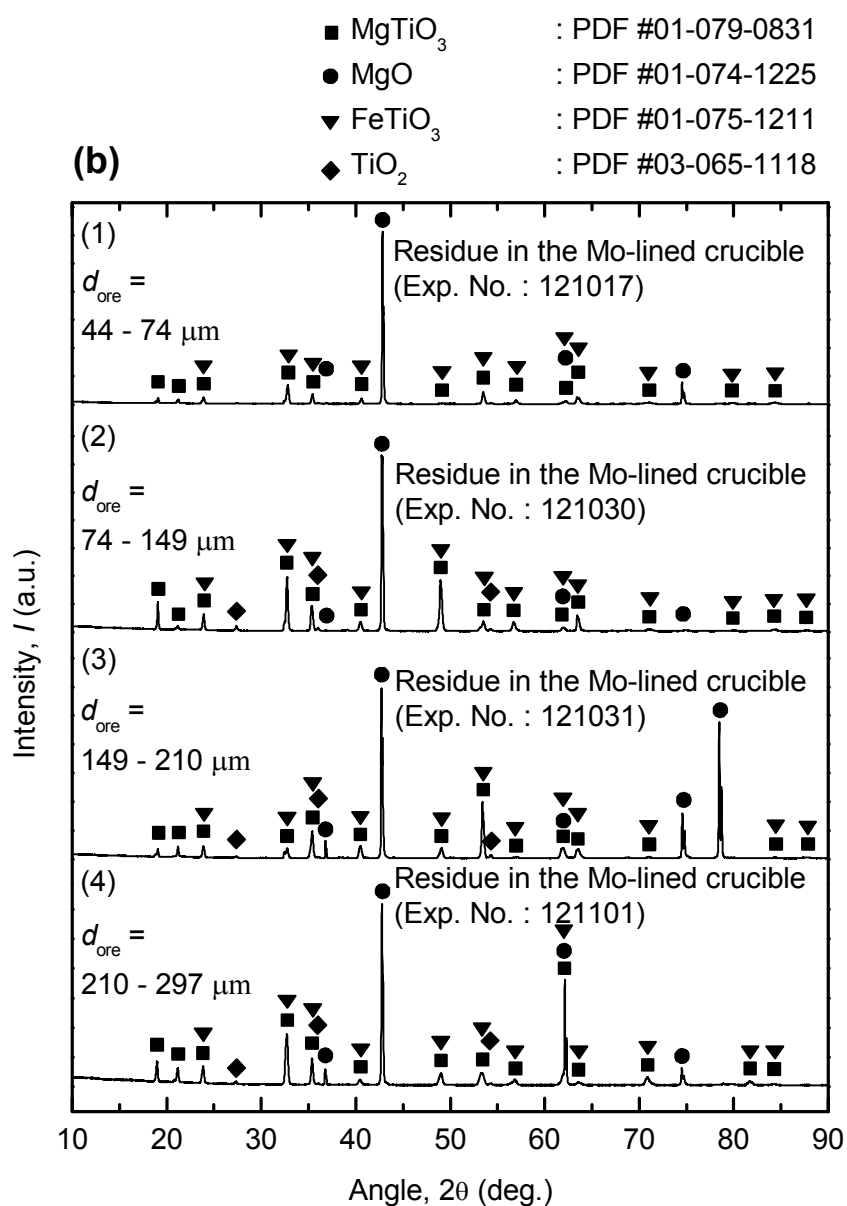
Figure 5-13 (b) XRD patterns of the residues obtained in the molybdenum-
lined quartz crucible when the ore particle size was in the
range: (1) 44 – 74 μm, (2) 74 – 149 μm, (3) 149 – 210 μm,
and (4) 210 – 297 μm. (*see* Table 5-3)

TiO$_2$ (rutile)   : PDF #01-072-1148
MgTiO$_3$: PDF #01-079-0831
FeTiO$_3$: PDF #01-075-0519
Fe$_3$O$_4$: PDF #01-089-0951
SiO$_2$: PDF #01-085-0865
TiO$_2$ (anatase)   : PDF #01-073-1764

(a)

(1) Residue in the quartz crucible (Exp. No. : 121020, Australia)

(2) Residue in the quartz crucible (Exp. No. : 121029, China)

Intensity, I / (a.u.)

Angle, 2θ (deg.)
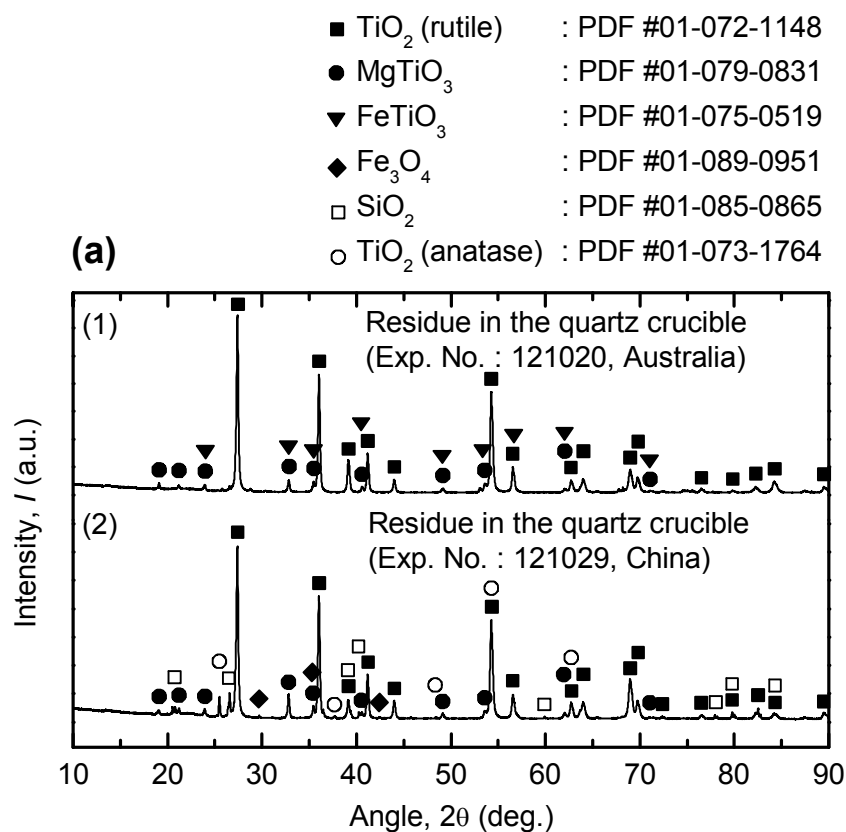
Figure 5-14 (a) XRD patterns of the residues obtained in the quartz crucible when various types of titanium ore were used as feedstock: (1) Australian ilmenite and (2) Chinese ilmenite. (*see* Table 5-4)
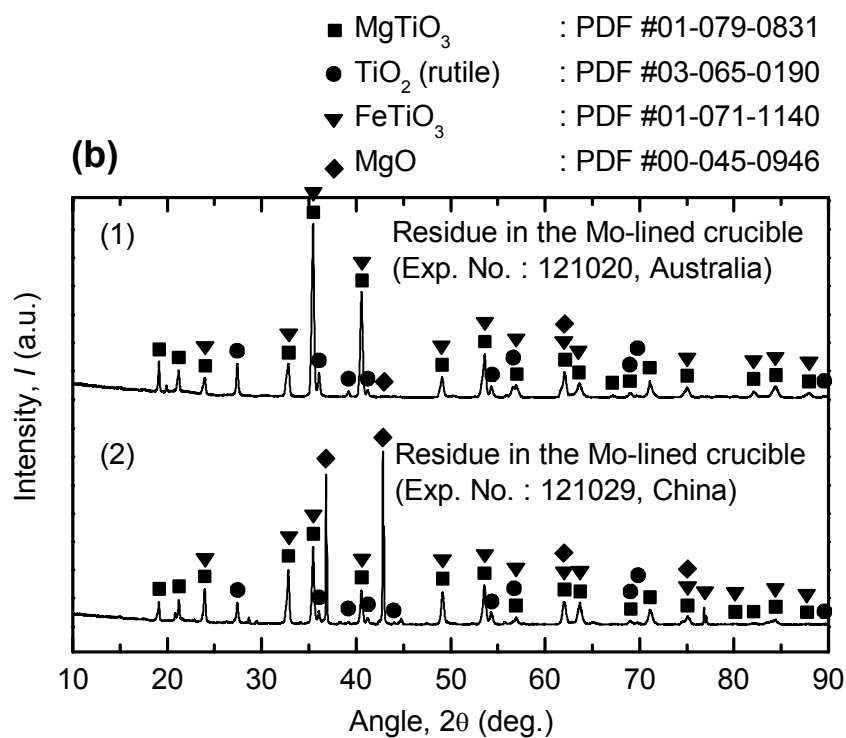
Figure 5-14 (b) XRD patterns of the residues obtained in the
molybdenum-lined quartz crucible when various
types of titanium ore were used as feedstock:
(1) Australian ilmenite and (2) Chinese ilmenite. (*see* Table 5-4)

206

Chapter 6 Selective chlorination of low-grade titanium ore using titanium tetrachloride under low oxygen chemical potential

6.1 Introduction

Titanium (Ti) is produced by the Kroll process in current industrial manufacturing. Among several important issues involved in the effective operation of the Kroll process, one of the most important issues is the grade (or purity) of the TiO_2 feed for the chlorination process.[1,2] Generally, the use of high-grade TiO_2 with a purity above 95 % is preferred to decrease the chlorine loss, prevent pipe clogging, and prevent damage to the refractory materials in the chlorinator. However, the use of a high-grade TiO_2 feed has become more difficult nowadays, mainly because the price of high-grade TiO_2 feed has increased owing to the increase in consumption of TiO_2 feed in China and other developing countries.[3] In this situation, Ti metal production companies in Japan have started to investigate the usage of lower grade feed, of about 90 % TiO_2 feed, instead of the 95 % TiO_2 feed.[3,4]

Currently, high-grade TiO_2 feed is produced by the Becher process,[5-9] Benilite process,[10-12] and slag process with post-treatment (the UGS process).[13-14] However, these processes have drawbacks such as multiple steps for removal of iron or the production of a large amount of acid aqueous waste solution. Some countries such as Japan have strict environmental regulations for the disposal and treatment of industrial wastes.[15] Therefore, when the upgrading of low-grade Ti ore is considered in these countries, an environmentally sound process that does not produce a large amount of acid aqueous waste solution or that can recycle the wastes must be established.

Extensive studies have been carried out to improve the current processes for the effective production of high-grade TiO_2 feed at reduced costs, and selective chlorination using a pyrometallurgical method has been found to be promising for upgrading low-grade Ti ore. Comprehensive research was conducted on selective chlorination using a pyrometallurgical method. For example, selective chlorination of Ti ore by Cl_2 gas in the presence of carbon[16-20] or under a CO/Cl_2 mixed atmosphere[21-24] was conducted. Recently, selective chlorination using calcium chloride ($CaCl_2$) or $MgCl_2$ as a

chlorinating agent has been investigated.[25] In addition, a new selective chlorination process using HCl gas produced in the presence of CaCl$_2$ or MgCl$_2$ as a chlorine source was developed as shown in chapters 3 and 5, and 97 % TiO$_2$ was obtained from a low-grade Ti ore containing 51 % TiO$_2$ under certain conditions.[3,26] Although the effectiveness of selective chlorination using CaCl$_2$ or MgCl$_2$ was demonstrated, several technical problems regarding its practical application have remained unresolved. One such problem is the damage to the chlorinator used in the Kroll process by the condensed chlorides, such as CaCl$_2$ or MgCl$_2$, because they lead to a corrosive environment at high temperatures.

Meanwhile, among the researchers studying selective chlorination using metal chlorides in the past, Othmer extensively investigated chlorination processes using TiCl$_4$.[27-29] First, Othmer researched oxidation-chlorination, where the chlorination of Fe$_2$O$_3$ by TiCl$_4$ was claimed. Practically, this reaction is a replacement reaction of oxide(s) and chloride(s) in an oxidative atmosphere rather than an oxidation reaction. The second approach was reduction-chlorination. Generally, this process is called carbo-chlorination. Othmer claimed that Ti ore containing iron oxides could be chlorinated using Cl$_2$ gas in the presence of carbon to produce TiCl$_4$. In addition, the chlorination of Ti ore containing FeO by TiCl$_4$ in the presence of carbon was also claimed. In this process, the exhaust gas stream containing TiCl$_4$ produced by carbo-chlorination in a reactor was directly used for chlorinating the Ti ore in another reactor that contains carbon. In any case, no systematic thermodynamic analysis considering the partial pressures of oxygen (p_{O_2}) and chlorine (p_{Cl_2}) was conducted.

Based on this background research, a fundamental study on a novel carbo-selective-chlorination method was conducted by using TiCl$_4$ as a chlorinating agent in the presence of carbon in order to selectively remove iron from Ti ores to produce high-grade TiO$_2$. In addition, a systematic thermodynamic analysis utilizing chemical potential diagrams was carried out to verify the mechanism of this process, which had not been done in the past.

Fig. 6-1 shows the flow diagram for the new Ti smelting process based on carbo-selective-chlorination investigated in this study. There are several advantages of this carbo-selective-chlorination using TiCl$_4$ when applied to a practical process. As shown in Fig. 6-1, first, because a large amount of TiCl$_4$ is circulated in the current Ti smelting

process, the carbo-selective-chlorination process can easily be adapted into the Kroll process. Second, Cl_2 gas can be collected from the chloride wastes produced, because they are produced in a dry form not containing any water. In addition, if this process is used for the pretreatment of low-grade TiO_2 feed, the problems with the chlorinator in the current chlorination process, such as chlorine loss and pipe clogging, can be decreased. Moreover, a large amount of acid aqueous waste solution is not generated, because no concentrated acid is necessary for removing iron from Ti ore. Furthermore, even though carbon powder is mixed with Ti ore as a feedstock for carbo-selective-chlorination, the mixture of the ore and carbon powder can be supplied directly to the current chlorination process. Finally, high-grade TiO_2 feed can be obtained directly from the low-grade Ti ore in a single step.

6.2   Thermodynamic analysis of selective chlorination using TiCl₄ under low oxygen chemical potential

Thermodynamically, the iron oxides and titanium oxides in the Ti ore can be considered to exist as a mixture of both oxides, because the Gibbs energy of formation of $FeTiO_3$ at 1100 K is a small negative value, as shown in Eq. 6-1. Therefore, the thermodynamic analysis of the mechanism of the chlorination of the Ti ore can be conducted by utilizing the chemical potential diagrams of the Fe-O-Cl and Ti-O-Cl systems at 1100 K.

$$FeO\ (s) + TiO_2\ (s) = FeTiO_3\ (s) \tag{6-1}$$
$$\Delta G^{\circ}_r = -11.0\ \text{kJ at 1100 K}^{[30]}$$

Fig. 6-2 shows the combined chemical potential diagram of the Fe-O-Cl and Ti-O-Cl systems at 1100 K plotted with the logarithms of p_{Cl_2} and p_{O_2} as the abscissa and ordinate, respectively. By overlapping the two chemical potential diagrams, the potential region for the selective chlorination can be analyzed, and this potential region is indicated as a hatched region in Fig. 6-2. As shown in Fig. 6-2, the $FeCl_x$ (x=2, 3) and the TiO_2 are stable in the hatched region. Therefore, if p_{Cl_2} and p_{O_2} are located in that region, iron oxides in the Ti ore will be transformed to $FeCl_x$ (x=2, 3) and titanium oxides will remain

as TiO$_2$ (s). In the case of FeCl$_2$ (l), although it is thermodynamically stable as a condensed phase at 1100 K, its vapor pressure at 1100 K is 0.09 atm,[30] which is high enough for the FeCl$_2$ (l) to evaporate. Therefore, if the chemical potentials of the oxygen and the chlorine are located in the selective chlorination region, the iron in the Ti ore can be selectively chlorinated as FeCl$_x$ (l,g) (x=2, 3), and TiO$_2$ (s) can be obtained.

Since an excess amount of TiCl$_4$ gas was used as a chlorinating agent in this study, the equilibrium line of the TiO$_2$ (s)/TiCl$_4$ (g) eq. in Fig. 6-2 dominates the chlorination reactions in the reaction system. This equilibrium line passes the borderline of the potential region for selective chlorination. In addition, the oxygen chemical potential in the reaction system is controlled by the C (s)/CO (g) eq. or the CO (g)/CO$_2$ (g) eq., because carbon was used in the reaction system. In this case, point d1 or d2 in Fig. 6-2 controls the chemical potentials of the reaction system. If the oxygen chemical potentials of the iron oxides in the Ti ore are considered, the p_{O_2} in the reaction system might be locally controlled by the FeO (s)/ Fe$_3$O$_4$ (s) eq. (point e1 in Fig. 6-2) or Fe$_3$O$_4$ (s)/ Fe$_2$O$_3$ (s) eq. (point e2 in Fig. 6-2). However, because the chlorination reaction was carried out in the presence of carbon, thermodynamically, the reaction system in this study is controlled by the conditions indicated by point d1 or d2 in Fig. 6-2.

Fig. 6-3 shows equilibrium lines of the FeO$_x$ (s)/FeCl$_y$ (l,g) eq. and the TiO$_2$ (s)/TiCl$_4$ (g) eq. and the potential regions for several chlorination reactions at 1100 K. The potential region for the carbo-selective-chlorination investigated in this study is depicted as the cross-hatched region in Fig. 6-3. For reference, the potential regions for the oxidation-selective-chlorination investigated by Othmer and for the carbo-chlorination in the conventional chloride process are also shown in Fig. 6-3. It is worth noting that the carbo-chlorination process already has established applications in industry, whereas the carbo-selective-chlorination discussed here has not been applied in practical manufacturing so far.

Thermodynamically, if a large excess amount of TiCl$_4$ and carbon exist in the reaction system and the reaction system is in the equilibrium state, the chemical potential of the carbo-selective-chlorination is fixed at point d1 or d2 in Fig. 6-3. However, when the redox potential of solid FeO in Ti ore is considered, the carbo-selective-chlorination works in a wider oxygen chemical potential range. In this case, the oxygen chemical potential ranges from the log p_{O_2} value that is determined by the Fe (s)/FeO (s) eq. to

point e1 in Fig. 6-3. Therefore, when the carbon in the system and the redox potential of solid FeO in Ti ore are considered, the oxygen chemical potential ranges from point d1 to point e1 in Fig. 6-3. Meanwhile, when the chlorination of a Ti ore particle is considered, the outermost boundary of the ore particle reacting with $TiCl_4$ is controlled by the TiO_2 (s)/$TiCl_4$ (g) eq., and the center of the ore particle not yet reacting with $TiCl_4$ is controlled by the FeO_x (s)/$FeCl_y$ (l,g) eq. If the chemical potential gradient between the two equilibriums is considered, the chemical potential pair of p_{Cl_2} and p_{O_2} can be placed between the equilibrium lines of the FeO_x (s)/$FeCl_y$ (l,g) eq. and the TiO_2 (s)/$TiCl_4$ (g) eq. As a result, the potential region between the equilibrium lines of the FeO_x (s)/$FeCl_y$ (l,g) eq. and the TiO_2 (s)/$TiCl_4$ (g) eq. can be identified as the potential region for the selective chlorination of iron in Ti ore. Thus, under these two conditions, the cross-hatched region shown in Fig. 6-3 becomes the potential region for the carbo-selective-chlorination in this study.

The potential region for the carbo-selective-chlorination is located within the stability region of $FeCl_2$ (l), and the vapor pressure of $FeCl_2$ (l) at 1100 K is high enough to allow for evaporation, as mentioned before. Therefore, when $TiCl_4$ is used as a chlorinating agent for the carbo-selective-chlorination at 1100 K, the iron oxide in the Ti ore is removed as $FeCl_2$ (l,g) and the TiO_2 remains, according to the following overall chemical reaction.

$$FeO\ (s,\ in\ the\ ore) + 1/2\ TiCl_4\ (g) = FeCl_2\ (l) + 1/2\ TiO_2\ (s) \qquad (6\text{-}2)$$
$$\Delta G°_r = -\,69.1\ kJ\ at\ 1100\ K^{[30]}$$
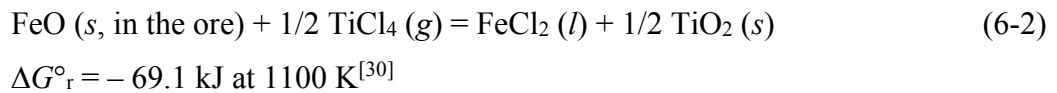
6.3   Experimental

Figs. 6-4 and 6-5 show schematic diagrams of the experimental apparatuses used in this study and photographs of the quartz reaction tubes taken before the experiment. In addition, detailed experimental conditions for this study are summarized in Table 6-1.

Prior to the experiments, Ti ore (*see* Table 6-2) and carbon powder (Kojundo Chemical Lab. Co., Ltd., purity $\geq$ 99.9 %) were placed in separate quartz crucibles (crucible for carbon: ϕ = 26 mm, I.D.; d = 24 mm, depth; crucible for Ti ore: ϕ = 25 mm, I.D.; l = 120 mm, length), which were subsequently positioned in the quartz tube (ϕ =

44.5 mm, I.D.; l = 820 mm, length), as shown in Fig. 6-4. As exceptional cases, in Exp. no. 130626, carbon was not used in the experiments in order to increase the p_{O_2} in the system, and in Exp. no. 130730, a mixture of Ti ore and carbon was used. In addition, in Exp. 131118, a crucible made by attaching four quartz crucibles (each crucible: ϕ = 12 mm, I.D.; l = 120 mm, length) was used as shown in Fig. 6-5. This crucible was used for reacting multiple samples simultaneously. After the samples were placed in the quartz tube, the tube was plugged by a Viton rubber plug. Afterward, liquid $TiCl_4$ (Wako Pure Chemical Industries Ltd., purity ≥ 99.0 %) was transferred from the reagent bottle to a glass bottle filled with argon gas (Ar, purity ≥ 99.9995 %) in a glove bag purged with nitrogen gas (N_2, purity ≥ 99.999 %) to prevent the reaction between $TiCl_4$ and the H_2O present in air as much as possible.

After the samples and liquid $TiCl_4$ were prepared, the quartz tube was evacuated thrice for 5 min each, and the tube was filled with Ar gas between the evacuations until the internal pressure reached 1 atm. After the final filling with Ar gas, Ar gas was flowed through the quartz tube at a controlled rate using a mass flow controller (MFC) while the internal pressure of the tube was maintained at 1 atm. In all the procedures, Ar gas was supplied into the quartz tube through magnesium perchlorate ($Mg(ClO_4)_2$, Kanto Chemical Co., Inc., purity ≥ 75 %) to remove the H_2O in the Ar gas.

After these atmosphere control procedures, the quartz tube was placed in a horizontal furnace preheated up to 1100 K for 30 min. The reaction temperature of 1100 K was chosen by considering the reduction of energy consumption and reaction kinetics for the production of TiO_2 (s). The quartz tube was placed at an angle of 1.7° relative to the horizontal axis of the horizontal furnace, and the front part of the quartz tube outside the furnace was cooled by a fan to promote effective $TiCl_4$ circulation inside the quartz tube. After the quartz tube was heated for 30 min in the furnace, liquid $TiCl_4$ (boiling temperature: 408 K) was fed into the tube by a peristaltic pump (Cole-Parmer Instrument Co., MasterFlex L/S Digital Drive, 7523-70; PTFE Tubing Pump, 77390-00) at a flow rate of 0.154 – 0.192 g/min. A continuous flow of liquid $TiCl_4$ into the quartz tube was used, except for in Exp. no. 130626. A $TiCl_4$ feeding pattern including periodic breaks was examined in order to decrease the amount of $TiCl_4$ discharged from the quartz tube without participating in the chlorination reaction.

In most cases, the quartz tube was instantly removed from the furnace after the reaction at a preset time and cooled down at room temperature. However, for Exp. nos. 130730 and 131118, evacuation using a diaphragm pump (As One Co., MAS-1) was performed 10 min and 20 min prior to the removal of the quartz tube from the furnace until the quartz tube was cooled down, respectively. The aim of this step was to remove the exhaust gas remaining in the quartz tube. Afterward, the quartz tube was filled with Ar gas until the internal pressure reached 1 atm, and Ar gas was flowed at room temperature while the internal pressure of the tube was maintained at 1 atm.

Three methods were applied to collect the residues from the quartz tube after the experiments. In Exp. no. 130704, the quartz tube was placed in a furnace preheated up to 500 K for 4 h under a N_2 gas atmosphere before the tube was taken out. Then, the quartz tube was filled with Ar gas until the internal pressure of the tube reached 1 atm, and subsequently Ar gas was flowed through the tube at room temperature until the $TiCl_4$ inside the tube was dried. The vapor pressure of $TiCl_4$ (l) at 300 K is 0.02 atm,[30] which is sufficient for evaporation. Therefore, the $TiCl_4$ in the quartz tube could be dried by supplying Ar gas. In Exp. no. 130730 and 131118, the Ar gas was flowed through the quartz tube at room temperature until the $TiCl_4$ inside the tube was dried. For all the other experiments, a small amount of acetone was injected into the quartz tube through the outlet pipe while the Ar gas flow was maintained to remove $TiCl_4$ from the front part of the tube. After the residues were taken out of the quartz tube, they were dissolved in deionized water and sonicated for over one hour at room temperature.

The chemical compositions of the residues obtained after the experiments were analyzed using X-ray fluorescence spectroscopy (XRF: JEOL, JSX-3100RII). The crystalline phases were identified by X-ray diffraction (XRD: RIGAKU, RINT 2500, Cu-Kα radiation), and the microstructures and compositions were analyzed by scanning electron microscopy/energy dispersive X-ray spectroscopy (SEM/EDS: JEOL, JSM-6510LV).

6.4   Results and discussion

6.4.1   Verification of selective chlorination using TiCl$_4$ under low oxygen chemical potential

Fig. 6-6 shows the results of XRD analysis of the Vietnamese, Australian, and Chinese Ti ores used in this study. As shown in Fig. 6-6, the main crystalline phase in the Ti ores was FeTiO$_3$. In addition, TiO$_2$ was also identified depending on the types of Ti ores.

Fig. 6-7 shows representative photographs of the low-temperature part of the quartz reaction tube during and after the experiment. TiCl$_4$ has a high vapor pressure even at room temperature, as mentioned before. Therefore, a certain amount of TiCl$_4$ that did not react with Ti ore was discharged from the quartz tube during the experiments and then condensed in a liquid form in the middle of the outlet line. To minimize the loss of unreacted TiCl$_4$, several methods were used to facilitate TiCl$_4$ circulation in the quartz tube, such as the use of a cooling fan or setting the quartz tube at a small tilting angle. As a result, as shown in Fig. 6-7 (a), a certain amount of unreacted TiCl$_4$ discharged from the reaction zone was cooled and condensed into a liquid in the cooling zone, and this liquid flowed back towards the reaction zone during the experiment because the horizontal quartz tube was slightly tilted.

After the experiments, yellow (and white) and brown deposits were generated inside the quartz tube, as shown in Fig. 6-7 (b). The brown deposits became yellow after the quartz tube was dried. Therefore, it is supposed that the TiCl$_4$ remaining in the low-temperature part of the quartz tube was evaporated and removed when Ar gas was flowed through the tube. Fig. 6-8 shows the results of XRD analysis of the two different yellow deposits obtained after drying brown or yellow deposits in the quartz tube. As shown in Fig. 6-8, FeCl$_2$ and FeCl$_2$·2(H$_2$O) were identified by the XRD analysis. Regarding the H$_2$O in the FeCl$_2$·2(H$_2$O), it seems H$_2$O in air had attached to FeCl$_2$ when the Viton rubber plug was removed from the quartz tube in order to obtain the residues.

Fig. 6-9 shows SEM images of the surface of a Ti ore particle obtained before and after the carbo-selective-chlorination experiment. As shown in Fig. 6-9, small pores were formed on the surfaces of the residues obtained after experiment. It is expected that the

214

majority of the pores were formed by the evaporation of iron chloride. This is because the vapor pressure of $FeCl_2$ generated by the reaction at 1100 K is high enough for the $FeCl_2$ to evaporate, and the evaporated $FeCl_2$ was condensed at the low-temperature part of the quartz tube. Therefore, it is concluded that the iron in the Ti ore was removed as $FeCl_2$ (*l,g*) by $TiCl_4$ at 1100 K as expected from the thermodynamic analysis.

Table 6-2 summarizes the analytical results for the feedstock used and the residues obtained after the experiments. As mentioned before, to increase the circulation of $TiCl_4$ inside the quartz tube, two types of $TiCl_4$ feeding patterns were examined: continuous feeding of $TiCl_4$ and feeding of $TiCl_4$ with periodic breaks. However, in the results from Exp no. 130626 and Exp no. 130703 shown in Table 6-2, even though different feeding patterns of $TiCl_4$ were adopted, no significant difference in the TiO_2 purity (98 % in both cases) was observed under the experimental conditions applied in this study.

6.4.2 Influence of various types of titanium ores

Fig. 6-10 shows the results of XRD analysis of the residues obtained after experiments when the Vietnamese Ti ore (Exp. no. 130703), Australian Ti ore (Exp. no. 130704), and Chinese Ti ore (Exp. no. 130708) were used as feedstock. As shown in Table 6-2 and Fig. 6-10, when the Vietnamese and Australian Ti ores were used as feedstock, the concentrations of titanium increased from 45 % to 98 % and from 49 % to 98 %, respectively, after the selective removal of iron from the Ti ore. As a result, 98 % TiO_2 was obtained in both cases. The purity of TiO_2 was calculated by converting all the elements measured by XRF to their nominal simple oxides. In addition, when the Chinese Ti ore was used as feedstock, 95 % TiO_2 was obtained after the experiment. Therefore, it can be claimed that various types of Ti ores can be upgraded to the TiO_2 with a purity of above 95 % by selectively removing iron directly from the ores in a single step through carbo-selective-chlorination.

Ti ore contains several impurities besides iron, such as manganese (Mn), aluminum (Al), or silicon (Si). Among these impurities, it was found that manganese oxide (MnO) was also removed from Ti ore by the carbo-selective-chlorination, as shown in Table 6-2. The chemical reaction between MnO and $TiCl_4$ is shown in Eq. 6-3.

$$\text{MnO } (s, \text{ in the ore}) + 1/2 \text{ TiCl}_4 \text{ } (g) = \text{MnCl}_2 \text{ } (l) + 1/2 \text{ TiO}_2 \text{ } (s) \qquad (6\text{-}3)$$

$\Delta G^\circ_r = -98.9$ kJ at 1100 K[30]
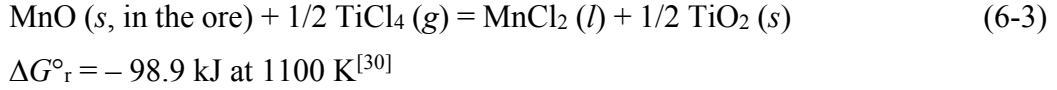
The analytical results showed decreased concentrations of aluminum in the residues after experiments. However, in the case of aluminum, from a thermodynamic point of view, Al_2O_3 is difficult to remove with $TiCl_4$, as shown in Eq. 6-4. Therefore, further study is required to investigate the behavior of aluminum and other impurities in the Ti ore during the carbo-selective-chlorination process.

$$\text{Al}_2\text{O}_3 \text{ } (s, \text{ in the ore}) + 3/2 \text{ TiCl}_4 \text{ } (g) = 2 \text{ AlCl}_3 \text{ } (g) + 3/2 \text{ TiO}_2 \text{ } (s) \qquad (6\text{-}4)$$

$\Delta G^\circ_r = 102.4$ kJ at 1100 K[30]
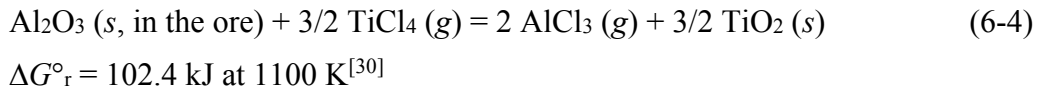
6.4.3 Influence of atmosphere in the reaction system

As discussed regarding the thermodynamic analysis of the carbo-selective-chlorination method (*see* Fig. 6-3), the potential region of this study is considered to be the cross-hatched region in which the oxygen chemical potential ranges from point d1 (C (*s*)/ CO (*g*) eq.) to point e1 (FeO (*s*)/Fe$_3$O$_4$ (*s*) eq.) in Fig. 6-3. When carbon and TiCl$_4$ exist in the reaction system, the potential of the system is located in the oxygen chemical potential ranges from point d1 to point d2 in the cross-hatched region in Fig. 6-3. The experimental conditions for Exp. nos. 130626 and 130703 can be considered examples of two conditions: one in which the p_{O_2} is located in the range from the log p_{O_2} value determined by the Fe (*s*)/FeO (*s*) eq. to point e1, and another in which the p_{O_2} value is located in the range from point d1 to point d2. In both cases, the iron in the Ti ore was selectively removed, and 98 % TiO$_2$ was obtained. Therefore, it can be claimed that if the chemical potentials of oxygen and chlorine are located in the potential region for carbo-selective-chlorination shown in Fig. 6-3, iron can be selectively removed from Ti ore and a high-grade TiO$_2$ can be obtained.

6.4.4 Influence of particle size of titanium ore

As shown in the results of Exp. no. 131118 in Table 6-2, when the Ti ore with various particle sizes was reacted with TiCl$_4$, the concentration of iron in the Ti ore decreased from about 50 % to 0.5 – 5.3 %, and the concentration of titanium in the Ti ore increased from 45 % to 93 – 98 % because of the selective removal of iron from the Ti ore. These results show that high-grade TiO$_2$ feed was produced by selective chlorination using TiCl$_4$ under low p_{O_2} regardless of the titanium ore particle sizes. The selective chlorination could proceed because TiCl$_4$ could pass through pores generated on the surfaces of Ti ore particles, as shown in Fig. 6-9 (b), and reacted with the iron at the central portions of the particles. The XRF analysis results in Table 6-2 show the tendency of slight decrease in the amount of iron removed from the Ti ore with an increase in the particle size of the Ti ore feed. However, it is expected that more amount of iron in the Ti ore will be removed with an increase in reaction time, because the pores exist on the surfaces of Ti ore particles. In addition, it can also be confirmed that Mn in the Ti ore was removed by the selective chlorination.

6.5 Summary

In order to selectively remove iron directly from low-grade titanium ore (*e.g.* FeTiO$_3$), thermodynamic analysis considering the chemical potentials of oxygen and chlorine was conducted. Then, the suitable chemical potential region for carbo-selective-chlorination using TiCl$_4$ as a chlorinating agent was investigated for the selective removal of iron from Ti ore to produce high-grade TiO$_2$. When the selective chlorination experiments were conducted under Ar or Ar + C atmospheres at 1100 K using low-grade Ti ores produced from Vietnam, Australia, and China as feedstock, the iron in the ores was selectively removed in the form of iron chloride (FeCl$_2$). As a result, 98 % TiO$_2$ was produced directly from low-grade Ti ore containing 51 % TiO$_2$ in a single step under certain conditions. Thus, the carbo-selective-chlorination investigated in this study is demonstrated to be a feasible process for upgrading low-grade titanium ore for the production of high-grade titanium dioxide.

References

[1]   T.H. Okabe and J. Kang: "*The Latest Technological Trend of Rare Metals*", CMC Publishing Co. LTD., Tokyo, 2012, Chap. 6-1, pp. 83-94. (in Japanese)

[2]   J.E. Kogel, N.C. Trivedi, J.M. Barker, and S.T. Krukowski: "*Industrial Minerals & Rocks Commodities, Markets, and Uses*", 7th ed., Society for Mining, Metallurgy, and Exploration, Inc. (SME), Littleton, Colorado, USA, 2006, pp. 987–1013.

[3]   J. Kang and T.H. Okabe: "*Removal of Iron from Titanium Ore through Selective Chlorination Using Magnesium Chloride*", Mater. Trans., 2013, 54 (8), pp. 1444-1453.

[4]   The Japan Titanium Society: Titanium Japan, 2013, vol. 61, pp. 84. (in Japanese)

[5]   K.S. Geetha and G.D. Surender: "*Experimental and modelling studies on the aeration leaching process for metallic iron removal in the manufacture of synthetic rutile*", Hydrometallurgy, 2000, vol. 56 (1), pp. 41-62.

[6]   R.G. Becher, R.G. Canning, B.A. Goodheart, and S. Uusna: "*A new process for upgrading ilmenitic mineral sands*", Proceeding of the Australasian Institute of Mining and Metallurgy, 1965, vol. 21, pp. 21-44.

[7]   S. Jayasekera, Y. Marinovich, J. Avraamides, and S.I. Bailey: "*Pressure leaching of reduced ilmenite: electrochemical aspects*", Hydrometallurgy, 1995, vol. 39 (1), pp. 183-199.

[8]   W. Hoecker: "*Process for the production of synthetic rutile*", United States Patent 5601630, 1997.

[9]   J.B. Farrow, I.M. Ritchie, P. Mangano: "*The reaction between reduced ilmenite and oxygen in ammonium chloride solutions*", Hydrometallurgy, 1987, vol. 18 (1), pp. 21-38.

[10]   J.H. Chen: "*Beneficiation of Titaniferous Ores*", United States Patent 3825419, 1974.

[11]   J.H. Chen and L.W. Huntoon: "*Beneficiation of ilmenite ore*", United States Patent 4019898, 1977.

[12]   J.H. Chen: "*Pre-leaching or reduction treatment in the beneficiation of titaniferous iron ores*", United States Patent 3967954, 1976.

[13]   M. Gueguin and F. Cardarelli: "*Chemistry and mineralogy of titania-rich slags. Part 1-hemo-ilmenite, sulphate, and upgraded titania slags*", Miner. Process. Extr. Metall. Rev., 2007, vol. 28, pp. 1–58.

[14]   K. Borowiec, A.E. Grau, M. Gueguin, and J-F. Turgeon: "*Method to upgrade titania slag and resulting product*", United States Patent 5830420, 1998.

[15]   T. Wako: "*Industrial Wastewater Management in Japan*", Conference of WEPA Dialogue in Sri Lanka, 2012.
http://www.env.go.jp/en/focus/docs/files/20120801-51.pdf.

[16]   S. Fukushima and E. Kimura: "*Ilmenite Upgrading: Particulary Concerning Mitsubishi Process*", Titanium·Zirconium, 1975, vol. 23 (2), pp. 67-74. (In Japanese)

[17]   A. Fuwa, E. Kimura, and S. Fukushima: "*Kinetics of Iron Chlorination of Roasted Ilmenite Ore, Fe_2TiO_5 in a Fluidized-Bed Reactor*", Metallurgical Transactions B, 1978, vol. 9B (4), pp. 643-652.

[18]   V.G. Neurgaonkar, A.N. Gokarn, and K. Joseph: "*Beneficiation of ilmenite to rutile by selective chlorination in a fluidised bed*", Journal of Chemical Technology and Biotechnology, 1986, vol. 36 (1), pp. 27-30.

[19]   J.S.J. Van Deventer: "*Kinetics of the selective chlorination of ilmenite*", Thermochimica Acta, 1988, vol. 124, pp. 205-215.

[20]   K.I. Rhee and H.Y. Sohn: "*The selective carbochlorination of iron from titaniferous magnetite ore in a fluidized bed*", Metallurgical Transactions B, 1990, vol. 21B (2), pp. 341-347.

[21]   L.K. Doraiswamy, H.C. Bijawat, and M.V. Kunte: "*Chlorination of ilmenite in a fluidized bed*", Chemical Engineering Progress, 1959, vol. 55 (10), pp. 80-88.

[22]   W.E. Dunn: "*High-temperature chlorination of TiO_2 bearing minerals*", Transactions of the Metallurgical Society of AIME, 1960, vol. 218 (1), pp. 6-12.

[23]   C.M. Lakshmanan, H.E. Hoelscher, and B. Chennakesavan: "*The kinetics of ilmenite beneficiation in a fluidised chlorinator*", Chemical Engineering Science, 1965, vol. 20 (12), pp. 1107-1113.

[24]   K.I. Rhee and H.Y. Sohn: "*The selective chlorination of iron from llmenite ore by $CO-Cl_2$ mixtures: Part I. intrinsic kinetics*", Metallurgical Transactions B, 1990, vol. 21B (2), pp. 321-330.

[25]   H. Zheng: "*Development of a Novel Titanium Production Process Using Selective Chlorination*", Doctoral Thesis, The University of Tokyo, 2007.

[26]   J. Kang and T.H. Okabe: "*Upgrading Titanium Ore Through Selective Chlorination Using Calcium Chloride*", Metallurgical and Materials Transactions B, 2013, vol. 44B (3), pp. 516-527.

[27]   D.F. Othmer: "*Manufacture of titanium chloride, synthetic rutile and metallic iron from titaniferous materials containing iron*", United States Patent 3859077, 1975.

[28]   D.F. Othmer and R. Nowak: "*Halogen affinities–A new ordering of metals to accomplish difficult separations*", AIChE J., 1972, 18 (1), pp. 217-220.

[29]   D.F. Othmer: "*Manufacture of titanium chloride and metallic iron from titaniferous materials containing iron oxides*", United States Patent 3989510, 1976.

[30]   I. Barin: "*Thermochemical Data of Pure Substances*", 3rd ed., VCH Verlagsgesellschaft mbH, Weinheim, Germany, 1995.

Table 6-1 Experimental conditions used in this study.

Exp no.[a]	Source country for Ti ore	Reaction time, t_r' / h	Particle size of Ti ore, d_{ore} / μm	Weight of carbon, w_c / g	Weight of Ti ore, w_{ore} / g	TiCl$_4$ feed[f]		
						Rate, f_{TiCl_4} / g·min^{-1}	Feeding pattern	Feeding time, t_{TiCl_4}' / ks
130626[b]	Vietnam	5	74 – 149	–	2.00	0.185	1	10.5
130703[c]	Vietnam	6	74 – 149	0.50	2.00	0.164	2	9.12
130704[c]	Australia	6	74 – 149	0.50	2.00	0.163	2	9.18
130708[c]	China	6	74 – 149	0.50	2.00	0.167	2	9.00
130730[d]	Vietnam	4	74 – 149	0.50	2.00	0.192	2	7.80
131118[e]	Vietnam	9	74 – 149	2.00	1.00	0.154	2	9.72
			149 – 210		1.00			
			210 – 297		1.00			
			297 – 510		1.00			

a : Experimental conditions;
   Reaction temperature, T = 1100 K.
b : Ar flow rate for entire reaction time with fan, f_{Ar} = 500 sccm.
   carbon was not used.
c : Ar flow rate for 5 h (from 0 h to 5 h) with fan, f_{Ar} = 500 sccm.
   Ar flow rate for 1 h (from 5 h to 6 h) without fan, f_{Ar} = 1000 sccm.
d : Ar flow rate for entire reaction time with fan, f_{Ar} = 500 sccm.
   Time for evacuation before taking out the quartz tube from furnace = 10 min.,
   and when evacuation was performed, exhaust gas was captured in the glass bottle cooled by
   liquid nitrogen.
   Titanium ore was and carbon was physically mixed.
e : Ar flow rate for entire reaction time with fan, f_{Ar} = 500 sccm.
   Time for evacuation before taking out the quartz tube from furnace = 20 min.,
   and when evacuation was performed, exhaust gas was captured in the glass bottle cooled by
   liquid nitrogen.
f : Amount of TiCl$_4$ used, w_{TiCl_4} = 25 g.
   TiCl$_4$ feeding pattern 1 : feeding for 30 min and break of feeding for 10 min.
   TiCl$_4$ feeding pattern 2 : continuous feeding without break.
   Feeding time of feeding pattern 1 includes periodic breaks.

Table 6-2 Analytical results for the feedstock used and residues obtained
     after experiments.

Exp. no.	Source country for Ti ore	Particle size of Ti ore, d_{ore} / µm	Concentration of element i, C_i (mass%)[a]				
			Ti	Fe	Mn	Si	Al
Feedstock (Initial)	Vietnam		45.0	49.7	3.47	0.57	0.33
	Australia		48.5	46.7	1.69	1.00	1.02
	China		47.2	45.4	2.79	1.65	1.41
130626	Vietnam	74 – 149	98.0	0.69	0.05	0.36	N.D
130703	Vietnam	74 – 149	97.7	0.39	0.05	0.96	N.D
130704	Australia	74 – 149	97.6	0.39	0.04	0.63	N.D
130708	China	74 – 149	94.8	2.28	0.15	0.83	N.D
130730	Vietnam	74 – 149	97.6	0.50	0.11	0.71	N.D
131118	Vietnam	74 – 149	98.3	0.50	0.09	0.46	N.D
		149 – 210	96.9	1.72	0.13	0.29	N.D
		210 – 297	93.1	5.33	0.35	0.19	N.D
		297 – 510	94.8	3.52	0.17	0.35	N.D

a : Determined by XRF analysis (excluding oxygen and other gaseous element).
   N.D : Not Detected. Below the detection limit of the XRF (<0.01 mass%),
   Values are determined by average of analytical results of five samples.
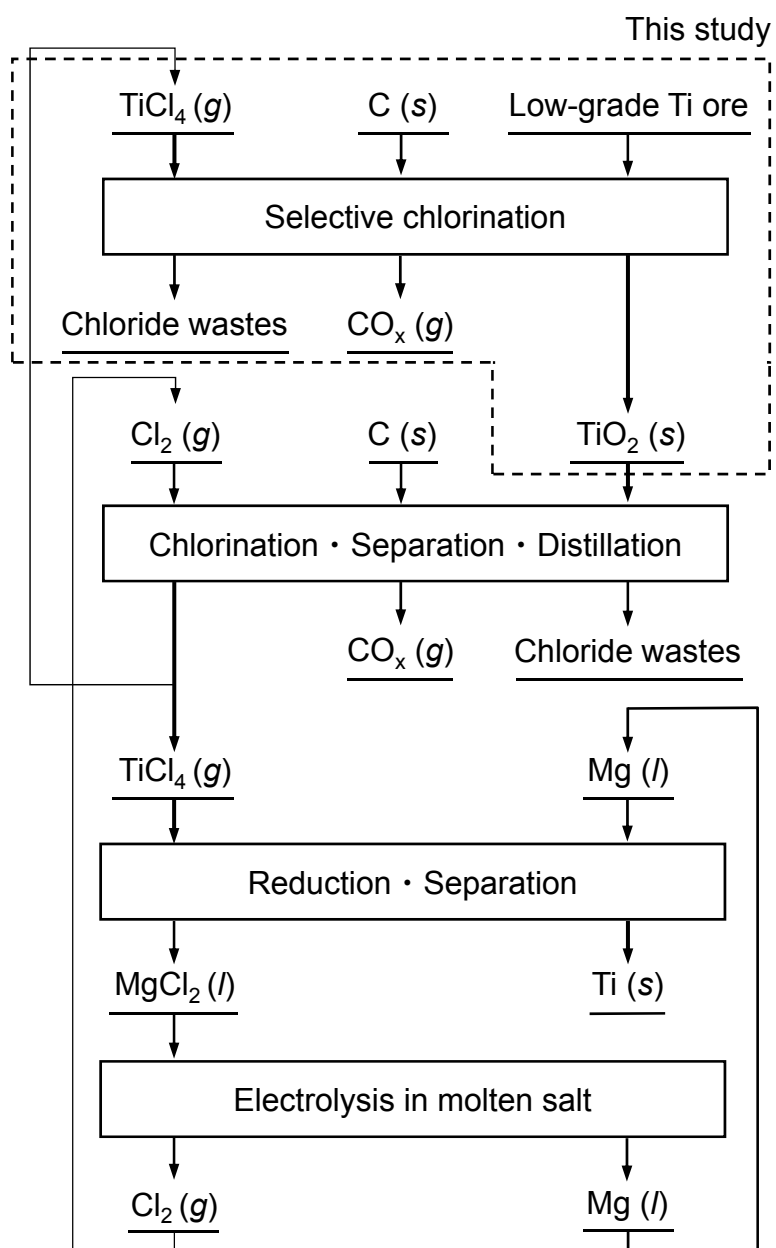
Figure 6-1 Flow diagram for new titanium smelting adopting
the selective chlorination process investigated in this study.

Fe-O-Cl system,

Ti-O-Cl system, *T* = 1100 K
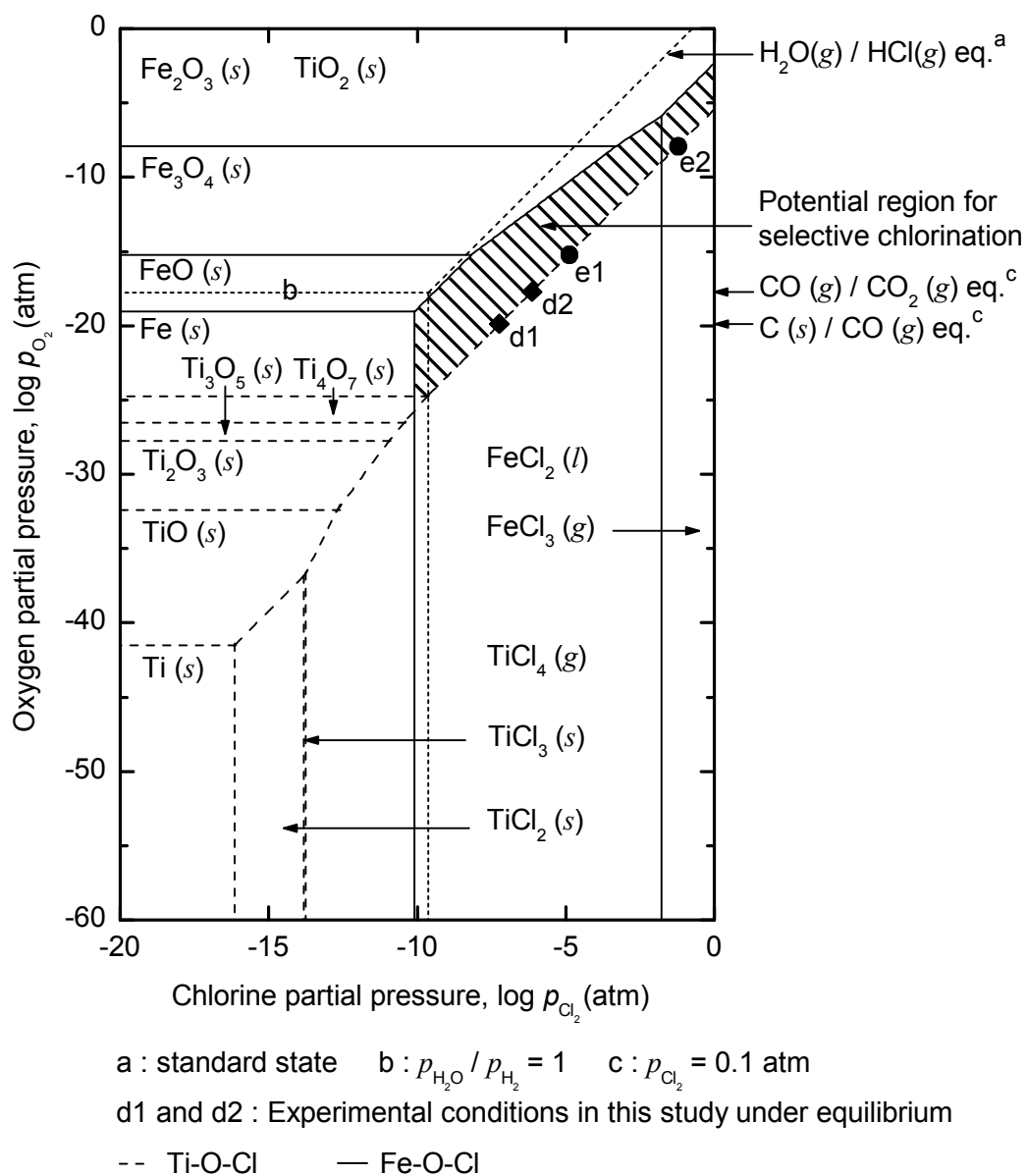
Figure 6-2 Chemical potential diagrams of the Fe-O-Cl system (solid line)
and the Ti-O-Cl system (dotted line) overlapped at 1100 K.
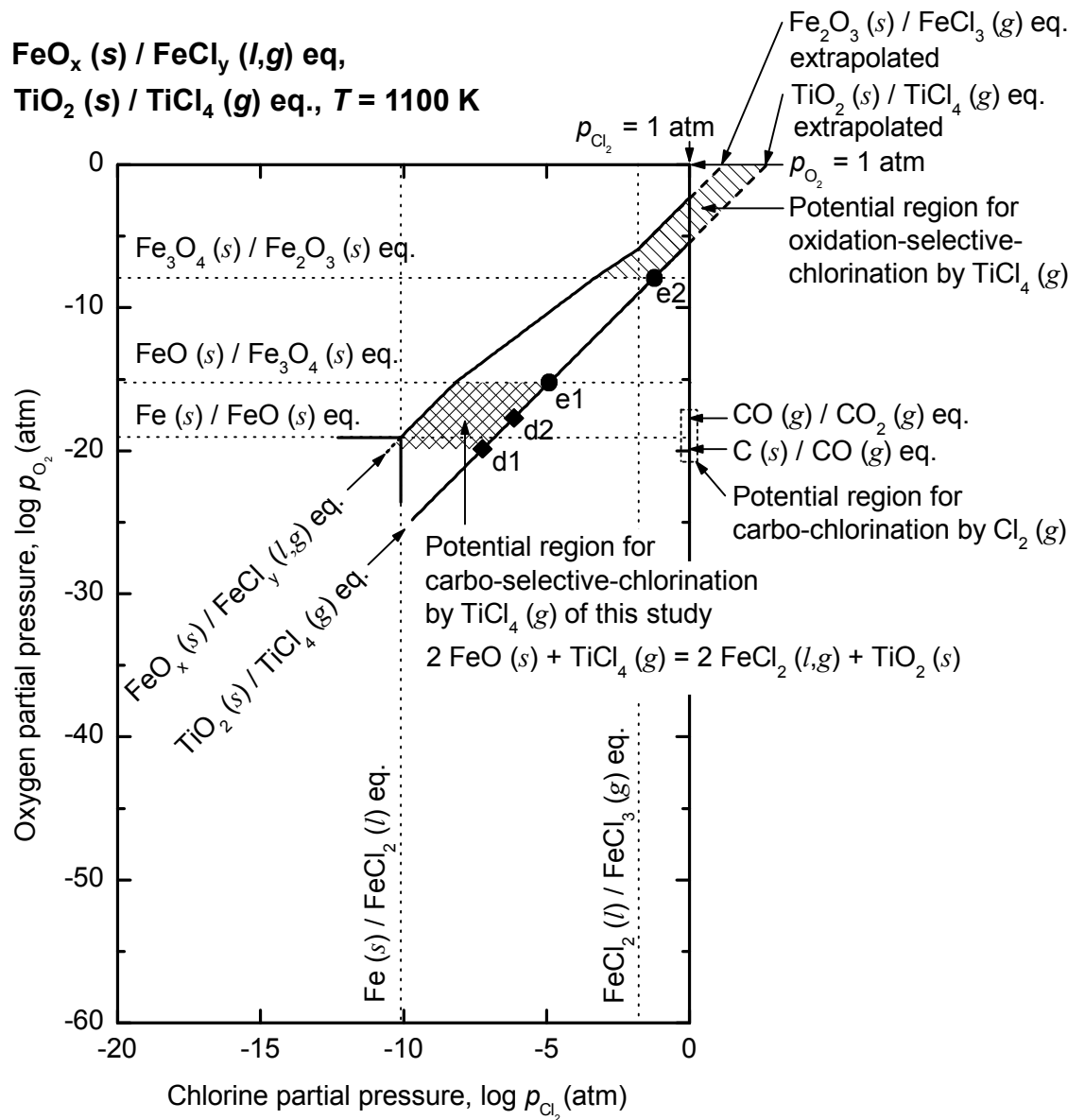
Figure 6-3 Comparison of potential regions for this study, carbo-chlorination, and oxidation chlorination using the modified chemical potential diagram of the Fe-O-Cl and the Ti-O-Cl systems at 1100 K.

(a)

Peristaltic pump

Teflon tube

Vacuum

Liquid N$_2$

Exhaust gas

Empty Water

Teflon valve

Ar gas inlet

Teflon cover

Glass bottle

TiCl$_4$

Heater

Electric furnace

Quartz tube

Quartz

Viton plug

Ti ore

Carbon

Angle = 1.7°

Mg(ClO$_4$)$_2$

Cooling Fan

Ti ore was mixed with carbon
(Exp. no. 130730 only).

Mass flow controller

Carbon was placed except Exp. no. 130626
and Exp. no. 130730.

Ar or N$_2$ gas inlet

(b)

10 mm
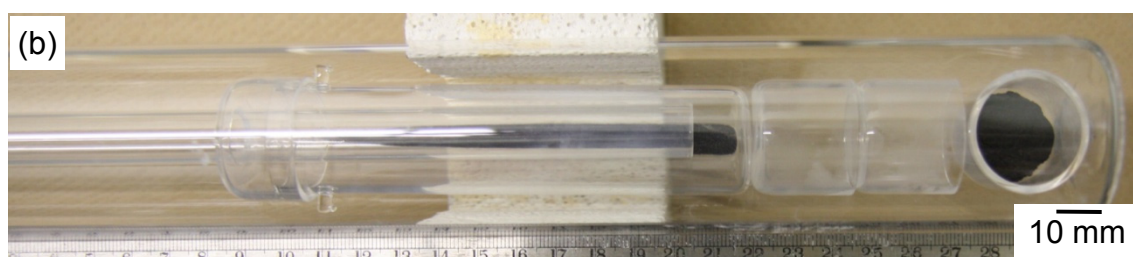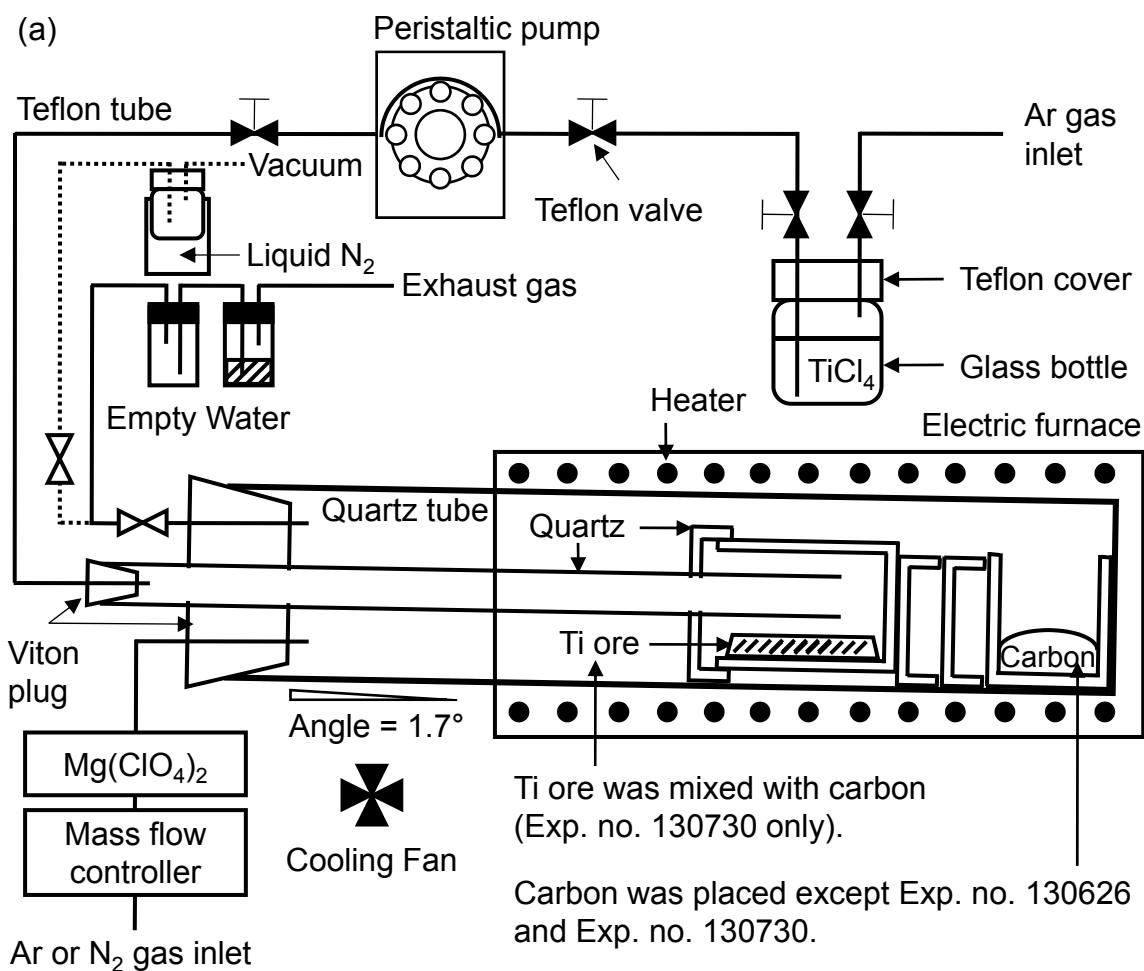
Figure 6-4 (a) Schematic diagram of the experimental apparatus and
(b) photograph taken before the experiments showing some of
the samples placed in the quartz tube.

(a)

Peristaltic pump

Teflon tube

Vacuum

Liquid N$_2$

Exhaust gas

Empty Water

Ar gas inlet

Teflon valve

Teflon cover

Glass bottle

TiCl$_4$

Heater

Electric furnace

Quartz tube

Quartz

Ti ore

Viton plug

carbon carbon

Angle = 1.7°

Mg(ClO$_4$)$_2$

Mass flow controller

Cooling Fan

Ar gas inlet

(b)

20mm

(c)

20mm
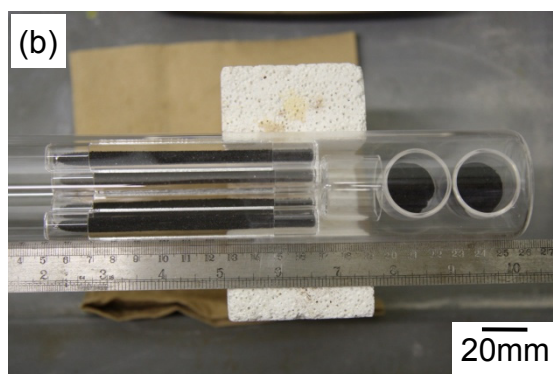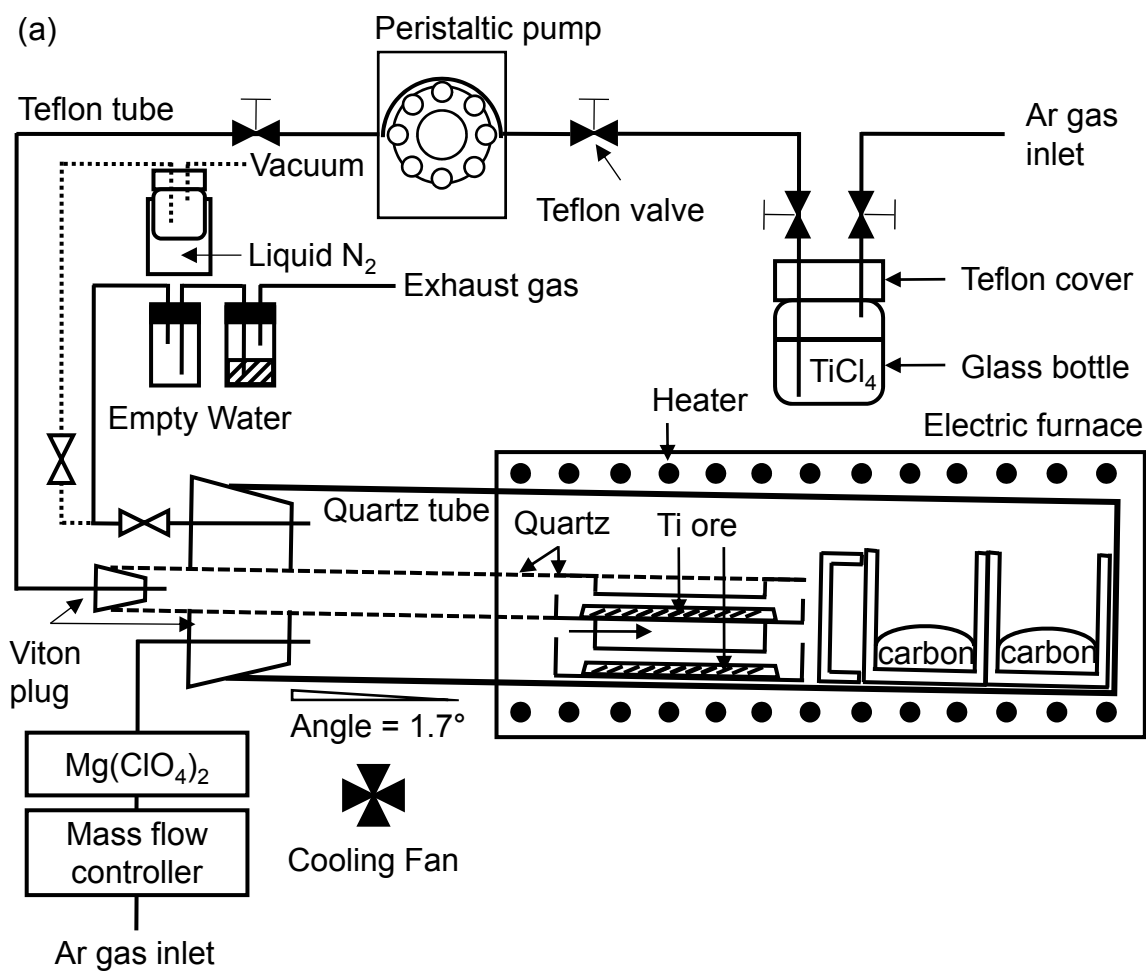
Figure 6-5 (a) Schematic diagram of the experimental apparatus and
(b) and (c) photographs taken before the experiments
showing some of the samples placed in the quartz tube.
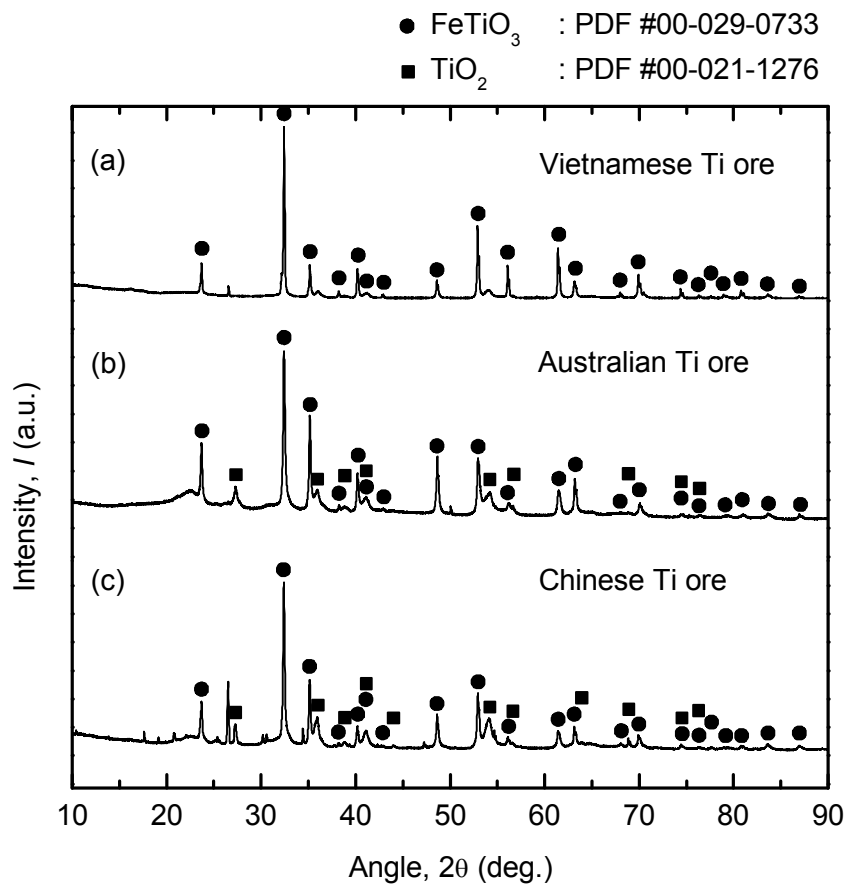
Figure 6-6 Results of XRD analysis of the (a) Vietnamese, (b) Australian, and (c) Chinese Ti ores used in this study. (*see* Table 6-2)
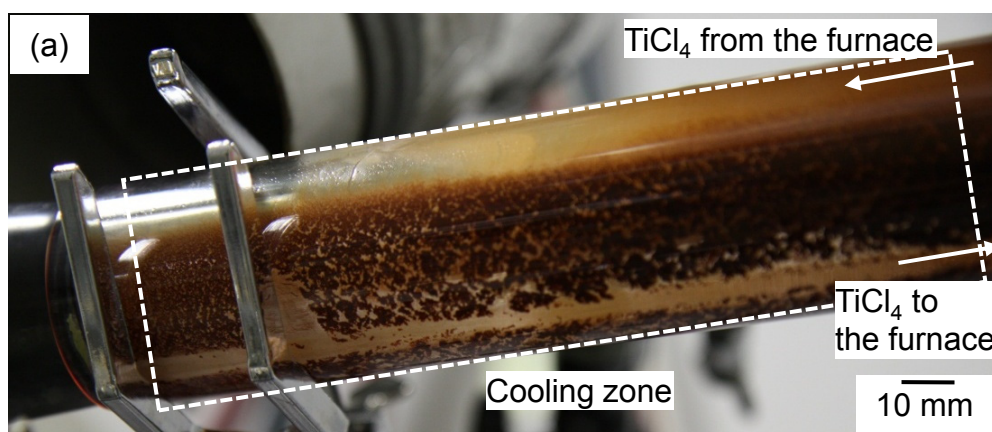
Figure 6-7 Representative photographs of low-temperature part of
the quartz tube (a) during the experiment (Exp. no. 130626)
and (b) after the experiment (Exp. no. 130704).

229
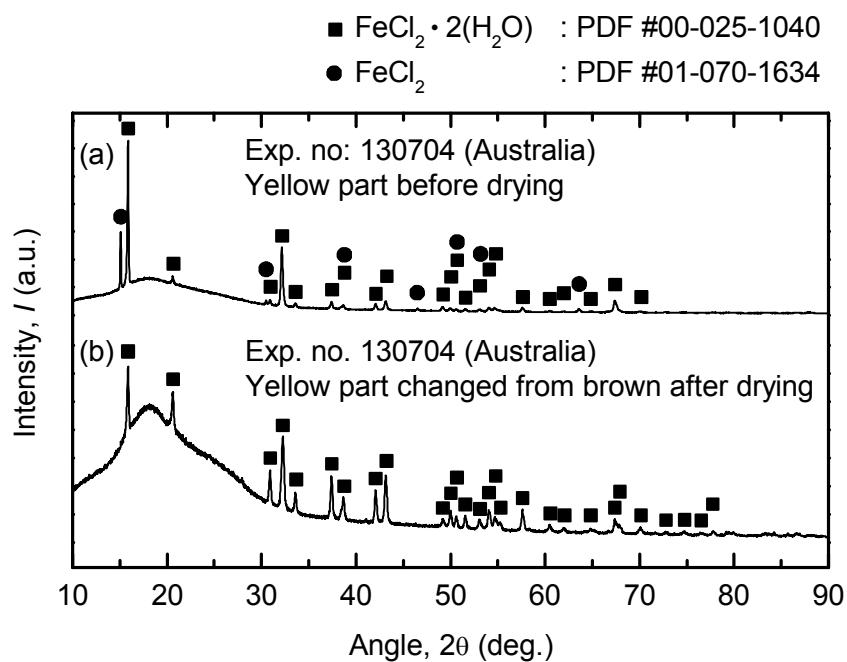
Figure 6-8　Results of XRD analysis of the powders condensed
in the low-temperature part of the quartz tube (Exp. no. 130704):
(a) yellow part before the quartz tube was dried and (b) yellow part
changed from brown after the quartz tube was dried.
(*see* Tables 6-1 and 6-2)
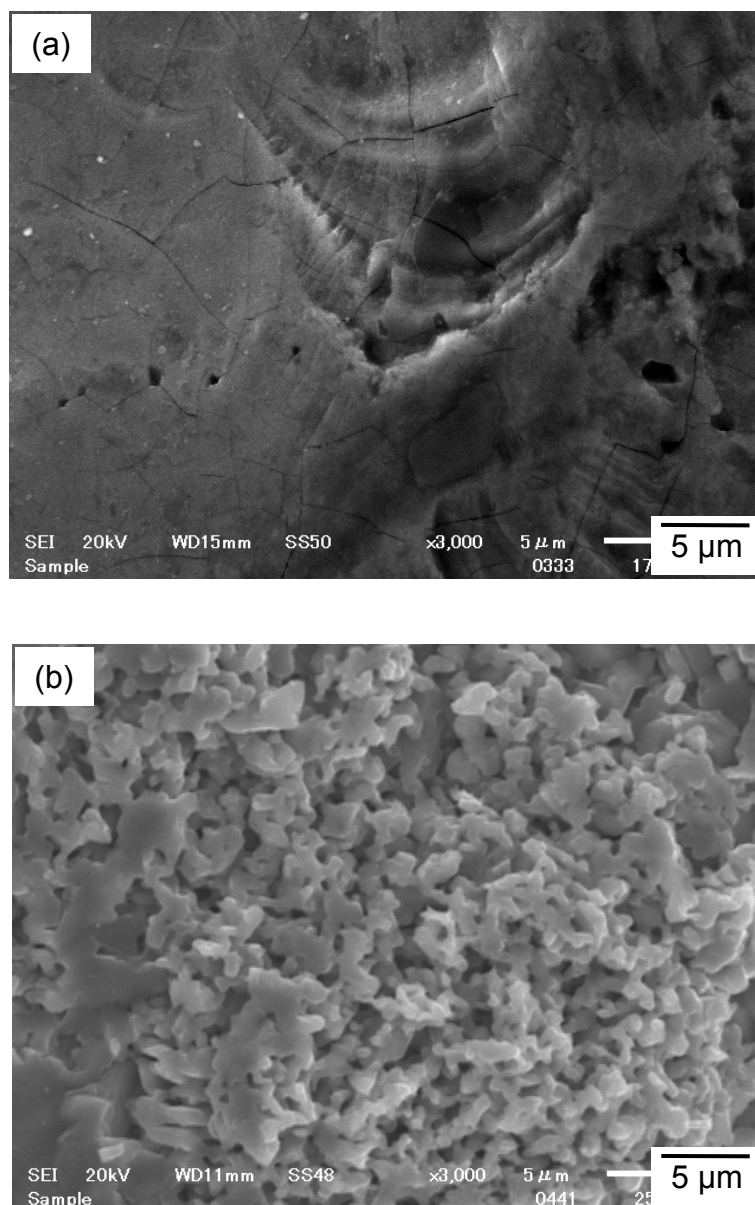
Figure 6-9 SEM images of the surface of a Vietnamese Ti ore particle
(a) before the experiment and (b) after the selective chlorination
experiment (Exp. no. 130703). (*see* Tables 6-1 and 6-2)
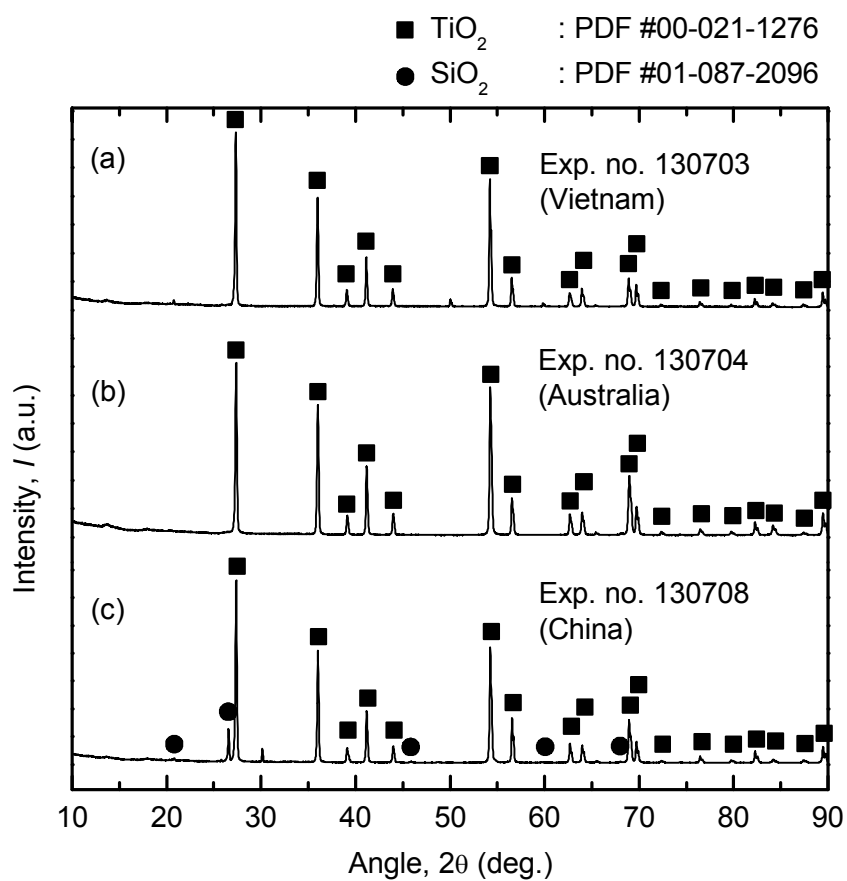
Figure 6-10 Results of XRD analysis of the residues obtained after experiments when the (a) Vietnamese (Exp. no. 130703), (b) Australian (Exp. no. 130704), and (c) Chinese (Exp. no. 130708) Ti ores were used as feedstock. (*see* Tables 6-1 and 6-2)

Chapter 7   Selective chlorination of low-grade titanium ore using titanium tetrachloride under high oxygen chemical potential

7.1   Introduction

The Kroll process is the industrial process for the production of titanium (Ti) metal.[1] Low-grade Ti ore (ilmenite) is upgraded to high-grade TiO_2 by removing iron (Fe) from the ore. Then the high-grade TiO_2 is used as feedstock for the Kroll process. In the first step of the Kroll process, the upgraded Ti ore containing $90 - 95$ % TiO_2 and other oxides is chlorinated in the chlorinator by chlorine gas (Cl_2) in the presence of carbon to produce $TiCl_4$. Most impurities in the ore are also chlorinated to form metal chlorides in this carbo-chlorination process.[2,3] Therefore, if Ti ore containing a large amount of impurities is used as a feedstock for the chlorinator, the chlorine loss increases because extra Cl_2 gas is consumed to chlorinate the impurities.[4] Simultaneously, a large amount of chloride waste is generated, which leads to clogging of pipes in the chlorinator. In addition, treatment of large amount of chloride waste is costly in several countries with stringent environmental restrictions for the treatment of industrial waste. For these reasons, most Ti metal production companies in Japan use TiO_2 feed with a purity of above 95 % (and purities above 90 % are used worldwide).[4]

Currently, the industrial processes for upgrading low-grade Ti ore are the Becher process,[5-9] the Benilite process,[10-12] and the slag and UGS processes.[13-14] Among these processes, the slag and UGS processes are the main processes for upgrading low-grade Ti ore based on the production of processes. For example, 1.4 Mt of titania–rich slag and 0.2 Mt of TiO_2 were produced by the slag process and UGS process, respectively, while 0.8 Mt of TiO_2 (synthetic rutile) was produced by other processes in 2003.[15]

Fig. 7-1 shows a representative flow chart for the slag and UGS processes. As can be seen, the processing necessary to remove Fe from low-grade Ti ore is quite complex and time-consuming. One reason for this complexity is the need to prevent the loss of Ti from the Ti ore and to enhance the removal of Fe from the ore during the upgrading process. This is achieved by the oxidation and reduction reactions for the Ti ore. Furthermore, the slag process consumes a large amount of energy, because the reaction

temperature for reducing iron oxides is very high, about 1923 − 1973 K. The advantage of the slag process is its speed and waste management. In the slag process, Fe in the ore is directly removed as pig-iron (Fe-C alloy), and this pig-iron is used for the iron industry.

The purity of TiO_2 feed produced by the slag process is 75 − 86 %, which is low for it to be used as feedstock for the Kroll process. Therefore, the UGS process uses concentrated acid such as 18 − 20 % hydrochloric acid (HCl) for the further removal of Fe and other impurities from the Ti ore as metal chlorides (e.g. $FeCl_2$ and $MnCl_2$) or oxychlorides. In addition, a large amount of aqueous acid waste solution containing heavy metals is dumped out because of the use of concentrated acid. The treatment of this large amount of acid waste solution containing heavy metals is costly in some countries with strict environmental regulations, such as Japan.[16]

To resolve these problems, extensive research has been conducted in the past. One representative method is selective chlorination through pyrometallurgical method. For example, selective chlorination of low-grade Ti ore was carried out using Cl_2 gas in the presence of carbon,[17-21] under a mixed CO and Cl_2 atmosphere,[22-25] using Cl_2 under presence of low-valence titanium oxide (TiO_x, $0 < x < 2$),[26] or using metal chlorides such as $CaCl_2$ or magnesium chloride ($MgCl_2$) as the chlorine source.[27-29] However, the direct use of Cl_2 gas is a problem in some situations from the viewpoint of safety and environmental concerns. In addition, the use of metal chlorides such as $CaCl_2$ or $MgCl_2$ also causes problems such as damage to the interior of the chlorinator, because these metal chlorides are highly corrosive at high temperatures.

Among the several potential processes, selective chlorination of low-grade Ti ore using $TiCl_4$ was suggested by Othmer in the past.[30-31] First, Othmer claimed Ti ore containing Fe_2O_3 could be selectively chlorinated by $TiCl_4$ under an oxidative atmosphere. This process is called oxidation-selective-chlorination. However, to the author's knowledge, experimental results on this process cannot be found in the literature. Second, Othmer claimed to have carried out the selective chlorination of Ti ore containing FeO by $TiCl_4$ in the presence of carbon. In all cases, systematic thermodynamic analysis considering the chemical potentials of oxygen (p_{O_2}) and chlorine (p_{Cl_2}) was not conducted.

In this study, thermodynamic analysis of selective chlorination of low-grade Ti ore using $TiCl_4$ under a high p_{O_2} was carried out in order to establish a new process for selective removal of Fe from the ore. Fig. 7-2 shows the selective chlorination method

investigated in this study. This process has the following advantages. (i) High-grade TiO_2 feed can be obtained directly from various types of low-grade Ti ores using a simple pyrometallurgical method in a single step. (ii) The $TiCl_4$ used as a chlorinating agent is easy to obtain, because a large amount of $TiCl_4$ is circulated in the Kroll process. (iii) There is no large amount of aqueous acid waste solution to be dumped out, because concentrated acid is not used. (iv) Recovery of chlorine is possible, because chloride waste such as $FeCl_x$ (x = 2, 3) is generated in a dry form.

7.2   Experimental

Fig. 7-3 shows a schematic diagram of the experimental apparatus used in this study, and Table 7-1 lists the experimental conditions. All samples used were oxidized at 1100 K for 13 h under an air atmosphere in advance. Before the experiments were conducted, the oxidized Ti ore was placed in quartz crucible (ϕ = 25 mm, I.D.; d = 120 mm, depth). Afterward, the quartz crucible was positioned in the quartz tube (ϕ = 44.5 mm, I.D.; l = 820 mm, length), and the tube was plugged with a Viton rubber plug.

After the sample was prepared, the atmosphere was controlled as follows. The quartz tube was evacuated for 5 min, and then the tube was filled with the Ar + 1 ppm O_2, Ar + 1 % O_2, or Ar + 10 % O_2 corresponding to the experimental atmosphere until the internal pressure of the tube reached 1 atm. This procedure was performed three times. After the quartz tube was finally filled with the appropriate atmosphere gas, the same gas was flowed through the quartz tube while the internal pressure of the tube was maintained at 1 atm. All the gas was supplied using a mass flow controller (MFC) and was passed through magnesium perchlorate ($Mg(ClO_4)_2$, Kanto Chemical Co., Inc., purity $\geq$ 75 %) to remove any H_2O in the gas.

After the atmosphere was controlled, the quartz tube was positioned in a horizontal furnace preheated to up to the experimental temperature of 1100 K or 1200 K. When the quartz tube was placed, it was tilted by 1.7° relative to the horizontal axis of the horizontal furnace. The front part of the tube outside the furnace was cooled by a fan to enhance the circulation of $TiCl_4$ inside the tube. Before $TiCl_4$ was fed into the quartz tube, Ti ore was oxidized at each experimental temperature for 1 h under each oxidative atmosphere. Afterward, liquid $TiCl_4$ (Wako Pure Chemical Industries Ltd., purity $\geq$

99.0 %) was fed into the quartz tube by a peristaltic pump at a flow rate of 0.126 – 0.160 g/min. During the experiments, the exhaust gas discharged from the outlet pipe was passed through deionized water for twice and then through 9.1 % $Na_2S_2O_3$ aq. solution.

After the designated reaction time had passed, the quartz tube was immediately removed from the furnace and cooled down at the room temperature. To collect the residues from the quartz tube, the each atmosphere gas used during experiment was flowed through the tube at room temperature until the $TiCl_4$ inside the tube was dried. The vapor pressure of $TiCl_4$ (l) is 0.02 atm at 300 K[32], which is high enough for evaporation to occur. The collected residues were dissolved in deionized water with sonication for at least one hour at room temperature. The chemical compositions of the residues obtained after the experiments were analyzed by X-ray fluorescence spectroscopy (XRF: JEOL, JSX-3100RII). The crystalline phases were identified using X-ray diffraction (XRD: RIGAKU, RINT 2500, Cu-Kα radiation), and the microstructures and compositions were analyzed by scanning electron microscopy/energy dispersive X-ray spectroscopy (SEM/EDS: JEOL, JSM-6510LV).

7.3 Thermodynamic analysis of selective chlorination using $TiCl_4$ under high oxygen chemical potential

Fe_2TiO_5 was the main complex oxide in the Ti ore when the ore was oxidized under an air atmosphere at 1100 K for 13 h (*see* Fig. 7-11 (e)). From the thermodynamic viewpoint, Fe_2TiO_5 can be considered as a mixture of iron oxide and titanium oxide, because the Gibbs energy of formation of Fe_2TiO_5 at 1200 K is a small negative value, as shown in Eq. 7-1. Therefore, thermodynamic analysis of the selective chlorination of Ti ore under oxidative atmosphere can be performed by utilizing the chemical potential diagrams of the Fe-O-Cl and Ti-O-Cl systems at 1200 K.

$$Fe_2O_3 \ (s) + TiO_2 \ (s) = Fe_2TiO_5 \ (s) \tag{7-1}$$
$$\Delta G°_r = -2.4 \text{ kJ at } 1200 \text{ K}^{[33]}$$

Fig. 7-4 shows the chemical potential diagram constructed by overlapping the chemical potential diagrams of the Fe-O-Cl (solid line) and Ti-O-Cl (dotted line) systems

at 1200 K. The hatched region with the solid lines is the potential region where $FeCl_x$ (l,g) [x=2, 3] and TiO_2 (s) are stable. Therefore, if the p_{O_2} and p_{Cl_2} are located in this hatched region, iron oxides will be transformed to $FeCl_x$ (l,g) [x=2, 3] and titanium oxides will be retained as TiO_2 (s). When the iron oxides are transformed to $FeCl_2$ (l), this $FeCl_2$ will evaporate, even though the liquid state of $FeCl_2$ is the thermodynamically stable phase at 1200 K. This is because the vapor pressure of $FeCl_2$ at 1200 K is 0.32 atm[32], which is sufficient for evaporation. Therefore, the hatched region with the solid lines is called the potential region for selective chlorination, because when p_{O_2} and p_{Cl_2} are in this region, the iron oxides in the Ti ore can be selectively chlorinated as $FeCl_x$ (l,g) [x=2, 3], and TiO_2 (s) can be obtained.

Because an excess amount of $TiCl_4$ was used as the chlorinating agent in the experiments, the TiO_2 (s) / $TiCl_4$ (g) eq. in Fig. 7-4 controls the p_{O_2} and p_{Cl_2} of the reaction system. As shown in Fig. 7-4, this equilibrium line is the borderline of the potential region for selective chlorination. In addition, oxygen concentration in atmosphere controls the p_{O_2} of the reaction system in the experimental condition employed in this study. Therefore, when the experiment was conducted under an Ar + 1 ppm O_2 atmosphere, the p_{O_2} and p_{Cl_2} were fixed at point a in Fig. 7-4. To analyze the p_{O_2} and p_{Cl_2} for the experiments conducted under the Ar + 1 % O_2 and Ar + 10 % O_2 atmospheres, an extrapolated equilibrium line for the TiO_2 (s) / $TiCl_4$ (g) eq. was assumed, as shown in Fig. 7-4. On the basis of this assumption, when the experiments were conducted under the Ar + 1 % O_2 and Ar + 10 % O_2 atmospheres, the p_{O_2} and p_{Cl_2} were fixed at points b and c, respectively, where the p_{Cl_2} is larger than 1 atm. As a result, even though the internal pressure of the quartz tube was maintained at 1 atm during the experiments, it is expected that the nominal p_{Cl_2} in some local reaction spots instantaneously exceeded 1 atm as a chemical potential during the experiment. Therefore, when an excess amount of $TiCl_4$ is used under Ar + 1 ppm O_2, Ar + 1 % O_2, or Ar + 10 % O_2 atmosphere and the reaction system is in an equilibrium state, the Fe_2O_3 in the Ti ore can be removed as $FeCl_3$ (g), because the p_{O_2} and p_{Cl_2} of the reaction system are fixed at points a, b, or c in Fig. 7-4, and TiO_2 (s) can be obtained.

Even though pure Cl_2 gas is used as a chlorinating agent for the chlorination of Fe_2O_3 (s) and TiO_2 (s), these oxides cannot be chlorinated by Cl_2 gas, as shown in Eqs. 7-2 and 7-3, where the $\Delta G°_r$ values are both positive. These calculation results show that chlorination of Fe_2O_3 (s) and TiO_2 (s) by pure Cl_2 gas is not feasible when p_{O_2} is high.

When the p_{O_2} is lowered by using carbon or another reducing agent, Fe_2O_3 (s) and TiO_2 (s) can be chlorinated by Cl_2 gas, which was explained in detail in chapter 2. Specifically, chlorination process using Cl_2 gas in the presence of carbon is well known as carbo-chlorination reaction. However, as discussed above, Fe_2O_3 (s) can be chlorinated by $TiCl_4$ (g), as shown in Eq. 7-4, which is the combined chemical reaction of the reactions shown in Eqs. 7-2 and 7-3. It is worth noting that the chlorination reaction of Fe_2O_3 (s) by $TiCl_4$ (Eq. 7-4) is independent of p_{Cl_2} and p_{O_2}. This thermodynamic analysis suggests that the chlorination reaction of Ti ore can proceed regardless of the p_{Cl_2} and p_{O_2} when $TiCl_4$ is used as a chlorinating agent.

$$2/3\ Fe_2O_3\ (s) + 2\ Cl_2\ (g) = 4/3\ FeCl_3\ (g) + O_2\ (g) \qquad (7\text{-}2)$$
$$\Delta G°_r = 36.0\ \text{kJ at 1200 K}^{[32]}$$

$$TiO_2\ (s) + 2\ Cl_2\ (g) = TiCl_4\ (g) + O_2\ (g) \qquad (7\text{-}3)$$
$$\Delta G°_r = 108.6\ \text{kJ at 1200 K}^{[32]}$$

$$2/3\ Fe_2O_3\ (s) + TiCl_4\ (g) = 4/3\ FeCl_3\ (g) + TiO_2\ (s) \qquad (7\text{-}4)$$
$$\Delta G°_r = -\ 72.6\ \text{kJ at 1200 K}^{[32]}$$
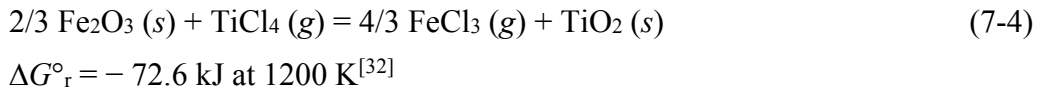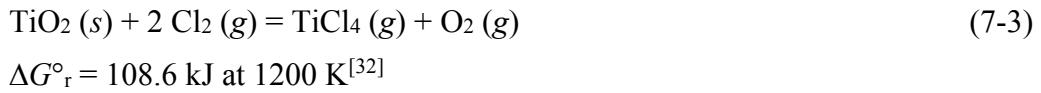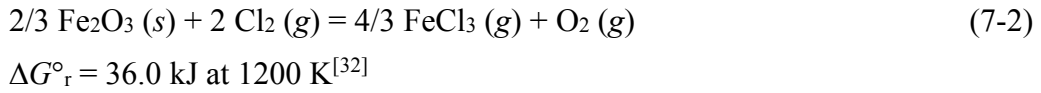
As mentioned before, if the reaction system is in equilibrium with an excess amount of $TiCl_4$, the p_{Cl_2} and p_{O_2} of the system are fixed at points a, b, or c depending on the oxygen chemical potential. However, the actual p_{Cl_2} and p_{O_2} for selective chlorination of Ti ore under high p_{O_2} can be in a wider chemical potential area not restricted to just these three points when several factors such as the redox potential of iron oxide are considered. This area is called potential region for oxidation-selective-chlorination, as shown in Fig. 7-5.

Fig. 7-5 shows the equilibrium lines of the FeO_x (s) / $FeCl_y$ (l,g) eq. and TiO_2 (s) / $TiCl_4$ (g) eq. at 1200 K and the potential region for oxidation-selective-chlorination under high p_{O_2} as the hatched area. When the redox potential of solid Fe_2O_3 (s) in Ti ore is considered, the log p_{O_2} value ranges from the log p_{O_2} determined by Fe_3O_4 (s) / Fe_2O_3 (s) eq. to 0 ($p_{O_2} = 1$). In addition, when the chlorination of Ti ore particles by $TiCl_4$ is considered, the outer boundary of the ore particle reacting with $TiCl_4$ is controlled by the

TiO$_2$ (s) / TiCl$_4$ (g) eq., and the center of the ore particle not yet reacting with TiCl$_4$ is controlled by the FeO$_x$ (s) / FeCl$_y$ (l,g) eq. Then if the chemical potential gradient of p_{Cl_2} and p_{O_2} between the two equilibriums is considered, the p_{Cl_2} and p_{O_2} can be located at any position between those two equilibrium lines. Thus, under these two conditions and the oxidative atmospheres used in this study, the hatched region shown in Fig. 7-5 becomes the potential region for the oxidation-selective-chlorination of Ti ore under high p_{O_2}.

As shown in Fig. 7-5, the potential region for oxidation-selective-chlorination exists in the stability region of FeCl$_3$ (g) and TiO$_2$ (s). Furthermore, the vapor pressure of FeCl$_3$ (g) is high enough for evaporation at 1200 K, and the vapor pressure of TiO$_2$ (s) is negligible. Therefore, when the TiCl$_4$ is used as a chlorinating agent for oxidation-selective-chlorination at 1200 K, the iron oxide in the Ti ore can be removed as FeCl$_3$ (g), and TiO$_2$ (s) can be obtained.

7.4   Results and discussion

7.4.1   Verification of selective chlorination using TiCl$_4$ under high oxygen chemical potential

Fig. 7-6 (a), (b), and (c) show photographs taken when 1 min, 2 min, and 4 min had elapsed after the quartz tube was removed from the furnace, respectively, when the experiment was conducted at 1100 K for 5 h under Ar + 1 ppm O$_2$ atmosphere. As shown in Fig. 7-6 (a), (b), and (c), as the time elapsed, the thick yellow fog inside the quartz tube became thinner, and the fog had disappeared when 6 min had elapsed. Fig. 7-7 (b) shows brown and yellow deposits condensed in the low-temperature part of the quartz tube after the experiment was conducted at 1200 K for 9 h under Ar + 1 ppm O$_2$ atmosphere (Exp. no. 131128). After the quartz tube was dried by flowing Ar + 1 ppm O$_2$ gas, the color of the deposits changed from brown to yellow because the TiCl$_4$ remaining was evaporated and removed from the tube.

Fig. 7-7 (a) shows the XRD results of the yellow deposits condensed in the low-temperature part of the quartz tube (Exp. no. 131128). As can be seen, the main crystalline phases of the deposits were FeCl$_2\cdot$4H$_2$O, FeCl$_3\cdot$6H$_2$O, and TiO$_2$. If the reactions in the system proceeded under equilibrium, all the Fe in the Ti ore should be removed as FeCl$_3$

under high p_{O_2}, as discussed in the section 7-3. However, the selective chlorination of Ti ore under a high p_{O_2} did not proceed under equilibrium, because $FeCl_2$ was also identified from the reaction product. The generation of $FeCl_2$ is presumed to be due to insufficient oxidation of the center parts of the Ti ore particles during the pretreatment and experiments, because $FeTiO_3$ was identified in the center of the particle after the experiment (*see* Fig. 7-10). Iron chlorides were identified in the form of $FeCl_x \cdot y(H_2O)_z$. It is expected that the H_2O was attached to the iron chlorides when they were exposed to air as the Viton rubber plug was removed from the quartz tube to collect the residues.

$Na_2S_2O_3$ aq. solution is frequently used as a dechlorinating agent.[34-35] The color of the $Na_2S_2O_3$ aq. solution through which the exhaust gas was passed changed from transparent to white and opaque when the experiments were conducted under $Ar + 1$ ppm O_2 and $Ar + 1$ % O_2 atmospheres. The color of the $Na_2S_2O_3$ aq. solution changed from transparent to bright yellow (and white) and opaque when the experiments were conducted under the $Ar + 10$ % O_2 atmosphere. After the $Na_2S_2O_3$ aq. solution was filtered, powders were obtained and dried under air at room temperature. These powders were identified as sulfur by XRD analysis as shown in Fig. 7-8. Sulfur is produced by the reaction between $Na_2S_2O_3$ aq. solution and Cl_2 gas. In addition, the generation of Cl_2 gas can also be inferred from the yellow fog inside the quartz tube after removal of the tube from the furnace as shown in Fig. 7-6 and from the TiO_2 identified by XRD analysis of the yellow deposits in the low-temperature part of the quartz tube as shown in Fig. 7-7. It is supposed that Cl_2 gas was mainly generated by the oxidation of $TiCl_4$ under high p_{O_2}.

Fig. 7-9 shows SEM images of the surfaces of Ti ore particles obtained before and after the experiment conducted at 1200 K under an $Ar + 1$ ppm O_2 atmosphere. As shown in Fig. 7-9, small pores were present on the surface of the Ti ore particle after the experiment. Therefore, it can be claimed that the Fe in the Ti ore was removed as $FeCl_x$ (*l,g*) [x = 2,3] and was subsequently condensed at the low-temperature part of the quartz tube owing to the high vapor pressure of $FeCl_x$ (*l,g*) [x = 2,3] at 1200 K.

In this study, oxidation of the Ti ore was performed before its use as feedstock for the experiment. This pretreatment of the Ti ore guarantees that the log p_{O_2} value is between the log p_{O_2} determined by Fe_3O_4 (*s*) / Fe_2O_3 (*s*) eq. and 0 in Fig. 7-5. In addition, the generation of Cl_2 gas shows that selective chlorination using $TiCl_4$ under high p_{O_2} proceeded in the high p_{Cl_2} region. Furthermore, the porous structure on the surface of the

Ti ore particle implies that the pair of p_{Cl_2} and p_{O_2} was located between the TiO_2 (s) / $TiCl_4$ (g) eq. and FeO_x (s) / $FeCl_y$ (l,g) eq. On the basis of these results, it is expected that the selective chlorination using $TiCl_4$ under high p_{O_2} proceeded in the potential region for oxidation-selective-chlorination in Fig. 7-5, as discussed in section 7-3.

7.4.2   Influence of oxidation state of iron and reaction temperature

Table 7-2 lists the analytical results for the initial feedstock used and for the residues obtained after the experiments. When the experiment was conducted at 1100 K for 9 h under an Ar + 1 ppm O_2 atmosphere (Exp. no. 131126), the concentration of Fe in the Ti ore decreased from 49.7 % to 7.41 %. Even though the selective chlorination using $TiCl_4$ proceeded under high p_{O_2}, 7.41 % Fe remained in the Ti ore. On the other hand, it was reported in chapter 6 that the amount of Fe in Ti ore decreased from 49.7 % to 0.50 % when selective chlorination using $TiCl_4$ was conducted at 1100 K for 4 h in the presence of carbon (low p_{O_2}). The difference in the concentration of Fe per reaction time for the high p_{O_2} and low p_{O_2} results from the oxidation state of the iron in the Ti ore. The oxidation state of the Fe in the Ti ore under high p_{O_2} is 3+, whereas that under low p_{O_2} is 2+. Generally, the reaction rate for chlorination of Fe_2O_3 (or Fe^{3+} in compounds) is slower than that for chlorination of FeO (or Fe^{2+} in compounds),[41] which is why industrial processes for upgrading Ti ore have a reduction step. Therefore, when the experiment was conducted at 1200 K for 9 h under an Ar + 1 ppm O_2 atmosphere (Exp. no. 131127), the concentration of Fe in the ore decreased from 49.7 % to below 0.01%, because reaction rate was enhanced at the higher reaction temperature.

7.4.3   Influence of particle size of titanium ore

The influence of the size of the Ti ore particles on the removal of Fe from Ti ore by selective chlorination was investigated. Table 7-2 shows that as the particle size increased, less Fe was removed from Ti ore when the other experimental conditions were identical. For example, when Ti ore particle with sizes in the range of 297 – 510 μm were used, 11.4 % Fe remained, and 87 % TiO_2 was obtained. On the other hand, when Ti ore particles of 74 – 149 μm were used, less than 0.01 % Fe remained, and 98 % TiO_2 was

obtained. The purity of TiO_2 was calculated by converting all the elements measured by XRF to their nominal simple oxides. Fig. 7-10 shows an SEM image and EDS results for a cross section of a Ti ore particle obtained when the experiment was conducted using Ti ore particles of $297 - 510$ μm (Exp. no. 131217). As shown by EDS results in Fig. 7-10, $FeTiO_3$ was detected in the center part, and TiO_2 was produced at the outer part of Ti ore particle. The detection of $FeTiO_3$ demonstrates that selective chlorination of Ti ore did not proceed completely and that oxidation of the Ti ore before its use was insufficient when the particle size of the Ti ore was large.

Fig. 7-11 shows the results of XRD analysis of the feedstock and residues obtained when the experiment was conducted using Ti ore with various particle sizes at 1200 K under the Ar + 1 ppm O_2 atmosphere. As shown in Fig. 7-11, TiO_2 was obtained when the Ti ore particles of $74 - 149$ μm and $149 - 210$ μm were used, because almost all of the Fe was selectively removed from the Ti ore. When Ti ore particles of $210 - 297$ μm and $297 - 510$ μm were used, $FeTiO_3$ and Fe_2TiO_5 were identified, respectively, in addition to TiO_2. Therefore, it is expected that when Ti ore particles of $297 - 510$ μm were used, the center parts of the Ti ore particles that were not oxidized by pretreatment ($FeTiO_3$) and portions of the rest of the Ti ore particles that were oxidized by pretreatment (Fe_2TiO_5) were not selectively chlorinated by $TiCl_4$ under high p_{O_2}.

7.4.4 Influence of various types of titanium ores and atmosphere

The influence of various types of Ti ore on the removal of Fe from Ti ore by selective chlorination was also investigated. As shown in Table 7-2, when the Australian and Chinese Ti ores were used as feedstock, the concentrations of Fe in the Ti ores decreased from 46.7 % to 0.75 % and from 45.4 % to 3.37 %, respectively. As a result, 97 % and 93 % TiO_2 were obtained when the Australian and Chinese Ti ores were used, respectively. Therefore, it can be concluded that selective chlorination using $TiCl_4$ can proceed for various types of Ti ores under Ar + 1 ppm O_2 atmosphere to produce high-grade TiO_2.

Furthermore, the influence of atmosphere in the reaction system on the removal of Fe from Ti ore by selective chlorination under oxidative atmosphere was investigated. When the experiments were conducted under Ar + 1 % O_2 and Ar + 10 % O_2 atmospheres,

the concentrations of Fe in the Ti ores decreased from 49.7 % to below 0.01 % and from 49.7 % to 0.25 %, respectively, and 98 % TiO_2 were obtained in both atmospheres. Therefore, selective chlorination using $TiCl_4$ can proceed under various oxygen chemical potentials, for example, $Ar + 1$ ppm O_2, $Ar + 1$ % O_2, and $Ar + 10$ % O_2, to produce high-grade TiO_2.

7.4.5 Comparisons of selective chlorination developed in the past and in this study

Table 7-3 shows the comparisons of experimental results of the selective chlorination processes developed in the past and in this study. According to the literature, by selective chlorination using Cl_2 gas under a reducing atmosphere, a high-grade TiO_2 feed with a purity of $93 - 97$ % was obtained. In addition, the results show that a high percentage of iron was removed from the Ti ore: $90 - 99$ %. However, as mentioned in section 7.1, the direct use of Cl_2 gas is a problem in some situations from the viewpoint of safety and environmental concerns. In addition, because Cl_2 was used as a chlorinating agent in the presence of carbon or under a CO gas atmosphere, there is a possibility of loss of Ti from the Ti ore under certain conditions.

In order to overcome these problems, the selective chlorination using metal chlorides such as $CaCl_2$ or $MgCl_2$ was proposed by Okabe's group. However, as shown in Table 7-3, when $CaCl_2$ and $MgCl_2$ were used, the purities of TiO_2 feeds obtained were 77 % and 81 %, respectively. In addition, the percentage of iron removed from the Ti ore was low. Furthermore, after the selective chlorination is completed, complex oxides, such as $CaTiO_3$, were obtained instead of high-grade TiO_2.

Thus, in this study, selective chlorination using HCl gas generated from $CaCl_2$ or $MgCl_2$, or $TiCl_4$ for the production of high-grade TiO_2 feeds was developed. Consequently, as shown in Table 7-3, high-grade TiO_2 feeds with a purity of 97 % – 98 % were obtained in a single step. However when $CaCl_2$ or $MgCl_2$ was used as the chlorine source, iron in the Ti ore was removed in a wet form because H_2O existed in the reaction system. In this case, the effective recovery of chlorine from chloride waste is difficult, even though HCl gas can be produced from the chloride waste. One of the problems is the difficulty in the choice for the material of the reactor because the environment of the reactor becomes highly corrosive. When $TiCl_4$ was used as the chlorine source in dry

(H$_2$O free) atmosphere, iron in the Ti ore was removed in the dry form because H$_2$O did not participate in the reaction. As a result, the effective recovery of chlorine from the chloride waste is feasible by oxidation. Thus, an environmentally friendly selective chlorination method can be established when TiCl$_4$ gas is used as the chlorinating agent.

Conventionally, it was considered that chlorination of iron oxides cannot proceed when p_{O_2} is high. However, in this study, the appropriate conditions for the selective chlorination of iron oxides under the high p_{O_2} was analyzed through thermodynamic study, and the feasibility of the selective chlorination of iron oxides under the high p_{O_2} was experimentally verified.

7.5   Summary

In order to produce high-grade TiO$_2$ directly from low-grade Ti ore in a single step, selective removal of iron from Ti ore using TiCl$_4$ under high p_{O_2} was investigated. The appropriate chemical potential region for selective chlorination under high p_{O_2} was studied by utilizing the chemical potential diagram considering p_{Cl_2} and p_{O_2}.

When the selective chlorination of Ti ore was conducted at 1200 K under high p_{O_2}, the iron in the ore was directly removed as FeCl$_x$ (l,g) [x = 2,3], and 98 % TiO$_2$ was obtained in a single step under certain conditions. When the selective chlorination using Ti ore particles of 74 – 297 μm was conducted at 1200 K under an Ar + 1 ppm O$_2$ atmosphere, $\geq$ 95 % TiO$_2$ was obtained. When the selective chlorination was conducted using Vietnamese, Australian, and Chinese Ti ores at 1200 K under Ar + 1 ppm O$_2$ atmosphere, 98 %, 97 %, and 93 % TiO$_2$ was obtained, respectively. Furthermore, when the selective chlorination of Ti ore was conducted at 1200 K under Ar + 1 ppm O$_2$, Ar + 1 % O$_2$, or Ar + 10 % O$_2$, 98 % TiO$_2$ was obtained. Therefore, selective chlorination of low-grade Ti ore using TiCl$_4$ under a high oxygen chemical potential is demonstrated to be a feasible process for producing high-grade titanium dioxide.

References

[1]   W. Kroll: "*The production of ductile titanium*", Trans. Electrochem. Soc., 1940, 78 (1), pp. 35–47.

[2]   T. Iida: Kinzoku Materials Science & Technology, 2012, 82, pp. 218–221. (in Japanese)

[3]   N. Nakamura: "*Current state of titanium sponge production technology*", Molten Salts, 2013, 56, pp. 121–124. (in Japanese)

[4]   T.H. Okabe and J. Kang: "*The Latest Technological Trend of Rare Metals*", CMC Publishing Co. LTD., Tokyo, 2012, Chap. 6-1, pp. 83-94. (in Japanese)

[5]   K.S. Geetha and G.D. Surender: "*Experimental and modelling studies on the aeration leaching process for metallic iron removal in the manufacture of synthetic rutile*", Hydrometallurgy, 2000, vol. 56 (1), pp. 41-62.

[6]   R.G. Becher, R.G. Canning, B.A. Goodheart, and S. Uusna: "*A new process for upgrading ilmenitic mineral sands*", Proceeding of the Australasian Institute of Mining and Metallurgy, 1965, vol. 21, pp. 21-44.

[7]   S. Jayasekera, Y. Marinovich, J. Avraamides, and S.I. Bailey: "*Pressure leaching of reduced ilmenite: electrochemical aspects*", Hydrometallurgy, 1995, vol. 39 (1), pp. 183-199.

[8]   W. Hoecker: "*Process for the production of synthetic rutile*", United States Patent 5601630, 1997.

[9]   J.B. Farrow, I.M. Ritchie, P. Mangano: "*The reaction between reduced ilmenite and oxygen in ammonium chloride solutions*", Hydrometallurgy, 1987, vol. 18 (1), pp. 21-38.

[10]   J.H. Chen: "*Beneficiation of Titaniferous Ores*", United States Patent 3825419, 1974.

[11]   J.H. Chen and L.W. Huntoon: "*Beneficiation of ilmenite ore*", United States Patent 4019898, 1977.

[12]   J.H. Chen: "*Pre-leaching or reduction treatment in the beneficiation of titaniferous iron ores*", United States Patent 3967954, 1976.

[13]   M. Gueguin and F. Cardarelli: "*Chemistry and mineralogy of titania-rich slags. Part 1-hemo-ilmenite, sulphate, and upgraded titania slags*", Miner. Process. Extr. Metall. Rev., 2007, vol. 28, pp. 1–58.

[14] K. Borowiec, A.E. Grau, M. Gueguin, and J-F. Turgeon: "*Method to upgrade titania slag and resulting product*", United States Patent 5830420, 1998.

[15] J.E. Kogel, N.C. Trivedi, J.M. Barker, and S.T. Krukowski: "*Industrial Minerals & Rocks Commodities, Markets, and Uses*", 7th ed., Society for Mining, Metallurgy, and Exploration, Inc. (SME), Littleton, Colorado, USA, 2006, pp. 987–1013.

[16] T. Wako: "*Industrial Wastewater Management in Japan*", Conference of WEPA Dialogue in Sri Lanka, 2012.
http://www.env.go.jp/en/focus/docs/files/20120801-51.pdf.

[17] S. Fukushima and E. Kimura: "*Ilmenite Upgrading: Particularly Concerning Mitsubishi Process*", Titanium·Zirconium, 1975, vol. 23 (2), pp. 67-74. (in Japanese)

[18] A. Fuwa, E. Kimura, and S. Fukushima: "*Kinetics of Iron Chlorination of Roasted Ilmenite Ore, Fe_2TiO_5 in a Fluidized-Bed Reactor*", Metallurgical Transactions B, 1978, vol. 9B (4), pp. 643-652.

[19] V.G. Neurgaonkar, A.N. Gokarn, and K. Joseph: "*Beneficiation of ilmenite to rutile by selective chlorination in a fluidised bed*", Journal of Chemical Technology and Biotechnology, 1986, vol. 36 (1), pp. 27-30.

[20] J.S.J. Van Deventer: "*Kinetics of the selective chlorination of ilmenite*", Thermochimica Acta, 1988, vol. 124, pp. 205-215.

[21] K.I. Rhee and H.Y. Sohn: "*The selective carbochlorination of iron from titaniferous magnetite ore in a fluidized bed*", Metallurgical Transactions B, 1990, vol. 21B (2), pp. 341-347.

[22] L.K. Doraiswamy, H.C. Bijawat, and M.V. Kunte: "*Chlorination of ilmenite in a fluidized bed*", Chemical Engineering Progress, 1959, vol. 55 (10), pp. 80-88.

[23] W.E. Dunn: "*High-temperature chlorination of TiO_2 bearing minerals*", Transactions of the Metallurgical Society of AIME, 1960, vol. 218 (1), pp. 6-12.

[24] C.M. Lakshmanan, H.E. Hoelscher, and B. Chennakesavan: "*The kinetics of ilmenite beneficiation in a fluidised chlorinator*", Chemical Engineering Science, 1965, vol. 20 (12), pp. 1107-1113.

[25] K.I. Rhee and H.Y. Sohn: "*The selective chlorination of iron from llmenite ore by CO-Cl_2 mixtures: Part I. intrinsic kinetics*", Metallurgical Transactions B, 1990, vol. 21B (2), pp. 321-330.

[26]   K. Ichimura, S. Oka, and Y. Takahashi: "*Method to produce high-grade TiO₂ feed*", Japan Patent 1994-191847, 1994. (in Japanese)

[27]   H. Zheng: "*Development of a Novel Titanium Production Process Using Selective Chlorination*", Doctoral Thesis, The University of Tokyo, 2007.

[28]   J. Kang and T.H. Okabe: "*Upgrading Titanium Ore Through Selective Chlorination Using Calcium Chloride*", Metallurgical and Materials Transactions B, 2013, vol. 44B (3), pp. 516-527.

[29]   J. Kang and T.H. Okabe: "*Removal of Iron from Titanium Ore through Selective Chlorination Using Magnesium Chloride*", Mater. Trans., 2013, 54 (8), pp. 1444-1453.

[30]   D.F. Othmer: "*Manufacture of titanium chloride, synthetic rutile and metallic iron from titaniferous materials containing iron*", United States Patent 3859077, 1975.

[31]   D.F. Othmer and R. Nowak: "*Halogen affinities–A new ordering of metals to accomplish difficult separations*", AIChE J., 1972, 18 (1), pp. 217-220.

[32]   I. Barin: "*Thermochemical Data of Pure Substances*", 3rd ed., VCH Verlagsgesellschaft mbH, Weinheim, Germany, 1995.

[33]   A. Roine: "*HSC Chemistry® 6.1 Outokumpu HSC Chemistry for Windows*", version 6.1, Outokumpu Research Oy Information Center, Finland, 2006.

[34]   C. Ohkawa: "*New Extraction Process of Precious Metals from Scrap by Using Chloride*", Master thesis, The University of Tokyo, 2005. (in Japanese)

[35]   American Water Works Association: "*Water Chlorination/Chloramination Practices and Principles*", 2nd ed., American Water Works Association, Denver, Colorado, USA, 2006.

[36]   A. Roine *et al.*: "*HSC Chemistry® version 7.11*", Outotec Oy Information Center, Finland, 2011.

[37]   A.S. Athavale and V.A. Altekar: "*Kinetics of Selective Chlorination of Ilmenite Using Hydrogen Chloride in a Fluidized Bed*", Industrial & Engineering Chemistry Process Design and Development, 1971, 10 (4), pp. 523-530.

[38]   R. Matsuoka: "*Iron Removal from Titanium Ore Using Selective Chlorination and Effective Utilization of Chloride Waste*", Master thesis, The University of Tokyo, 2005. (in Japanese)

[39] J. Kang and T.H. Okabe: "*Production of Titanium Dioxide Directly from Titanium Ore Through Selective Chlorination Using Titanium Tetrachloride*", Meter. Trans., 2014, vol. 55 (3), pp. 591-598.

[40] J. Kang and T.H. Okabe: "*Removal of Iron from Titanium Ore by TiCl$_4$ under High Oxygen Potential through Selective Chlorination*", International Journal of Mineral Processing, 2014 (submitted).

[41] A. Janssen and A. Putnis: "*Process of oxidation and HCl-leaching of Tellnes ilmenite*", Hydrometallurgy, 2011, vol. 109, pp. 194-201.

Table 7-1 Experimental conditions used in this study for experiments conducted under high oxygen partial pressure.

Exp no.[a]	Source country for Ti ore	Particle size of Ti ore, d_{ore} / μm	Temp., T / K	Atmosphere	Reaction time, t'_r / h	TiCl$_4$ feed[b]	
						Feeding rate, f_{TiCl_4} / g·min^{-1}	Feeding time, t_{TiCl_4}' / ks
131125	Vietnam	74 – 149	1100	Ar + 1 ppm O$_2$	5	0.160	9.36
131126	Vietnam	74 – 149	1100	Ar + 1 ppm O$_2$	9	0.158	9.48
131127	Vietnam	74 – 149	1200	Ar + 1 ppm O$_2$	9	0.158	9.48
131128	Vietnam	149 – 210	1200	Ar + 1 ppm O$_2$	9	0.144	10.44
131202	Vietnam	210 – 297	1200	Ar + 1 ppm O$_2$	9	0.158	9.48
131217	Vietnam	297 – 510	1200	Ar + 1 ppm O$_2$	9	0.152	9.84
131220	Australia	74 – 149	1200	Ar + 1 ppm O$_2$	9	0.154	9.72
131223	China	74 – 149	1200	Ar + 1 ppm O$_2$	9	0.154	9.72
131227	Vietnam	74 – 149	1200	Ar + 1 % O$_2$	9	0.126	11.88
140103	Vietnam	74 – 149	1200	Ar + 10 % O$_2$	9	0.144	10.44

a : Experimental conditions;
Weight of feedstock used for Ti ore, w_{ore} = 1.50 g.
Ar flow rate for entire reaction time with fan, f_{Ar} = 500 sccm.
All feedstocks were oxidized at 1100 K for 13 h under dried air before experiments.
All feedstocks were oxidized for 1 h before supplying TiCl$_4$ at each reaction temperature and under each atmosphere.
b : Amount of TiCl$_4$ used, w_{TiCl_4} = 25 g.
TiCl$_4$ feeding pattern : continuous feeding without breaks.

Table 7-2 Analytical results for initial feedstock used and for residues obtained after experiments under high oxygen partial pressure (high p_{O_2}).

Exp. no.	Source country for Ti ore	Atmosphere (Ar based)	Conditions of chemical potentials in Figs. 7-4,7-5	Concentration of element i, C_i (mass%)[a]					Note (related Figs.)
				Ti	Fe	Mn	Si	Al	
Feedstock (Initial)	Vietnam			45.0	49.7	3.47	0.57	0.33	Fig. 7-9 (a)
	Australia			48.5	46.7	1.69	1.00	1.02	
	China			47.2	45.4	2.79	1.65	1.41	
131125	Vietnam	1 ppm O₂	Point a	85.7	11.6	1.42	0.38	N.D	Fig. 7-6 (a) – (c)
131126	Vietnam	1 ppm O₂	Point a	89.8	7.41	1.48	0.40	N.D	
131127	Vietnam	1 ppm O₂	Point a	97.2	N.D	1.12	0.40	N.D	Fig. 7-11 (a), Fig. 7-9 (b)
131128	Vietnam	1 ppm O₂	Point a	95.5	0.62	2.52	0.39	N.D	Fig. 7-11 (b), Fig. 7-7
131202	Vietnam	1 ppm O₂	Point a	93.3	2.82	2.46	0.42	N.D	Fig. 7-11 (c)
131217	Vietnam	1 ppm O₂	Point a	84.5	11.4	2.32	0.60	N.D	Fig. 7-11 (d), Fig. 7-10
131220	Australia	1 ppm O₂	Point a	96.6	0.75	0.64	0.56	N.D	
131223	China	1 ppm O₂	Point a	92.0	3.37	1.42	1.66	N.D	
131227	Vietnam	1 % O₂	Point b	97.2	N.D	1.34	0.53	N.D	
140103	Vietnam	10 % O₂	Point c	98.0	0.25	0.33	0.51	N.D	

a : Determined by XRF analysis (excluding oxygen and other gaseous element),
N.D : Not Detected. Below the detection limit of the XRF (<0.01 mass%),
Values are determined by average of analytical results of five samples.

250

Table 7-3 Selective chlorination processes using pyrometallurgical method developed in the past and in this study.

Author	Chlorinating agent	Reducing agent	Temp., T / K	Composition of Ti ore, C_i (mass%)					After selective chlorination		Notes
				TiO$_2$	Fe$_2$O$_3$	FeO	Ti¶	Fe§	TiO$_2$ purity, p_{TiO_2} (mass%)	Fe removal, R_{Fe} (%)	
Doraiswamy et al.[1]	Cl$_2$	CO	1173	62.6	23.4	11.0	(60.1)	(39.9)	-	97.0*	-
Dunn[2]	Cl$_2$	CO	1173	-	-	-	-	-	97.0	-	-
Lakshmanan et al.[3]	Cl$_2$	CO	1173	59.3	24.9	10.8	(55.0)	(45.0)	-	83.2*	-
Rhee and Sohn[4]	Cl$_2$	CO	1123	37.5	18.5	33.7	(36.5)	(63.5)	-	94.0#	-
Fukushima and Kimura[5]	Cl$_2$	C	1223	53.4	19.5	19.9	(52.4)	(47.6)	87.5	(85.9)+¶¶	Roasted Ti ore, pilot
Fuwa et al.[6]	Cl$_2$	C	1153	53.4	19.7	20.2	(52.1)	(47.9)	-	99.0#	Roasted Ti ore
Neurgaonkar et al.[7]	Cl$_2$	C	1273	61.1	23.3	9.6	(60.7)	25.2 (39.3)	94.0	96.9*	O$_2$ supply, Cl$_2$:O$_2$=8:1
Deventer[8]	Cl$_2$	C	1243	49.7	-	-	-	35.9	94.0	≈ 90.0#	-
Rhee and Sohn[9]	Cl$_2$	C	973	20.2	44.6	21.4	(20.2)	(79.8)	-	≈ 90.0#	-
Ichimura et al.[10]	Cl$_2$	TiO$_x$	1123	84.7	0.2	11.1	(85.3)	8.8	93.0	97.4+	TiO$_x$ (0 < x < 2)
Athavale and Altekar[11]	Cl$_2$ + H$_2$ (HCl)	(H$_2$)	1073	61.5	36.0	-	(59.4)	(40.6)	-	90.0&	98% HCl generated
Othmer[12]	TiCl$_4$	C	-	-	-	-	-	-	-	-	No actual data
Matsuoka and Okabe[13]	MgCl$_2$	-	1123	-	-	-	44.5	48.4	(76.6)¶¶	48.2+	Carbon crucible
Zheng and Okabe[14]	CaCl$_2$ + H$_2$O	-	1293	-	-	-	43.8	51.3	(80.6)¶¶	67.4+	Carbon crucible
Kang and Okabe[15]	HCl (from CaCl$_2$)	-	1100	51.1	-	-	45.0	51.3	96.8	98.9+	Under Vacuum
Kang and Okabe[16]	HCl (from MgCl$_2$)	-	1000	51.1	-	-	45.0	51.3	97.0	96.4+	Under Ar
Kang and Okabe[16]	HCl (from MgCl$_2$)	-	1000	51.1	-	-	45.0	51.3	97.4	97.5+	Under Ar + H$_2$O
Kang and Okabe[17]	TiCl$_4$	C	1100	51.1	-	-	45.0	51.3	98.2	99.0+	Under Ar
Kang and Okabe[18]	TiCl$_4$	-	1200	51.1	-	-	45.0	51.3	97.5	100.0+ (not detected)	Under Ar + 1 ppm O$_2$
Kang and Okabe[18]	TiCl$_4$	-	1200	51.1	-	-	45.0	51.3	97.6	100.0+ (not detected)	Under Ar + 1 % O$_2$
Kang and Okabe[18]	TiCl$_4$	-	1200	51.1	-	-	45.0	51.3	98.0	99.5+	Under Ar + 10 % O$_2$

1: Ref.[22]; 2: Composition of Ti ore was not provided in Ref.[23]; 3: Ref.[24]; 4: Composition of Ti ore is average values in Ref.[25]; 5: Ref.[17]; 6: Ref.[18]; 7: Ref.[19]; 8: Values are roughly estimated based on graph.[20];
9: Values are roughly estimated based on graph.[21]; 10: Ref.[26]; 11: Ref.[37]; 12: Ref.[30,31]; 13: Ref.[38]; 14: Ref.[27]; 15: Ref.[28]; 16: Ref.[29]; 17: Ref.[39]; 18: Ref.[40].
*: Removal percentage of Fe$_2$O$_3$, calculated by residual weight of the ore when all iron oxides present in the ore are assumed as Fe$_2$O$_3$.
#: Removal percentage of iron from the ore as total Fe.
&: Removal percentage of iron oxide. Form of iron oxide was not provided.
+: Removal percentage of iron (%) = 100×(w_{Fe} in feed – w_{Fe} in residue) / w_{Fe} in feed.
¶: Total Ti composition excluding gaseous elements. Values in parenthesis are calculated by the authors assuming pseudo-binary TiO$_2$ – FeO$_x$ system.
§: Total Fe composition excluding gaseous elements. Values in parenthesis are calculated by the authors assuming pseudo-binary TiO$_2$ – FeO$_x$ system.
¶¶: Values in parenthesis are calculated by the authors assuming TiO$_2$ – FeO$_x$ – MO$_x$ system given by the authors
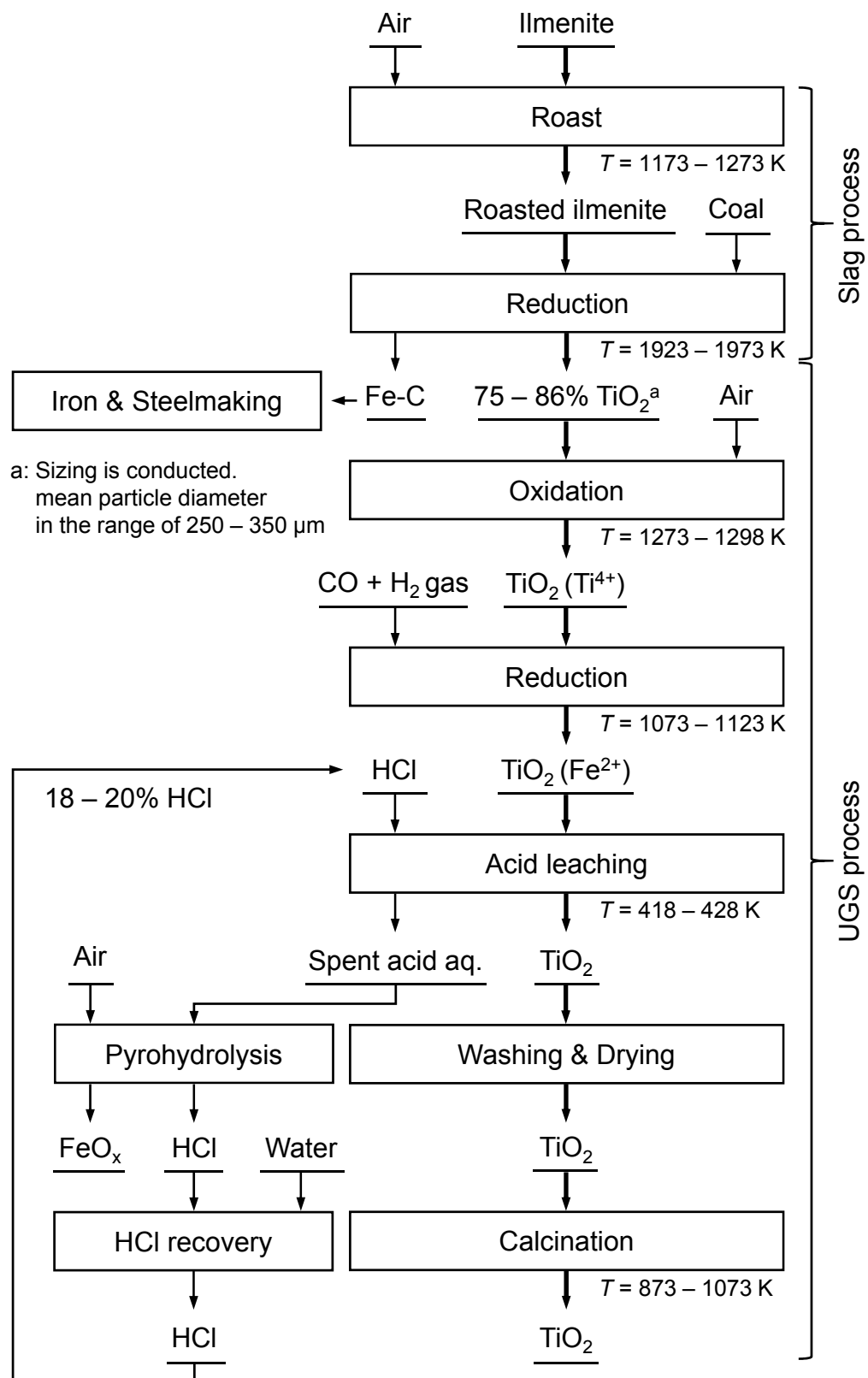
Figure 7-1 Flow chart of the slag and UGS processes.
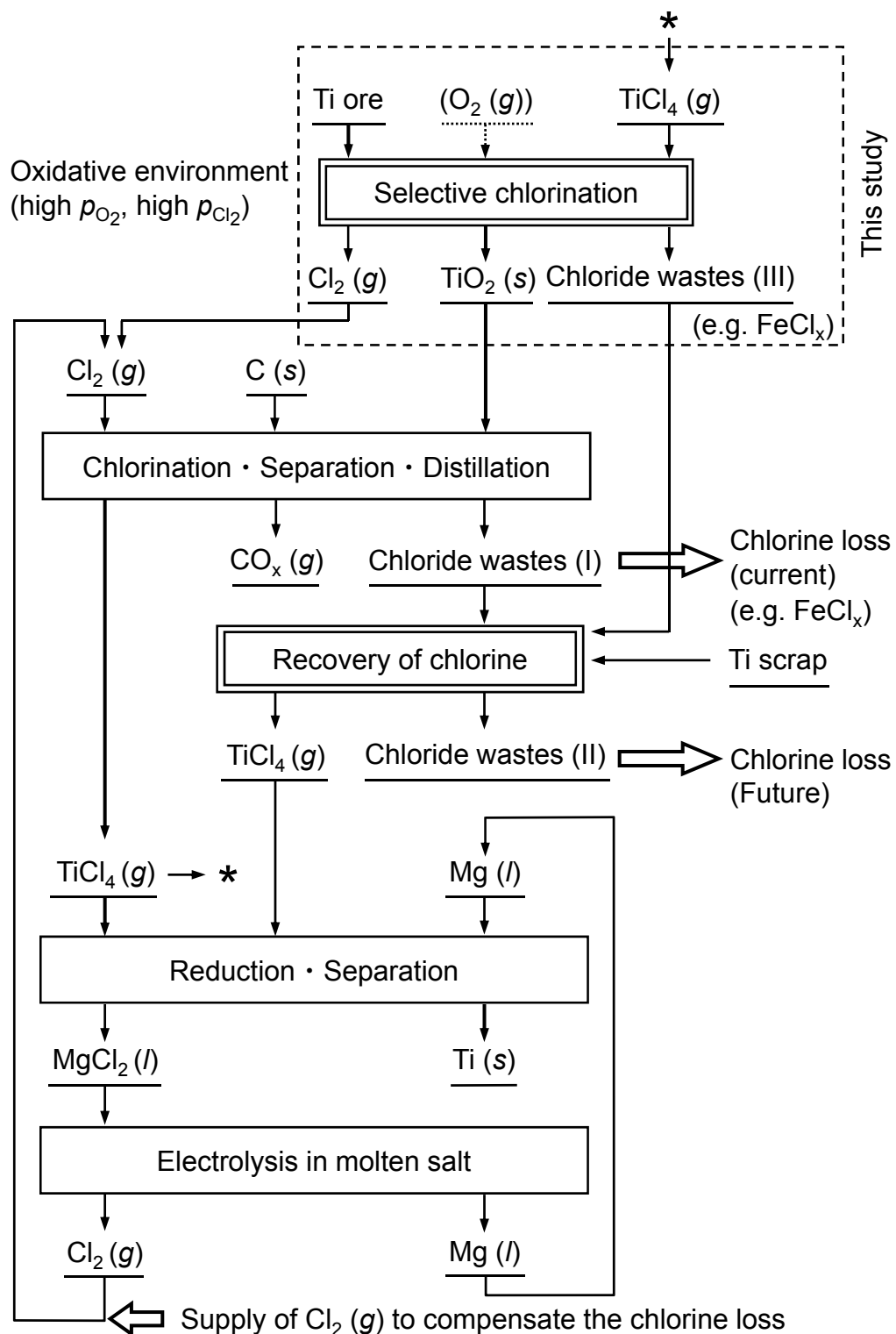
Figure 7-2 Flow chart for new titanium smelting process adopting
the selective chlorination process investigated in this study.
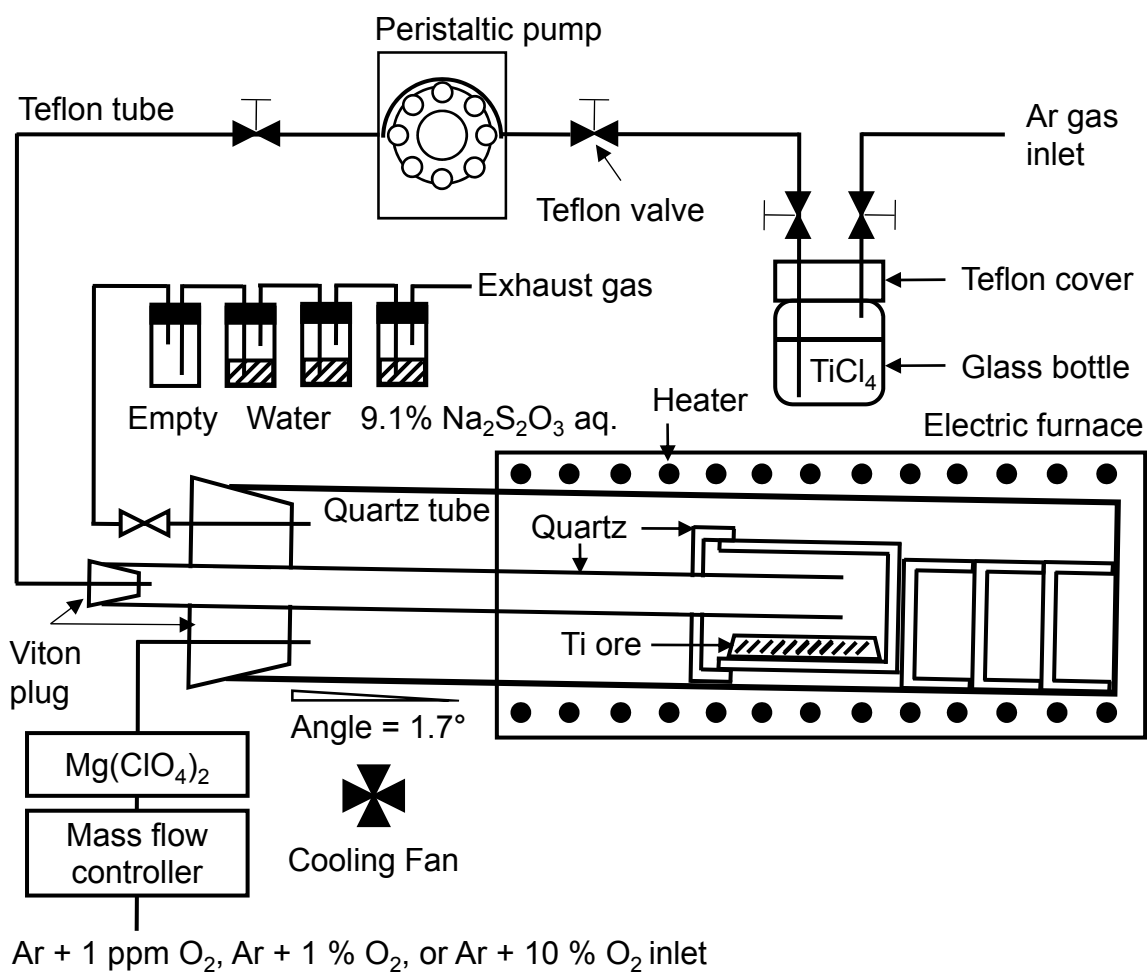
Figure 7-3 Schematic diagram of the experimental apparatus.
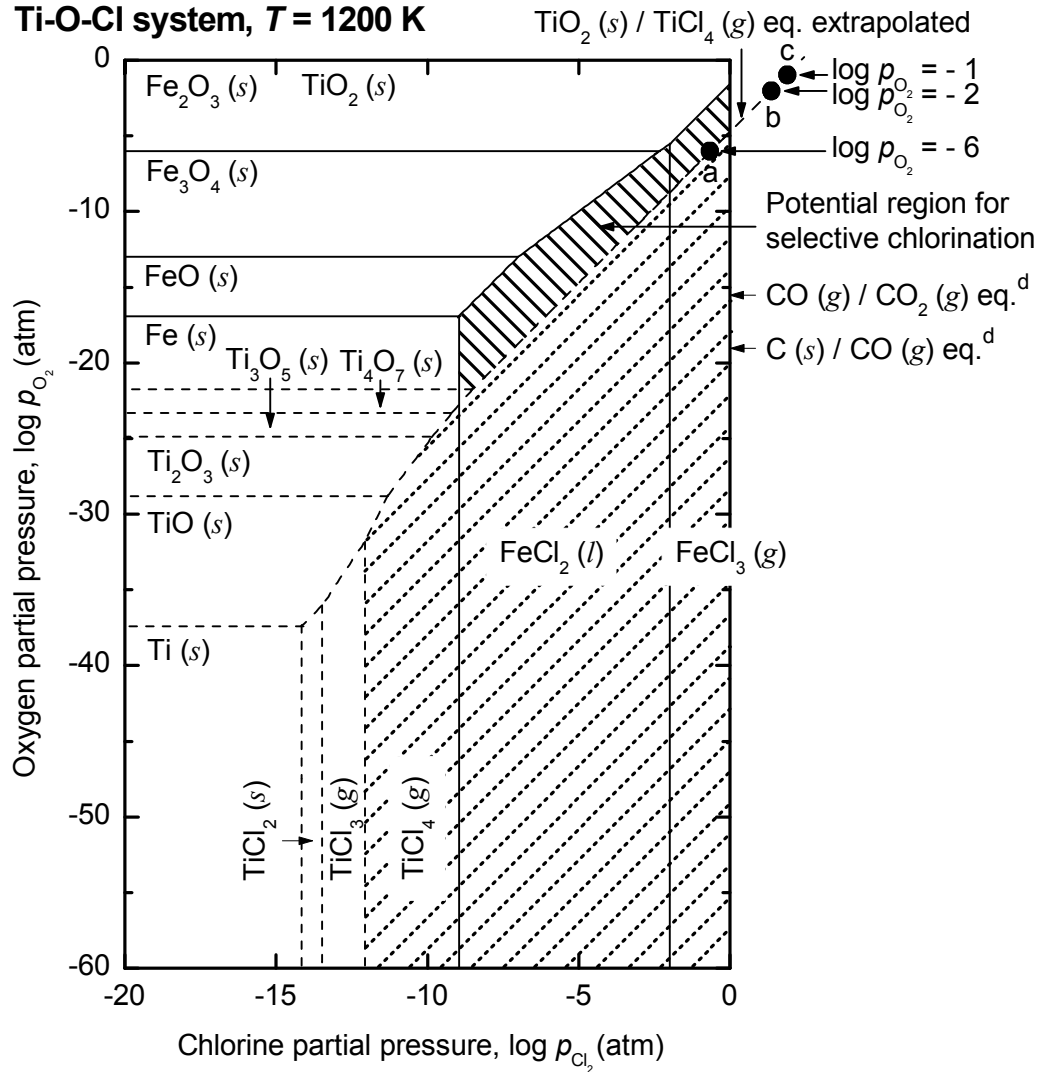
Figure 7-4 Chemical potential diagram of the Fe-O-Cl (solid line) and Ti-O-Cl (dotted line) systems overlapped at 1200 K. The hatched region with solid lines in the diagram is the TiO_2 (s) and $FeCl_x$ (l,g) stability region. The hatched region with dotted lines is the $TiCl_4$ (g) stability region.
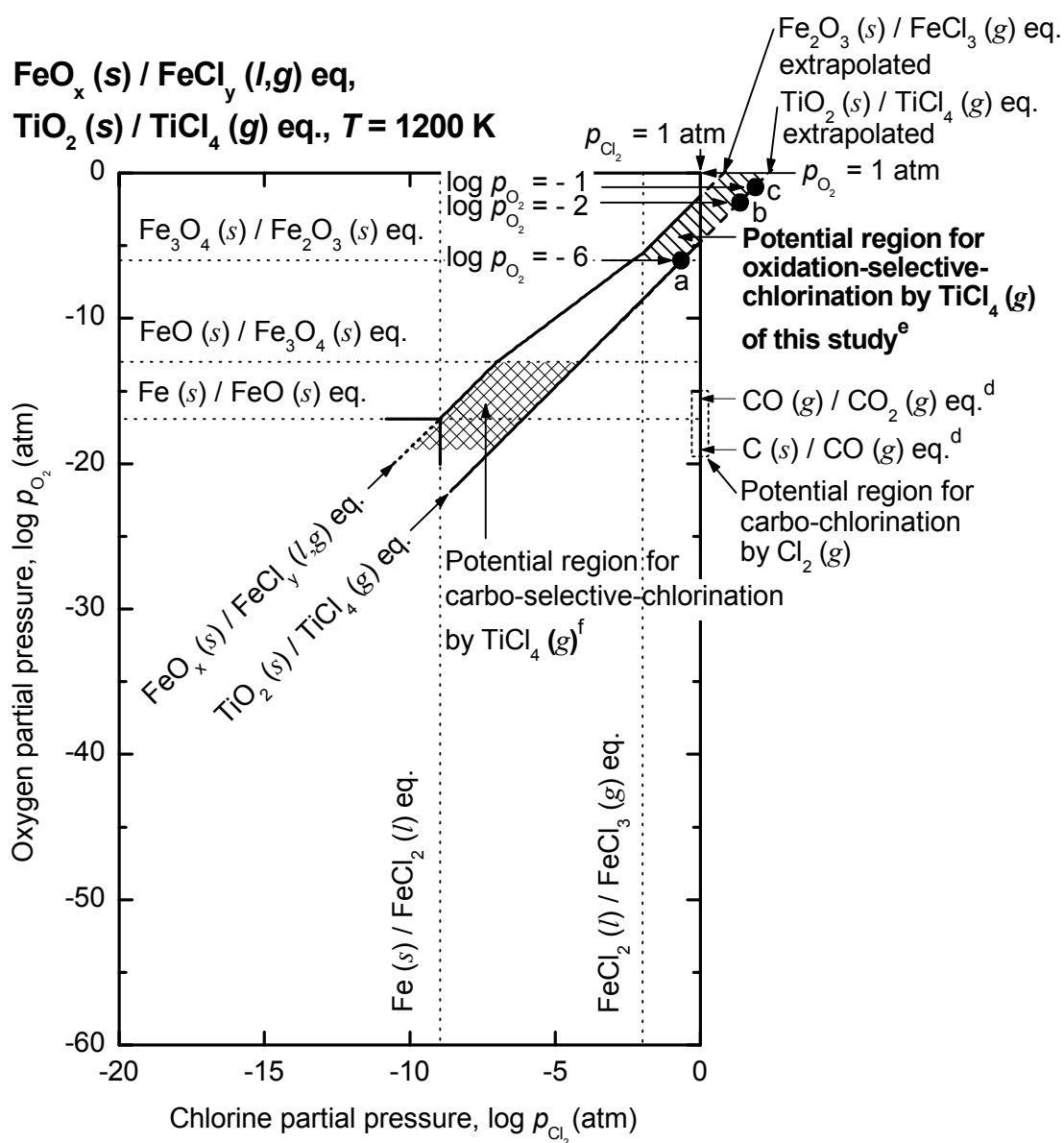
Figure 7-5 Comparison of potential regions for oxidation-selective-chlorination
in this study, carbo-chlorination, and carbo-selective-chlorination
using a modified chemical potential diagram of the Fe-O-Cl and
Ti-O-Cl systems at 1200 K.

256
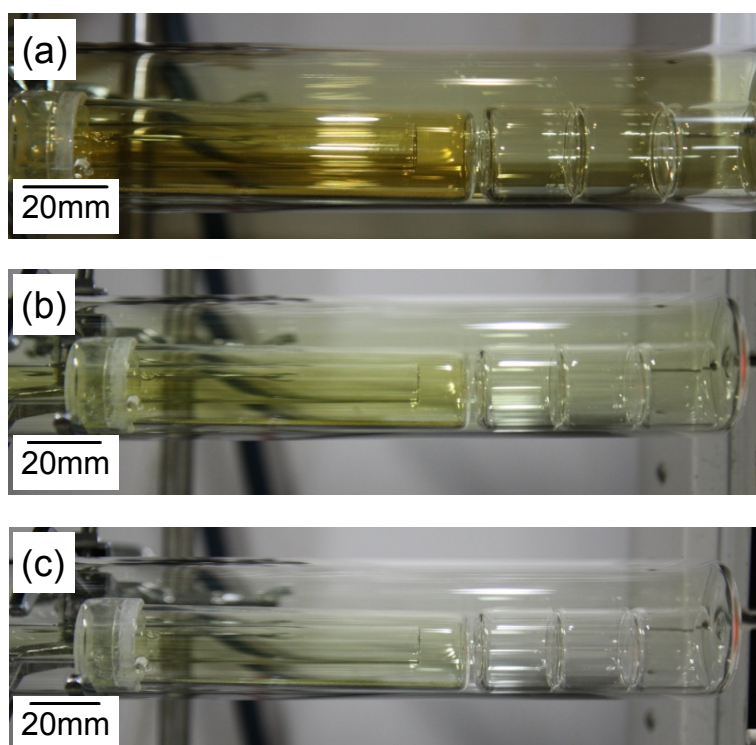
Figure 7-6 Photographs taken after the quartz tube was removed from the furnace after (a) 1 min (Exp. no. 131125), (b) 2 min, and (c) 4 min had elapsed. (*see* Table 7-1)
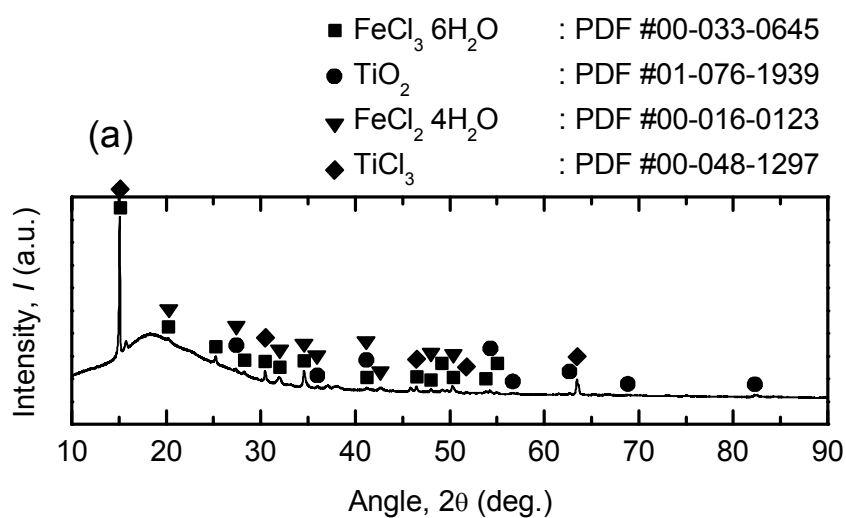
Figure 7-7 (a) XRD results for the yellow (and white) powders condensed in the low-temperature part of the quartz tube after the tube was dried, and (b) photograph of the low-temperature part of the quartz tube after the experiment when the experiments were conducted under the Ar + 1 ppm O_2 (Exp. no. 131128) atmosphere.
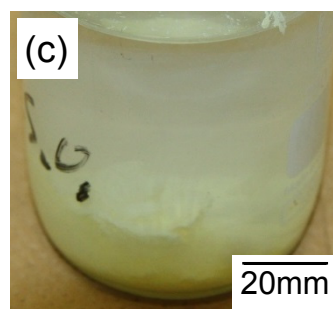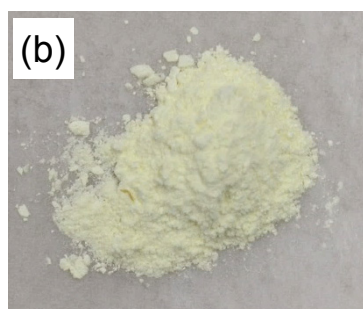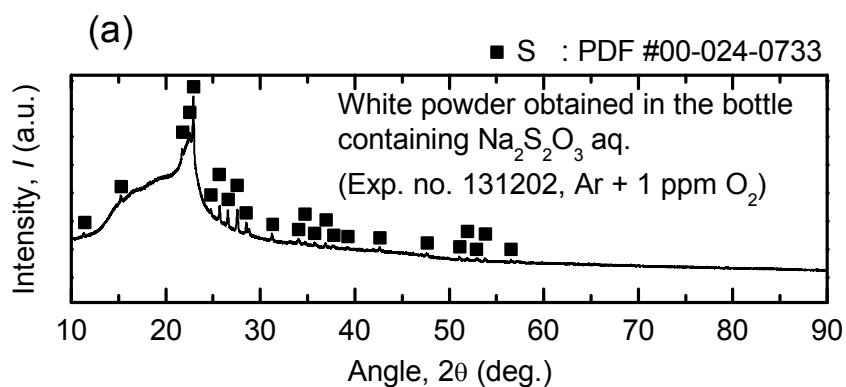
Figure 7-8 (a) XRD analysis results of the white deposits obtained in the bottle containing $Na_2S_2O_3$ aq. when the experiment was conducted under Ar + 1 ppm O_2 atmosphere (Exp. no. 131202), (b) photograph of the residues obtained after filtering and drying of $Na_2S_2O_3$ aq. after the experiment (Exp. no. 131202), and (c) photograph of $Na_2S_2O_3$ aq. taken after the experiment was conducted under Ar + 10 % O_2 atmosphere (Exp. no. 140103).
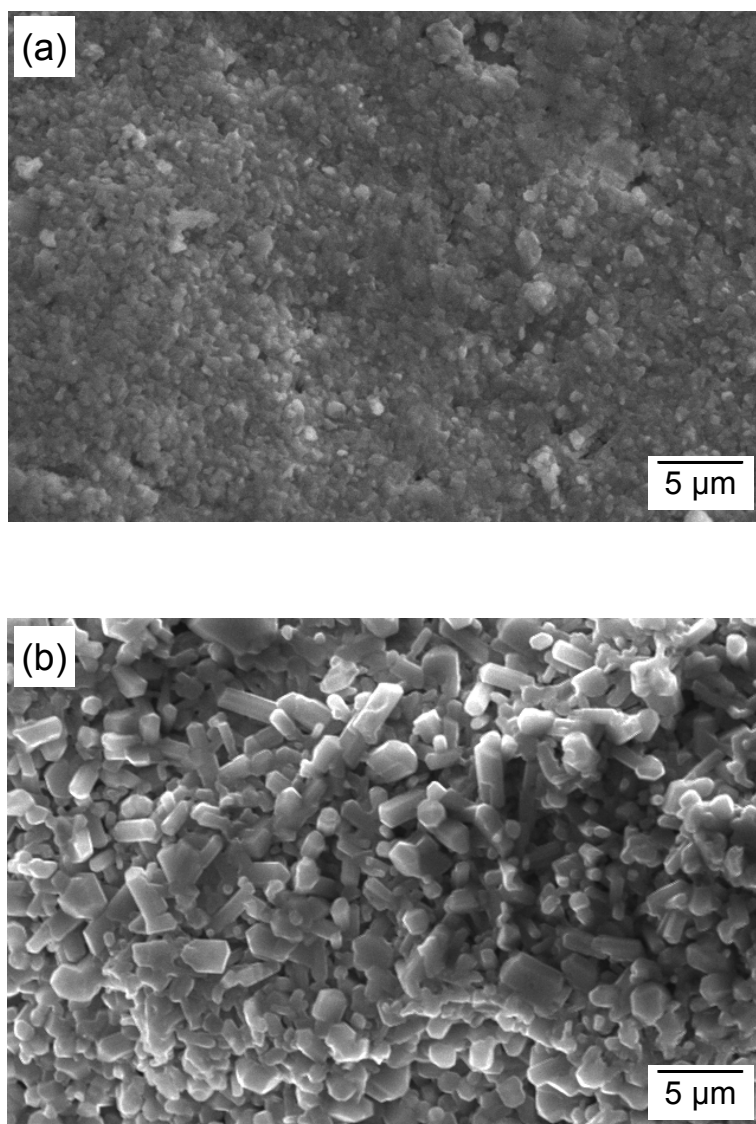
Figure 7-9 SEM images of the surface of a Vietnamese Ti ore particle obtained
(a) before the experiment (after being oxidized at 1100 K for 13 h
under dried air) and (b) after the experiment (Exp. no. 131127).
(*see* Table 7-2)
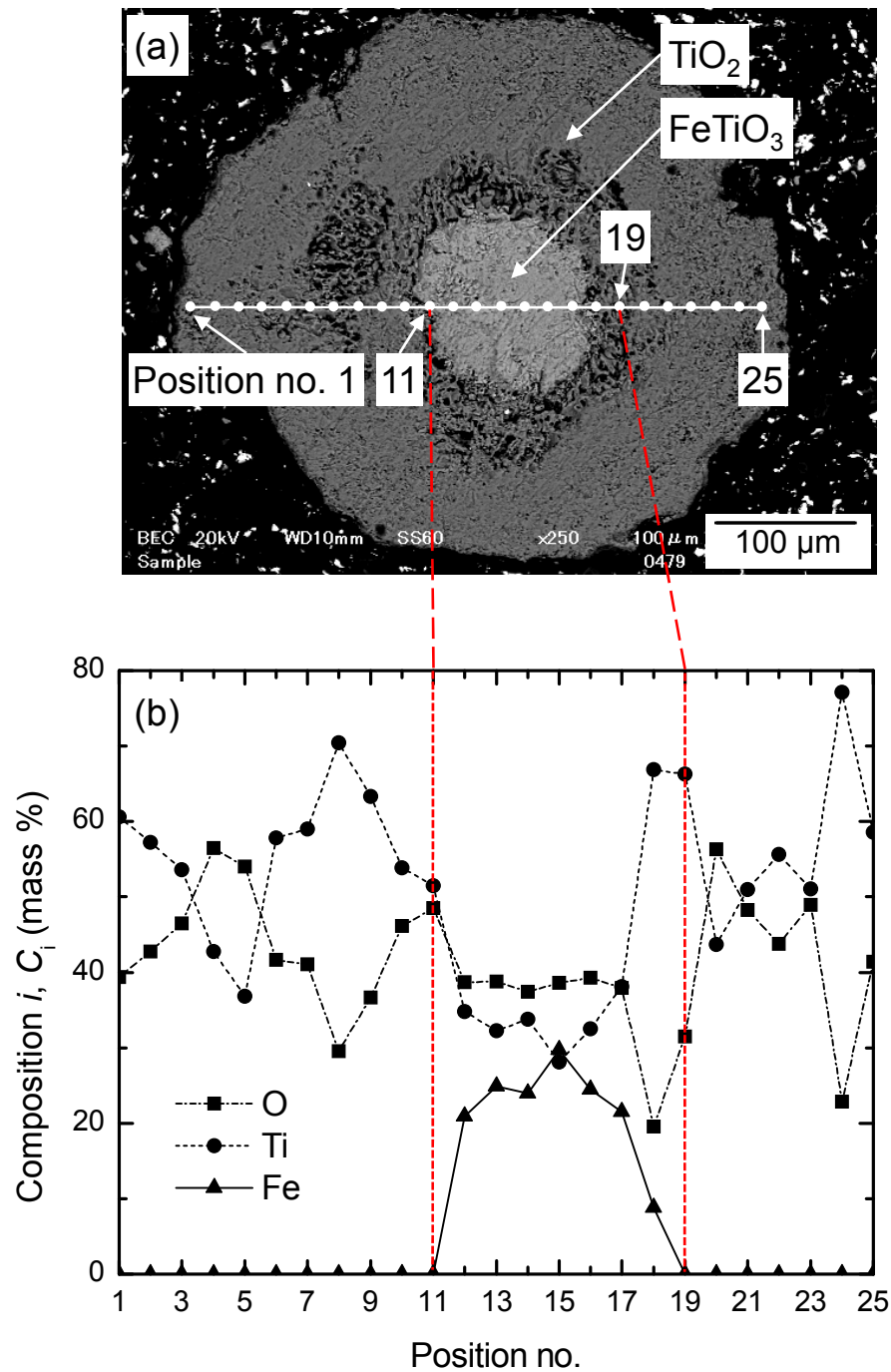
Figure 7-10 (a) SEM image of a cross section of a Ti ore particle obtained
after the experiment was conducted using Ti ore particles of
297 – 510 μm under the Ar + 1 ppm O_2 atmosphere (Exp. no. 131217)
and (b) EDS results of the Ti ore particle. (*see* Table 7-2)
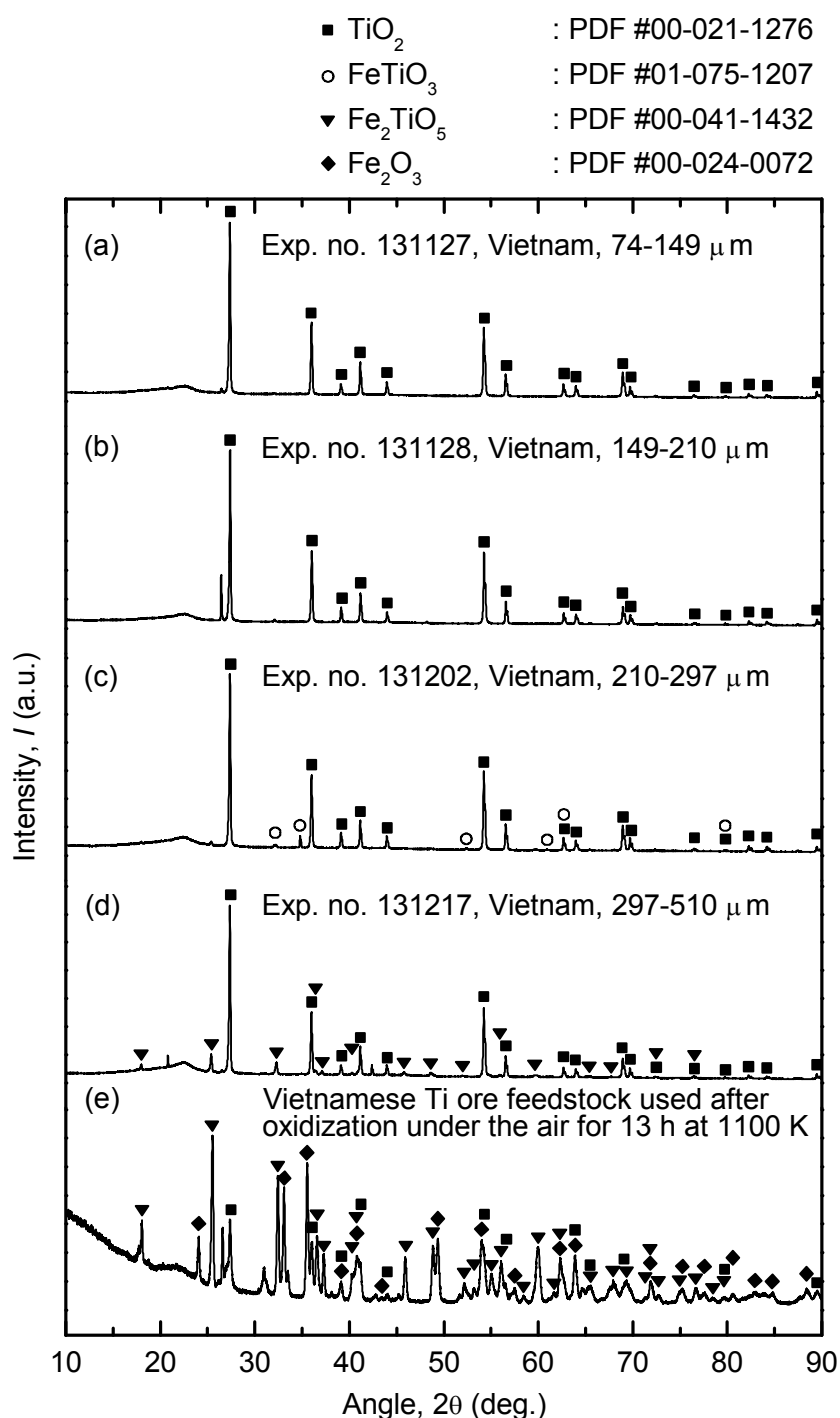
Figure 7-11 XRD results for the residues obtained when the experiment
was conducted under Ar + 1 ppm O_2 atmosphere Ti ore particles
with various sizes: (a) 74 – 149 μm, (b) 149 – 210 μm, (c) 210 – 297 μm,
and (d) 297 – 510 μm. (e) Results for the Vietnamese Ti ore feedstock
(74 – 149 μm) before the experiment. (*see* Table 7-2)

Chapter 8   Selective chlorination of titania slag using titanium tetrachloride

8.1   Introduction

Of the two major mineral resources of titanium, i.e., ilmenite and rutile ores, it is the former that is considered the more important when both production and reserves are considered. For example, global production of ilmenite in 2012 accounted for 90 % of the total titanium ore mineral production,[1] with this ilmenite ore consisting of approximately 50 % titanium oxides and 50 % iron oxides.

Currently, the Kroll process is used for the industrial-scale production of titanium metal.[2] The first step of this process is the chloride process, and almost all the oxides in the feedstock are chlorinated by chlorine gas (Cl_2) in the presence of carbon. Consequently, if a low-grade ilmenite is directly used as the feedstock, then a large amount of chloride waste is generated, and the chlorine loss is increased. The generation of a large amount of chloride waste is undesirable, as it results in operational problems such as the clogging of reactor pipes. Therefore, high-grade TiO_2 feed with a purity of above 90 % TiO_2 (or 95 % TiO_2 in Japan) produced in advance through the removal of iron from a low-grade ilmenite ore is used as the feedstock for the Kroll process.[2]

There are several major processes for the upgrading of low-grade ilmenite ores, such as the Becher[3-7] or Benilite[8-10] process, to produce the high-grade TiO_2 feed. Among these processes, the most representative titanium ore upgrading processes are the slag and UGS processes.[11-12] Fig. 8-1 shows flow chart of the slag and UGS processes.

In the slag process, titania slag with a purity of 75 – 86 % TiO_2 is produced by carbothermic reduction in an electric furnace operating at 1923 – 1973 K, and the iron in a low-grade titanium ore is removed as a Fe-C alloy (pig iron).[13-15] The removal of iron in the titanium ore as pig iron is the large advantage, because the iron is not a waste material, and it can be sold as a feed for steel manufacturing. However, the purity of the titania slag produced is not sufficient for use as a feedstock for the Kroll process. In addition, the slag process consumes a large amount of energy owing to the high reaction temperature operating in a huge electric furnace. This makes it particularly difficult to establish the slag process in Japan, where the cost of electricity is relatively high.

In order to remove residual iron in the titania slag, and produce a high-grade TiO_2 feed, the UGS process is often employed. As shown in Fig. 8-1, this entails both oxidation and reduction pretreatments prior to an acid leaching process. In the oxidation process, the titania slag is oxidized at $1273 – 1298$ K to ensure transformation of all low-valence titanium oxides to a higher oxidation state as TiO_2 (Ti^{4+}). By converting titanium into +4 valence, dissolution of titanium in the slag by following acid treatment can be hindered. Subsequently, this oxidized titania slag is reduced to convert ferric iron to ferrous iron (FeO). This iron reduction treatment increases the dissolution rate of iron during acid leaching process, in which an $18 – 20$ % HCl acid solution is used as a chlorinating agent to remove the iron and a TiO_2 feed with a purity of about 95 % is produced. However, this generates a large amount of acid waste solution containing heavy metals, because highly concentrated acid is used to remove the iron. The treatment or disposal of this acid waste solution is quite costly in countries with strict environmental regulations, such as Japan.

The price of a high-grade TiO_2 feed is one of the important factors in determining the processing cost of the Kroll process. Thus, in order to reduce the processing cost of the Kroll process in Japan, the development of an effective titanium ore or titania slag upgrading process that does not discharge a large amount of waste is required. In order to achieve this goal, an effective process for the selective chlorination of low-grade titanium ore, using $TiCl_4$ as the chlorinating agent, was developed for producing high-grade TiO_2 feed with a purity of $97 – 98$ % TiO_2 under certain conditions, as described in chapters 6 and 7. In addition, no acid waste solution is discharged by this process, and recovery of chlorine from the chloride waste is a feasible, because chloride waste in dry form is produced after the selective chlorination process using $TiCl_4$.

In this chapter, the selective chlorination of titania slag using $TiCl_4$ was investigated for the production of high-grade TiO_2 feed. There are several advantages in using titania slag as a feedstock rather than low-grade ilmenite, such as reduction in the amount of chloride waste generated due to the lower iron oxide content of the slag. Furthermore, an effective upgrading process of titania slag that does not discharge acid waste solution has the potential to replace the current UGS process when considering environmental impact and related cost in the future.

In this study, the feasibility of a new method for the upgrading of slag by selective chlorination using $TiCl_4$ was assessed. Fig. 8-2 shows a flow chart for this novel selective chlorination process, which offers the following advantages: (i) High-grade TiO_2 feed can be obtained directly from titania slag using a simple pyrometallurgical method in a single step. (ii) Large amount of acid waste solution is not dumped out, because highly concentrated acid is not used. (iii) Recovery of chlorine is possible, because the iron in a titania slag is chlorinated in a dry form. (iv) It is easily applied as a pretreatment for the Kroll process, because large amount of $TiCl_4$ is circulated in the Kroll process.

8.2   Experimental

Fig. 8-3 shows a schematic diagrams of the experimental apparatus and crucible used, and a photograph of the quartz crucibles containing the various types of feedstocks and carbon powders. The experimental conditions used in this study are listed in Table 8-1.

In order to examine the possibility of replacing the UGS process, four types of feedstocks (*cf.* Exp. no. 131028 in Table 8-1) were prepared before use by applying identical conditions to the UGS process. As shown in Table 8-1, this entailed first oxidizing a titania slag produced in China under ambient atmosphere at 1273 K for 9 hours, then reducing it at 1073 K under 10 % CO and 90 % Ar mixed atmosphere for 12 hours. The UGS (upgraded slag) feedstock used in Exp. no. 131028 (UGS_China_Xinli) was produced from the titania slag in Exp. no. 131028 (Slag_China_Xinli) as a feedstock for the UGS process in the Chinese company. In addition, various types of titania slag feedstocks used in Exp. no. 140626 were oxidized in advance under ambient atmosphere at 1273 K for 9 hours. No pretreatment was conducted on the feedstocks used in Exps. no. 140623.

Prior to the experiments, the feedstocks and a carbon powder (Kojundo Chemical Lab. Co., Ltd., purity $\geq$ 99.9 %) were positioned in separate quartz crucibles (crucible for carbon: ϕ = 26 mm, I.D.; d = 24 mm, depth). These crucibles were then placed in a quartz tube (ϕ = 44.5 mm, I.D.; l = 820 mm, length), as shown in Fig. 8-3; a single crucible for the slag samples being made by combining four of the quartz crucibles (each crucible: ϕ = 12 mm, I.D.; l = 120 mm, length) to allow reaction of multiple samples simultaneously.

The quartz tube was then sealed by a Viton rubber plug, and liquid $TiCl_4$ (Wako Pure Chemical Industries Ltd., purity $\geq$ 99.0 %) was transferred from a reagent bottle to a glass bottle filled with argon gas (Ar, purity $\geq$ 99.9995 %) in a glove bag purged with nitrogen gas (N_2, purity $\geq$ 99.999 %).

After the samples were installed in the reaction tube, it was evacuated thrice for 5 min each time. The tube was filled with Ar gas between each evacuation until the internal pressure reached 1 atm. During each experiment, the Ar gas was flowed through the quartz tube at a controlled rate using a mass flow controller (MFC, Aera Japan LTD., Model: RO-100), while the internal pressure of the tube was maintained at 1 atm. In all the procedures, the Ar gas was delivered into the quartz tube through magnesium perchlorate ($Mg(ClO_4)_2$, Kanto Chemical Co., Inc., purity $\geq$ 75%) to remove any H_2O in the Ar gas.

The quartz tube was placed into a horizontal furnace at an angle of 1.7° relative to the horizontal axis; the furnace having been first preheated to 1100 K. After heating the quartz tube for 30 min in the furnace, the feeding of liquid $TiCl_4$ (boiling temperature: 408 K) into the tube by a peristaltic pump (Cole-Parmer Instrument Co., MasterFlex L/S Digital Drive, 7523-70; PTFE Tubing Pump, 77390-00) at a flow rate of 0.156 – 0.159 g/min was commenced. The part of quartz tube extending outside the furnace was cooled by a fan to promote effective circulation of $TiCl_4$ inside the quartz tube. The $TiCl_4$ was periodically or continuously fed into the tube depending on experiment until the end of supply of amount of $TiCl_4$ prepared.

In Exp. no. 131028, evacuation of the quartz tube was performed using a diaphragm pump (As One Co., MAS-1) 10 min prior to its removal from the furnace after being allowed to react for a preset time. After cooling the quartz tube at room temperature, the tube was filled with Ar gas until an internal pressure of 1 atm was reached, and Ar gas was flowed at room temperature while the internal pressure of the tube was maintained at 1 atm. In the other experiments, the quartz tube was instantly removed from the furnace after reaction for a preset time, and then cooled at room temperature. The residues removed from the quartz tube were dissolved in deionized water and sonicated for over one hour at room temperature.

The chemical compositions of the residues obtained after each experiment were determined using X-ray fluorescence spectroscopy (XRF: JEOL, JSX-3100RII). The

crystalline phases were also identified by X-ray diffraction (XRD: RIGAKU, RINT 2500, Cu-Kα radiation), and the microstructures/compositions were analyzed by scanning electron microscopy/energy dispersive X-ray spectroscopy (SEM/EDS: JEOL, JSM-6510LV).

8.3 Thermodynamic analysis of selective chlorination using $TiCl_4$

Fig. 8-4 shows the results of XRD analysis for the four feedstocks prepared for use in Exp. no. 131028: as-received titania slag, oxidized titania slag, reduced titania slag, and UGS. As shown in Fig. 8-4, the $FeTi_2O_5$ and TiO_2 were mainly identified in titania slag. In addition, the Fe_2TiO_5 and TiO_2 were mainly identified in the oxidized titania slag, the reduced titania slag, and UGS. In particular, as shown in the results of XRD analysis of the reduced slag, even though the oxidized titania slag was reduced at 1073 K under a mixed atmosphere of 10 % CO – 90 % Ar, Fe_2TiO_5 was still identified in addition to $FeTiO_3$.

From a thermodynamic viewpoint, these iron titanium compounds can be considered as a mixture of iron oxide and titanium oxide, from thermodynamic viewpoint, because the Gibbs energy of formation for these compounds at 1100 K is positive or small negative value, as shown in Eqs. 8-1 – 8-3. Thus, a thermodynamic analysis of the selective chlorination of titania slag can be conducted by utilizing the chemical potential diagrams of the Fe-O-Cl and Ti-O-Cl systems at 1100 K.

$$Fe_2O_3\ (s) + TiO_2\ (s) = Fe_2TiO_5\ (s) \tag{8-1}$$
$$\Delta G°_r = -1.9\text{ kJ at }1100\text{ K}^{[16]}$$

$$FeO\ (s) + TiO_2\ (s) = FeTiO_3\ (s) \tag{8-2}$$
$$\Delta G°_r = -11.0\text{ kJ at }1100\text{ K}^{[17]}$$

$$FeO\ (s) + 2\ TiO_2\ (s) = FeTi_2O_5\ (s) \tag{8-3}$$
$$\Delta G°_r = 101.7\text{ kJ at }1100\text{ K}^{[18]}$$

Fig. 8-5 shows the chemical potential diagram of the Fe-O-Cl (solid line) and Ti-O-Cl (dotted line) systems overlapped at 1100 K, and plotted with the logarithms of chlorine chemical potential (p_{Cl_2}) and oxygen chemical potential (p_{O_2}) as the abscissa and ordinate, respectively. The hatched region is denoted as a potential region for selective chlorination, because if the p_{Cl_2} and p_{O_2} are located within this hatched region, then iron oxides are transformed to volatile $FeCl_x$ (x=2,3) (l,g) and titanium oxides are transformed to TiO_2. The vapor pressure of $FeCl_2$ (l) at 1100 K is 0.09 atm,[17] which is high enough to ensure that the $FeCl_2$ (l) evaporates. In addition, the stable phase of $FeCl_3$ (g) at 1100 K is gas. Moreover, the vapor pressure of TiO_2 (s) is negligible. Therefore, if both p_{Cl_2} and p_{O_2} of the reaction system are controlled so as to be located within this hatched region in Fig. 8-5, then the iron in the titania slag will be selectively removed as iron chlorides, and titania slag itself will be converted to high-grade TiO_2.

Given that an excess amount of $TiCl_4$ gas was used as the chlorinating agent, the TiO_2 (s)/$TiCl_4$ (g) eq. in Fig. 8-5 dominates the chlorination reactions of the reaction system, and this equilibrium line is on the borderline of the potential region for selective chlorination. Furthermore, the p_{O_2} of the reaction system is controlled by either the C (s)/CO (g) eq. or CO (g)/CO_2 (g) eq., because carbon powder was placed in the reactor. The combination of these two conditions means that the chemical potentials for the selective chlorination of titania slag using $TiCl_4$ in the presence of carbon are thermodynamically controlled by point d1 or d2 in Fig. 8-5.

Fig. 8-6 shows equilibrium lines of the FeO_x (s)/$FeCl_y$ (l,g) eq. and TiO_2 (s)/$TiCl_4$ (g) eq. and the potential regions for various kinds of chlorination reactions at 1100 K. In Fig. 8-6, the carbo-selective-chlorination process is shown as a cross hatched region, whereas the oxidation-selective-chlorination process is shown as a hatched region. The carbo-chlorination process, which is already well-established in the titanium smelting industry, is also shown in Fig. 8-6. With regards to the oxidation-selective-chlorination process carried out under a high p_{Cl_2}, the details of this are described in chapter 7.

If an excess amount of $TiCl_4$ and carbon powder is present in the reaction system, then the chemical potential of the reaction system is fixed at point d1 or d2 in Fig. 8-6 under equilibrium state. However, when the redox potential of solid FeO in titania slag is taken into consideration, the p_{O_2} ranges from the Fe (s)/FeO (s) eq. to FeO (s)/Fe_3O_4 (s) eq. in Fig. 8-6. Thus, when both the carbon in the system and the redox potential

of solid FeO in titania slag are considered, the p_{O_2} ranges from C (*s*)/CO (*g*) eq. to FeO (*s*)/ Fe$_3$O$_4$ (*s*) eq. in Fig. 8-6. In addition, when the chlorination of titania slag particle is taken into account, the outermost boundary of particle reacting with TiCl$_4$ is controlled by the TiO$_2$ (*s*)/TiCl$_4$ (*g*) eq., but the center of the particle unreacted by TiCl$_4$ is controlled by the FeO$_x$ (*s*)/FeCl$_y$ (*l,g*) eq. If we consider the chemical potential gradient between the two equilibriums, the chemical potential pair of p_{Cl_2} and p_{O_2} is placed at any position between the equilibrium lines of the FeO$_x$ (*s*)/FeCl$_y$ (*l,g*) eq. and the TiO$_2$ (*s*)/TiCl$_4$ (*g*) eq. Thus, under these two conditions, the cross-hatched region shown in Fig. 8-6 becomes the potential region for selective chlorination, wherein the iron in the titania slag is selectively removed as FeCl$_2$ by Eq. (8-4)

FeO (*s*, in the ore) + 1/2 TiCl$_4$ (*g*) = FeCl$_2$ (*l*) + 1/2 TiO$_2$ (*s*)   (8-4)

$\Delta G^\circ_r = -$ 69.1 kJ at 1100 K[17]
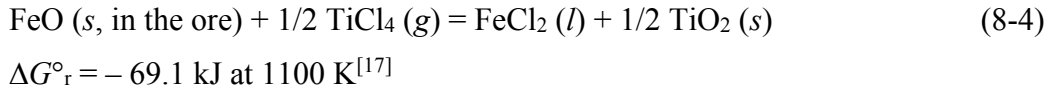
As shown in Fig. 8-4, the existence of Fe$_2$TiO$_5$ in the reduced titania slag implies that although the reduction process was performed at 1073 K under a 10 % CO – 90 % Ar mixed atmosphere, equilibrium of the reaction system controlled by the CO (*g*)/ CO$_2$ (*g*) eq. is not easily achieved, because not all of the Fe$_2$O$_3$ was reduced. From these results, it can be inferred that the p_{O_2} controlled by the redox potential of solid Fe$_2$O$_3$ in titania slag also needs to be considered, despite the fact that the selective chlorination was conducted in the presence of carbon. When the redox potential of solid Fe$_2$O$_3$ in titania slag is considered, the p_{O_2} of the reaction system ranges from Fe$_3$O$_4$ (*s*)/Fe$_2$O$_3$ (*s*) eq. to high p_{O_2} (10^{-3} – 1 atm) in Fig. 8-6. In addition, when the selective chlorination of the slag particle is taken into consideration, the TiO$_2$ (*s*)/TiCl$_4$ (*g*) eq. controls the outermost boundary of those particles reacting with TiCl$_4$, whereas the FeO$_x$ (*s*)/FeCl$_y$ (*l,g*) eq. controls the unreacted particle center. When the chemical potential gradient between the two equilibriums is considered, the chemical potentials of p_{Cl_2} and p_{O_2} exist at any position between the equilibrium lines of the FeO$_x$ (*s*)/FeCl$_y$ (*l,g*) eq. and TiO$_2$ (*s*)/ TiCl$_4$ (*g*) eq. Consequently, under these two conditions, the hatched region shown in Fig. 8-6 becomes the potential region for the selective chlorination of the slag under certain conditions, and the iron in the titania slag is selectively removed as FeCl$_3$ by the reaction shown in Eq. (8-5)

$$2/3 \; Fe_2O_3 \; (s) + TiCl_4 \; (g) = 4/3 \; FeCl_3 \; (g) + TiO_2 \; (s) \qquad\qquad (8\text{-}5)$$

$\Delta G^{\circ}_r = -\; 65.5 \; kJ \; at \; 1100 \; K^{[17]}$
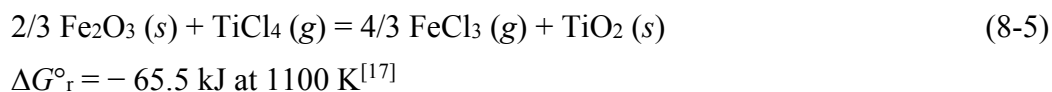
8.4 Results and discussion

8.4.1 Verification of selective chlorination using TiCl₄

Fig. 8-7 (c) shows that brown and yellow deposits were condensed inside the low-temperature part of the quartz tube during the selective chlorination of titania slags using TiCl₄ in the presence of carbon (Exp. no. 131028). The color of the brown deposits were changed to yellow when the inside of the quartz tube was dried by flowing Ar gas at room temperature after the experiment. The vapor pressure of TiCl₄ (*l*) at 300 K is 0.02 atm,[17] which is sufficient for evaporation. Therefore, the solid deposits obtained were not pure TiCl₄, but contained a certain amount of TiCl₄. Fig. 8-7 (d) shows the result of XRD analysis of the yellow deposits obtained after the quartz tube was dried, which shows that the iron in the titania slags was removed as $FeCl_2$ or $FeCl_2 \cdot 2(H_2O)$. It is expected that the H_2O was adhered to the $FeCl_2$ when the Viton plug was removed from the quartz tube to collect residues.

The thermodynamic analysis of the selective chlorination of titania slags using TiCl₄ in the presence of carbon revealed the possibility for the selective removal of Fe_2O_3 in titania slag feedstock as $FeCl_3$ in addition to the selective removal of FeO as $FeCl_2$. However, Fig. 8-7 (d) shows that $FeCl_3$ was not identified when the deposits were analyzed. It is supposed that $FeCl_3$ was not identified by XRD analysis, because amount of $FeCl_3$ in the deposits was relatively small owing to the generation of a large amount of $FeCl_2$ or because most of the Fe_2O_3 in the titania slag feedstock was reduced to FeO during the experiment. However, the precise reason for this is not clear at this stage.

Fig. 8-8 shows SEM images of the surface of an untreated titania slag particle prior to oxidation/reduction reaction, and a slag particle obtained after experiment. It is clear from this that small pores were generated on the surface of titania slag particles through selective chlorination using TiCl₄ in the presence of carbon at 1100 K. On the basis of Figs. 8-7 and 8-8, it is concluded that iron in the titania slags was selectively

chlorinated by TiCl$_4$ as FeCl$_2$ (*l,g*) when the selective chlorination proceeded under reducing atmosphere, and pores were generated.

8.4.2   Influence of slag pretreatment

Table 8-2 lists the analytical results for feedstock used in this study, and for residues obtained after experiments. In addition, Fig. 8-9 shows the results of XRD analysis of the residues obtained when the experiment was conducted at 1100 K in the presence of carbon using titania slag, oxidized titania slag, reduced titania slag, and UGS as feedstocks (Exp. no. 131028). These results show that when the oxidized titania slag and reduced titania slag were reacted with TiCl$_4$, the concentration of iron decreased from 13.9 % to 0.12 % and 0.11 %, and thus 95.1 % and 94.8 % of TiO$_2$ feed were obtained directly from the slag, respectively. In addition, when the UGS was reacted with TiCl$_4$, the iron in the feedstock was further removed, and 96.1 % of TiO$_2$ feed was produced. However, although the concentration of iron in the slag decreased from 13.9 % to 0.79 % when the untreated titania slag was reacted with TiCl$_4$, a mixture of TiO$_2$, Ti$_9$O$_{17}$, and Ti$_3$O$_5$ was obtained as shown in Fig. 8-2. Low-valence titanium oxides were also identified in residues obtained when the selective chlorination using various types of slags with no pretreatment as a feedstock was conducted (Exp. no. 140623).

One of the reasons for the production of Ti$_3$O$_5$ seen in Fig. 8-9 (a) is expected that the Ti$_3$O$_5$ in the slag feedstock shown in Fig. 8-4 (a) was identified from the residues. Since Ti$_9$O$_{17}$ was not identified in the titania slag feedstock, as shown in Fig. 8-4 (a), it is supposed that this Ti$_9$O$_{17}$ was produced from TiO$_2$ and not from TiO$_x$ (0 < x < 2) in the feedstock during the experiment, because the p_{O_2} of the reaction system was not high owing to the existence of carbon powder. However, the detailed reason for the production of low-valence titanium oxides is still being investigated.

In order to produce high-grade TiO$_2$ feed that does not contain low-valence titnium oxides, various types of the slags oxidized in advance were used as a feedstock for the selective chlorination process in the presence of carbon (Exp. no. 140626). Fig 8-10 shows the results of XRD analysis of the residues obtained when the various types of slags were used as a feedstock. Fig. 8-10 shows that TiO$_2$ was obtained after the experiment. In addition, as shown in Table 8-2, the concentration of titanium in the slags

increased from 78.1 – 90.2 % to 94.0 – 96.7 %, and the concentration of iron in the slags decreased from 4.29 – 13.9 % to 0.03 – 0.35 %. Therefore, it claims that the production of low-valence titanium oxides can be prevented and high-grade TiO_2 feed can be obtained by oxidizing the feedstock before conducting the selective chlorination.

8.5 Summary

A fundamental study on the selective chlorination of titania slag using $TiCl_4$ as a chlorinating agent was conducted in order to produce high-grade TiO_2 directly from the slag. It was found that the iron in titania slag, oxidized titania slag, reduced titania slag, and UGS was selectively removed as $FeCl_2$ at 1100 K under a reducing atmosphere. XRF and XRD analysis revealed that a 95 − 96 % TiO_2 feed could be obtained by the selective removal of iron from the titania slags. However, a mixture of TiO_2 and low-valence titanium oxides was obtained when a Chinese slag with no pretreatment were used as a feedstock. On the other hand, when the oxidized Chinese slags in advance was used as a feedstock for the selective chlorination process, high-grade TiO_2 feed was obtained in a single step. Thus, it was demonstrated that production of a high-grade TiO_2 feed directly from a titania slag is feasible when the selective chlorination of the slag using $TiCl_4$ was conducted at 1100 K under a reducing atmosphere in a single step.

References

[1] G.M. Bedinger: "*Mineral Commodity Summaries: Titanium Mineral Concentrates*", U.S. Geological Survey, Washington DC, February, 2014, pp. 172-173.

[2] T.H. Okabe and J. Kang: "*The Latest Technological Trend of Rare Metals*", CMC Publishing Co. LTD., Tokyo, 2012, Chap. 6-1, pp. 83-94. (in Japanese)

[3] K.S. Geetha and G.D. Surender: "*Experimental and modelling studies on the aeration leaching process for metallic iron removal in the manufacture of synthetic rutile*", Hydrometallurgy, 2000, vol. 56 (1), pp. 41-62.

[4] R.G. Becher, R.G. Canning, B.A. Goodheart, and S. Uusna: "*A new process for upgrading ilmenitic mineral sands*", Proceeding of the Australasian Institute of Mining and Metallurgy, 1965, vol. 21, pp. 21-44.

[5] S. Jayasekera, Y. Marinovich, J. Avraamides, and S.I. Bailey: "*Pressure leaching of reduced ilmenite: electrochemical aspects*", Hydrometallurgy, 1995, vol. 39 (1), pp. 183-199.

[6] W. Hoecker: "*Process for the production of synthetic rutile*", United States Patent 5601630, 1997.

[7] J.B. Farrow, I.M. Ritchie, P. Mangano: "*The reaction between reduced ilmenite and oxygen in ammonium chloride solutions*", Hydrometallurgy, 1987, vol. 18 (1), pp. 21-38.

[8] J.H. Chen: "*Beneficiation of Titaniferous Ores*", United States Patent 3825419, 1974.

[9] J.H. Chen and L.W. Huntoon: "*Beneficiation of ilmenite ore*", United States Patent 4019898, 1977.

[10] J.H. Chen: "*Pre-leaching or reduction treatment in the beneficiation of titaniferous iron ores*", United States Patent 3967954, 1976.

[11] M. Gueguin and F. Cardarelli: "*Chemistry and mineralogy of titania-rich slags. Part 1-hemo-ilmenite, sulphate, and upgraded titania slags*", Miner. Process. Extr. Metall. Rev., 2007, vol. 28, pp. 1–58.

[12] K. Borowiec, A.E. Grau, M. Gueguin, and J-F. Turgeon: "*Method to upgrade titania slag and resulting product*", United States Patent 5830420, 1998.

[13] J.E. Kogel, N.C. Trivedi, J.M. Barker, and S.T. Krukowski: "*Industrial minerals & rocks: commodities, markets, and uses*", 7th ed., Society for Mining, Metallurgy, and Exploration, Inc. (SME), Littleton, Colorado, United States of America, 2006.

[14]   D. Filippou and G. Hudon: "*Iron removal and recovery in the titanium dioxide feedstock and pigment industries*", JOM, 2009, vol. 61 (10), pp.36–42.

[15]   G.E. Williams and J.D. Steenkamp: "*Heavy Mineral Processing at Richards Bay Minerals*", Southern African Pyrometallurgy 2006, The South African Institute of Mining and Metallurgy, 2006, pp. 181-188.

[16]   A. Roine: "*HSC Chemistry*® 6.1 *Outokumpu HSC Chemistry for Windows*", version 6.1, Outokumpu Research Oy Information Center, Finland, 2006.

[17]   I. Barin: "*Thermochemical Data of Pure Substances*", 3rd ed., VCH Verlagsgesellschaft mbH, Weinheim, Germany, 1995.

[18]   A. Roine et al.: "*HSC Chemistry*® *version 7.11*", Outotec Oy Information Center, Finland, 2011.

Table 8-1 Experimental conditions used in this study for experiments.

Exp. no.[a]	Source country for Ti slag	Pretreatment				Weight of Ti slag, w_{slag} / g	Particle size of Ti slag, d_{slag} / μm	TiCl₄ feed	
		Reaction	Temp., T / K	Atmosphere	Time, t_p' / h			Feeding rate, f_{TiCl_4} / g·min⁻¹	Feeding time, t_{TiCl_4}' / ks
131028[b]	Slag_China_Xinli	–	–	–	–	2.0	–	0.159	9.42
	Slag_China_Xinli_Oxidized	Oxidation[d]	1273	Air	9	2.0			
	Slag_China_Xinli_Reduced	Reduction[e]	1073	10 % CO – 90 % Ar	12	2.0			
	UGS_China_Xinli	–	–	–	–	2.0			
140623[c]	Slag_China_Xinli	–	–	–	–	1.0	74 – 149	0.156	9.60
	Slag_China_Biotan	–	–	–	–	1.0			
	Slag_China_Hualong	–	–	–	–	1.0			
	Slag_China_Chengde	–	–	–	–	1.0			
140626[c]	Slag_China_Xinli_Oxidized	Oxidation[d]	1273	Air	9	1.0	74 – 149	0.156	9.60
	Slag_China_Biotan_Oxidized	Oxidation[d]	1273	Air	9	1.0			
	Slag_China_Hualong_Oxidized	Oxidation[d]	1273	Air	9	1.0			
	Slag_China_Chengde_Oxidized	Oxidation[d]	1273	Air	9	1.0			

a: Experimental conditions;
Reaction temperature, T = 1100 K.
Ar flow rate for entire reaction time with fan, f_{Ar} = 500 sccm.
Reaction time, t_r' = 5h.
Atmosphere: Ar gas in the presence of carbon, Weight of carbon, w_c = 2.00 g. (1.00 g of carbon was placed in each crucible)
b: Time for vacuum before taking out the quartz tube from furnace = 10 min., and
when vacuum was performed, exhaust gas were captured in the glass bottle cooled by liquid nitrogen.
Sieving was not performed to determine the particle size of Ti slag.
Amount of TiCl₄ used, w_{TiCl_4} = 25 g. TiCl₄ feeding pattern : feeding for 30 min and break of feeding for 10 min. Feeding time excludes periodic breaks.
c: Amount of TiCl₄ used, w_{TiCl_4} = 25 g. TiCl₄ feeding pattern : continuous feeding.
d : Ti slag was oxidized at 1273 K under ambient atmosphere for 9 h.
e : Oxidized Ti slag under d condition was reduced at 1073 K under 10 % CO + 90 % Ar mixed atmosphere for 12 h. Mixed gas flow rate, f_{CO_Ar} = 210 sccm.

275

Table 8-2 Analytical results for initial feedstock used and for residues obtained after experiments.

Exp. no.	Crucible no.	Source country for Ti slag	Pretreatment	Concentration of element i, C_i (mass%)[a]						Notes
				Ti	Fe	Mn	Si	Al		
Feedstock (Initial)		Slag_China_Xinli		78.1	13.9	1.47	2.86	0.60		Figs. 8-4 (a) and 8-8 (a)
		UGS_China_Xinli		93.8	2.50	0.23	1.87	N.D		Fig. 8-4 (d)
		Slag_China_Biotan		85.3	7.53	3.49	1.49	0.62		
		Slag_China_Hualong		85.0	7.01	1.82	2.43	0.86		
		Slag_China_Chengde		90.2	4.29	1.37	1.00	0.66		
131028	1	Slag_China_Xinli	–	94.0	0.79	0.22	2.65	N.D		Figs. 8-7, 8-8 (b), and 8-9 (a)
	2	Slag_China_Xinli_Oxidized	Oxidation	95.7	0.12	0.09	3.04	N.D		Figs. 8-7 and 8-9 (b)
	3	Slag_China_Xinli_Reduced	Reduction	95.3	0.11	0.07	2.62	N.D		Figs. 8-7 and 8-9 (c)
	4	UGS_China_Xinli	–	96.7	0.18	0.05	2.23	N.D		Figs. 8-7 and 8-9 (d)
140623	1	Slag_China_Xinli	–	95.7	0.36	0.22	2.03	0.03		
	2	Slag_China_Biotan	–	97.5	0.10	0.30	1.48	N.D		
	3	Slag_China_Hualong	–	94.2	0.35	0.36	2.80	0.28		
	4	Slag_China_Chengde	–	97.8	0.06	0.15	1.11	N.D		
140626	1	Slag_China_Xinli_Oxidized	Oxidation	96.0	0.21	0.11	2.45	N.D		Fig. 8-10 (a)
	2	Slag_China_Biotan_Oxidized	Oxidation	94.0	0.35	0.38	3.33	N.D		Fig. 8-10 (b)
	3	Slag_China_Hualong_Oxidized	Oxidation	95.7	0.03	0.51	2.32	N.D		Fig. 8-10 (c)
	4	Slag_China_Chengde_Oxidized	Oxidation	96.7	0.31	0.30	1.37	N.D		Fig. 8-10 (d)

a : Determined by XRF analysis (excluding oxygen and other gaseous element),
N.D : Not Detected. Below the detection limit of the XRF (<0.01 mass%),
Values are determined by average of analytical results of five samples.

276

Air Ilmenite

Roast T = 1173 – 1273 K

Slag process

Roasted ilmenite Coal

Reduction T = 1923 – 1973 K

Iron & Steelmaking ← Fe-C 75 – 86% TiO_2[a] Air

a: Sizing is conducted.
   mean particle diameter
   in the range of 250 – 350 μm

Oxidation T = 1273 – 1298 K

$CO + H_2$ gas TiO_2 (Ti^{4+})

Reduction T = 1073 – 1123 K

18 – 20% HCl HCl TiO_2 (Fe^{2+})

Acid leaching T = 418 – 428 K

UGS process

Air Spent acid aq. TiO_2

Pyrohydrolysis Washing & Drying

FeO_x HCl Water TiO_2

HCl recovery Calcination T = 873 – 1073 K

HCl TiO_2
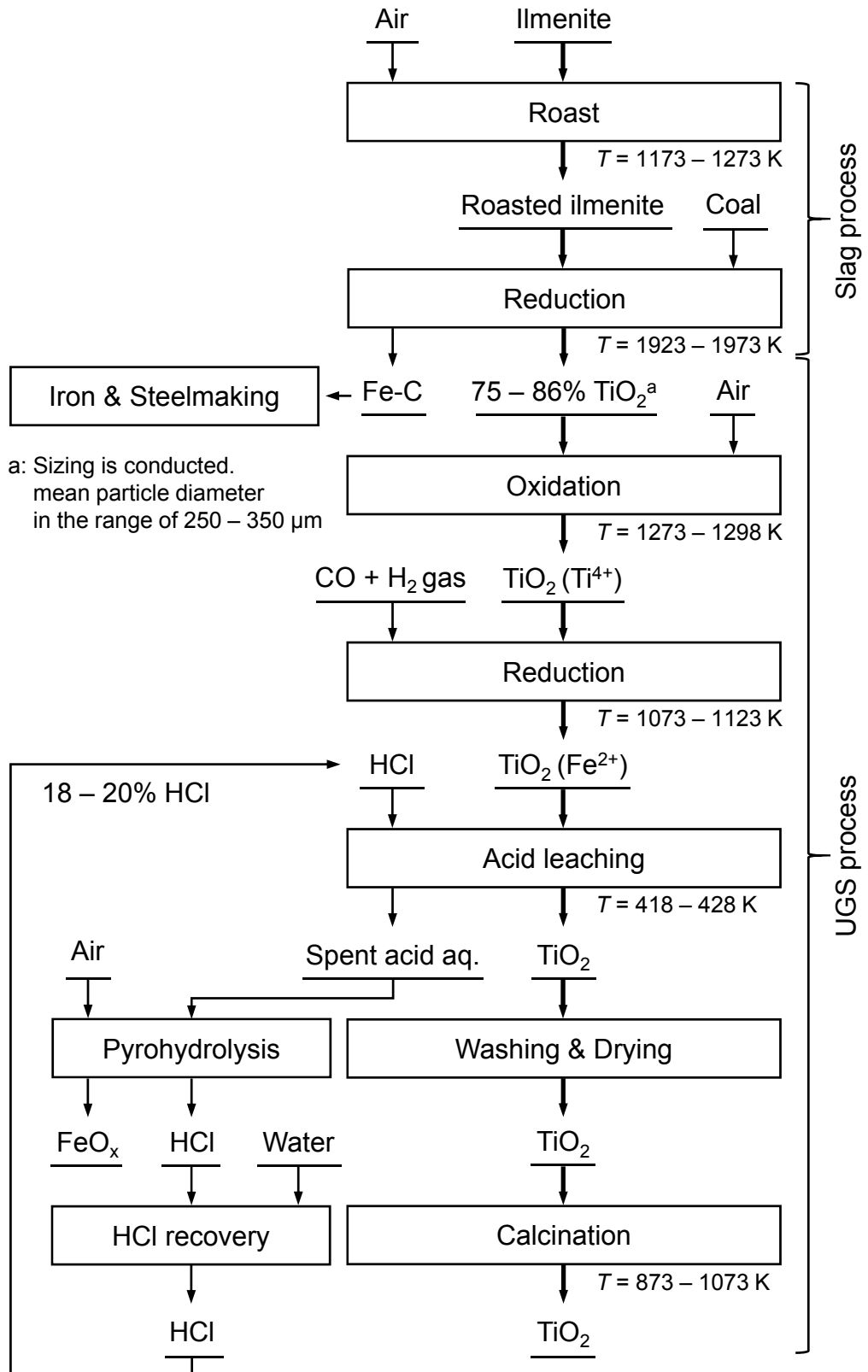
Figure 8-1 Flow chart of the slag and UGS processes.[11-13]

277
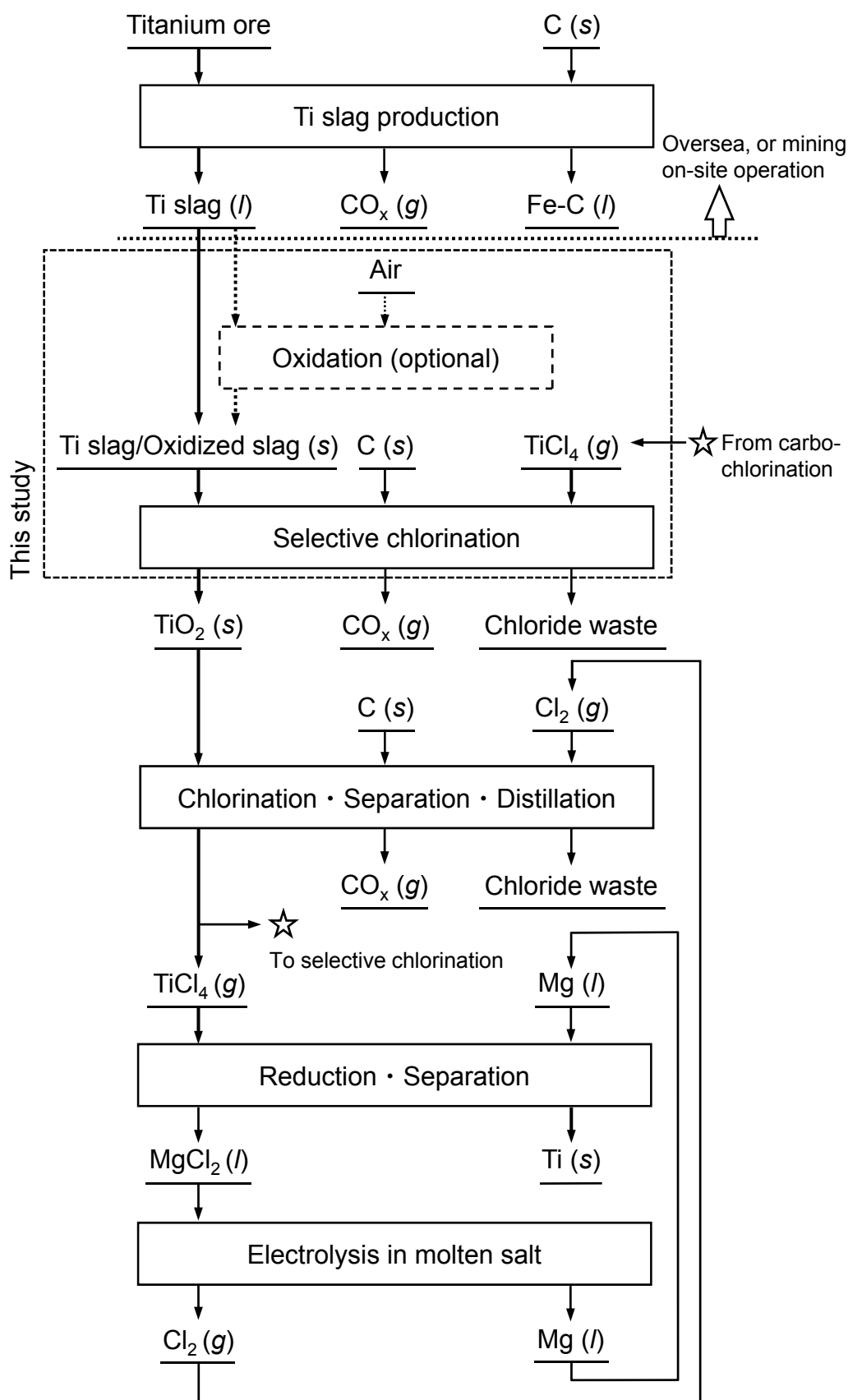
Figure 8-2 Flow chart for new selective chlorination process investigated in this study for upgrading Ti slag.

(a)

Peristaltic pump

Teflon tube

Vacuum

Liquid N_2

Exhaust gas

Empty Water

Quartz tube

Heater

Ar gas inlet

Teflon valve

Teflon cover

Glass bottle

$TiCl_4$

Electric furnace

Quartz

Ti slag or ore

carbon carbon

Viton plug

Angle = 1.7°

$Mg(ClO_4)_2$

Mass flow controller

Cooling Fan

Ar gas inlet

(b)

Ti slag

Oxidized Ti slag

Reduced Ti slag

UGS (Upgraded slag)

10mm
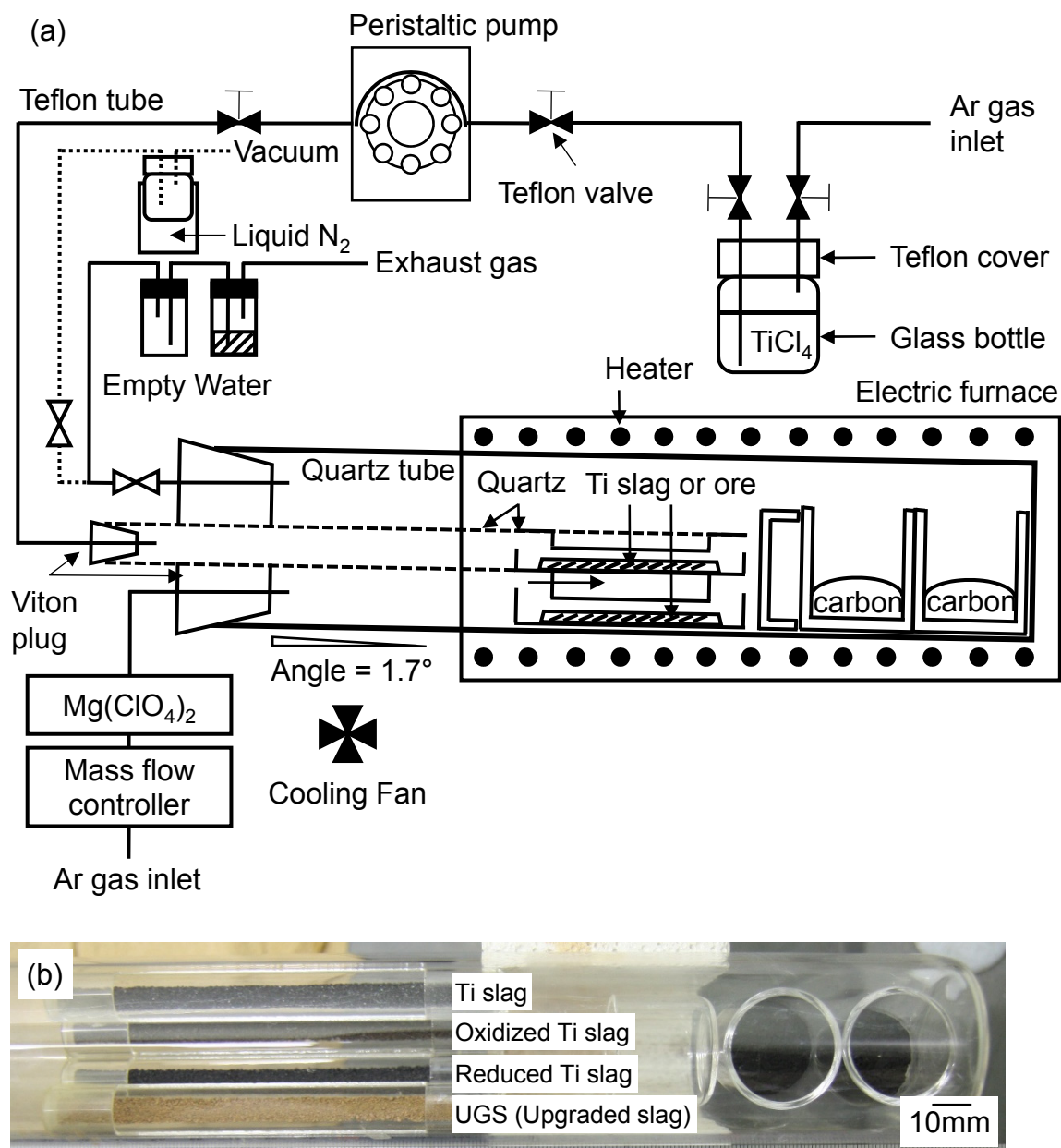
Figure 8-3 (a) Schematic diagram of the experimental apparatus used and
(b) a photograph taken after the quartz crucibles were placed
in the quartz tube before the experiment (Exp. no. 131028).

(c)

O.D ϕ 14 mm
I.D ϕ 12 mm

open

blockage

Weld

open

blockage

(d)

O.D ϕ 14 mm
I.D ϕ 12 mm

open

blockage

20 mm

7 mm

20 mm

14 mm

Weld

120 mm
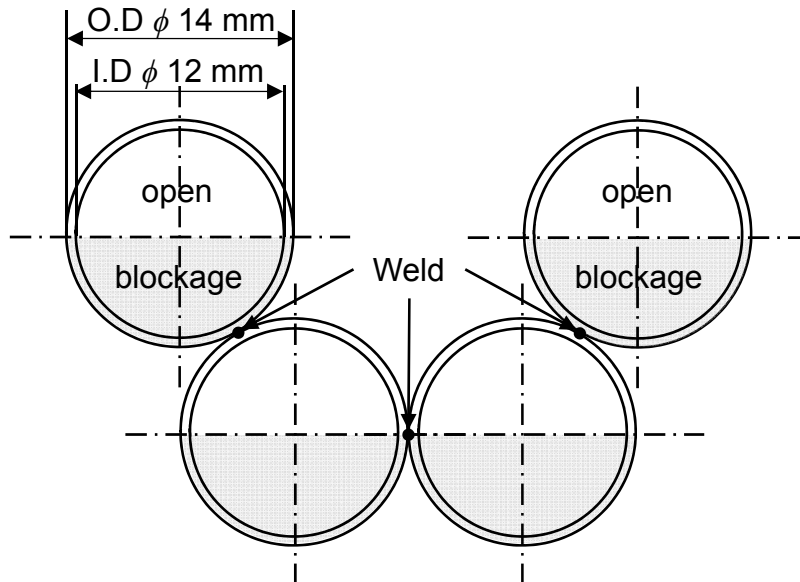
Weld
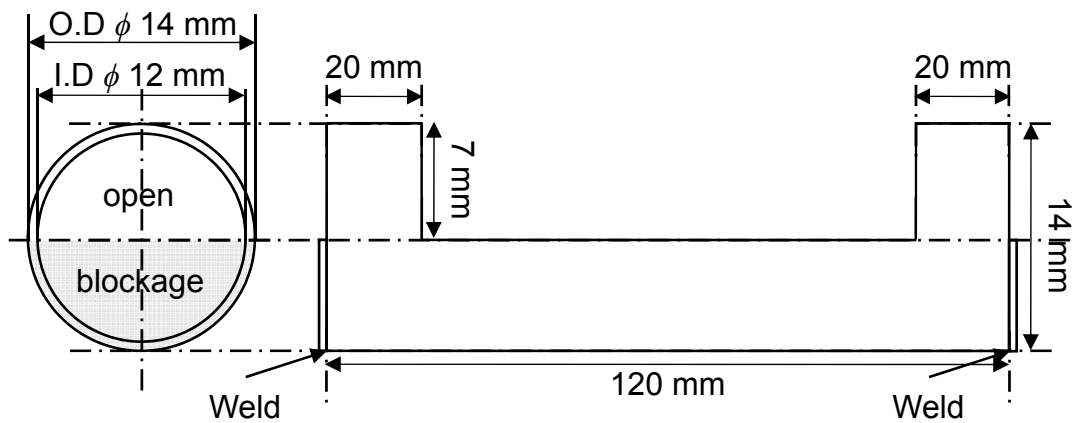
Figure 8-3 (c) Schematic diagram of the crucible for the slag samples
being made by combining four of the quartz crucibles, and
(d) schematic diagram of the one of the four quartz crucibles.
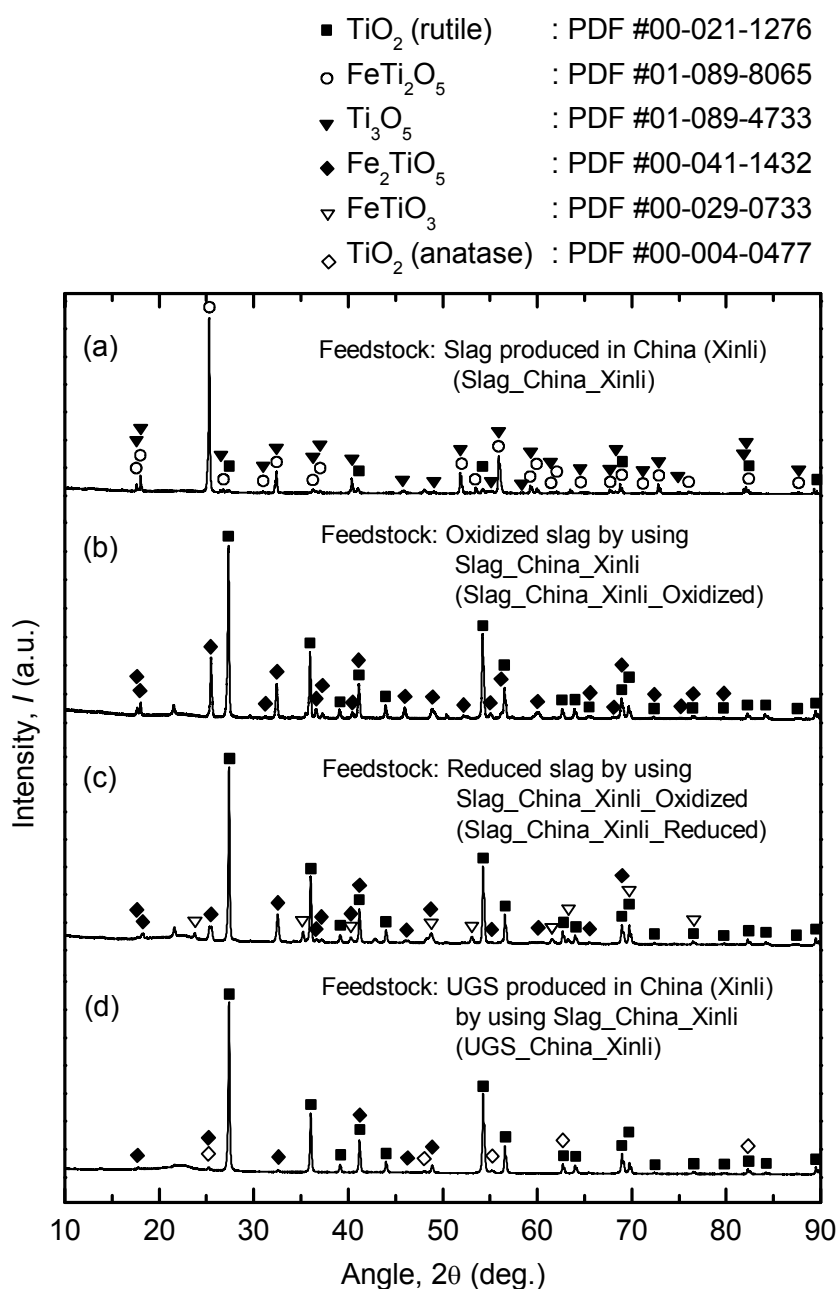
Figure 8-4 Results of XRD analysis of (a) the titania slag, (b) the oxidized titania slag by using titania slag of (a), (c) the reduced titania slag by using the oxidized titania slag of (b), and (d) UGS (upgraded slag) by using titania slag of (a). (*see* Table 8-2)

Fe-O-Cl system,
Ti-O-Cl system, *T* = 1100 K
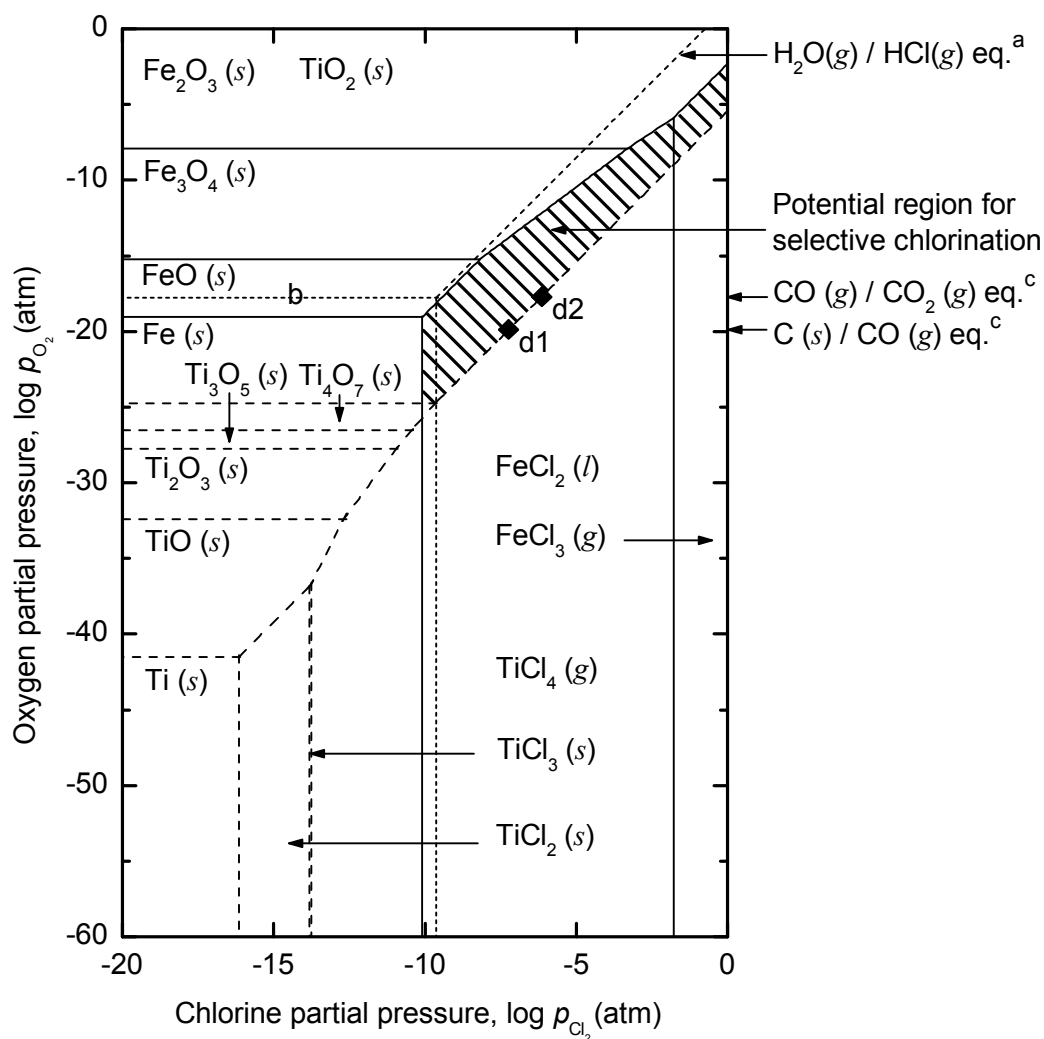
Figure 8-5 Chemical potential diagrams of the Fe-O-Cl (solid line)
and Ti-O-Cl (dotted line) systems overlapped at 1100 K.
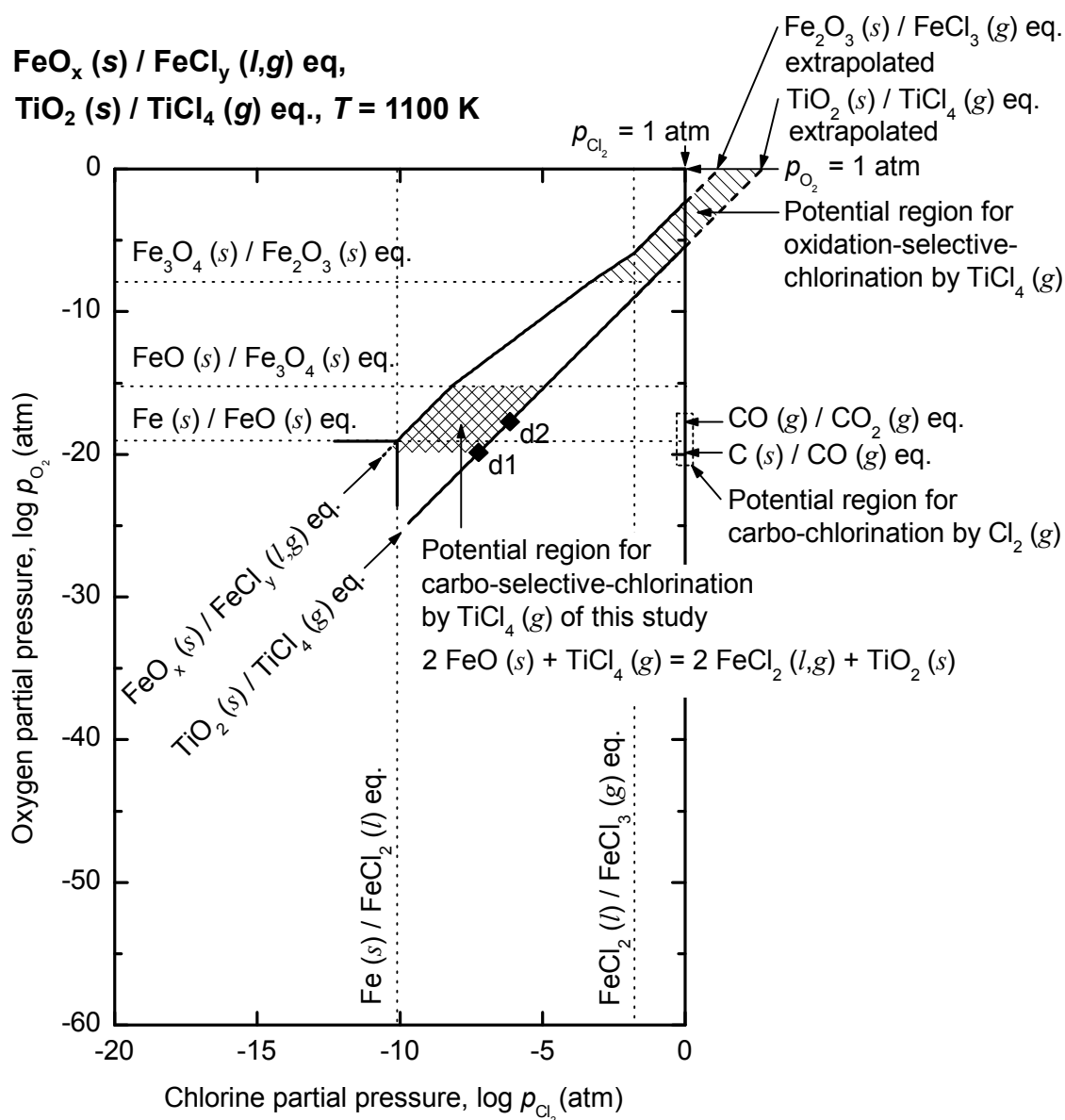
Figure 8-6 Potential regions for carbo-selective chlorination,
oxidation-selective-chlorination, and carbo-chlorination
using modified chemical potential diagram of the Fe-O-Cl and
Ti-O-Cl systems at 1100 K.
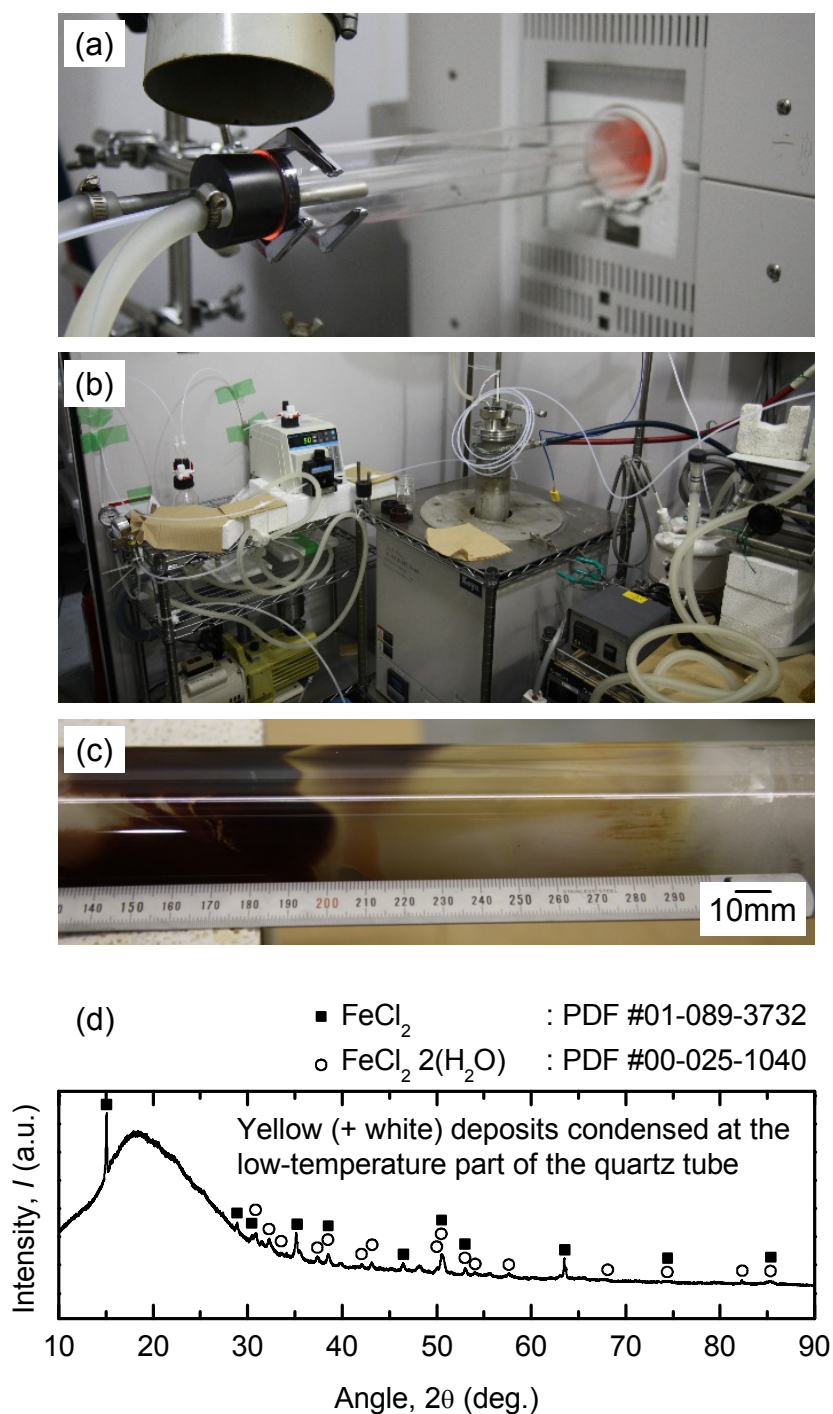
Figure 8-7 (a) Photograph of the front part of the quartz tube when
the tube was just placed in the furnace, and (b) photograph
of the TiCl$_4$ supply system, and (c) photograph of the quartz
tube taken out from the furnace after reaction, and (d) results
of XRD analysis of the yellow deposits condensed at the
low-temperature part of the tube after the inside of the tube
was dried. (Exp. no. 131028)
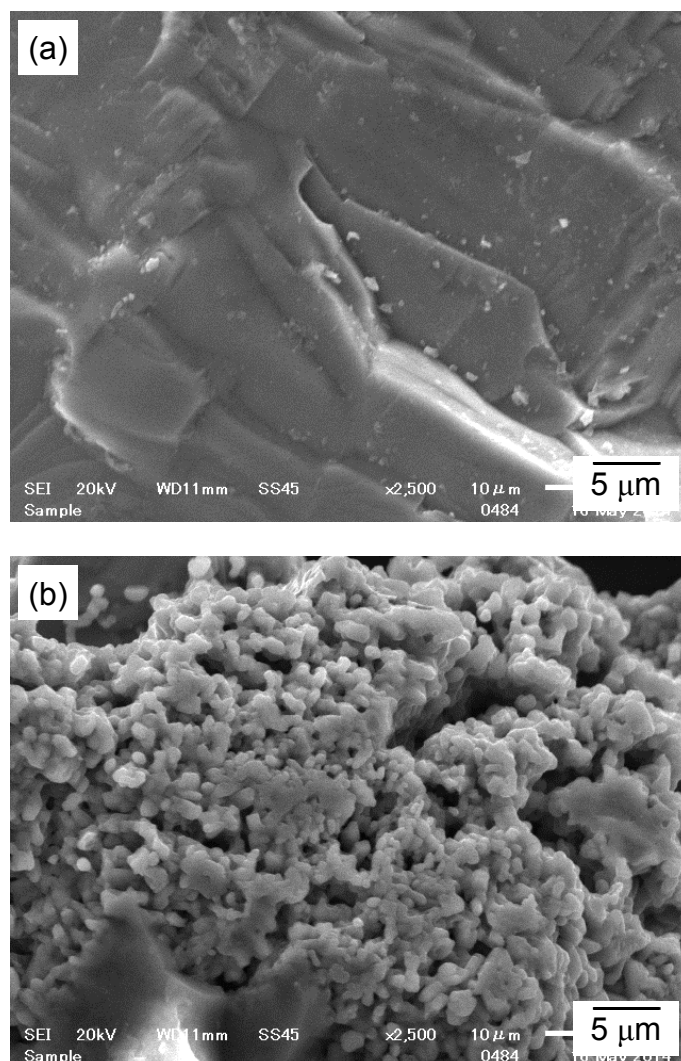
Figure 8-8 SEM images of surfaces of (a) the titania slag particle without
pretreatment before experiment and (b) the residues of the titania
slag particle without pretreatment after experiment. (Exp. no. 131028)
(*see* Table 8-2)
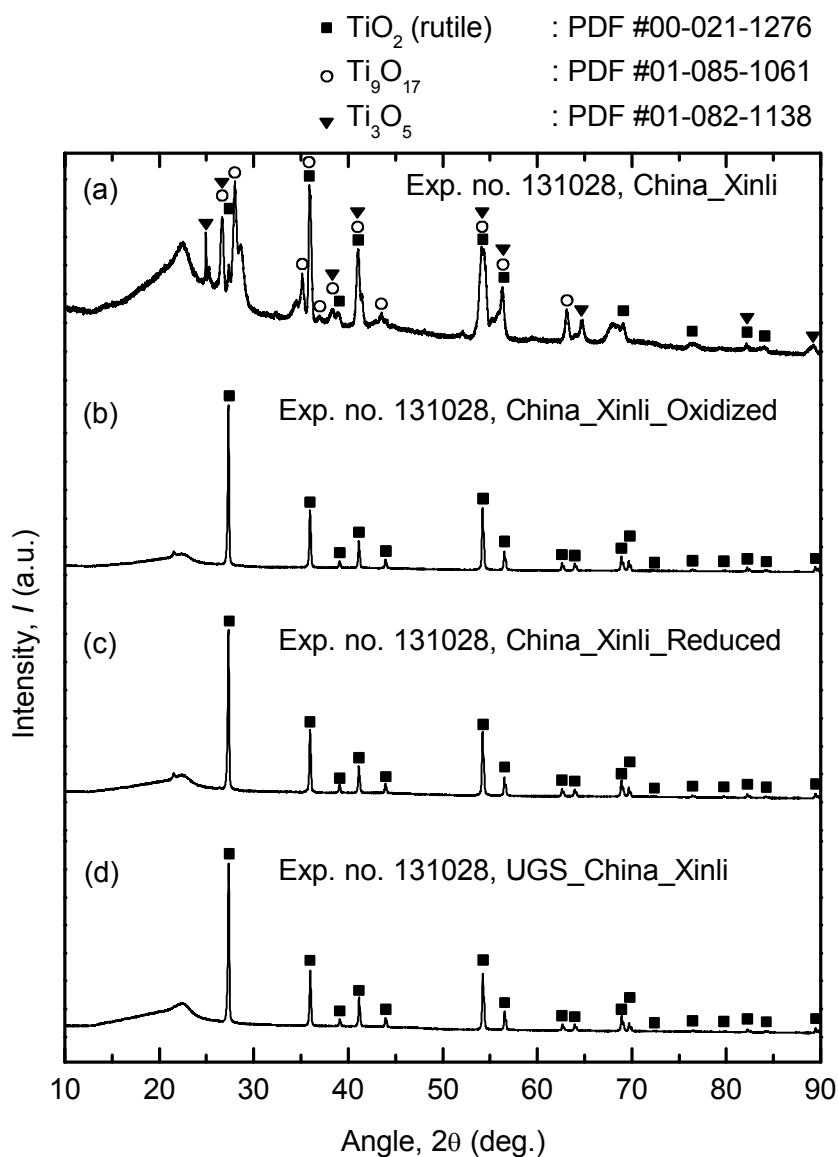
Figure 8-9 Results of XRD analysis of residues obtained when the experiment
was conducted by using (a) titania slag, (b) oxidized titania slag,
(c) reduced titania slag, and (d) UGS as feedstock (Exp. no. 131028).
(*see* Table 8-2)
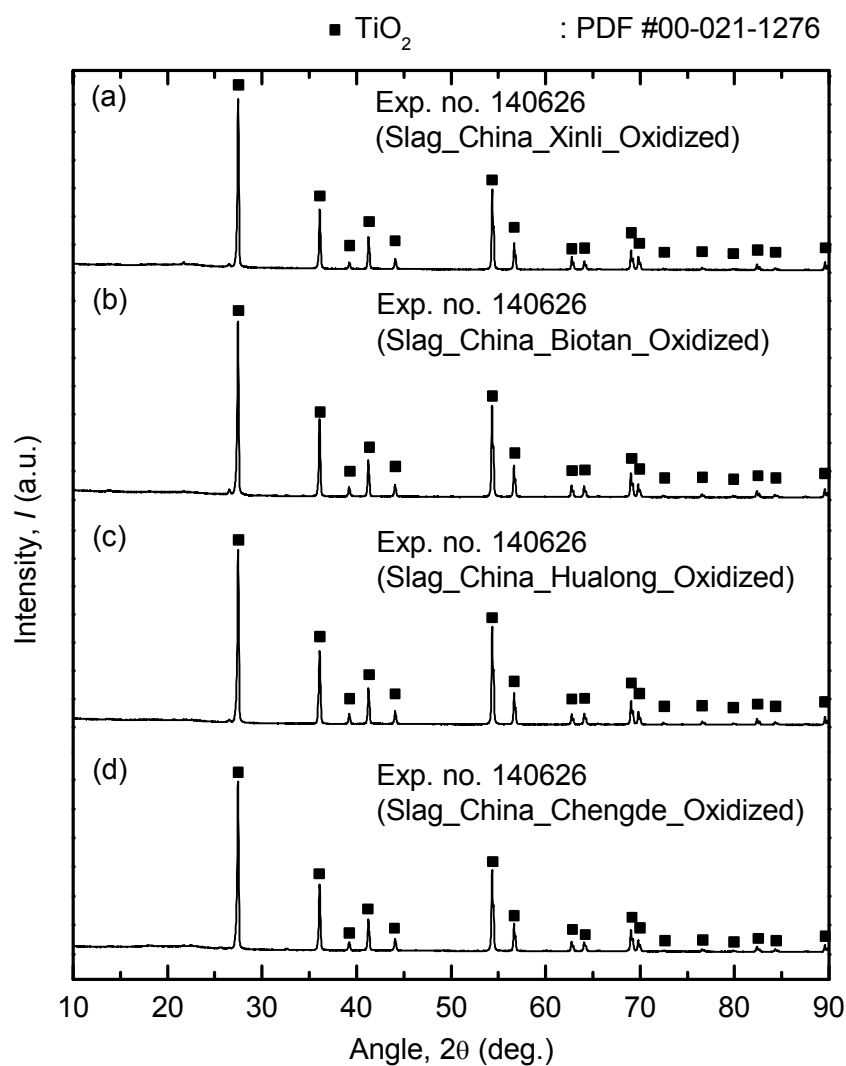
Figure 8-10 Results of XRD analysis of residues obtained when the experiment
was conducted in the presence of carbon by using (a) the oxidized
Chinese slag in Xinli, (b) oxidized Chinese slag in Biotan, (c) oxidized
Chinese slag in Hualong, and (d) oxidized Chinese slag in Chengde
as a feedstock (Exp. no. 140626). (*see* Table 8-2)

Chapter 9   Proposal of a novel environmentally friendly titanium upgrading process

9.1   Introduction

Titanium metal has many excellent properties such as a high specific strength (strength to weight ratio) and high corrosion resistance. Therefore, titanium is a material with huge possibilities for future applications.

Titanium is the ninth most abundant element in the Earth's crust. In addition, the amount of the main mineral resource of titanium, which is ilmenite (chemical formula: $FeTiO_3$), is essentially unlimited from the viewpoint of reserves of the mineral resource. Even though titanium has very little restriction on its resource abundance, titanium metal and its alloys are currently not widely used as structural materials in our society. The main reason for this is that the removal of impurities such as iron and oxygen from low-grade titanium ore is technically difficult for the production of high-purity titanium metal.[1]

Currently, although the latest technology is used, the production cost is still about $10,000 per ton, and a long processing time of at least two weeks is required to produce titanium metal from titanium ore.[1] In addition, for extracting the metal from the ore, a high amount of energy is required, and a large amount of waste solution or chloride waste is generated during the smelting process.

Taking into consideration of the growth of the titanium industry in the near future, problems regarding the treatment of the waste solution or chloride waste generated by the smelting process will become important issue. Therefore, in this study, the possibility of establishing an environmentally friendly titanium smelting process is discussed, and a novel titanium smelting process that does not discharge waste solution or chloride waste is proposed.

9.2   Review of flow chart of titanium smelting and the main titanium upgrading methods

Fig. 9-1 shows the outline of the current flow chart of titanium production from ore to metal.[2] As shown in Fig. 9-1, the main ore used as feedstock in the titanium

industry is ilmenite ore, which contains approximately 50 % iron oxides as impurities. In addition, rutile ore (chemical formula: TiO_2) is partly used as feedstock. Although rutile ore is high-grade TiO_2 and has a low concentration of iron, which makes it useful as a feedstock, it is not practical for use in large-scale titanium industry in the future. This is because, reserves of rutile ore are scarce, and the price of the ore is seven times higher than that of ilmenite ore.[3]

As shown in Fig. 9-1, a large amount of titanium ore is consumed to produce the titania (TiO_2) pigment used mainly for coatings, polymers, and paper. The total production volume of titania pigment is 21.5 times larger than that of the TiO_2 feed consumed for titanium metal production.[3,4]

For the production of titania pigment or titanium metal, it is necessary to remove the iron from the titanium ore. Currently, as shown in Fig. 9-1, several smelting processes are used in industry to upgrade low-grade titanium ore.

The slag process in Fig. 9-1 uses high-temperature reactions to remove iron from titanium ore as pig iron (Fe-C alloy).[5,6] When the titanium ore reacts with the carbon (*s*) and/or CO (*g*) powder reductant in an electric furnace at 1923 – 1973 K, the iron in the titanium ore is reduced and is removed separately as liquid Fe-C alloy.[7-9] As a result, TiO_2 is produced as a slag (molten oxide) called titania slag. Because the reactions proceed at high temperature, the slag process consumes a high amount of energy. Nonetheless, it is appropriate for large-scale process owing to the low amount of waste generated and high reaction rate. However, the purity of the titanium oxide obtained is not high enough, because the titania slag still contains FeO as impurity. As a result, the purity of TiO_2 in titania slag is generally 75 – 86 %. Therefore, the UGS or sulfate process is used to upgrade titania slag into high-grade TiO_2 feed.

The sulfate,[10-14] UGS,[5,6] Becher,[15-19] and Benilite[20-22] processes in Fig. 9-1 are hydrometallurgical processes in which aqueous solutions are used to leach iron to remove it from the titanium ore or titania slag. These processes can upgrade titanium ore or titania slag to a purity of above 95 % TiO_2, which is considered high-grade TiO_2. However, the reaction rate of the hydrometallurgical processes is slower than that of the pyrometallurgical process, and a large amount of acid waste solution or chloride waste is generated owing to the use of a large amount of concentrated acid solution.

On the other hand, the chloride process is a pyrometallurgical process utilizing high-temperature reactions.[7,10,23,24] Therefore, the reaction rate is fast, and it is suitable for large-scale process. However, when low-grade titanium ore is used as feedstock, a large amount of chloride waste is generated, because the other oxides in the titanium ore are also chlorinated. Therefore, when the chloride process or the Kroll process using a carbo-chlorination process is used, almost all impurities in titanium ore are removed and discharged as chloride waste. Generation of a large amount of chloride waste makes the chlorinator difficult to operate owing to problems such as clogging of pipes by condensed chlorides.

For example, when the ilmenite is directly chlorinated in the chloride process, a large amount of iron chlorides is discharged as chloride waste because the molar amount of iron is almost identical to that of titanium in the titanium ore, and it is chlorinated. If a large amount of chloride waste can be disposed of inexpensively, a chloride process that directly chlorinates ilmenite will become effective. However, generally, to decrease the amount of chloride waste generated as well as the chlorine loss in the process, upgraded TiO_2 feed produced by removing iron from titanium ore in advance is used as feedstock for the chloride process.

Among the processes shown in Fig. 9-1, the slag process is the only one that does not discharge waste solution or chloride waste. When the other processes except the slag process shown in Fig. 9-1 are used, problems regarding the treatment of the discharged waste arise. Therefore, given the anticipated growth of the titanium industry, a novel environmentally friendly titanium smelting process that does not discharge waste solution or chloride waste and that use low-grade titanium ore will become important.

9.3　A novel environmentally friendly titanium smelting process free from waste solution or chloride waste discharge

Fig. 9-2 shows, as an example, the process flow chart of the new titanium smelting method that is currently being investigated fundamentally in this thesis. When the selective chlorination method and the recovery of chlorine through pyrometallurgical method shown in Fig. 9-2 are used, titanium metal can be produced without generating

waste solution or chloride waste, even though a low-grade titanium feed such as ilmenite or titania slag is used.

9.3.1 Selective chlorination process using metal chlorides

As mentioned before, the slag process can produce TiO_2 feed without discharging waste solution or chloride waste. However, the production of a feed with a purity of above 90 % TiO_2 is difficult, and the feed still contains FeO. Therefore, in this thesis, the selective chlorination method for selectively removing iron as iron chlorides was investigated to produce high-grade TiO_2 with a purity of above 95 % using titanium ore or titania slag as feedstock.[25-28] Because this selective chlorination process is a pyrometallurgical process and is conducted at high temperatures such as 1100 K or 1200 K, the reaction rate is fast, and it is suitable for mass production. In addition, because this process does not use aqueous solution, the recovery of chlorine from the iron chlorides generated is possible.[27,28] The recovered chlorine can be reused as a chlorinating agent for the carbo-chlorination in the Kroll process.

The selective chlorination method ((A) Selective chlorination) in Fig. 9-2 was reported in detail in chapters 3, 5, 6, 7, and 8 in this thesis and by Othmer.[2,27-31] Furthermore, in the past, extensive studies were conducted on selective chlorination. For example, selective chlorination using Cl_2 gas in the presence of low-valence titanium oxide (TiO_x, $0 < x < 2$) was investigated in Japan.[32] However, unfortunately, none of this research is used in the current industry, except for the processes shown in Fig. 9-1.

The representative chemical reaction for the production of high-grade TiO_2 feed using the selective chlorination method is as follows:

(A) FeO_x (s, in Ti ore) + x/2 $TiCl_4$ (g) = $FeCl_{2x}$ (g) + x/2 TiO_2 (s)   (9-1)
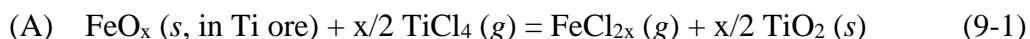
As shown in Table 9-1, for example, a feed with a purity of about 97 % TiO_2 could be obtained by reacting $TiCl_4$ (or HCl) gas with ilmenite or titania slag.[25-28,33,34]

In this chapter, a novel selective chlorination process is suggested as a pre-treatment method to upgrade low-grade titanium ore or titania slag into high-grade TiO_2 feed for the titanium metal smelting process. The abovementioned reaction can also be

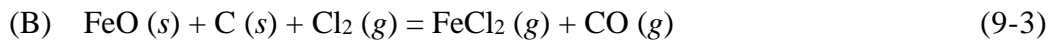applied to produce high-grade TiO_2 feed directly from low-grade titanium ore for titania pigment production.

9.3.2   Carbo-chlorination process

Currently, the carbo-chlorination process under a reducing atmosphere is used in the titanium metal smelting process. The carbo-chlorination process is carried out at 1073 – 1273 K, and, generally, the following reactions occur.[10,35] (In actual situation, it is considered that multiple complex reactions including the reaction shown in Eq. 9-1 simultaneously occur.)

(B) TiO_2 (s) + 2 C (s) + 2 Cl_2 (g) = $TiCl_4$ (g) + 2 CO (g)   (9-2)

(B)   FeO (s) + C (s) + Cl_2 (g) = $FeCl_2$ (g) + CO (g)   (9-3)

In the reaction shown in Eq. 9-1, TiO_2 is not chlorinated, and only FeO_x is chlorinated. However, TiO_2 and almost all impurities including iron oxides in the TiO_2 feed are simultaneously chlorinated by the reactions shown in Eqs. 9-2 and 9-3, and chlorides waste is generated. In the current industry, recovery of chlorine from the generated chloride waste is not conducted, and the chloride waste is disposed of as industrial waste.

Fig. 9-3 shows the chemical potential diagram of the Fe-O-Cl and Ti-O-Cl systems overlapped at 1100 K, plotted with the partial pressure of chlorine (p_{Cl_2}) as the abscissa and the partial pressure of oxygen (p_{O_2}) as the ordinate, for indicating the chemical potential region where the reactions shown in Eqs. 9-1 ~ 9-3 proceed. The detailed thermodynamic analysis of the potential regions in Fig. 9-3 can be found in chapters 2, 6, and 7 of this thesis. It is worth noting that even though the chlorination of iron proceeds, the chemical potential regions where the chlorination reaction proceeds are different depending on the chemical potentials of chlorine and oxygen, as shown by chemical potential region A and point B in Fig. 9-3.

9.3.3 Recovery of chlorine by the oxidation of chlorides

In addition, the main reaction of the process indicated as C in Fig. 9-2, which is for the recovery of chlorine from $FeCl_x$, is as follows:

$$(C) \quad FeCl_x \ (s,g) + 3/4 \ O_2 \ (g) = 1/2 \ Fe_2O_3 \ (s) + x/2 \ Cl_2 \ (g) \qquad (9\text{-}4)$$
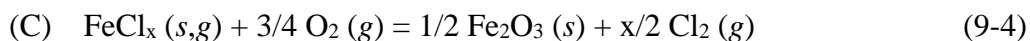
This reaction proceeds under high p_{Cl_2} and high p_{O_2} conditions. These conditions are indicated by point C in the upper-right corner of the chemical potential diagram in Fig. 9-3. Therefore, the chemical potential conditions for the progress of this reaction are different from those for the chlorination processes, which are indicated by chemical potential region A or point B in Fig. 9-3.

This method has been investigated by several researchers in the past.[36-41] Harris reported that 97 % of $FeCl_3$ was converted to Fe_2O_3 and Cl_2 gas when the dechlorination using a mixture of $FeCl_3$, Fe_2O_3, and NaCl as the feedstock was conducted at 773 K for 30 hours.[36] The influence of NaCl as a catalyst on the dechlorintion was investigated by Henderson, who also reported that more than 95 % of the $FeCl_3$ was converted to iron oxide at 773 K and 873 K.[37] Dunn reported that the dechlorination of iron chloride could be performed when iron chloride heated to 1250 – 1380 K was reacted with oxygen gas, and subsequently cooled to allow further oxidation.[38] In addition, Haack and Reeves of DuPont also reported that more than 95 % of iron chloride was converted to iron oxide at 823 – 1023 K under certain conditions.[39,40]

This dechlorination process by the oxidation of iron chloride is a straightforward reaction and not technically difficult to perform. However, Cardarelli pointed out that issues such as the deposition of Fe_2O_3 inside the reactor and the poor quality of the generated Cl_2 gas generated owing to contamination by unreacted volatile chlorides including $FeCl_3$ and the dilution of the Cl_2 gas by the unreacted O_2 gas. These problems must be resolved before the establishment of a commercial dechlorination process.[41]

9.3.4 Establishment of a novel titanium smelting process

Table 9-2 lists the chlorinating agents and conditions for selective removal of iron oxides in titanium ore as iron chlorides and for chlorination of TiO_2.[25-29,33,34] As shown in Table 9-2, $TiCl_4$ and HCl gas are appropriate chlorinating agents for selectively removing iron in titanium ore as iron chlorides.

Table 9-1 lists some representative results for the concentrations of iron in titanium ore before and after the titanium ore was reacted with chlorinating agents such as $TiCl_4$, $CaCl_2$, $MgCl_2$, and HCl.[25-28,33,34] As shown in Table 9-1, when the p_{Cl_2} and p_{O_2} in the reaction system are properly controlled, a purity of above 97 % TiO_2 feed is directly obtained in a single step. The concentration of iron in the titanium ore decreased from 50 % in the initial step to below 1% because of the selective chlorination reaction.

The selective chlorination (A) in Fig. 9-2, for example, uses $TiCl_4$ as chlorinating agent. HCl also can be used as a chlorinating agent instead of $TiCl_4$. However, when HCl is used as chlorinating agent, problems such as the difficulty in progress of the selective chlorination under high p_{O_2} and the highly corrosive environment in the reactor must be considered. (*see* chapter 2 in detail)

Table 9-3 lists the input materials, operation conditions, by-product, and product of the selective chlorination and the slag/UGS processes for considering the energy required for each process. As shown in Table 9-3, the energy required for the feedstock of the slag/UGS processes is higher than that for the feedstock of the selective chlorination process, because the feedstock of the UGS process, 75 – 86 % TiO_2, is produced by the slag process. In addition, the reaction temperature of the slag process is higher than that of the selective chlorination process. In case of reagents/supplies, it is difficult to compare the energy required for chlorinating agents. However, the energy required for treating and disposing the by-product of selective chlorination process is lower than that for treating and disposing the by-product of the slag/UGS process, because a large amount of acid waste solution is dumped out in the slag/UGS process.

In the future, new environmentally friendly processes for producing high-purity TiO_2 without the discharge of waste solution will be developed. Fig. 9-4 shows future flow chart and environmentally sound processes for the production of titania pigment and titanium. In Fig. 9-4, the processes and flow lines depicted by the dashed lines are the

proposed new processes and flow lines based on chloride metallurgy. These processes do not discharge waste solution and are suitable for large-scale operation. Therefore, these novel environmentally friendly processes will gain significant attention as solutions for establishment of sustainable titanium smelting process in the future.

9.4   Summary

In the current titanium smelting process for production of high-grade TiO_2 or titanium metal from low-grade titanium ore, a large amount of harmful waste solution or chloride waste is generated. In the future, when the demand for titanium increases, problems regarding the treatment or disposal of chloride waste could become significant.

Therefore, in this study, a novel environmentally friendly titanium smelting process that does not discharge waste solution or chloride waste was proposed and characterized in detail. In particular, the authors proposed the establishment of a new selective chlorination process through pyrometallurgical method (high-temperature process) to upgrade low-grade titanium ore directly in a single step to produce high-grade TiO_2 feed for titanium metal production.

In addition, when the selective chlorination is used, it is also possible to decrease the chlorine loss in the chlorination process, because the chlorine can be recovered using a pyrometallurgical method such as the oxidation reaction. Therefore, the environmental burden can be decreased, because the iron in the titanium ore is discharged from the system as pig iron or iron oxide (Fe_2O_3) in the titanium smelting process.

In recent years, the concerns regarding to the environment have increased, and, accordingly, a sustainability has been pursued in the titanium smelting industry. When the environmental burden caused by pollution and waste management are considered, it is essential to develop new environmentally sound processes that do not generate industrial wastes such as acid waste solution or chloride waste in the future. When these aspects are taken into consideration, the processes discussed in this chapter would be the solution for development of new processes in the future.

References

[1]   T.H. Okabe and J. Kang: "*The Latest Technological Trend of Rare Metals*", CMC Publishing Co. LTD., Tokyo, 2012, Chap. 6-1, pp. 83-94. (*in Japanese*)

[2]   J. Kang and T.H. Okabe: "T*hermodynamic Consideration of the Removal of Iron from Titanium Ore by Selective Chlorination*", Metall. Trans. B, 2014 (in print).

[3]   G.M. Bedinger: "*Mineral Commodity Summaries: Titanium Mineral Concentrates*", U.S. Geological Survey, Washington DC, January, 2013, pp. 174-175.

[4]   G.M. Bedinger: "*Mineral Commodity Summaries: Titanium and Titanium Dioxide, U.S. Geological Survey*", Washington DC, January, 2013, pp. 172-173.

[5]   M. Gueguin and F. Cardarelli: "*Chemistry and mineralogy of titania-rich slags. Part 1-hemo-ilmenite, sulphate, and upgraded titania slags*", Miner. Process. Extr. Metall. Rev., 2007, vol. 28, pp. 1–58.

[6]   K. Borowiec, A.E. Grau, M. Gueguin, and J-F. Turgeon: "*Method to upgrade titania slag and resulting product*", United States Patent 5830420, 1998.

[7]   J.E. Kogel, N.C. Trivedi, J.M. Barker, and S.T. Krukowski: "*Industrial minerals & rocks: commodities, markets, and uses*", 7th ed., Society for Mining, Metallurgy, and Exploration, Inc. (SME), Littleton, Colorado, United States of America, 2006.

[8]   D. Filippou and G. Hudon: "*Iron removal and recovery in the titanium dioxide feedstock and pigment industries*", JOM, 2009, vol. 61 (10), pp.36–42.

[9]   G.E. Williams and J.D. Steenkamp: "*Heavy Mineral Processing at Richards Bay Minerals*", Southern African Pyrometallurgy 2006, 2006, pp. 181-188.

[10]   F. Habashi: "*Handbook of Extractive Metallurgy*", vol. 2, VCH Verlagsgesellschaft mbH, Weinheim, Germany, 1997.

[11]   T. Tomonari: "*Titanium Industry-Its Growing Steps and Future Possibilities*", The Japan Titanium Society, Tokyo, Japan, 2001. (*in Japanese*)

[12]   M. Matsunaga: "*Titanium Dioxide Pigment*", Journal of the Japan Society of Colour Material, 1981, vol. 54 (11), pp. 680-689. (*in Japanese*)

[13]   E.G. Roche, A.D. Stuart, and P.E. Grazier: "*Production of Titania*", United States Patent 7485269 B2, 2009.

[14]   E.G. Roche, A.D. Stuart, P.E. Grazier, and H. Liu: "*Production of Titania*", United States Patent 7485268 B2, 2009.

[15]   K.S. Geetha and G.D. Surender: "*Experimental and modelling studies on the aeration leaching process for metallic iron removal in the manufacture of synthetic rutile*", Hydrometallurgy, 2000, vol. 56 (1), pp. 41-62.

[16]   R.G. Becher, R.G. Canning, B.A. Goodheart, and S. Uusna: "*A new process for upgrading ilmenitic mineral sands*", Proceeding of the Australasian Institute of Mining and Metallurgy, 1965, vol. 21, pp. 21-44.

[17]   S. Jayasekera, Y. Marinovich, J. Avraamides, and S.I. Bailey: "*Pressure leaching of reduced ilmenite: electrochemical aspects*", Hydrometallurgy, 1995, vol. 39 (1), pp. 183-199.

[18]   W. Hoecker: "*Process for the production of synthetic rutile*", United States Patent 5601630, 1997.

[19]   J.B. Farrow, I.M. Ritchie, P. Mangano: "*The reaction between reduced ilmenite and oxygen in ammonium chloride solutions*", Hydrometallurgy, 1987, vol. 18 (1), pp. 21-38.

[20]   J.H. Chen: "*Beneficiation of Titaniferous Ores*", United States Patent 3825419, 1974.

[21]   J.H. Chen and L.W. Huntoon: "*Beneficiation of ilmenite ore*", United States Patent 4019898, 1977.

[22]   J.H. Chen: "*Pre-leaching or reduction treatment in the beneficiation of titaniferous iron ores*", United States Patent 3967954, 1976.

[23]   M.K. Akhtar, Y. Xiong, and S.E. Pratsinis: "*Vapor Synthesis of Titania Powder by Titanium Tetrachloride Oxidation*", AIChE Journal, 1991, vol. 37 (10), pp. 1561-1570.

[24]   M.K. Akhtar, S. Vemury, and S.E. Pratsinis: "*Competition between TiCl$_4$ Hydrolysis and Oxidation and its Effect on Product TiO$_2$ Powder*", AIChE Journal, 1994, vol. 40 (7), pp. 1183-1192.

[25]   J. Kang and T.H. Okabe: "*Upgrading Titanium Ore Through Selective Chlorination Using Calcium Chloride*", Metall. Mater. Trans. B, 2013, vol.44B (3), pp.516-527.

[26]   J. Kang and T.H. Okabe: "*Removal of Iron from Titanium Ore through Selective Chlorination Using Magnesium Chloride*", Mater. Trans., 2013, vol.54 (8), pp.1444-1453.

[27]   J. Kang and T.H. Okabe: "*Production of Titanium Dioxide Directly from Titanium Ore Through Selective Chlorination Using Titanium Tetrachloride*", Mater. Trans., 2014, vol.55 (3), pp.591-598.

[28]   J. Kang and T.H. Okabe: "*Removal of Iron from Titanium Ore by TiCl₄ under High Oxygen Potential*", International Journal of Mineral Processing, 2014 (submitted).

[29]   T.H. Okabe and J. Kang: "*Thermodynamic Study on Chlorination Reactions of Oxides at Elevated Temperatures*", Molten Salts, 2013, vol. 56 (1), pp. 15-26. (*in Japanese*)

[30]   D.F. Othmer: "*Manufacture of titanium chloride, synthetic rutile and metallic iron from titaniferous materials containing iron*", United States Patent 3859077, 1975.

[31]   D.F. Othmer and R. Nowak: "*Halogen affinities–A new ordering of metals to accomplish difficult separations*", AIChE Journal, 1972, vol.18, no.1, pp.217-220.

[32]   K. Ichimura, S. Oka, and Y. Takahashi: "*Method to produce high-grade TiO₂ feed*", Japan Patent 1994-191847, 1994. (*in Japanese*)

[33]   H. Zheng: "*Development of a Novel Titanium Production Process Using Selective Chlorination*", Doctoral Thesis, The University of Tokyo, 2007.

[34]   R. Matsuoka and T.H. Okabe: "*Iron removal from titanium ore using selective chlorination and effective utilization of chloride waste*", Proceedings of the Symposium on Metallurgical Technology for Waste Minimization (134th TMS Annual Meeting), 2005, San Francisco, United States.
http://www.okabe.iis.u-tokyo.ac.jp/japanese/for_students/parts/pdf/050218_TMS_proceedings_matsuoka.pdf.

[35]   N. Nakamura: "*Current state of titanium sponge production technology*", Molten Salts, 2013, vol.56, no.3, pp.121-124. (in Japanese)

[36]   H.M. Harris, A.W. Henderson, J.I. Paige, and T.T. Campbell: "*Process for Chlorination of Titanium Bearing Materials and for Dechlorination of Iron Chloride*", World Mining and Metals Technology, The Society of Mining Engineers, New York, United States of America, Chap. 44, 1976, pp. 693-712.

[37]   A.W. Henderson, T.T. Campbell, and F.E. Block: "*Dechlorination of Ferric Chloride With Oxygen*", Metallurgical Transactions, 1972, vol. 3 (10), pp. 2579-2583.

[38]   W.E. Dunn, Jr.: "*Process for Beneficiating a Titaniferous Ore and Production of Chlorine and Iron Oxide*", United States Patent 3865920, 1975.

[39]   D.J. Haack and J.W. Reeves: "*Production of Chlorine and Iron Oxide from Ferric Chloride*", United States Patent 4144316, 1979.

[40]   J.W. Reeves, R.W. Sylvester, and D.F. Wells: "*Chlorine and Iron Oxide from Ferric Chloride – Apparatus*", United States Patent 4282185, 1981.

[41]   F. Cardarelli, S. Lefebvre, C. Tousignant, and G. Hudon: "*Electrochemical Process for the Recovery of Metallic Iron and Chlorine Values from Iron-rich Metal Chloride Wastes*", European Patent 2265749 B1.

Table 9-1 Representative analytical results for the titanium ore before and after
the selective chlorination experiments.

	Chlorinating agent	Chlorination conditions			Concentration of element i, C_i (mass%)[a]				Ref.
		Temp., T / K	Time, t_r' / h	Atmosphere	Ti	Fe	Ca	Mg	
Feed ilmenite[b]					43.8	51.3	N.D	N.A	
After Exp.	CaCl$_2$	1073	6	$N_2 + H_2O$	54.2	27.8	15.3	N.A	H. Zheng[33]
		1173	6	$N_2 + H_2O$	56.6	19.8	20.7	N.A	
		1293	12	$N_2 + H_2O$	77.3	16.7	3.36	N.A	
Feed ilmenite[c]					45.0	49.7	0.04	N.D	
After Exp.	HCl (from CaCl$_2$)	1100	5	Vacuum	96.7	0.54	0.04	N.D	J. Kang[25]
	CaCl$_2$	1100	5	Vacuum	52.5	18.1	28.0	N.D	
After Exp.	HCl (from MgCl$_2$)	1000	11	Ar	96.7	1.77	N.D	N.D	J. Kang[26]
	MgCl$_2$	1000	11	Ar	63.4	18.1	N.D	15.5	
	HCl (from MgCl$_2$)	1000	7	$Ar + H_2O$	97.2	1.24	N.D	N.D	
	MgCl$_2$	1000	7	$Ar + H_2O$	57.1	19.4	N.D	20.5	
After Exp.	TiCl$_4$	1100	5	Ar	98.0	0.69	N.D	N.D	J. Kang[27]
	TiCl$_4$	1100	4	$Ar + C$	97.6	0.50	N.D	N.D	
	TiCl$_4$	1200	9	$Ar + 1ppm\ O_2$	97.2	N.D	N.D	N.D	J. Kang[28]
	TiCl$_4$	1200	9	$Ar + 1\%\ O_2$	97.2	N.D	N.D	N.D	
	TiCl$_4$	1200	9	$Ar + 10\%\ O_2$	98.0	0.25	N.D	N.D	

a : Determined by XRF analysis (excluding oxygen and other gaseous elements),
N.D : Not Detected. Below the detection limit of the XRF (<0.01%).
N.A : Not Analyzed or unknown.
b : Titanium ore produced in the Vietnam, particle size is unknown: seiving was not performed.
c : Titanium ore produced in the Vietnam, particle size : 74 to 149 μm.

Table 9-2 Various conditions for the chlorination of iron oxides and titanium oxide at elevated temperatures.

Feed materials	Chlorinating agent				
	Cl_2	$Cl_2 + C$	$TiCl_4$	HCl	MCl_x (M = Ca, Mg, …)
Symbols in Fig. 9-3	○	☆			
FeO_x	✗ ($\Delta G° > 0$)	◎ ($\Delta G° \ll 0$) Current $TiCl_4$ production process	◎ ($\Delta G° \ll 0$)	○ ($\Delta G° \sim 0$)	○ ($\Delta G° \sim 0$)
			Selective chlorination of iron is feasible		
TiO_2	✗ ($\Delta G° > 0$)	◎ ($\Delta G° \ll 0$)	✗ ($\Delta G° > 0$)	✗ ($\Delta G° > 0$)	✗ ($\Delta G° \gg 0$)
Notes	high p_{Cl_2} high p_{O_2}	high p_{Cl_2} low p_{O_2}	$p_{Cl_2}{}^2/p_{O_2}$ = const	$p_{Cl_2}{}^2/p_{O_2}$ = const	$p_{Cl_2}{}^2/p_{O_2}$ = const
		Employed in Kroll process and Chloride process (Dupont)	Chapter 6-8	Chapter 3, 5	Chapter 3-5

Table 9-3 The input materials, operation conditions, by-product, and product of the selective chlorination and the slag/UGS processes.

	Slag and UGS processes[a]		Selective chlorination process	Dechlorination process	Note
	Slag	UGS			
Feedstock	Ilmenite, FeTiO$_3$ (30 – 65 % TiO$_2$)	Titania slag[c] (75 – 86 % TiO$_2$)	Ilmenite, FeTiO$_3$ (30 – 65 % TiO$_2$)	FeCl$_x$ (x = 2, 3)[b]	
Reaction temperature[d]	1923 – 1973 K (1173 – 1273 K)[d]	418 – 428 K (1273 – 1298 K)[e] (1073 – 1123 K)[f]	1100 K	773 – 1380 K	
Reagents / Supplies	–	18 – 20 % HCl	TiCl$_4$	–	Chlorinating agent
	Carbon	– (CO + H$_2$)[f]	Carbon or None	–	Reducing agent
	– (Air)[d]	– (Air)[e]	–	Air	Oxidizing agent
By-product	Fe-C	Spent HCl aq. FeCl$_x$ (x = 2, 3)	FeCl$_x$ (x = 2, 3)	FeO$_x$	
Product	75 – 86 % TiO$_2$	95 % TiO$_2$	95 – 98 % TiO$_2$	Cl$_2$	

a : *See* Figure 1-22 in chapter 1.
b : By-product of the selective chlorination process. Iron chlorides in a dry form are used as a feedstock .
c : Product of the slag process.
d : Conditions for the roasting of titanium ore before reduction process.
e : Conditions for the oxidation of titania slag before reduction step in the UGS process.
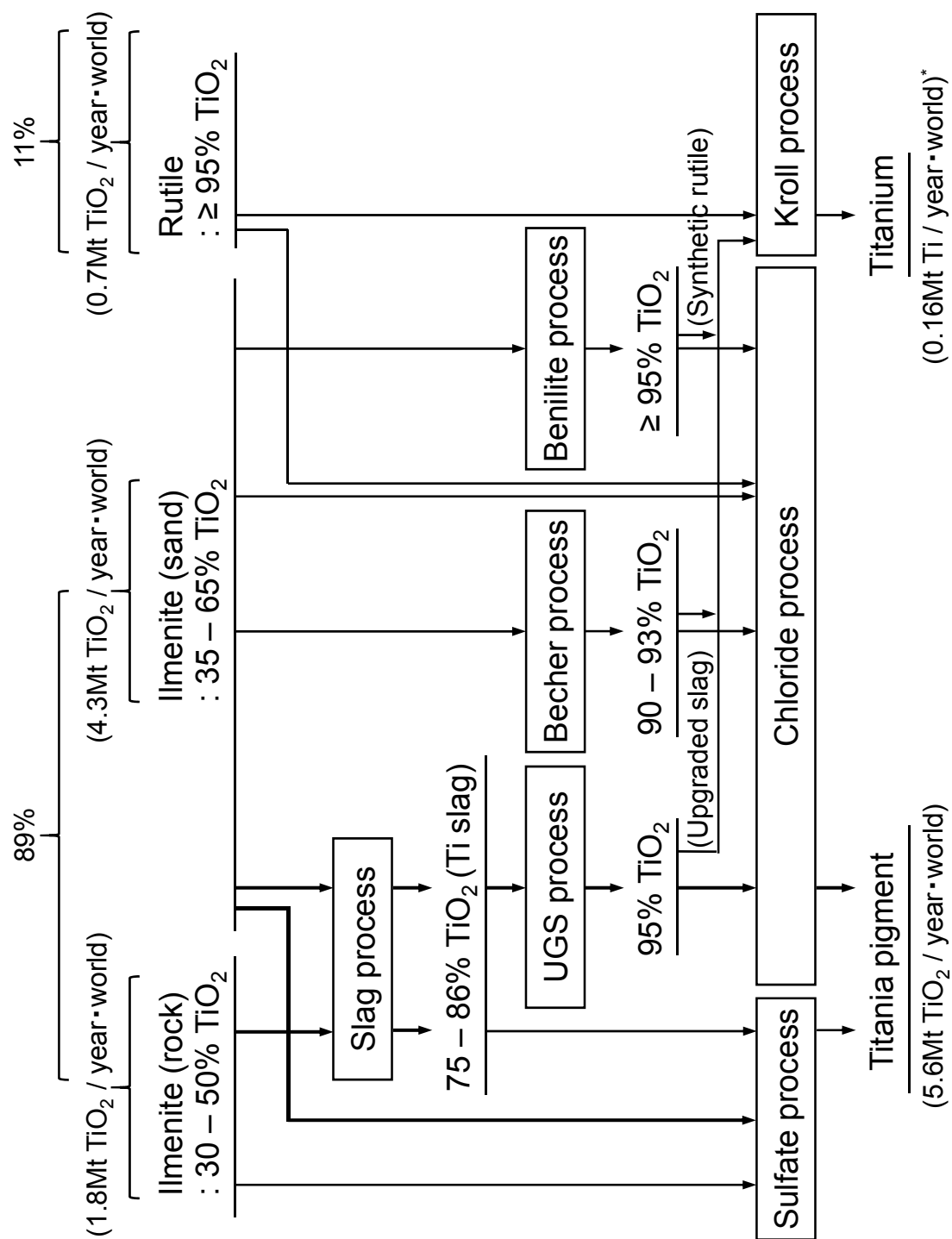f : Conditions for the reduction of oxidized titania slag before acid leaching process.

Ilmenite (rock)
: 30 – 50% TiO_2

(1.8Mt TiO_2 / year・world)

Ilmenite (sand)
: 35 – 65% TiO_2

(4.3Mt TiO_2 / year・world)

89%

Rutile
: ≥ 95% TiO_2

(0.7Mt TiO_2 / year・world)

11%

Slag process

75 – 86% TiO_2 (Ti slag)

UGS process

95% TiO_2
(Upgraded slag)

Becher process

90 – 93% TiO_2
(Upgraded slag)

Benilite process

≥ 95% TiO_2
(Synthetic rutile)

Kroll process

Sulfate process

Chloride process

Titania pigment

(5.6Mt TiO_2 / year・world)

Titanium

(0.16Mt Ti / year・world)*

*: Ti produced in USA is excluded. The estimated Ti production in USA in 2010 was 0.015 Mt Ti / year

Figure 9-1 The current flowchart of titanium production from titanium ore to titanium metal and titania pigment.

Titanium ore (*s*)   Carbon (*s*)

30 – 65 % TiO_2

Ti slag production

Oversea, or mining
on-site operation

Ti slag (*l*)   Fe-C (*l*) CO_x (*g*)

Supply of Cl_2 (*g*)
to compensate
the chlorine loss

Ti slag (*s*) $TiCl_4$ (*g*) ← ☆ From carbo-
chlorination

75 – 86% TiO_2

(A) Selective chlorination ←--- (C (*s*), Cl_2 (*g*))

95 – 98 % TiO_2

Cl_2 (*g*)   C (*s*) TiO_2 (*s*) $FeCl_x$ (*s,g*) O_2 (*g*)

(B) Carbo-chlorination · Distillation   (C) Recovery of chlorine

$TiCl_4$ (*g*) CO_x (*g*)   Chloride wastes (l) ---- Cl_2 (*g*) Fe_2O_3 (*s*)

☆
To selective
chlorination

Chlorine loss (e.g. $FeCl_x$ (*s*))
(current)

Wastes
(Future)

$TiCl_4$ (*l*)   Mg (*l*)

Reduction · Separation

$MgCl_2$ (*l*)   Ti (*s*)

Molten salt electrolysis

Cl_2 (*g*)   Mg (*l*)

Figure 9-2 Flowchart of the proposed novel environmentally sound
process for upgrading titanium ore and the Kroll process from
the viewpoint of circulation of chlorine gas and chloride waste.
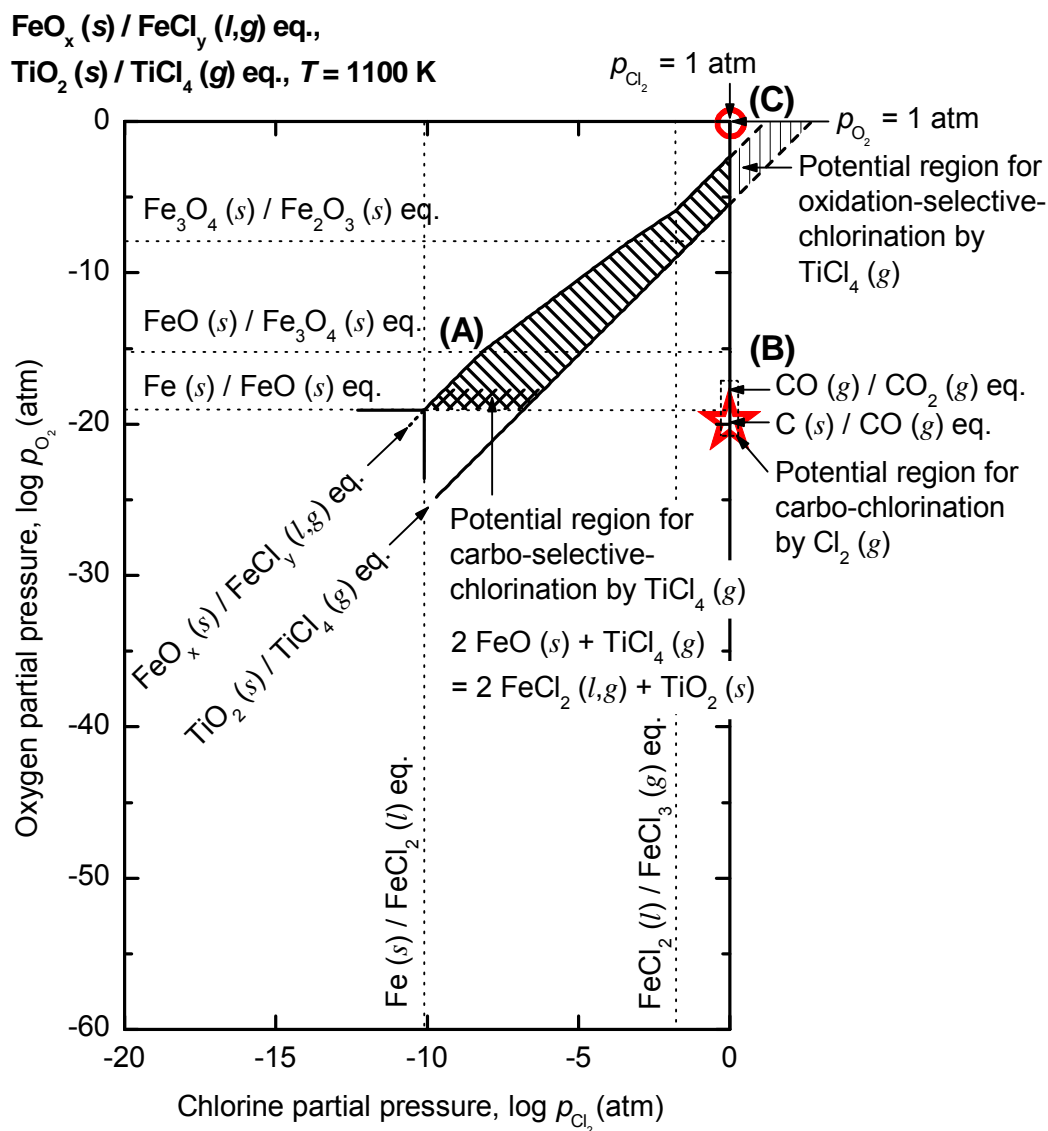
Figure 9-3 Comparison of potential regions for (A) selective chlorination
by $TiCl_4$ (g), (B) carbo-chlorination by Cl_2 (g), and (C) recovery
of chlorine from chloride waste using the modified chemical potential
diagram of the Fe-O-Cl and Ti-O-Cl systems at 1100 K.
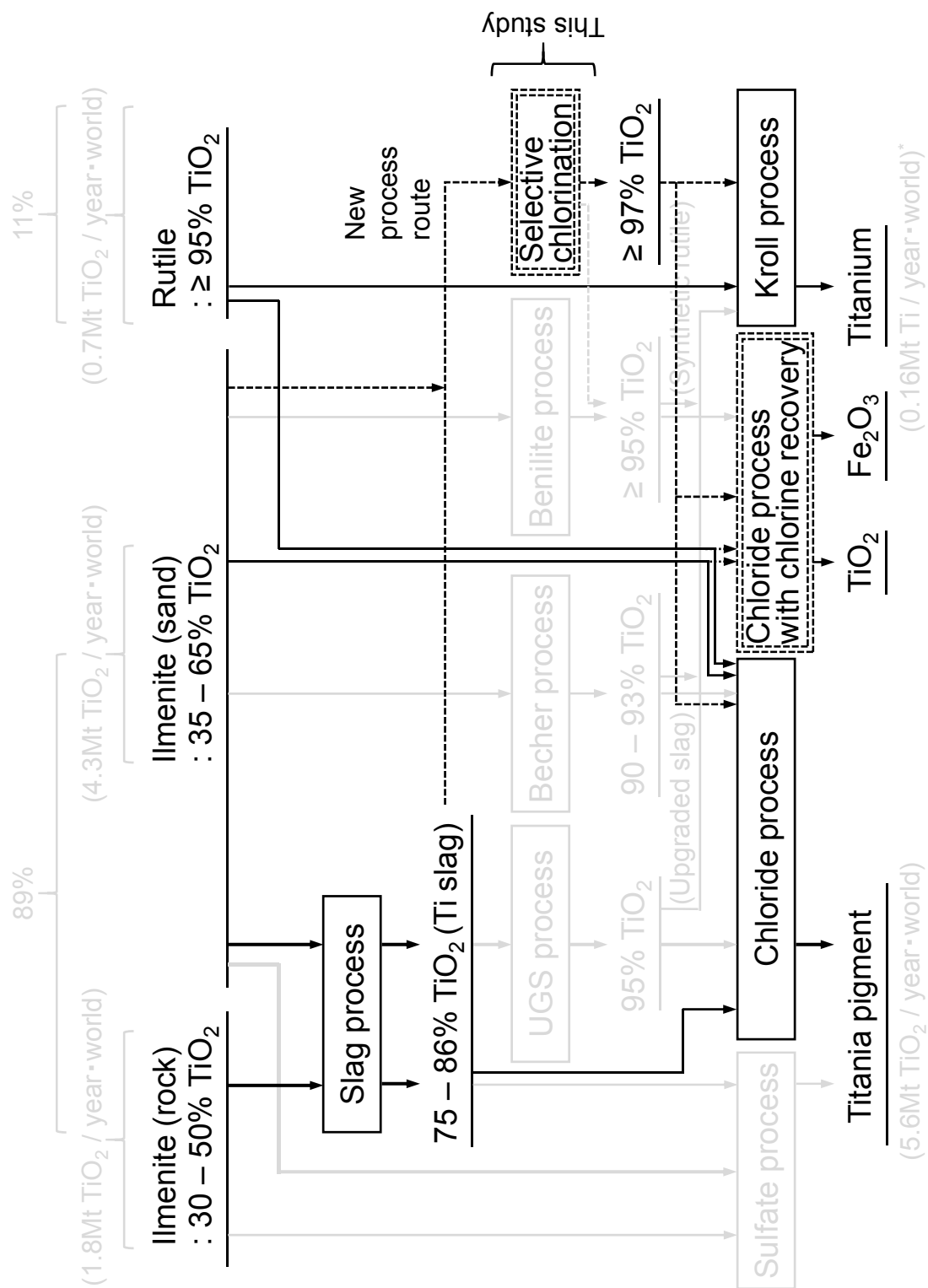
Figure 9-4 Future environmentally sound processes for production of titania pigment and titanium. The processes and flow lines depicted by the dashed lines are the proposed new processes, which is free from generating waste solution. (*see* Fig. 9-1)

Chapter 10 General overview and conclusions

Titanium (Ti) has excellent physical and chemical properties such as a high specific strength and corrosion resistance. In addition, titanium is the ninth most abundant element in the Earth's crust. However, titanium is not as widely used as aluminum or iron because of its high production costs and low productivity. For example, the cost for processing titanium ore is 15 times higher than that of processing iron ore. For these reasons, the development of an efficient process for upgrading low-grade titanium ore ($FeTiO_3$, 30 − 65 % TiO_2) to high-grade titanium dioxide (TiO_2) feed with a purity of above 95 % is important. Therefore, in this thesis, a method for the selective chlorination of low-grade titanium ore using metal chlorides or hydrogen chloride (HCl) gas as a chlorinating agent was developed to produce high-grade TiO_2 feed by selectively removing iron directly from the Ti ore in a single step.

In chapter 1, the current statuses of titanium metal, titania pigment, titanium mineral concentrates, and the upgraded TiO_2 feed were briefly introduced. In addition, the industrial titanium smelting processes for converting the ore to metal and pigment were reviewed from various viewpoints. The use of high-grade TiO_2 as a feedstock for the production of titanium metal or titania pigment is very important. When low-grade titanium ore is used as a feedstock, many operating problems arise, such as clogging of the reactor pipes and chlorine loss in a chlorinator by the generation of a large amount of chloride waste, or the generation of waste containing heavy metals. Currently, high-grade TiO_2 feed is produced by the Becher, Benilite, and slag and UGS processes. However, these upgrading processes still have several disadvantages such as the generation of a large amount of acid waste solution containing heavy metals owing to the use of the highly concentrated acid and the need for multiple steps to remove iron from the ore.

In order to improve these disadvantages, the efficient and environmentally friendly selective chlorination method using metal chlorides or HCl gas was studied. The selective chlorination processes investigated in this thesis all have the following advantages in common. (i) A high-grade TiO_2 feed can be obtained directly from the low-grade titanium ore in a single step. (ii) A highly concentrated acid or chlorine (Cl_2) gas is

not used. (iii) Various types of low-grade titanium ores can be used as starting materials. In addition, selective chlorination using titanium tetrachloride (TiCl$_4$) has the following additional advantages. (iv) Recovery of chlorine from chloride waste is possible, because the waste is generated in a dry form. (v) Finally, the TiCl$_4$ is easy to obtain, because a large amount of TiCl$_4$ is circulated in the Kroll process.

In chapter 2, a thermodynamic study of the chlorination reactions of metals or oxides at elevated temperature was carried out in order to consider the feasibility of the iron removal directly from low-grade titanium ore through selective chlorination. In particular, various chlorination reactions were analyzed by utilizing the chemical potential diagrams of M-O-Cl systems (M = Fe, Ti, H, Ca, Mg), which were found to be applicable and useful for analyzing the selective chlorination of low-grade titanium ore. Furthermore, chlorination reactions with various types of chlorinating agents were discussed from various viewpoints. It was shown that the selective chlorination of iron from low-grade titanium ore by HCl, CaCl$_2$, MgCl$_2$, or TiCl$_4$ is thermodynamically feasible and efficient for the production of high-grade TiO$_2$ feed. These thermodynamic analysis results showed that a new upgrading process for the titanium ore using a dry method that does not discharge any aqueous waste solution could be developed.

In chapter 3, a fundamental investigation of the selective chlorination of low-grade titanium ore using CaCl$_2$ to produce high-grade TiO$_2$ feed was carried out. The experimental results showed that iron in the low-grade titanium ore was selectively removed as FeCl$_x$ (l, g) (x = 2, 3) by HCl gas produced directly from the mixture of CaCl$_2$/titanium ore and CaCl$_2$ at 1100 K. When the HCl reacted with various types of low-grade titanium ores, 97 % TiO$_2$ feed with a porous microstructure was produced in a single step under certain conditions. In addition, when CaCl$_2$ directly reacted with low-grade titanium ore, the concentration of iron in the titanium ore decreased from about 50 % to 18 %, and CaTiO$_3$ was mainly produced. In some cases, iron was insufficiently removed from the titanium ore because the CaTiO$_3$ produced in the outmost parts of the titanium ore particles by the reaction between titanium ore and CaCl$_2$ hindered the removal of iron from the center of the titanium ore particles. On the other hand, the

production of $CaTiO_3$ helped to generate the HCl from $CaCl_2$ by lowering the activity of CaO in $CaCl_2$.

Chapter 4 describes a fundamental study on increasing the amount of iron removed from low-grade titanium ore by reaction with $CaCl_2$ through physical contact. In the experiment, iron was selectively removed as $FeCl_2$ (l, g) from various types of titanium ores, and high-grade $CaTiO_3$ was produced. When the selective chlorination was conducted using $\leq$ 74 μm titanium ore particles at 1240 K for at least 8 hours, the concentration of iron in the titanium ore decreased from about 50 % to 1.8 %. It was found that the amount of iron removed from a titanium ore increased when the reaction temperature or time were increased or particle size of titanium ore was decreased. In addition, the feasibility of the scale up of the selective chlorination using $CaCl_2$ was demonstrated.

In chapter 5, a method for the selective chlorination of low-grade titanium ore using $MgCl_2$ was developed for the production of high-grade TiO_2 feed. Iron was selectively removed from the low-grade titanium ore as $FeCl_2$ (l, g) directly by HCl gas generated from the $MgCl_2$/titanium ore mixture and $MgCl_2$ at 1000 K. When HCl reacted with various types of low-grade titanium ores, 97 % TiO_2 feed with a porous microstructure was produced in a single step under certain conditions. In addition, it was shown that the time required for the completion of the removal of iron from the titanium ore was decreased when the experiments were conducted in the presence of H_2O gas because of the accelerated production of HCl gas from the $MgCl_2$. When $MgCl_2$ directly reacted with low-grade titanium ore, the iron concentration in the titanium ore was decreased from about 50 % to 18 %. It was found that the formation of the $MgTiO_3$ at the outer part of the titanium ore particles physically hindered further reaction between $MgCl_2$ and iron in the central portions of the titanium ore particles.

In chapter 6, in order to selectively remove iron directly from low-grade titanium ore by $TiCl_4$ under a low oxygen chemical potential (p_{O_2}), thermodynamic analysis considering the chemical potentials of oxygen and chlorine was conducted. Then, the suitable chemical potential region for the selective chlorination of iron in the titanium ore

311

using TiCl$_4$ under low p_{O_2} was investigated to produce high-grade TiO$_2$ feed. When the experiments were conducted under a reducing atmosphere, which was maintained by the presence of carbon, at 1100 K, the iron in the various types of titanium ores was selectively removed in the form of FeCl$_2$ (l, g). As a result, 98 % TiO$_2$ feed with a porous microstructure was produced directly from low-grade titanium ore containing 51 % TiO$_2$ in a single step under certain conditions. In addition, the FeCl$_2$ was produced in a dry form, because H$_2$O did not participate in the reactions, which makes it possible to recover the chlorine from chloride waste.

In chapter 7, the selective removal of iron from the titanium ore using TiCl$_4$ under high p_{O_2} was investigated, in order to produce high-grade TiO$_2$ feed directly from low-grade titanium ore in a single step. The appropriate chemical potential region for selective chlorination under high p_{O_2} was studied by utilizing the chemical potential diagram considering chlorine chemical potential (p_{Cl_2}) and p_{O_2}. When the selective chlorination of various types of titanium ore particles with sizes of 74 – 149 μm was conducted at 1200 K under high p_{O_2} (1 ppm, 1 %, or 10 % O$_2$), the iron in the titanium ore was directly removed as FeCl$_x$ (l, g) (x = 2, 3) in a dry form, and 98 % TiO$_2$ feed with a porous microstructure was obtained in a single step under certain conditions. In addition, when the selective chlorination using titanium ore particles with sizes of 74 – 297 μm was conducted at 1200 K under an Ar + 1 ppm O$_2$ atmosphere, TiO$_2$ feed with more than 95 % purity was obtained. However, when the titanium ore particle size was larger than 297 μm, the concentration of iron in the titanium ore decreased from about 50 % to 11 %, because unreacted iron remained in the central portions of the titanium particles owing to the insufficient reaction time.

In chapter 8, the application of the selective chlorination using TiCl$_4$ under low p_{O_2} was investigated with the purpose of upgrading titania slag to produce the high-grade TiO$_2$ feed directly. Generally, titania slag with a purity of 75 – 86 % TiO$_2$ is further upgraded before use by the UGS process using highly concentrated acid to produce high-grade TiO$_2$ feed. As a result of the upgrading process, a large amount of acid waste solution containing heavy metals is generated. In the experiments, various types of titania slags, as-received titania slag, the oxidized titania slag, the reduced titania slag after

oxidation, and the upgraded slag, were reacted with $TiCl_4$ in the presence of carbon at 1100 K. The iron in the titania slag feedstocks was selectively removed as $FeCl_2$ (l, g) in a dry form, and TiO_2 feed with more than 94 % purity was directly obtained. These results show that the selective chlorination using $TiCl_4$ could be used instead of the UGS process for upgrading titania slag.

In chapter 9, the problems of the current titanium ore upgrading processes were briefly reviewed again. Thereafter, a novel environmentally friendly titanium ore upgrading process that does not discharge waste solution or chloride waste was proposed, and the features of the new process were characterized in detail. In particular, establishment of a novel selective chlorination process through pyrometallurgical method (high-temperature process) for the production of the high-grade TiO_2 feed for titanium metal and titania pigment production was proposed. When this selective chlorination process is used, it is also possible to decrease the chlorine loss in the chlorination process, because the chlorine can be recovered using a pyrometallurgical method such as the oxidation reaction. Thus, the environmental burden can be decreased, because the iron in the titanium ore is discharged from the system as pig iron or iron oxide (Fe_2O_3) in the new titanium smelting process.

In this thesis, thermodynamic analysis considering the chemical potentials of oxygen and chlorine was conducted in order to remove iron selectively and directly from low-grade titanium ore. Then, the suitable chemical potential region for the selective chlorination using HCl, $CaCl_2$, $MgCl_2$, or $TiCl_4$ as the chlorinating agent for the production of high-grade TiO_2 feed was investigated by utilizing the chemical potential diagrams. The experimental results showed that iron was selectively removed from low-grade titanium ore as iron chlorides by these chlorides, and 97 − 98 % TiO_2 feed was produced directly from titanium ore containing 51 % TiO_2 in a single step under certain conditions.

When the reaction rate, environment of a reactor during operation, recycling of chlorides waste, reduction in chlorine loss of chlorinating agent, and ease of obtaining chlorinating agent are considered, the selective chlorination process will be the most

efficient method for the production of the high-grade TiO_2 feed in the future. Especially, the selective chlorination process using $TiCl_4$ is an environmentally friendly method, because any acid waste solution is not discharged and recovery of chlorine from chlorides waste is possible.

In recent years, interest in a method that allows inexpensive low-grade titanium ore to be used in the titanium smelting industry has increased along with the rising price of titanium ore. Therefore, it is expected that the selective chlorination method investigated in this thesis will be used as a novel environmentally friendly process for the production of high-grade TiO_2 feedstock for titanium metal and titania pigment production.

Acknowledgment

Jumpei Mitsui, Kohei Matsutani, Akihiro Yoshimura, Akinari Suzue, Yuki Hamanaka, and Ryohei Yagi; Ms. Tomoko Miyazaki; Ms. Tomoko Inaba; Messrs. Tetsuo Watanabe, Keigo Nishimura, Yiannis G. Kipouros, and Daiki Nishikawa; Ms. Mei Hirotani; and Ms. Yukiko Miura.

The author owes a great deal of gratitude to Professors Kyung-Woo Yi, Han-Ill Yoo, and Eun Soo Park; Emeritus Professor Tak Kang of the Department of Materials Science and Engineering at Seoul National University in the Republic of Korea; and Messrs. Si Woo Lee, Ik Joon Kim, Hee Young Kim, Hoon Hui Lee, and Hyun Sik Jeong of POSCO in the Republic of Korea for their warm and constant guidance and support. In addition, the author is grateful to Dr. Seong-Jae Mun and Dr. Minsoo Kim of Samsung Electro-mechanics and Ms. Wonkyoung Ye of LG Chem. for their support.

Finally, the author would like to sincerely thank his parents, Mr. Seonghyul Kang and Mrs. Hyeonok Lee, for their generous supports and encouragement. The author also offers his thanks to his grandparents, Dr. Taekhyeon Kang and Mrs. Dalmak Oh, who passed away in 2013.

Jungshin Kang

Tokyo, Japan
August 2014

List of Publications

The main parts of this thesis are constructed from the following papers.

Original papers for journal with peer review, Review papers, Book, and Proceedings for international conference

Chapter 1

1. "レアメタルの最新動向"
   岡部 徹，姜 正信 (分担執筆):
   [監修] 岡部 徹、野瀬 勝弘、第 6 章 1 節 チタンの製錬技術の将来展望について、シーエムシー出版、東京、2012, pp. 83-94.

Chapter 2

2. "Thermodynamic Consideration of the Removal of Iron from Titanium Ore by Selective Chlorination":
   Jungshin Kang and Toru H. Okabe:
   Metallurgical and Materials Transactions B, 2014, vol. 45B, pp. 1260-1271.

3. "高温における酸化物の塩化反応に関する熱力学的考察",
   岡部 徹、姜 正信:
   溶融塩および高温化学, 2013, vol. 56 (1), pp. 15-26.

Chapter 3

4. "Upgrading Titanium Ore Through Selective Chlorination Using Calcium Chloride",
   Jungshin Kang and Toru H. Okabe:
   Metallurgical and Materials Transactions B, 2013, vol. 44B, pp. 516-527.

5. "Upgrade of Titanium Ore by Selective Chlorination Using Calcium Chloride",
   Jungshin Kang and Toru. H. Okabe:
   Proceedings of the 4th Asian Conference on Molten Salt Chemistry and Technology, and 44th Symposium on Molten Salt Chemistry, Edited by Y.Sato,
   [Matsushima, Japan, September 23-27, 2012] (2012.9.25), pp. 176-182.

Chapter 5

6. "Removal of Iron from Titanium Ore through Selective Chlorination Using
Magnesium Chloride",
Jungshin Kang and Toru H. Okabe:
Materials Transactions, 2013, vol. 54 (8), pp. 1444-1453.

　　　※ 62th Best Paper Awards (Kinzoku Gakkai Ronbun-shou)
from the Japan Institute of Metals and Materials.
(To be awarded at 155th Fall meeting of the Japan Institute of Metals and
Materials, Nagoya, 24-26 September, 2014)

Chapter 6

7. "Production of Titanium Dioxide Directly from Titanium Ore Through
Selective Chlorination Using Titanium Tetrachloride",
Jungshin Kang and Toru H. Okabe:
Materials Transactions, 2014, vol. 55 (3), pp. 591-598.

Chapter 7

8. "Removal of Iron from Titanium Ore by $TiCl_4$ under High Oxygen Potential
through Selective Chlorination",
Jungshin Kang and Toru H. Okabe:
International Journal of Mineral Processing (under revision)

Chapter 9

9. "Proposal of an Environmentally Friendly Titanium Smelting Process Free from
Waste Solution or Chloride Waste Discharge",
Jungshin Kang and Toru H. Okabe:
JOM (submitted)

Presentations at international conferences

1. "Upgrading Ti Ore by Selective Chlorination" [Poster Presentation],
Jungshin Kang, Toru H. Okabe
The 7th Workshop on Reactive Metal Processing,
Massachusetts Institute of Technology (MIT), Cambridge, USA (Mar. 16-17, 2012).

2. "Upgrade of Titanium Ore by Selective Chlorination" [Oral Presentation],
  Jungshin Kang and Toru H. Okabe
  The 11th GMSI-COSM-UT2 2012 Graduate Student Workshop,
  The University of Tokyo, Tokyo, Japan (Jun. 18-21, 2012).

3. "Upgrade of Titanium Ore by Selective Chlorination Using Calcium Chloride"
  [Oral Presentation],
  Jungshin Kang and Toru H. Okabe:
  The 4th Asian Conference on Molten Salt Chemistry and Technology, and
  44th Symposium on Molten Salt Chemistry, Matsushima, Japan (Sep. 23-27, 2012).

4. "Upgrade of Titanium Ore by Selective Chlorination" [Oral Presentation],
  Jungshin Kang and Toru H. Okabe:
  TMS 2013 142nd ANNUAL MEETING & EXHIBITION,
  4th International Symposium on High-Temperature Metallurgical Processing:
  Roasting, Reduction and Smelting, Henry B. Gonzalez Convention Center,
  San Antonio, Texas, USA (Mar. 3-7, 2013).

5. "Iron Removal from Titanium Ore to Prepare Titanium Dioxide through
  Selective Chlorination" [Oral Presentation],
  Jungshin Kang and Toru H. Okabe:
  The 8th Workshop on Reactive Metal Processing,
  Massachusetts Institute of Technology (MIT), Cambridge, USA (Mar. 8-9, 2013).

6. "Development of Selective Chlorination Process for Upgrading Ti Ore and
  Thermodynamic Analysis of Chlorination Reactions" [Oral Presentation],
  Jungshin Kang and Toru H. Okabe:
  The 12th COSM-UT2 2013 Graduate Student Workshop,
  The University of Toronto, Ontario, Canada (June. 5-7, 2013).

7. "Iron Removal from Titanium Ore for Titanium Dioxide Production
  by Selective Chlorination Using Metal Chlorides"
  [Poster Presentation], [Excellent Poster Presentation Award],
  Jungshin Kang and Toru H. Okabe:
  The 11th Japan/Korea International Symposium on Resources Recycling and
  Materials Science, Kansai University Centenary Memorial Hall, Osaka, Japan
  (June. 17-19, 2013).

8. "Thermodynamic Consideration on Selective Chlorination and Its Application for Upgrading Titanium Ore" [Oral Presentation], [Best Presentation Award], Jungshin Kang and Toru H. Okabe: The 9th TU-UT-SNU Student Workshop, Seoul National University, Seoul, Republic of Korea (Oct. 9-12, 2013).

9. "Iron Removal from Titanium Ore through Selective Chlorination and Its Reaction Analysis" [Oral Presentation], Jungshin Kang and Toru H. Okabe: TMS 2014 143rd ANNUAL MEETING & EXHIBITION, 5th International Symposium on High-Temperature Metallurgical Processing: Roasting, Reduction and Smelting, San Diego Convention Center, San Diego, California, USA (Feb. 16-20, 2014).

10. "Upgrading Titanium Ore through Selective Chlorination Using Titanium Tetrachloride" [Oral Presentation], Jungshin Kang and Toru H. Okabe: TMS 2014 143rd ANNUAL MEETING & EXHIBITION, Materials Processing Fundamentals, San Diego Convention Center, San Diego, California, USA (Feb. 16-20, 2014).

11. "Production of High-grade TiO_2 Feed from Ti Ore through Selective Chlorination Using $TiCl_4$" [Poster Presentation], Jungshin Kang and Toru H. Okabe: The 9th Workshop on Reactive Metal Processing, California Institute of Technology (Caltech), Pasadena, California, USA (Feb. 21-22, 2014).

12. "Development of a New Ti Ore Upgrading Process Using $TiCl_4$ for Production of High-grade TiO_2" [Oral and Poster Presentation], Jungshin Kang and Toru H. Okabe: 7th KIFEE International Symposium on Environment, Energy, and Materials, Doshisha University, Kyoto, Japan (Mar. 16-19, 2014).

Presentations at domestic conferences

1. "Upgrade of Titanium Ore by Selective Chlorination using Metal Chlorides" [Poster Presentation], Jungshin Kang and Toru H. Okabe:

資源・素材学会　関東支部 第 9 回「資源・素材・環境」技術と研究の
交流会, [東京大学浅野キャンパス・武田先端知ビル、東京] (2012.8.1).

2. "選択塩化法による低品位チタン鉱石のアップグレード" [Oral Presentation],
姜 正信、岡部 徹:
資源素材学会・秋季大会 [秋田大学、秋田] (2012.9.13).

3. "高温における酸化物の塩化反応に関する熱力学的考察" [Oral Presentation],
岡部 徹、姜 正信:
第 180 回溶融塩委員会役員会, [けやき会館, 千葉大学西千葉キャンパス,
千葉] (2013.1.24).

4. "チタン製錬と環境問題" [Oral Presentation],
岡部 徹、姜 正信:
新日鐵住金株式会社での勉強会, [新日鐵住金株式会社本社(丸の内南),
東京] (2013.2.27).

5. "金属塩化物を用いた選択塩化法によるチタン鉱石の脱鉄による酸化チタン
の製造" [Poster Presentation],
Jungshin Kang and Toru H. Okabe:
第 55 回 レアメタル研究会 特別企画：若手研究者、大学院生による
ポスター発表、[東京大学生産技術研究所、東京] (2013.3.22).

6. "Upgrading Titanium Ore through Selective Chlorination Using $MgCl_2$"
[Oral Presentation],
Jungshin Kang and Toru H. Okabe:
資源素材学会・春季大会 [千葉工業大学、千葉] (2013.3.29).

7. "選択塩化法によるチタン鉱石のアップグレードとその反応解析"
[Oral Presentation],
姜 正信、岡部 徹:
シンポジウム「チタン製錬技術の革新を目指して」、[主催：一般社団法人
日本チタン協会 産学連携委員会、新日鐵住金(株)本社、東京] (2013.5.8).

8. "選択塩化によるチタン鉱石からの脱鉄" [Oral Presentation],
姜 正信、岡部 徹:
チタン若手研究者・技術者交流会、[主催：一般社団法人日本チタン協会
産学連携委員会、新日鐵住金(株) 製鋼所、大阪] (2013.11.15).

Curriculum Vitae

Personal Information

Name:	Jungshin Kang
Sex:	Male
Nationality:	Republic of Korea

Current position:	Ph.D candidate
	Department of Materials Engineering,
	Graduate School of Engineering, The University of Tokyo

Address:	4-6-1 Komaba, Meguro-ku, Tokyo 153-8505
	Room Fw301, Institute of Industrial Science,
	The University of Tokyo

Tel.:	+81-3-5452-6314
Fax.:	+81-3-5452-6313
E-mail:	jskang@iis.u-tokyo.ac.jp / strongspirit@gmail.com

Education

Oct. 2011 – Present	Ph.D candidate in Materials Engineering,
	The University of Tokyo
Feb. 2011	M.Sc. in Materials Science and Engineering,
	Seoul National University
Aug. 2006	B.Sc. in Materials Science and Engineering,
	Seoul National University
	B.Sc. in Computer Science and Engineering,
	Seoul National University

Research/Professional Experience

May. 2013 – Mar. 2014	Research Assistant,
	Department of Materials Engineering,
	The University of Tokyo
Jan. 2013 – Mar. 2013	Research Assistant,
	Department of Materials Engineering,
	The University of Tokyo

Mar. 2011 – Dec. 2011	Research Associate, Research Institute of Advanced Materials, Seoul National University
Aug. 2006 – Mar. 2009	Engineer, Cold Rolling Department, Gwangyang Works, POSCO

Awards

Sep. 2014	62th Best Paper Awards (Kinzoku Gakkai Ronbun-shou) from the Japan Institute of Metals and Materials. (To be awarded at 155th Fall meeting of the Japan Institute of Metals and Materials, Nagoya, 24-26 September, 2014)
Oct. 2013	Best Presentation Award at the 9th TU-UT-SNU Student Workshop, Seoul National University, Korea, 9-12 October, 2013
Jun. 2013	Excellent Poster Presentation Award from RPSJ (Resources Processing Society of Japan) and KIGAM (Korea Institute of Geoscience and Mineral Resources) at The 11th Japan/Korea International Symposium on Resources Recycling and Materials Science, Kansai University, Osaka, 17–19 June, 2013
Aug. 2006	Best Research Award from Department of Materials Science and Engineering, Seoul National University

Funds

Scholarship

Oct. 2011 – Present	Government scholarship from Ministry of Education, Culture, Sports, Science and Technology (MEXT), Japan
May. 2013 – Mar. 2014	Scholarship as research assistant from "Grants for Excellent Graduate Schools" program, Department of Materials Engineering, The University of Tokyo
Jan. 2013 – Mar. 2013	Scholarship as research assistant from "Grants for Excellent Graduate Schools" program, Department of Materials Engineering, The University of Tokyo
Sep. 2009 – Feb. 2011	Scholarship from LG Yonam Cultural Foundation

Mar. 2009 – Aug. 2009	Scholarship from College of Engineering, Seoul National University
Mar. 2005 – Aug. 2006	Scholarship for academic achievement from Seoul National University
Mar. 2000 – Feb. 2002	Scholarship for academic achievement from Seoul National University

Grant Aid for Travel

Feb. 2013	"Grants for Excellent Graduate Schools" program, Department of Materials Engineering, The University of Tokyo (Feb. 15, 2013) Country or areas to visit: San Antonio and Boston, America Time period: Mar. 3 – 12, 2013 Purpose: Presentation at TMS 2013 142nd ANNUAL MEETING & EXHIBITION and The 8th Workshop on Reactive Metal Processing
Sep. 2012	The Foundations for the Promotions of Industrial Science, Institute of Industrial Science, The University of Tokyo (Sep. 21, 2012) Country or areas to visit: San Antonio and Boston, America Time period: Mar. 3 – 12, 2013 Purpose: Presentation at TMS 2013 142nd ANNUAL MEETING & EXHIBITION and The 8th Workshop on Reactive Metal Processing

Certifications

Aug. 2007 – Feb. 2009	Six Sigma Green Belt, POSCO

Other Skills

Programming	JAVA, C, and FORTRAN
Numerical modeling	CFD-GEOM, CFD-ACE+, and CFD-VIEW
Analysis equipment	Normal SEM/EDS, FE-SEM, XRF, XRD

Reference

Toru H. Okabe	Professor, Institute of Industrial Science, The University of Tokyo
Kyung-Woo Yi	Professor, Department of Materials Science and Engineering, Seoul National University